S. Boopathy Vijayaraghavan

Atlas of Fetal Imaging

Abdomen

Springer

Atlas of Fetal Imaging

S. Boopathy Vijayaraghavan

Atlas of Fetal Imaging

Abdomen

Springer

S. Boopathy Vijayaraghavan
SONOSCAN-Ultrasonic Scan Centre
Coimbatore
Tamil Nadu
India

ISBN 978-981-13-0931-1 ISBN 978-981-13-0932-8 (eBook)
https://doi.org/10.1007/978-981-13-0932-8

Library of Congress Control Number: 2018951068

This Springer imprint is published by the registered company Springer Nature Singapore Pte Ltd.
The registered company address is: 152 Beach Road, #21-01/04 Gateway East, Singapore 189721, Singapore

Preface

The field of fetal medicine has evolved as an independent specialty over this past decade. It is, to a major extent, due to the advancement in obstetric ultrasound. Because of improvement in the technology and resolution of machines, we are able to see more and earlier in gestation. Study of fetal abdomen has come to limelight, only recently. Most of the anomalies of fetal abdomen are rare, and their description has been mostly in the form of case reports or case series because of the lack of numbers. This atlas is designed to lead the reader from an abnormal ultrasound image of fetal abdomen to a precise diagnosis. This is made possible by the help of high-frequency probe in most of the cases and dynamic study in many cases. The dynamic study is illustrated in the form of cine loops which are made available online for the readers. This book is an atlas of fetal abdomen giving description of various anomalies of fetal abdomen using abundant illustrative scan images with essential descriptive text containing a brief mention of other aspects of the anomalies. The readers are encouraged to refer to more literature for detailed description of these aspects. This atlas will be a practical guide to the imaging specialists and those who practice fetal medicine.

Coimbatore, Tamil Nadu, India — S. Boopathy Vijayaraghavan

Acknowledgment

I acknowledge with thanks the support extended by my family and the professional help by my colleagues, fellows, and staff of SONOSCAN which made this book possible.

Contents

About the Author

S. Boopathy Vijayaraghavan graduated from Coimbatore Medical College and Madras Medical College, Chennai. He is a consultant diagnostic radiologist in Sonoscan-Ultrasonic Scan Centre and Director of the Sonoscan Institute of Ultrasound in Medicine. He was President of the Coimbatore Ultrasound Society and Chairperson of the Coimbatore subchapter of the Indian Radiological and Imaging Association. He is currently the Organizing Chairman of FOCUSSE, a periodical CME in ultrasonography, and he was on the editorial committees of the *Indian Journal of Radiology and Imaging* and the *Indian Journal of Medical Ultrasound*. He has published work in several books and journals and has delivered numerous lectures at various national and international CME events and conferences. He has received a number of awards, including the Sir JC Bose Award—the highest honor conferred by the Indian Radiology and Imaging Association—and Gnanadhara's distinguished teacher award.

List of Videos

1 Protocol of Performance of Sonography of Fetal Abdomen and Normal Appearance

1.1 Introduction

Fetal abdomen contains most structures forming part of fetal gastrointestinal tract and genitourinary tract. It is contained by the anterior abdominal wall anteriorly, diaphragm above, pelvic floor below and the spine and paraspinal muscles posteriorly.

1.2 Technique and Protocols

Most of the guidelines of performance of an anomaly scan recommend the following sections. First is the section along which the abdominal circumference is measured (Fig. 1.1).

In this section the structures to be studied are the spine posteriorly, the umbilico-portal vein seen as a hockey stick formed by the anteroposteriorly oriented left branch and horizontal right branch of portal vein, the stomach bubble, the liver, spleen, aorta and inferior vena cava. In this section abdominal organ situs is determined. The stomach bubble should be on the left side. The size of stomach bubble is variable due to gastric emptying. If stomach bubble is not visualized, the scan should be repeated after an interval. The second section is an axial scan just below the first one (Fig. 1.2).

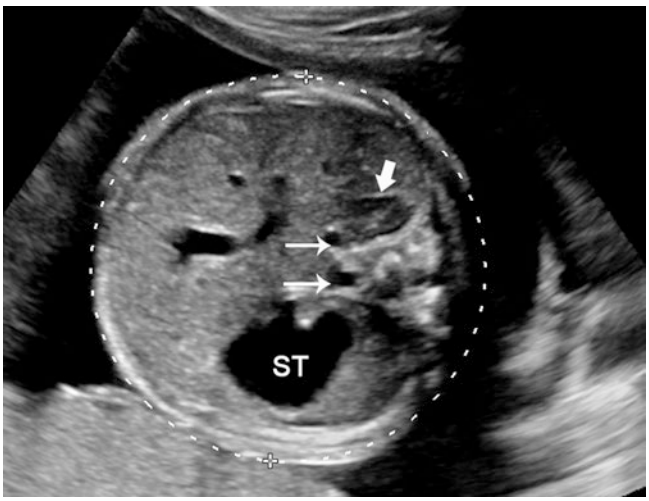

Fig. 1.1 Axial section of fetal abdomen along which the abdominal circumference is measured. The structures seen are stomach bubble (ST) on left side, umbilico portal vein, aorta on left side and inferior vena cava on right side (*thin arrows*) and the right adrenal (*bold arrow*)

S. B. Vijayaraghavan, *Atlas of Fetal Imaging*, https://doi.org/10.1007/978-981-13-0932-8_1

This will show the pyriform gall bladder on right side. This section is not a minimum requirement of the basic anomaly scan. The third section is taken to show the fetal insertion site of umbilical cord to rule out abdominal wall defects (Fig. 1.3).

This section will also show the mid abdomen containing the small bowels. The kidneys are seen on an axial scan with the spine either at 12 or 6 o'clock position (Fig. 1.4).

The kidneys are seen as round echopoor structures on either side of the spine with horizontally oriented slit like fluid filled renal pelvis. The urinary bladder is seen as an oval fluid filled structure in axial scan of pelvis (Fig. 1.5a).

With color Doppler study, in a slightly oblique scan of urinary bladder including the cord insertion, the two umbilical arteries are seen to skirt around the urinary bladder (Fig. 1.5b, c). When urinary bladder is not seen the umbilical arteries help to confirm that the urinary bladder is not seen in the appropriate section. When urinary bladder is not seen, scan has to be repeated since the urinary bladder may be empty due to fetal micturition. The last section in protocol is the coronal scan of the abdomen. It will show three fluid filled structures—the stomach in left upper abdomen, the gall bladder in the right upper abdomen and the urinary bladder in the midline in the pelvis (Fig. 1.6).

Any other additional fluid filled structure will need further evaluation. These are the standard sections of abdomen to be obtained as per guidelines. When an abnormal appearance is seen, the scan has to be extended appropriately.

The resolution of the ultrasound scanners have improved remarkably over the years. Hence the visualization of abdominal structures have improved to a great extent. The highest frequency probe, allowing adequate penetration for the structure to be seen, has to be used. The high frequency linear transducer has to be used to see better details of organs whenever possible. This may need a repeat scan to allow the fetus to move so that the organ comes nearer the anterior abdominal wall. The improved resolution of this technique and its utility is illustrated in the subsequent pages.

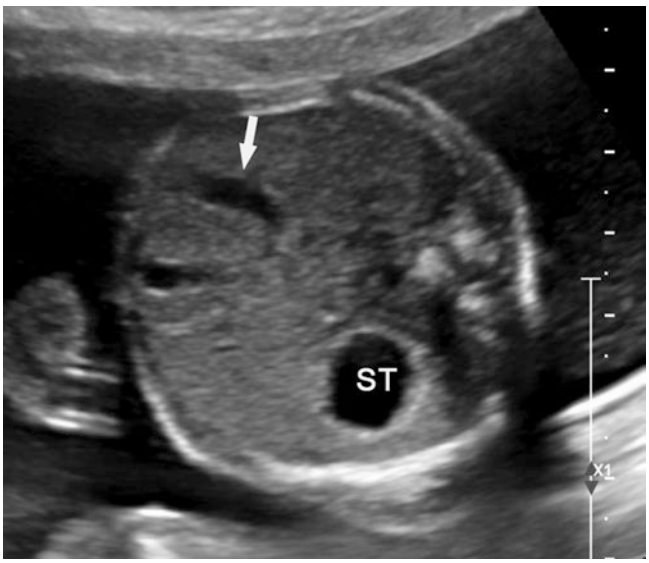

Fig. 1.2 Axial section below the section of Fig. 1.1 showing the pyriform gall bladder on right side

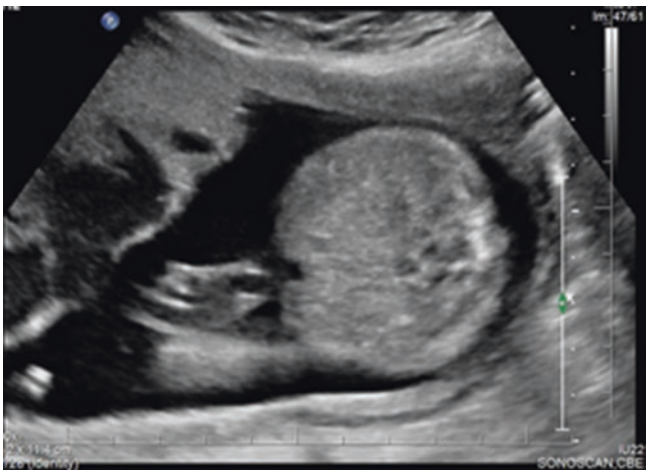

Fig. 1.3 Axial section of mid abdomen showing the fetal cord insertion and small bowels filling the abdomen

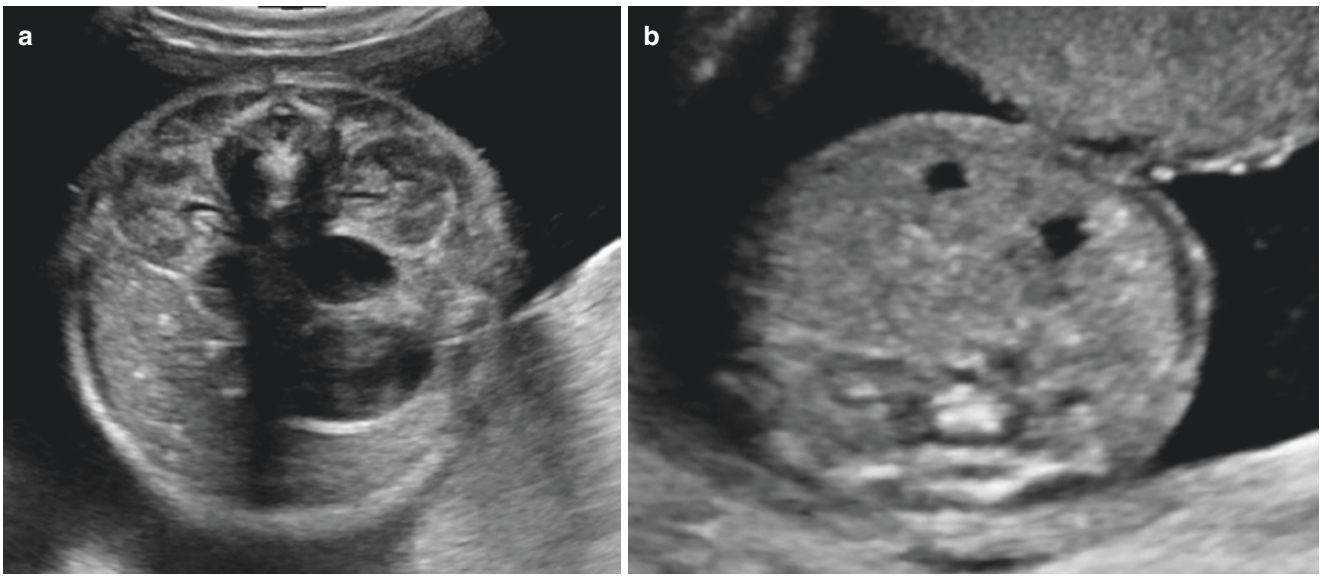

Fig. 1.4 Axial section with spine at (**a**) 12 o'clock and (**b**) 6 o'clock position showing the kidneys as round echopoor structures on either side of spine with central slit like fluid filled renal pelvis

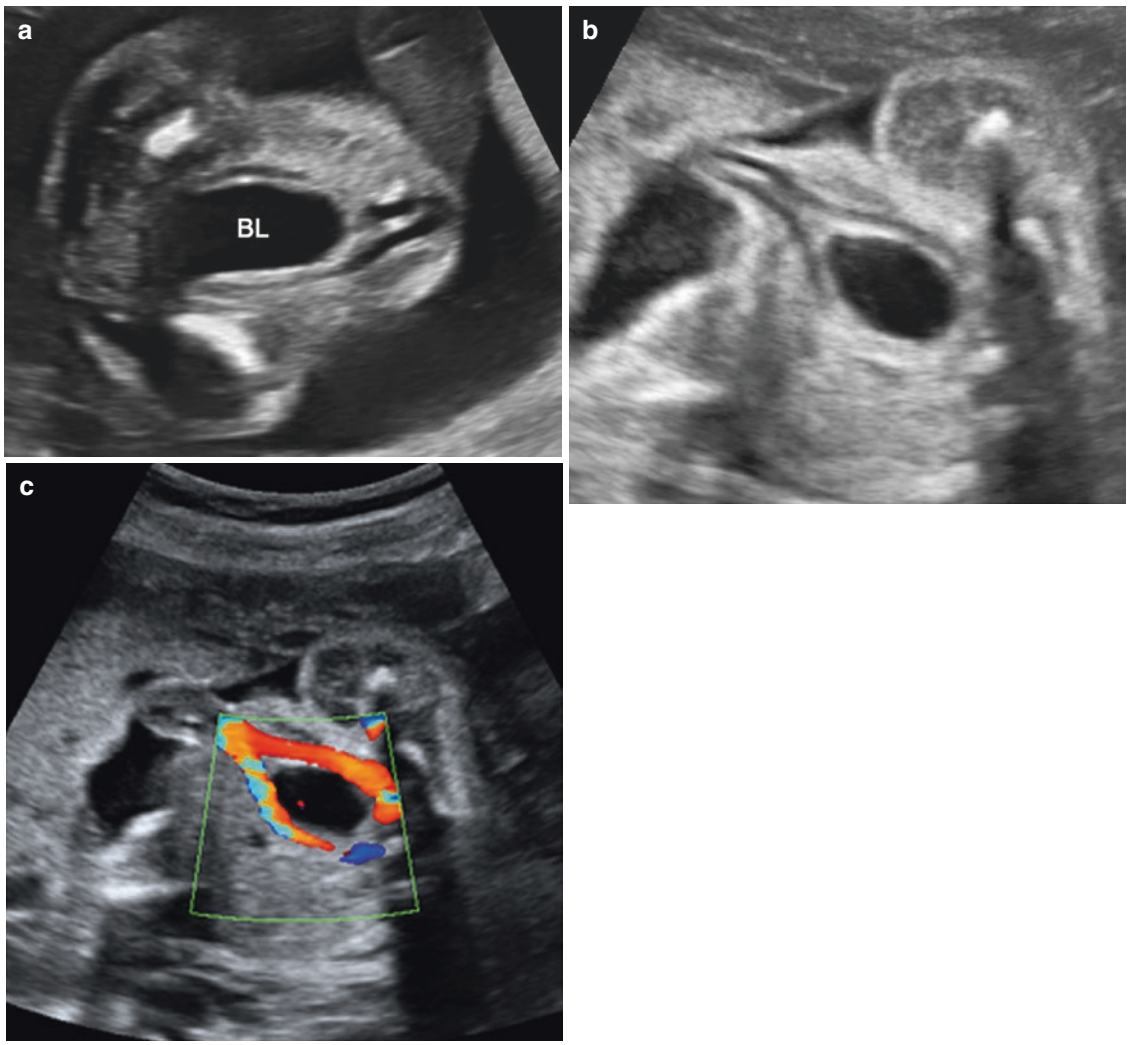

Fig. 1.5 (**a**) Axial section of fetal pelvis showing the fluid filled urinary bladder. (**b**) Gray scale and (**c**) colour Doppler oblique section of pelvis and cord insertion showing the urinary bladder and the two umbilical arteries skirting on either side of bladder

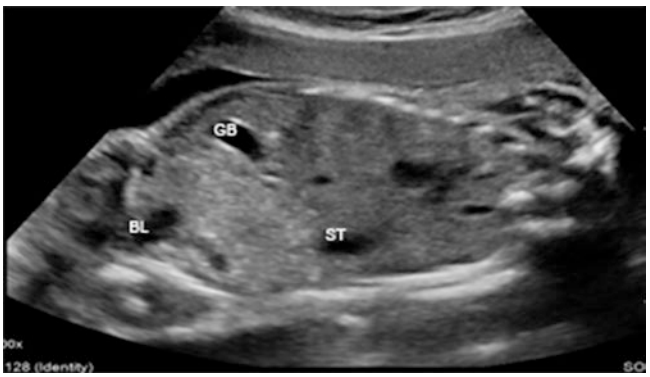

Fig. 1.6 Coronal scan of fetal abdomen showing the three fluid filled structures—stomach (ST), gall bladder (GB) and urinary bladder (BL)

1.3 Amniotic Fluid Dynamics

The amniotic fluid is vital for the well-being of the fetus. There is an association between the amniotic fluid dynamics and structures in fetal abdomen. Before 18 weeks the major source for the amniotic fluid is membranes followed by skin. So the fetal anomalies do not affect the amniotic fluid volume. After that period major source of amniotic fluid is fetal urine followed by the secretions of lungs and membranes. The fetus swallows the amniotic fluid which is absorbed by the fetal intestine. The amniotic fluid homeostasis is maintained by the balance between the inflow from fetal urinary tract and lung secretion and outflow by swallowing and absorption by the fetal GIT. Since the urinary tract and GIT are in the fetal abdomen, anomalies of these tracts are associated with change in the amniotic fluid volume—either as polyhydramnios when there is an obstructive anomaly of GIT or oligohydramnios in anomalies of urinary tract. In obstructive anomaly of the GIT, the more distal the obstruction, less is the degree of polyhydramniso.

Suggested Reading

American Institute of Ultrasound in Medicine. AIUM practice guideline for the performance of obstetric ultrasound examinations. J Ultrasound Med. 2013;32(6):1083–101.

Khurana A, Makhija B, Deka D, et al. Society of fetal medicine practice guidelines for the second trimester anomalies scan. J Fetal Med. 2014;1:11–5.

Salomon L, et al. Practice guidelines for performance of the routine mid-trimester fetal ultrasound scan. Ultrasound Obstet Gynecol. 2011;37:116–26.

Sonography of Fetal Gastrointestinal Tract (GIT)

2

The fetal gastro intestinal tract consists of

- Esophagus
- Stomach
- Small bowel and peritoneal cavity
- Large bowel

The sonographic appearance of fetal GIT is dynamic. The appearance varies with gestational age and during the period of each scan depending on the contents and peristalsis. This is the unique feature of fetal GI tract.

2.1 Oesophagus

The normal esophagus is a collapsed structure that is not routinely imaged. But it can be seen in second and third trimester. The esophagus is seen as a small round echogenic structure or a small round echopoor structure between the heart and the descending thoracic aorta in the axial section of fetal thorax at the level of 4 chamber view of the heart (Fig. 2.1).

On the longitudinal scan it is seen as a linear triple line structure. Occasionally it may be seen as fluid filled tube (Fig. 2.2).

In real time imaging the peristalsis can also be seen (Video 2.1). The presence of a patent and normally functioning esophagus is usually inferred by noting fluid in the fetal stomach. So direct visualization of esophagus is unnecessary.

Electronic Supplementary Material The online version of this chapter (https://doi.org/10.1007/978-981-13-0932-8_2) contains supplementary material, which is available to authorized users.

S. B. Vijayaraghavan, *Atlas of Fetal Imaging*, https://doi.org/10.1007/978-981-13-0932-8_2

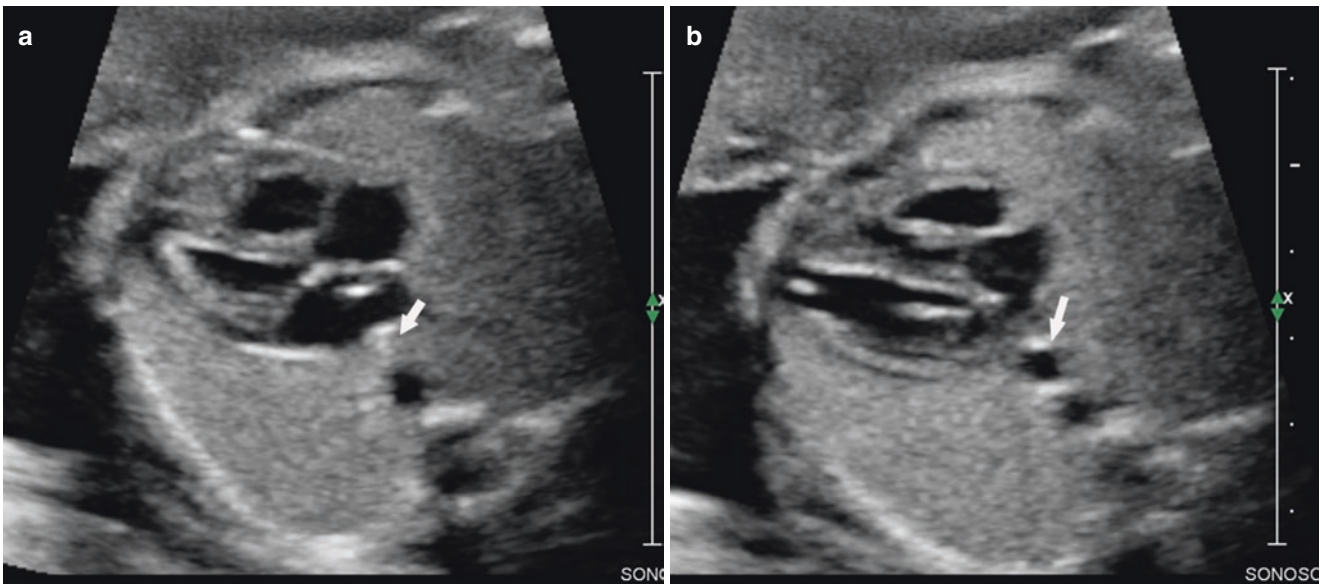

Fig. 2.1 Axial section of fetal chest at the level of four chamber view of the heart showing the collapsed echogenic (**a**) and round fluid filled (**b**) esophagus between the heart and descending aorta

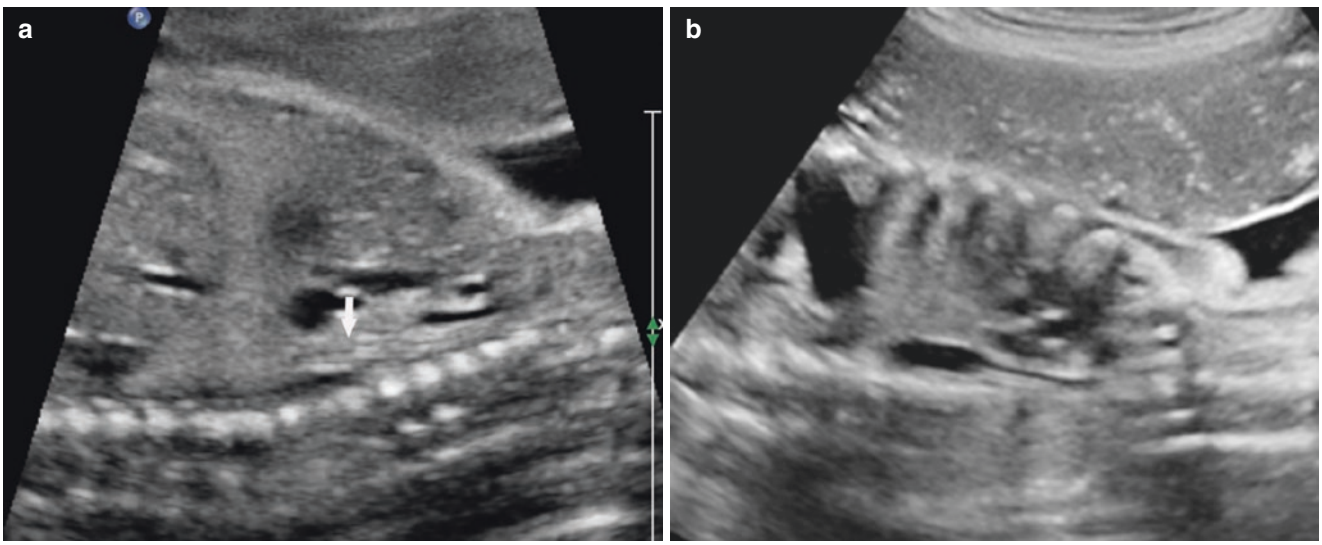

Fig. 2.2 Longitudinal section of the fetal chest showing the collapsed triple line (**a**) and fluid distended (**b**) esophagus (Video 2.1)

2.2 Visualisation of Stomach by Sonography

Fetal swallowing starts by 11 weeks of gestation and the fetal stomach can be visualized as a sonolucent area in the left upper quadrant of the fetal abdomen from 12 weeks onwards (Fig. 2.3).

There is marked variation in the size of fetal stomach among fetuses during second and third trimesters due to the fetal swallowing and gastric emptying over time and so the variation in the size of stomach does not carry any significance.

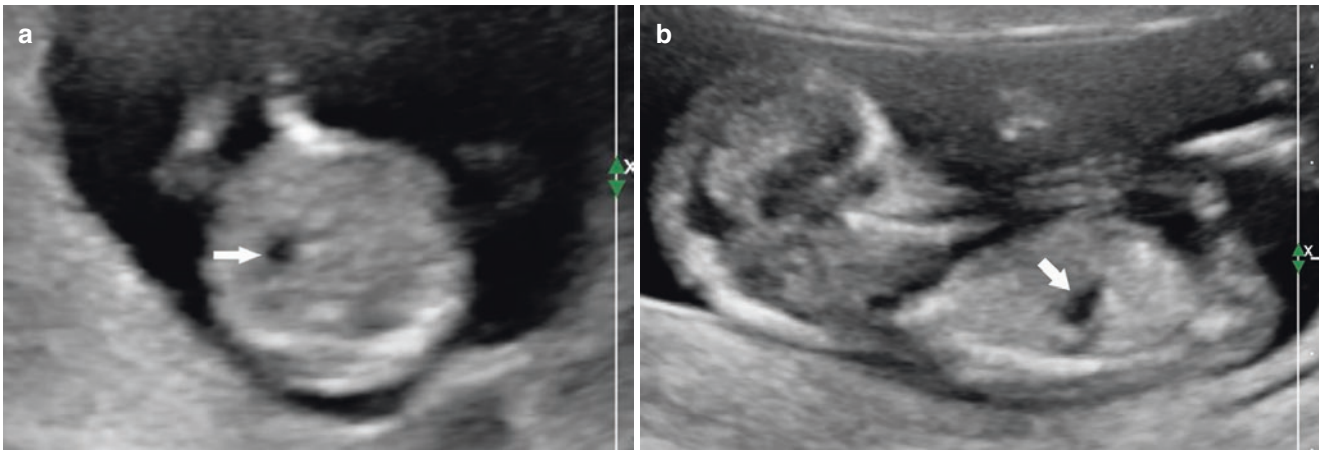

Fig. 2.3 (**a**) Axial and (**b**) Sagittal Scan of fetal abdomen at 12 weeks of gestation showing the stomach bubble

2.3 Esophageal Atresia

The incidence is 1 in 2500–4000 live births with male preponderance. There are five types of esophageal atresia (Fig. 2.4).

The commonest type is esophageal atresia with tracheoesophageal fistula between the trachea and distal segment of esophagus forming 85% of the cases.

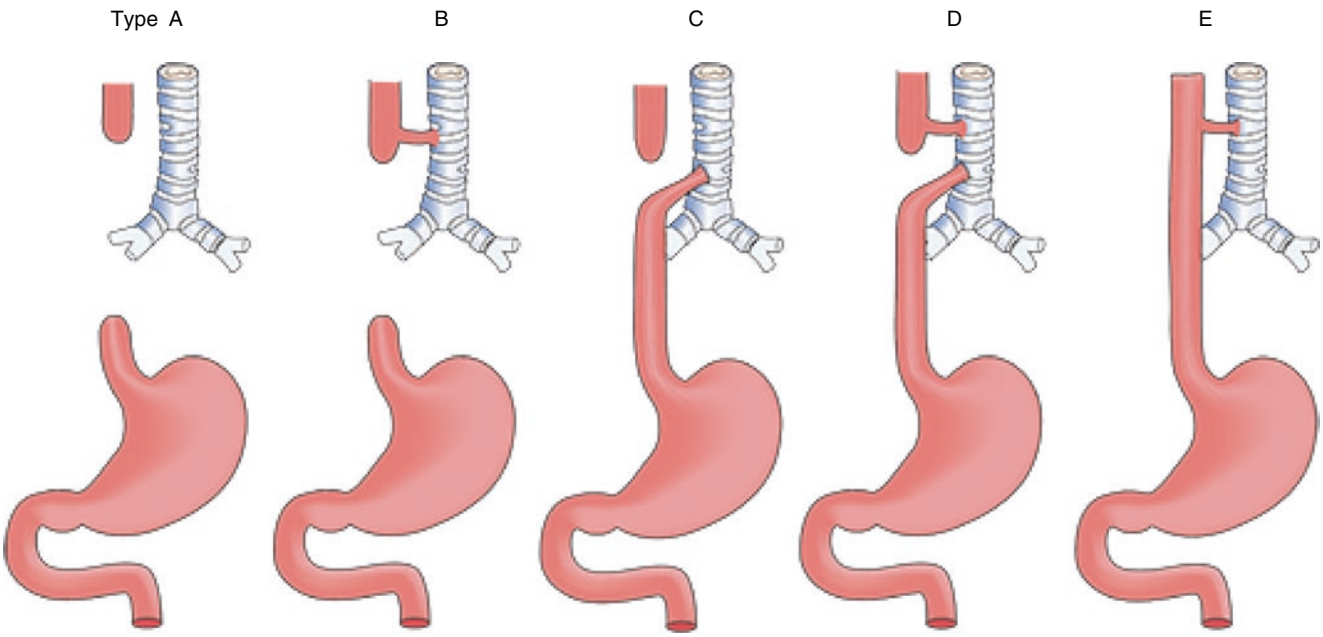

Fig. 2.4 Schematic diagram showing the types of esophageal atresia

2.3.1 Sonographic Features

In esophageal atresia the fetal stomach is persistently nonvisualised (Fig. 2.5).

There is polyhydramnios, which is not attributable to any other anomaly. The scan has to be repeated after an interval to confirm that the stomach is persistently nonvisualized. These features are diagnostic of esophageal atresia without tracheoesophageal fistula. But there are other conditions where the stomach bubble is not seen which have to be ruled out before diagnosing the esophageal atresia. Anomalies causing impaired fetal swallowing like cleft lip/palate, masses in oral cavity, neck or chest, esophageal compression due to vascular ring or masses and neuromuscular causes like anencephaly and fetal akinesia deformation sequence may have nonvisualized stomach bubble. The fetal stomach bubble is absent in cases of severe oligohydramnios also.

In the presence of polyhydramnios the visualization of stomach bubble does not rule out esophageal atresia since the commonest type is with tracheoesophageal fistula through which amniotic fluid reaches the stomach (Fig. 2.6a).

This type can be diagnosed by looking for the blind ending proximal esophagus which fills up and empties during fetal swallowing. This is called as ***pouch sign*** (Fig. 2.6b, c). To see the pouch sign a coronal scan of the neck is done and the transducer is rocked between the spine and the trachea (Video 2.2). The blind esophageal pouch can be seen as a transient finding when it fills up during fetal swallowing (Video 2.3). If it is persistent for some time the pouch can be imaged in transverse section also (Fig. 2.6d).

Features to differentiate trachea and esophageal pouch (Fig. 2.7).

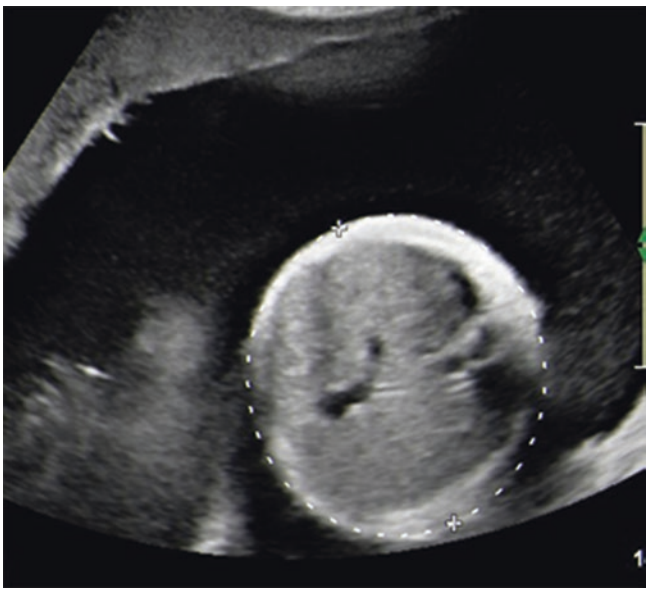

Fig. 2.5 Axial section of fetal upper abdomen in a fetus with oesophageal atresia without tracheooesophageal fistula showing the nonvisualised stomach bubble with polyhydramnios

Trachea	Esophagus pouch
Bifurcates low down	Does not bifurcate
Remain stationary Cylindrical in shape	Empties and fills up Oval in shape
Colour Doppler: during fetal breathing, colour change is noted indicating fluid movement	

Esophageal atresia can be isolated or form part of VACTERL association (Fig. 2.8).

Prognosis is good in isolated esophageal atresia.

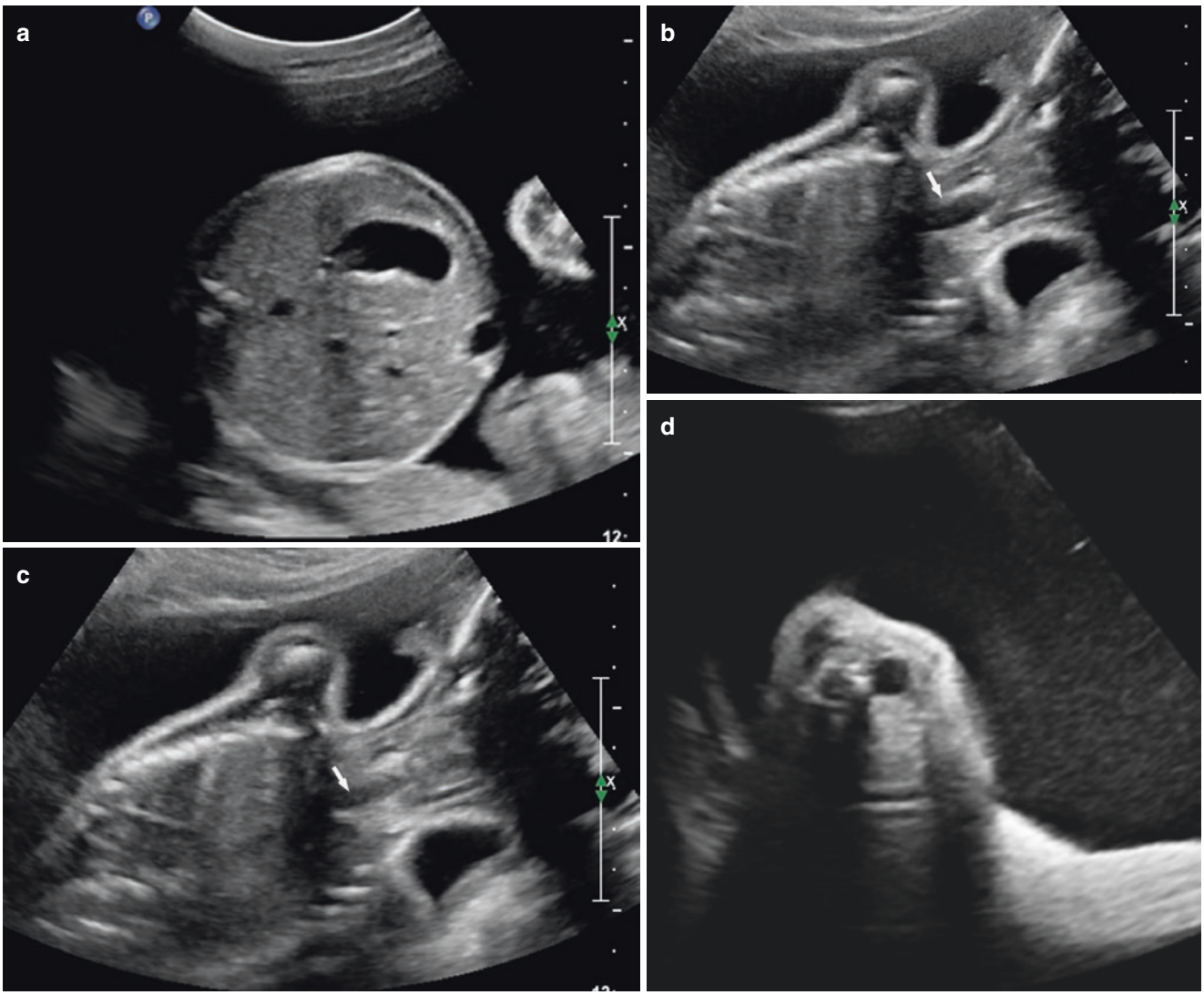

Fig. 2.6 Esophageal atresia with tracheoesophageal fistula—(**a**) Axial section a fetal upper abdomen showing polyhydramnios and the normal stomach bubble. Coronal scan of fetal neck showing the fluid distended blind esophageal pouch (**b**) and collapsed pouch (Video 2.3) (**c**). Axial scan of neck showing the round fluid distended pouch

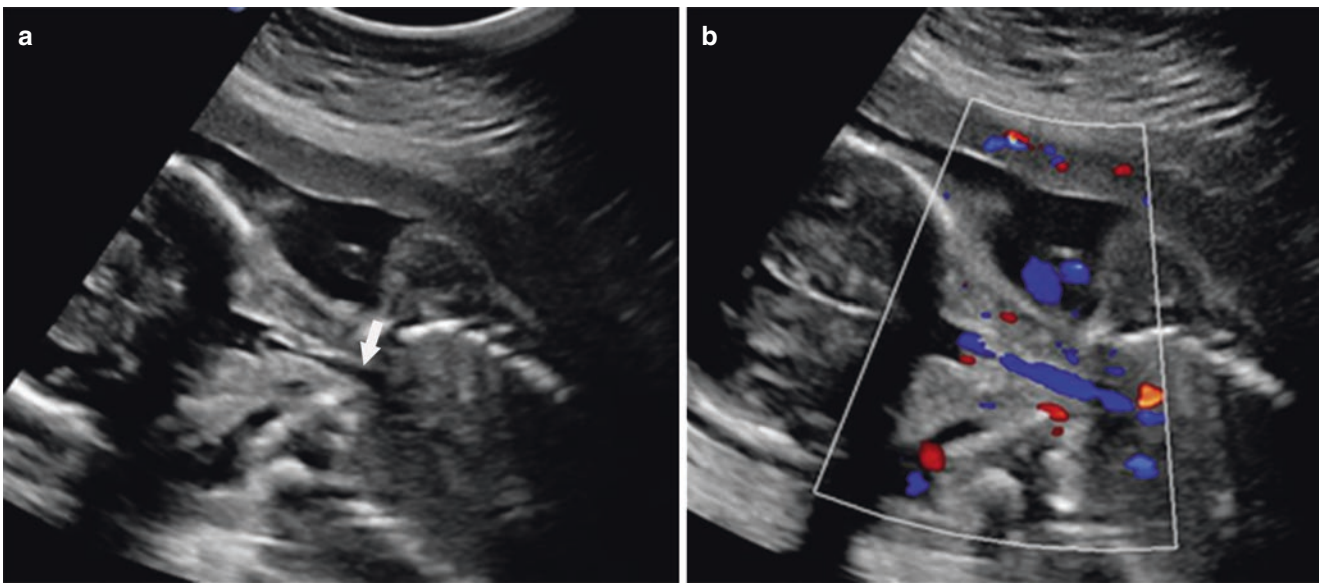

Fig. 2.7 (**a**) Gray scale and (**b**) Colour Doppler images of coronal scan of neck showing the fluid filled cylindrical trachea (arrow) filling with color due to fetal respiration (Video 2.4)

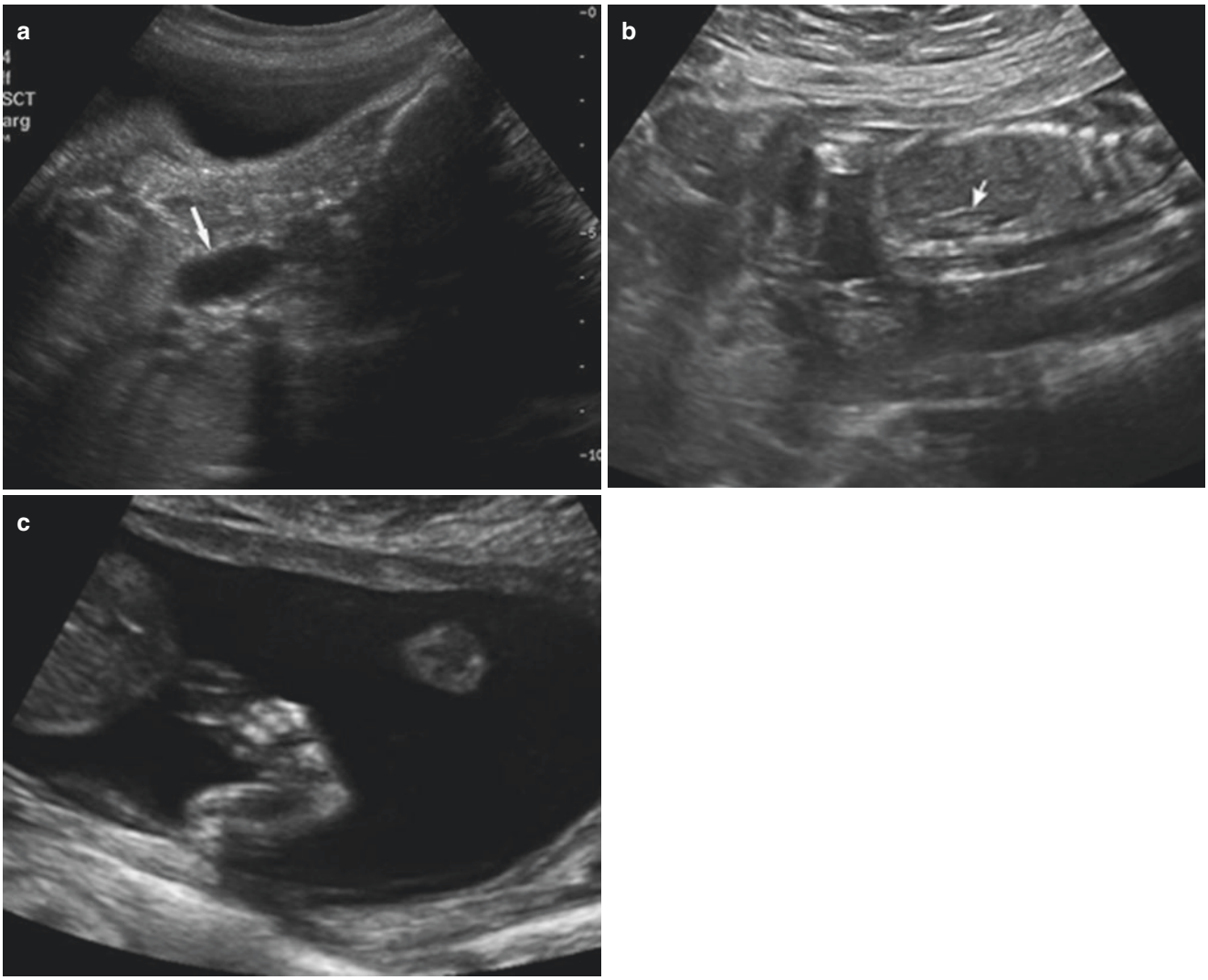

Fig. 2.8 Esophageal atresia in VACTERL association. (**a**) Pouch sign (arrow). (**b**) Unilateral renal agenesis with lying down adrenal sign (arrow). (**c**) One upper limb showing Radial Ray Aplasia

2.4 Gastric Pseudomass

Defined as an echogenic mass within the stomach (Figs. 2.9 and 2.10).

It is not a neoplasm. It has got variable sonographic appearance and may be mobile. The pseudomass is produced by aggregates of swallowed fetal cells denuded from the fetal skin. Usually it is a transient finding. There is increased incidence associated with bowel obstruction and ventral wall defects.

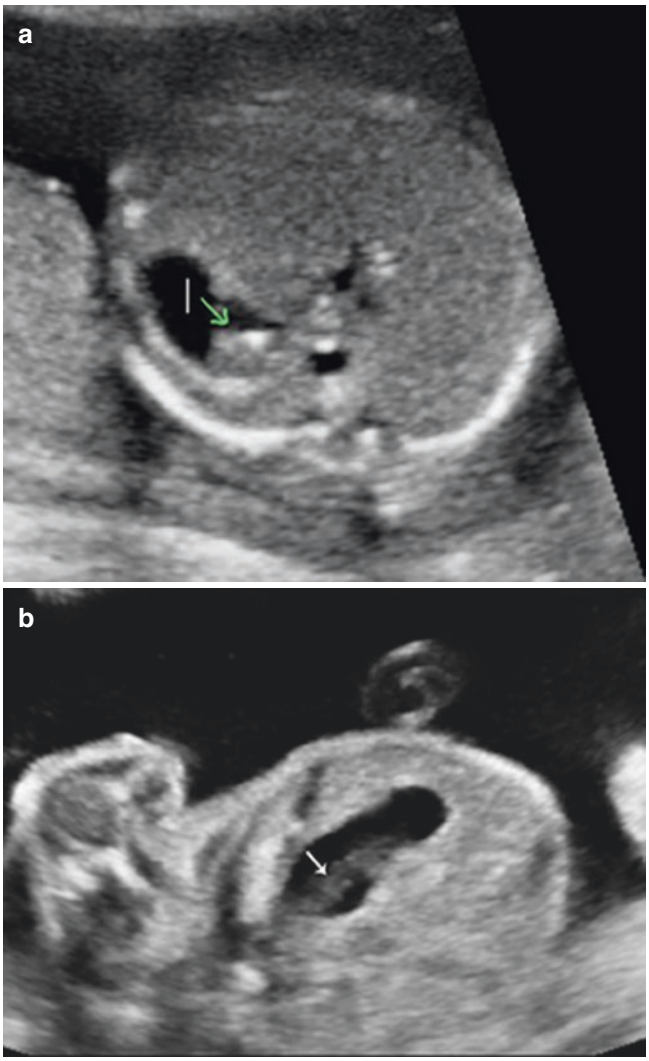

Fig. 2.9 (**a, b**) Gastric pseudomass (arrow) in two fetuses

2.5 Pyloric Atresia (PA)

Pyloric atresia is a very rare anomaly with an incidence of about 1 in 100,000 live births. It is seen in about 1% of all intestinal atresia. It can occur as an isolated anomaly or with associated anomalies—major association is with epidermolysis bullosa (PA–EB). Epidermolysis Bullosa is an autosomal recessive condition affecting the skin, manifesting as blisters, erosions and scars. Defect in ITGA6, ITGB4 and PLEC genes have been indicated. It has an incidence of 1 in 30,000 live births.

Sonographic features of pyloric atresia are polyhydramnios, grossly dilated stomach with hyperperistalsis and dilated esophagus due to regurgitation caused by the distal obstruction (Fig. 2.10). There will be no double bubble sign. In PA-EB syndrome, snow flake sign of echogenic debris in amniotic fluid may be seen in real-time scan (Fig. 2.10c, Video 2.5). There may be pseudomass in the stomach due to excess skin denudation. The sonographic signs are seen usually in late second trimester. Other associated anomalies may be seen, more commonly cardiac and urinary tract anomalies. PA-EB syndrome is a highly lethal condition. Early sonographic diagnosis is possible with family history. Early genetic diagnosis is possible.

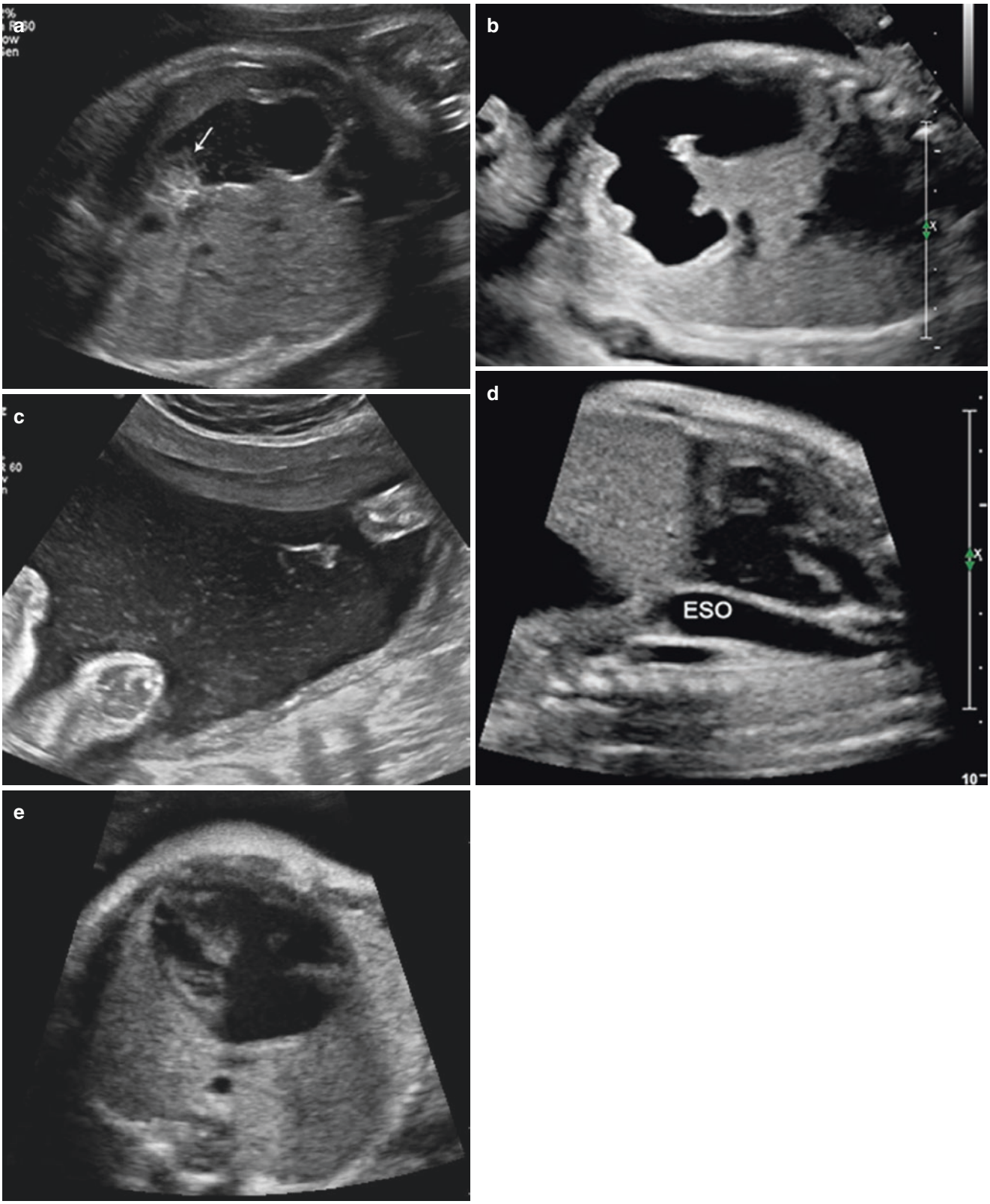

Fig. 2.10 Pyloric atresia (**a**) Axial and (**b**) Coronal scan showing the dilated stomach up to pylorus with pseudomass (arrow). (**c**) Snow flake sign in amniotic fluid (Video 2.5). (**d**) Sagittal scan of fetal chest showing fluid distended esophagus (ESO). (**e**) Four chamber view of heart showing AVSD

2.6 Duodenal Obstruction

Incidence of duodenal obstruction is 1 in 5000 pregnancies. It may be due to duodenal atresia (DA), malrotation of midgut or annular pancreas. Approximately 20–40% of all infants with duodenal atresia have Down syndrome and 8% of infants with Down syndrome have DA. DA occurs 1 in 5000–10,000 live births.

Sonographic sign of duodenal obstruction is double bubble sign in the axial section of fetal upper abdomen, with polyhydramnios (Fig. 2.11a).

The two bubbles are on either side of midline. The fluid distended stomach will cross the midline to the dilated duodenum. The continuity between the two bubbles through narrow pylorus should be demonstrated (Fig. 2.11b). Gastric hyperperistalsis will be seen (Fig. 2.11c, Video 2.6). If obstruction is partial, as it happens in fenestrated duodenal web, malrotation of midgut or annular pancreas, the manifestation may be delayed and dilatation of stomach and duodenum may be less marked. In case of malrotation of midgut, color Doppler study will show inversion of relationship of superior mesenteric artery and vein, with vein to left of artery (Fig. 2.12).

Prognosis of DA depends on associated anomalies. Down syndrome has to be ruled out. The risk of Down syndrome increases further if there is associated atrioventricular septal defect (AVSD).

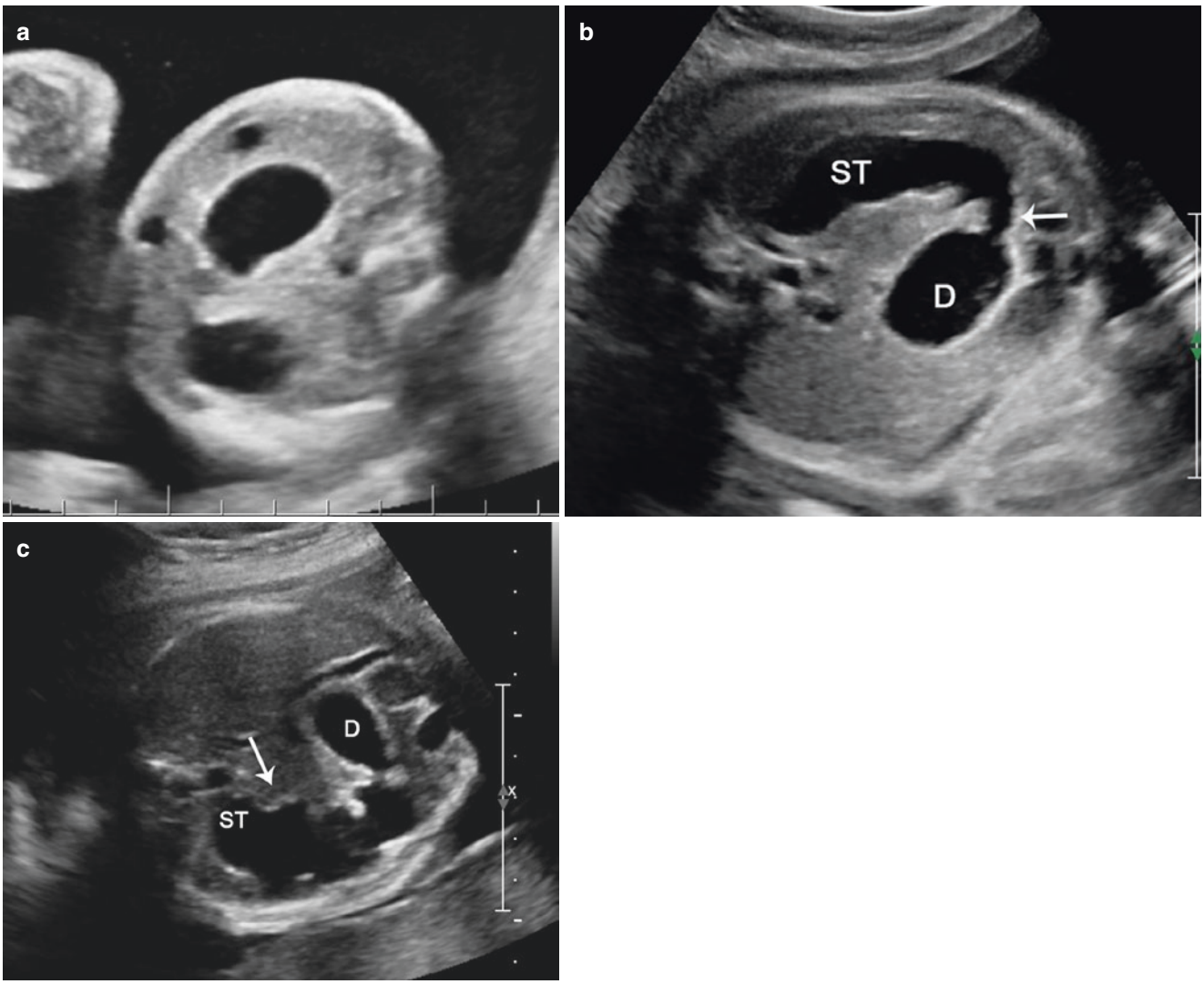

Fig. 2.11 Duodenal obstruction: Axial section of fetal upper abdomen showing the double bubble sign of dilated stomach and duodenum on either side of midline (**a**) continuity of the two bubbles through the narrow pylorus (arrow) (**b**) and hyperperistalsis of stomach seen as multiple constrictions (arrow) in (**c**) and also in Video 2.6

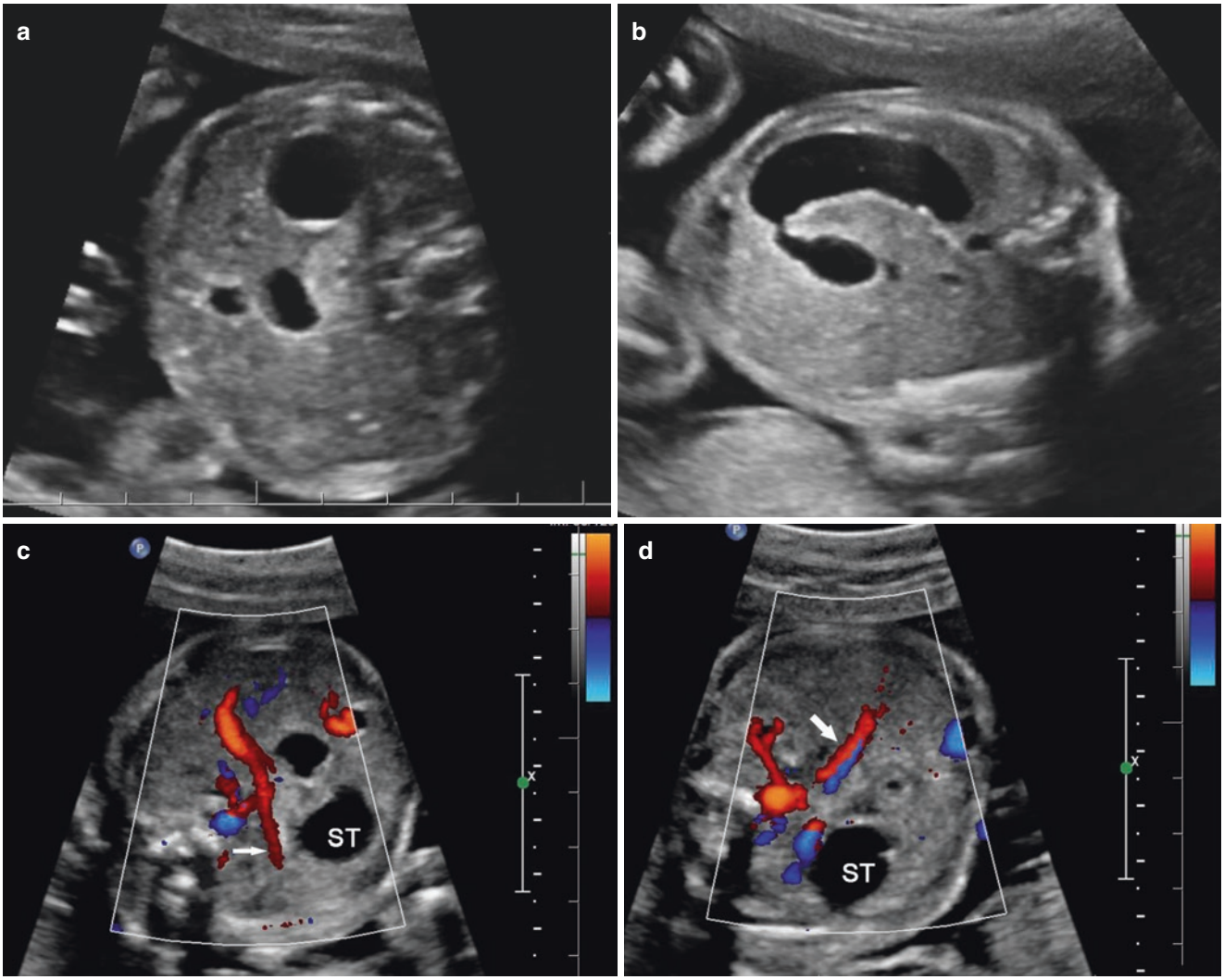

Fig. 2.12 Duodenal obstruction due to malrotation of midgut. Axial sections of a 30 weeks fetus showing the double bubble sign (**a**) and continuity of two bubbles (**b**). Colour Doppler image (**c**) through liver showing the splenic vein (arrow) extending from left side, posterior to stomach (ST), to right side as the portal vein with in the liver (**d**) through mid-abdomen showing the inversion of relationship of superior mesenteric artery (arrow) and vein with vein to the left of artery indicating malrotation

2.6.1 Differential Diagnosis

When stomach appears well distended it may mimic double bubble sign (pseudo double bubble sign) but the narrow pylorus will not be seen in coronal oblique scan. It will not cross the midline (Fig. 2.13).

A cystic mass in upper abdomen like liver/splenic cyst, choledochal cyst, adrenal cyst, dilated gall bladder, renal cyst etc. may be mistaken for a double bubble sign. Features of continuity and peristalsis will differentiate them.

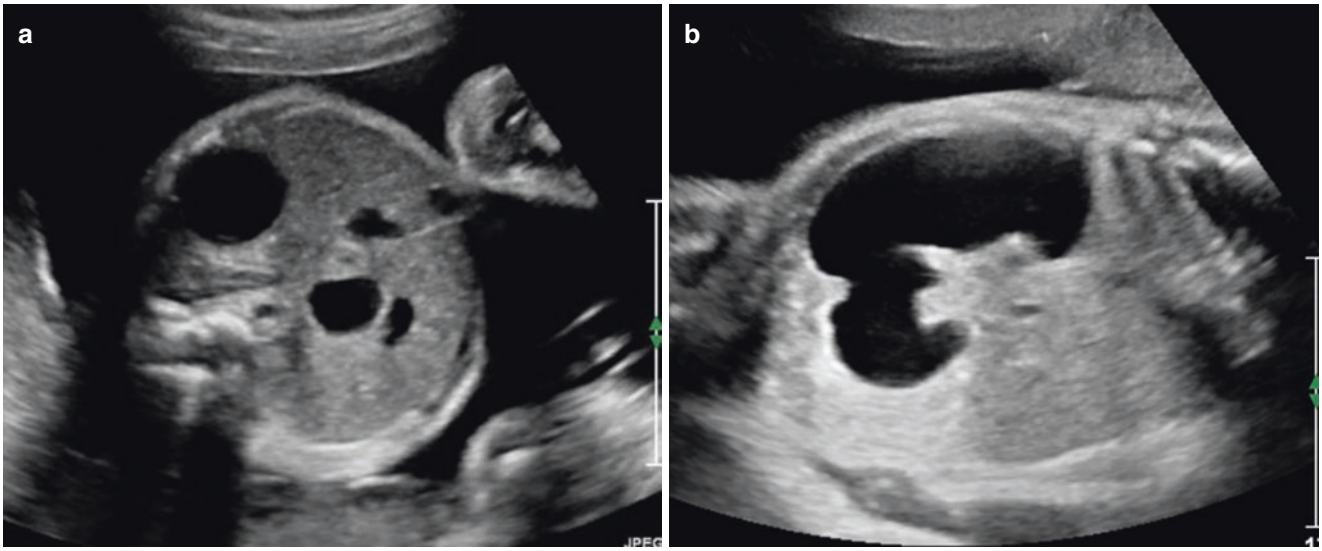

Fig. 2.13 Pseudodouble bubble sign: (**a**) Axial section showing double bubble and (**b**) coronal section showing only dilated stomach. Duodenal bubble is not seen

2.7 Duodenal and Esophageal Atresia

Very rarely there can be atresia of both the esophagus and duodenum resulting in closed loop obstruction of stomach. On sonography, the stomach is grossly dilated due to accumulated secretions. There is a large double bubble sign with dilated distal esophagus (Fig. 2.14).

The risk for Down syndrome is very high in double atresia.

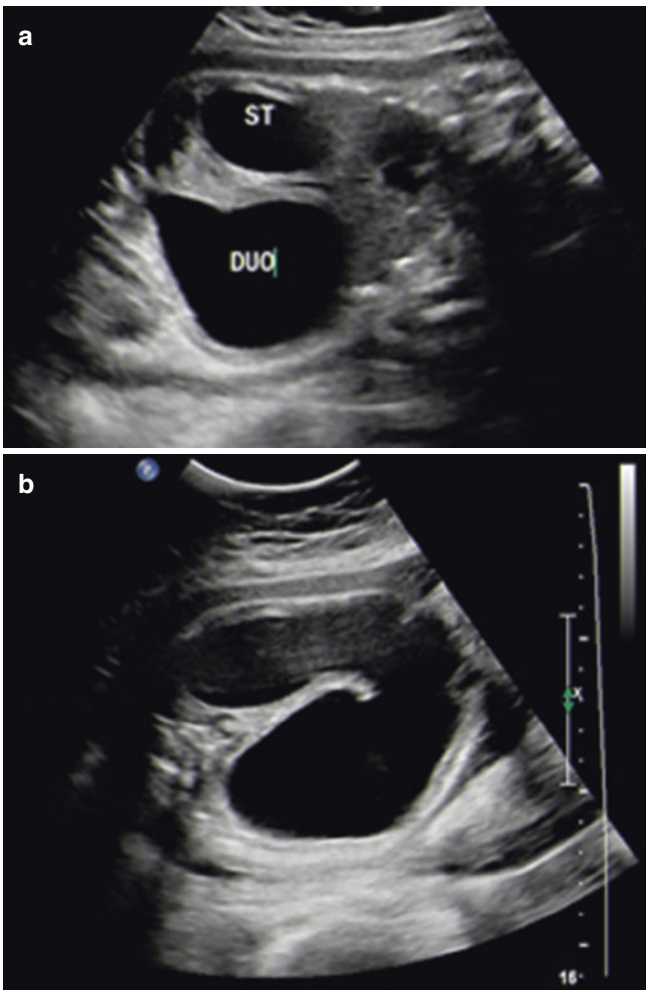

Fig. 2.14 Double atresia of oesophagus and duodenum: (**a**) Axial section showing the giant double bubble sign and (**b**) the continuity of the bubbles

2.8 Gastrointestinal Duplication Cysts

Gastrointestinal duplication cysts are rare congenital malformation of gastrointestinal tract (GIT). It can occur anywhere along the GIT, but is more common in ileum followed by esophagus, large bowel and stomach. It can be cystic (80%) or tubular (20%). Tubular type can vary in length and communicates with native lumen in one or more places. The wall of duplication cysts contains two layers, the mucosal layer and muscle layer referred to as bowel signature and shares blood supply of the adjacent bowel. In the bowel it is on the mesenteric side.

2.8.1 Gastric Duplication Cyst

Gastric Duplication cyst forms 7% of all gastrointestinal duplication cysts. Majority are non-communicating round cysts seen more commonly along the greater curvature of the stomach. It is attached to some part of the stomach and shares a common muscle and blood supply. In axial scan of fetal upper abdomen sonography shows a thick walled cyst close to the stomach bubble. It usually shows the two layers of the wall, the mucosal layer being echogenic (Fig. 2.15).

Postnatally most of them are asymptomatic. Since it can contain ectopic gastric glands, there can be ulcers that can penetrate and perforate as complications.

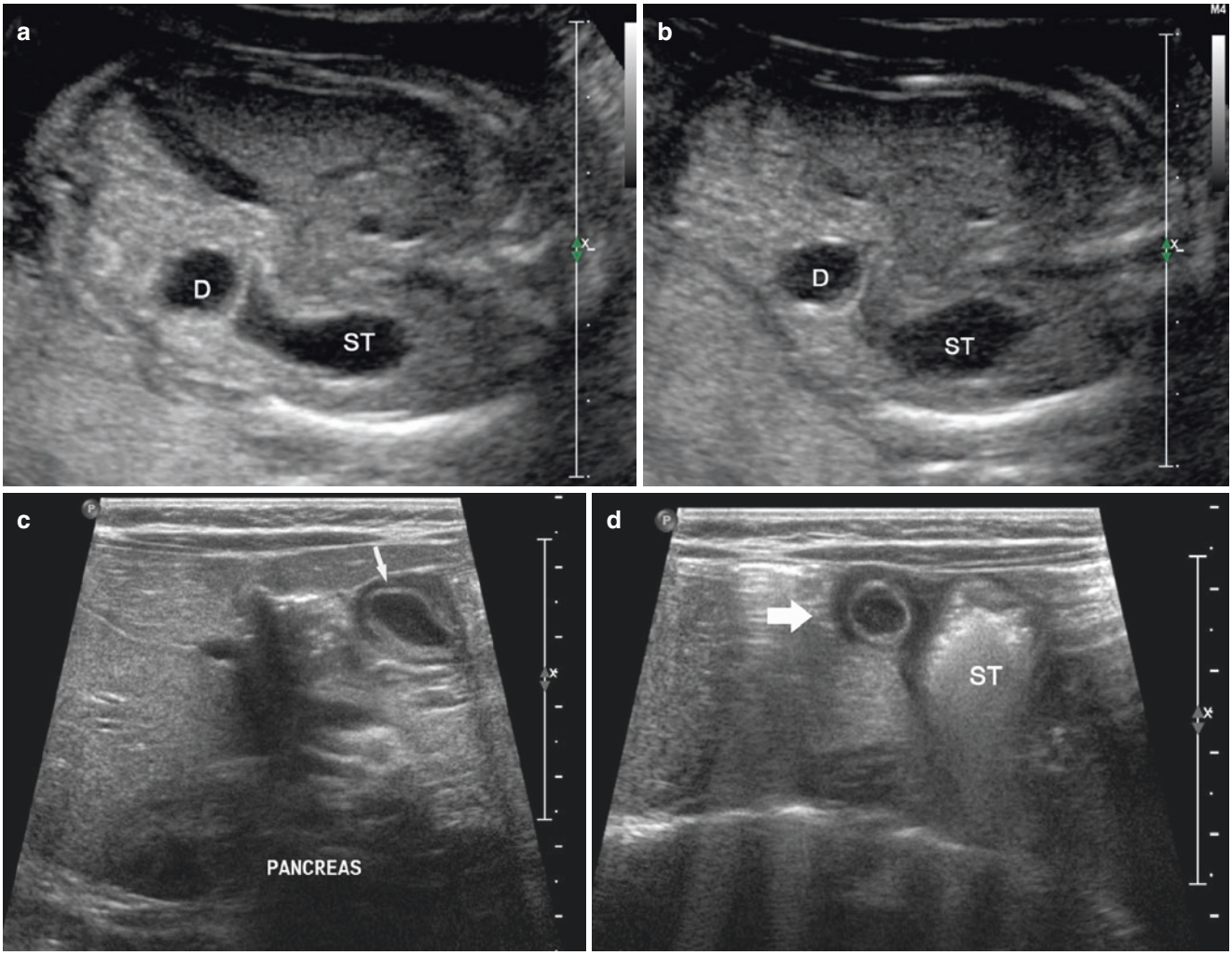

Fig. 2.15 Gastric duplication cyst: (**a**) Axial and (**b**) Coronal scan of fetal abdomen showing a cyst (D) indenting on the distal body of the stomach (ST) with two layer wall suggestive of duplication cyst of stomach (**c**) Axial and (**d**) oblique postnatal scans of the new born showing the typical bowel signature in the wall of the cyst (arrow) which is shared with the wall of body of stomach (ST) characteristic of gastric duplication

2.8.2 Small Bowel Duplication Cysts

Small bowel duplications cysts are the most common type of gastrointestinal tract duplication. They can be cystic or tubular. They have the echogenic mucosal lining and share muscle and blood supply with native small bowel. It is seen on the mesenteric side. They may cause intussusception or volvulus in the fetus.

On Sonography, the common presentation is an intraabdominal cystic mass. The signs of origin from known abdominal organs, like kidney, are absent. The characteristic feature is the two layer sign or the bowel signature in the wall. There is inner echogenic layer of mucosa and the outer echopoor muscle (Figs. 2.16 and 2.17).

It usually shows peristalsis which is diagnostic (Video 2.7). This differentiates the duplication cyst from mesenteric cyst and ovarian cyst which do not show peristalsis. It may be seen in changing location within the abdomen at different periods of scan since it is in the mobile mesentery. The tubular type is seen as a segmental dilated bowel loop with peristalsis (Fig. 2.18, Video 2.8).

The wall will show the bowel signature. This type has to be differentiated from a dilated loop of bowel in evolving small bowel obstruction, by repeating a scan after a few days. The tubular duplication will retain the same appearance, whereas small bowel obstruction will show extended dilated loops.

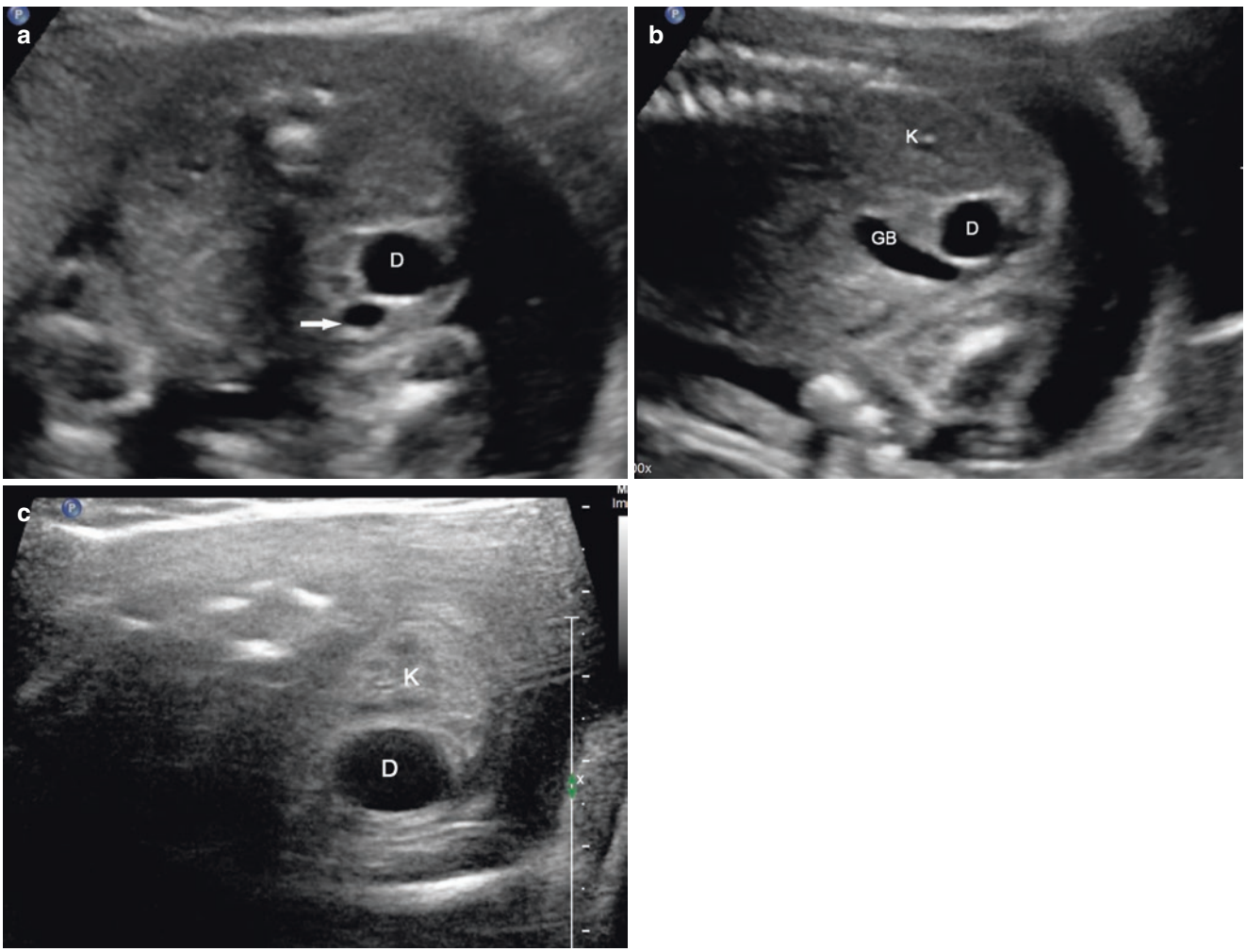

Fig. 2.16 Duodenal Duplication: (**a**) Axial and (**b**) Longitudinal Scan of fetal upper abdomen showing a cyst between gall bladder (arrow) and the right kidney. (**c**). High frequency scan reveals the bowel signature in the wall confirming duplication cyst of duodenum because of location

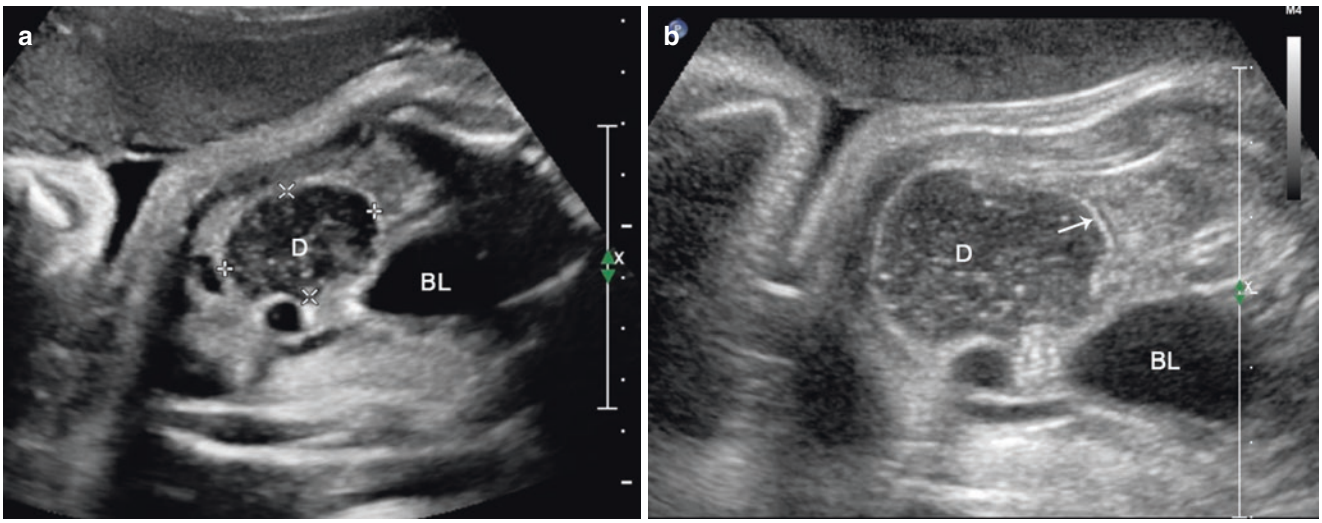

Fig. 2.17 Cystic duplication of small bowel: (**a**) Oblique scan of fetal lower abdomen shows a thick-walled spherical cyst (D) anterior and cephalic to urinary bladder (BL). (**b**) High frequency scan of the cyst shows the bowel signature in the wall (arrow) and Video 2.7 shows peristalsis in the cyst (D), confirming a duplication cyst of small bowel

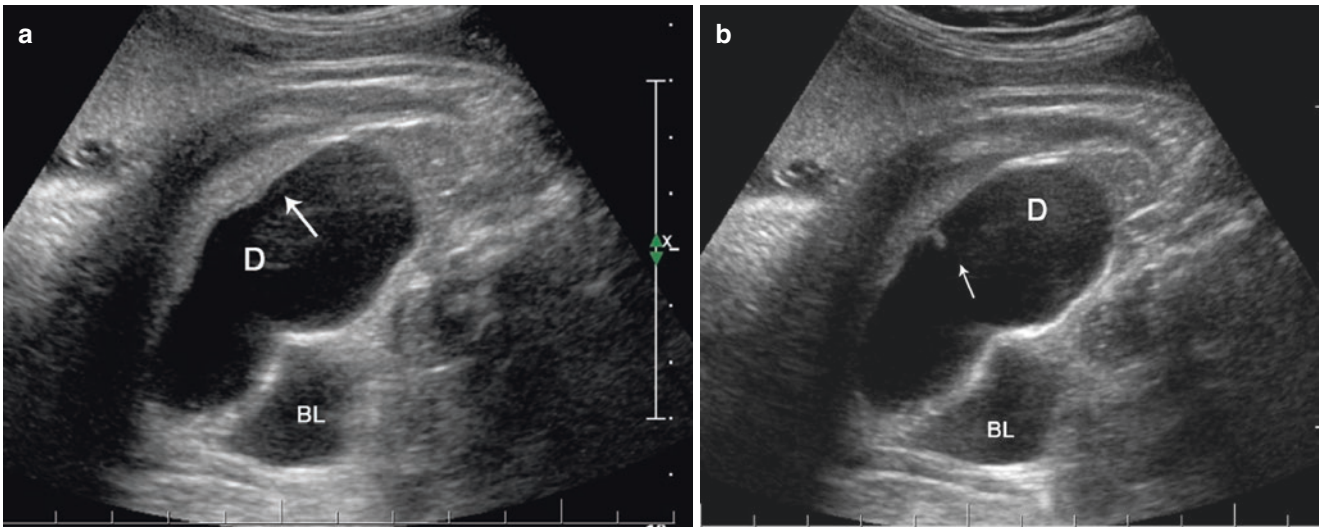

Fig. 2.18 Tubular duplication of the small bowel: (**a**) Axial scan of the fetal lower abdomen shows a focally dilated loop of small bowel (D) with bowel signature in the wall anterolateral to urinary bladder (BL). It reveals constriction (arrow) of peristalsis in (**b**) and peristalsis in Video 2.8

2.9 Small Bowel

Fetal small bowel loops are seen in the axial section of central abdomen. They are slightly echogenic and fill the central abdomen (Fig. 2.19).

With the high resolution of recent machines, small bowel is seen well. The individual serpiginous loops can be made out on high frequency scans (Fig. 2.19c). Occasionally fluid filled individual segments can be seen in the normal fetus, not exceeding 7 mm in diameter and 15 mm in length (Fig. 2.19d). Active peristalsis of normal small bowel can be observed in later gestation.

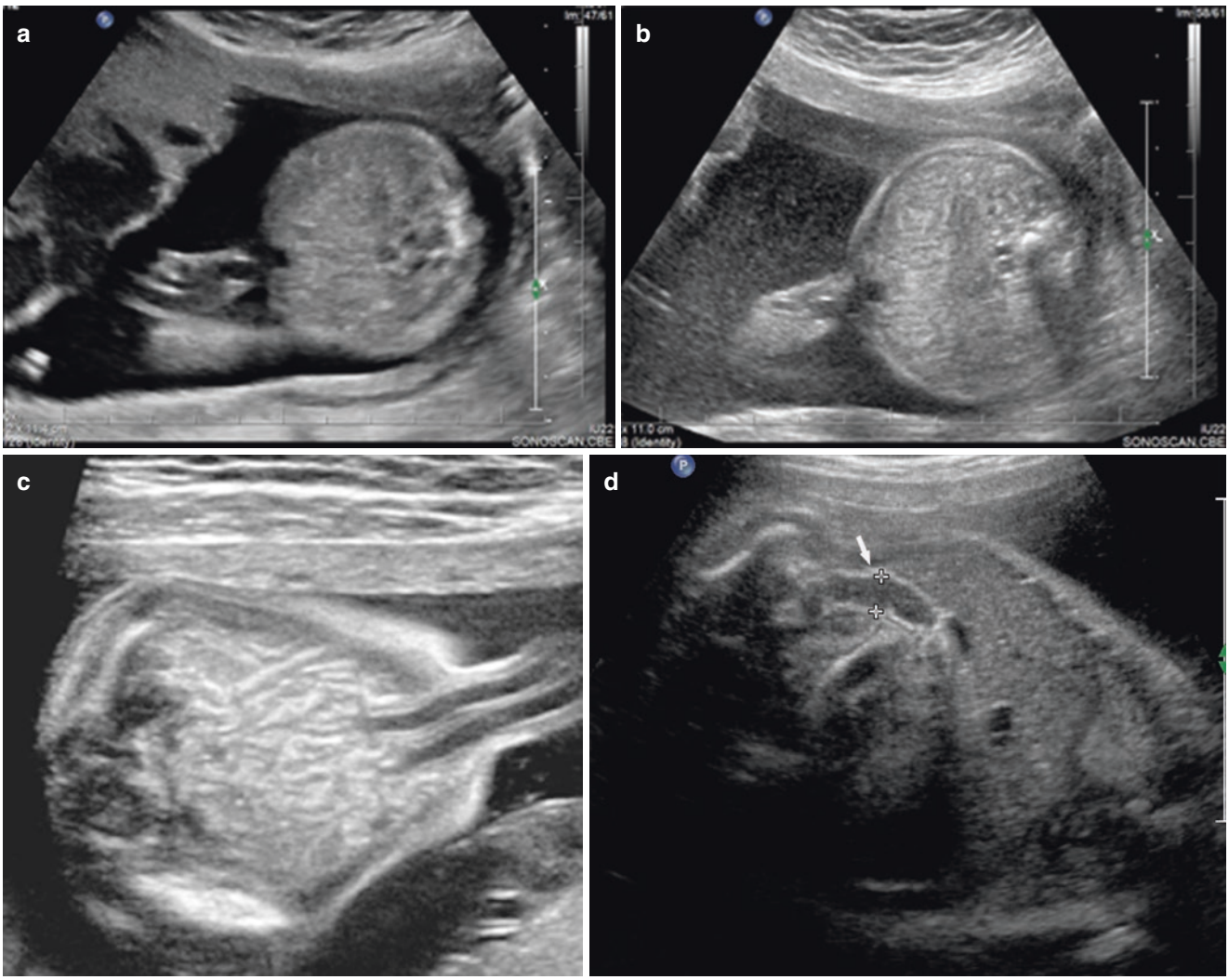

Fig. 2.19 Normal fetal small bowel with different transducer frequency. (**a**) Conventional 3.5 MHz probe showing echogenic bowel filling the mid abdomen. (**b**) With 5 MHz probe: small bowel loops are seen as echogenic curved lines. (**c**) High frequency 5–12 MHz probe shows the serpiginous echogenic small bowel loops. (**d**) Normal fetus showing a fluid distended small bowel of less than 7 mm in diameter (arrow)

2.9.1 Small Bowel Atresia

Bowel atresia is mostly due to a vascular insult to a segment of bowel. It results in obstruction with proximal dilatation. Incidence is 1 in 3000–8000 live births.

Sonographic features of small bowel obstruction are dilated interconnecting bowel loops with peristalsis or hyperperistalsis (Fig. 2.20) (Video 2.9).

Polyhydramnios is usually present. Small bowel obstruction usually manifests in late second or third trimester. Dilated stomach can be seen in jejunal atresia. In jejunal atresia there are only a few dilated loops in upper abdomen (Fig. 2.21).

In ileal atresia the whole abdomen is filled with dilated loops, dilatation increasing towards lower abdomen (Fig. 2.22).

Small bowel atresia may be secondary to mesenteric volvulus in malrotation of midgut. Here the inversion of superior mesenteric artery and vein can be seen on color Doppler study. In volvulus the real time "Whirl Pool" sign can be seen on gray scale and color Doppler study (Fig. 2.23) (Videos 2.10 and 2.11).

Small bowel obstruction has to be differentiated from congenital chloride diarrhea and mesenteric lymphangioma which are described subsequently. Grossly dilated ureter can mimic small bowel obstruction but can be differentiated by tracing the same to dilated calyces in the kidney (Fig. 2.24).

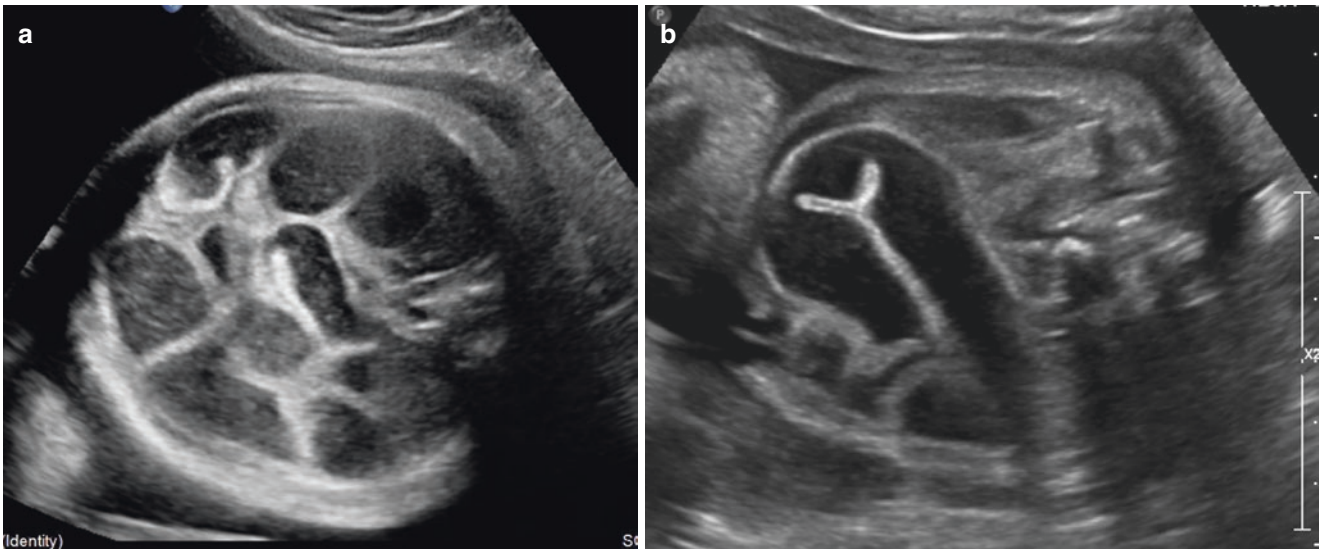

Fig. 2.20 Small bowel obstruction. (**a**) Axial scan of mid abdomen shows multiple dilated small bowel loops with hyperperistalsis seen in Video 2.9. (**b**) Oblique scan shows the intercommunicating dilated small bowel loops

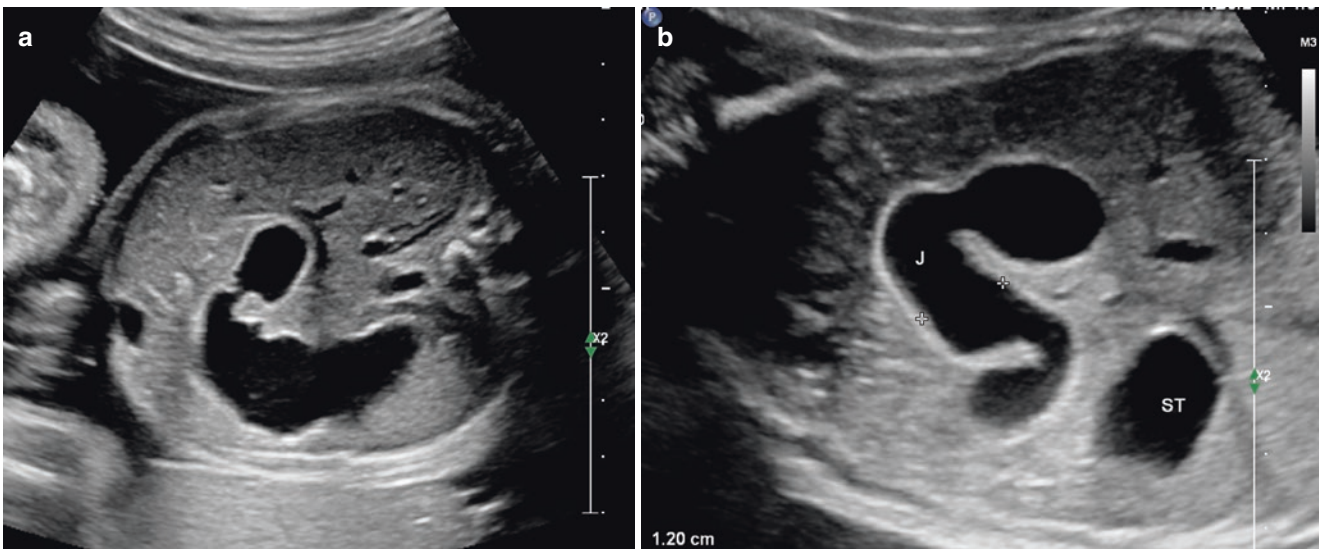

Fig. 2.21 Jejunal atresia: (**a**) Axial scan of upper abdomen shows dilated stomach and duodenum. (**b**) Coronal scan shows a few dilated jejunal loops (J)

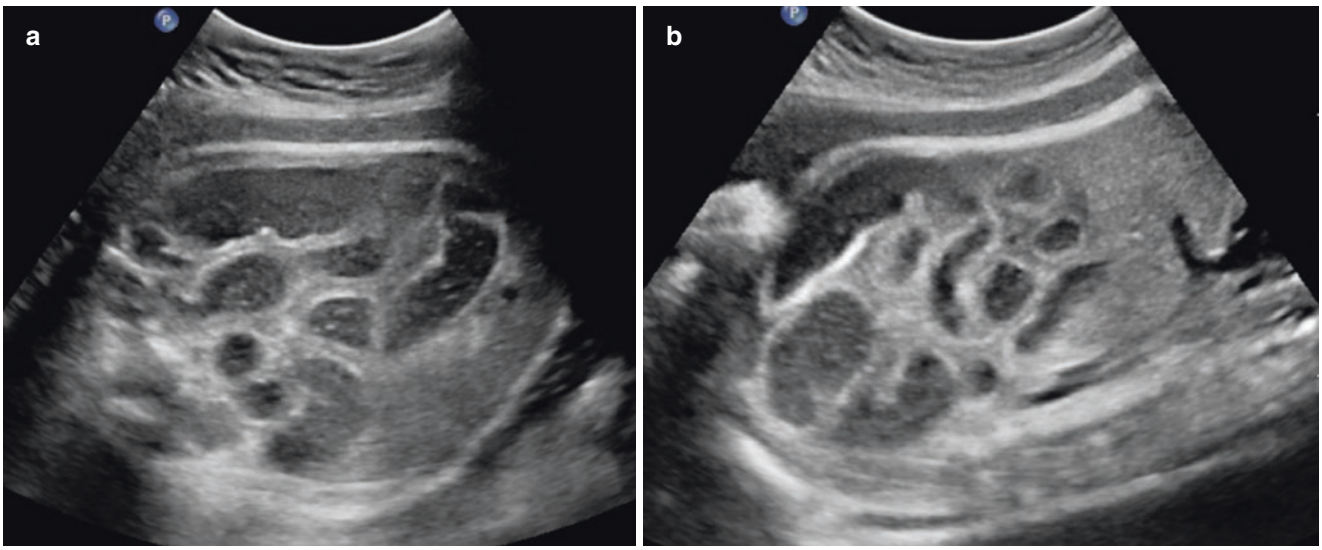

Fig. 2.22 Ileal atresia: (**a**) Axial scan shows multiple dilated small bowel loops filling the abdomen. (**b**) Longitudinal scan shows increasing dilatation towards lower abdomen indicating ileal atresia

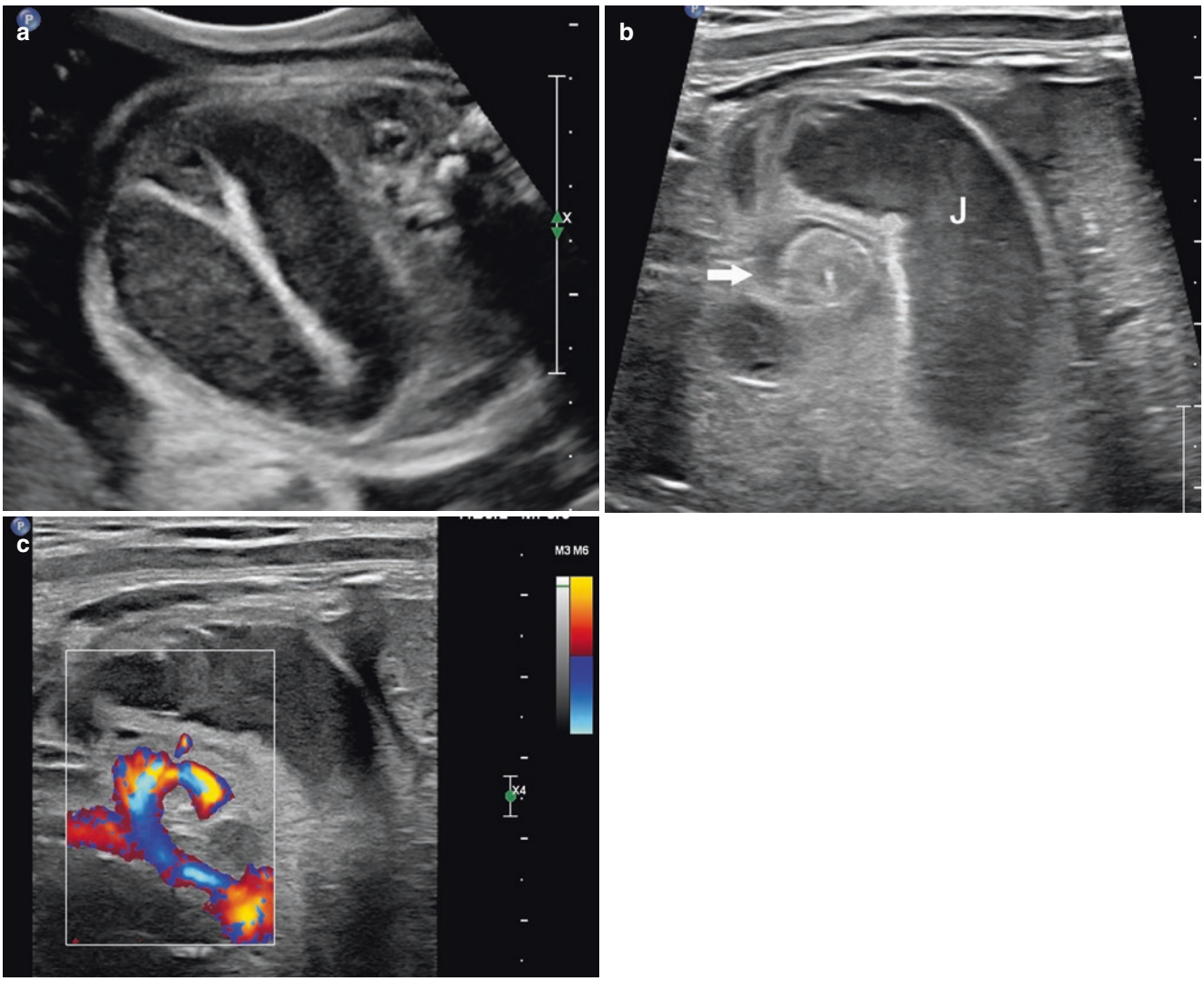

Fig. 2.23 Small bowel atresia due to malrotation of midgut with volvulus: (**a**) Axial scan showing the dilated small bowel loops with a coffee bean appearance. (**b**) High frequency oblique scan just below the dilated loop shows the mass of "Whirl Pool" in gray scale (arrow) and (**c**) Colour Doppler. Videos 2.10 and 2.11 show the "Whirl Pool" sign when the probe is moved down confirming the volvulus on gray scale and color Doppler study

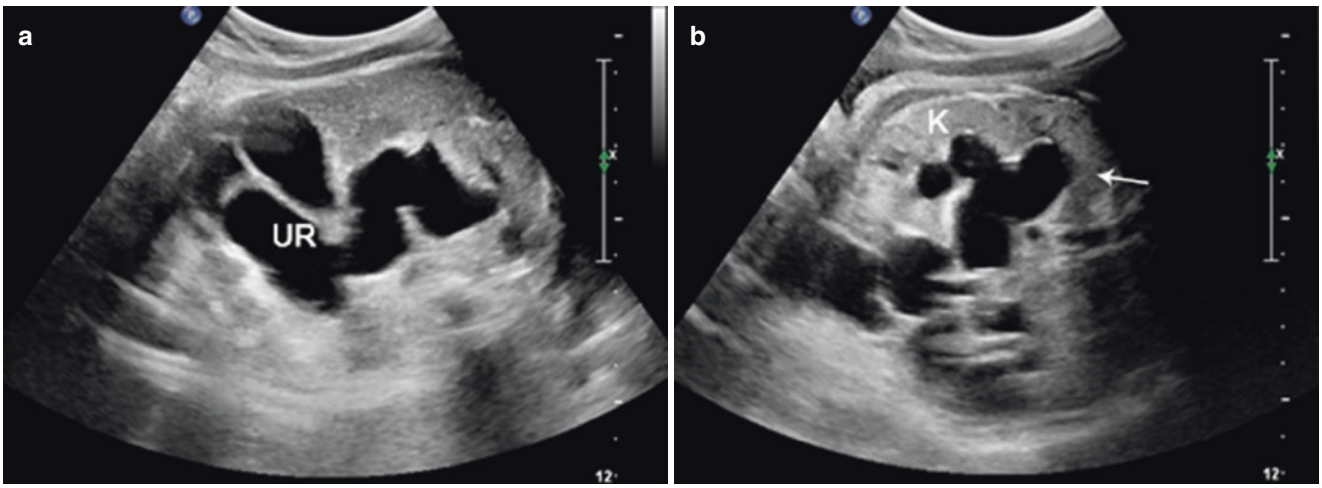

Fig. 2.24 (**a**) Oblique axial scan of fetal abdomen shows grossly dilated ureter (UR) mimicking dilated small bowel but on tracing it is connected to the dilated renal pelvis and calyces (arrow) in the kidney (K) confirming that it is grossly dilated ureter in (**b**)

2.10 Congenital Chloride Diarrhea (CCD)

Congenital Chloride Diarrhea is a very rare disorder, reported mainly in Finland. It is an autosomal recessive disorder. The underlying defect is in chloride resorption by intestine associated with impaired transport of bicarbonate. This results in hygroscopic retention of fluid in the intestine leading to watery diarrhea and polyhydramnios.

Sonography reveals distension of fetal abdomen with uniformly dilated small and large bowel filling the abdomen with hyperperistalsis (Fig. 2.25, Video 2.12).

There is polyhydramnios due to fetal diarrhea. Differential diagnosis is ileal atresia and anal atresia. There is uniform dilatation of bowels in CCD while the dilatation increases distally in ileal atresia. The fluid distended rectum can be seen in CCD while it is not seen in ileal atresia and occasionally the fetal diarrhea can also be seen as fluid gushing out from fetal anus (Video 2.13). Normal fetal anus will be seen, differentiating it from anal atresia.

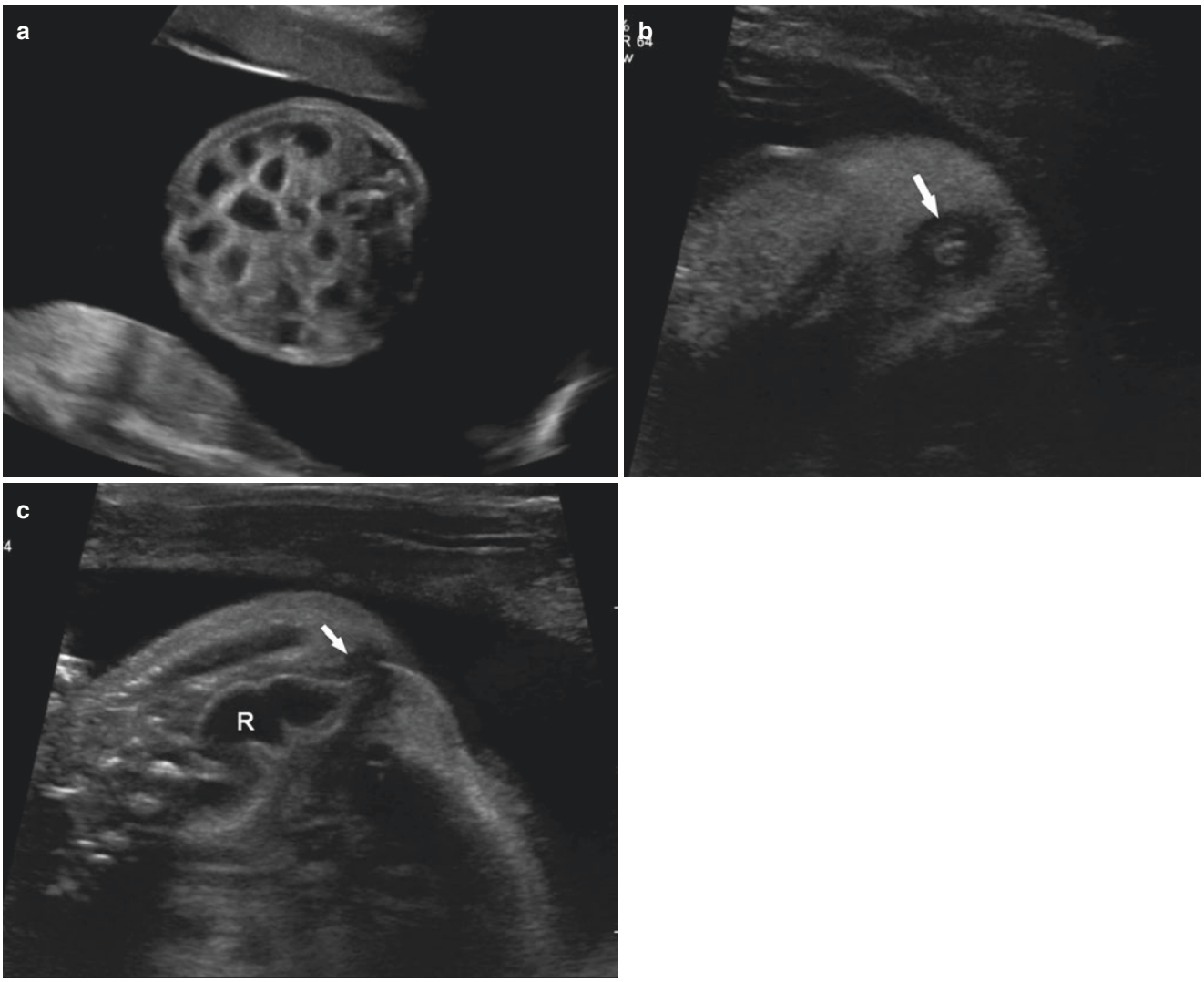

Fig. 2.25 Congenital Chloride Diarrhea: (**a**) Axial scan of the fetal abdomen shows distension of abdomen with uniformly dilated bowel loops with polyhydramnios. They show intense peristalsis as shown in Video 2.12. (**b**) Tangential scan of perineum shows the fetal anus ruling out anal atresia. (**c**) Sagittal scan of fetal pelvis and perineum showing the fluid distended rectum (R) that differentiates it from ileal atresia and the anal canal (arrow) reaching up to the skin of perineum. Video 2.13 shows the fetal diarrhea as gush of fluid from the anus

2.11 Echogenic Bowel (EB)

On fetal sonography echogenic bowel is diagnosed when bowel appears echogenic in different scan planes, across various transducer frequencies without harmonics and remains echogenic equal to bone when the gain is decreased to see only bones (Fig. 2.26, Videos 2.14 and 2.15).

It is detectable at the time of second trimester routine antenatal ultrasound in 0.2–1.8% of all fetuses. Echogenic bowel can be a normal variant or may be due to normal echogenic meconium near term (Fig. 2.28).

Abnormal situations of echogenic bowel are swallowed blood, a marker for Trisomy 21, feature of cystic fibrosis, CMV infection and fetal growth restriction. In fetuses with EB, the sonographic survey must be complete to exclude associated sonographic soft markers for trisomy 21, bowel dilation, fetal ascites, and peritoneal calcification or extra-intestinal anomalies that may correlate with an increased risk of adverse neonatal outcome.

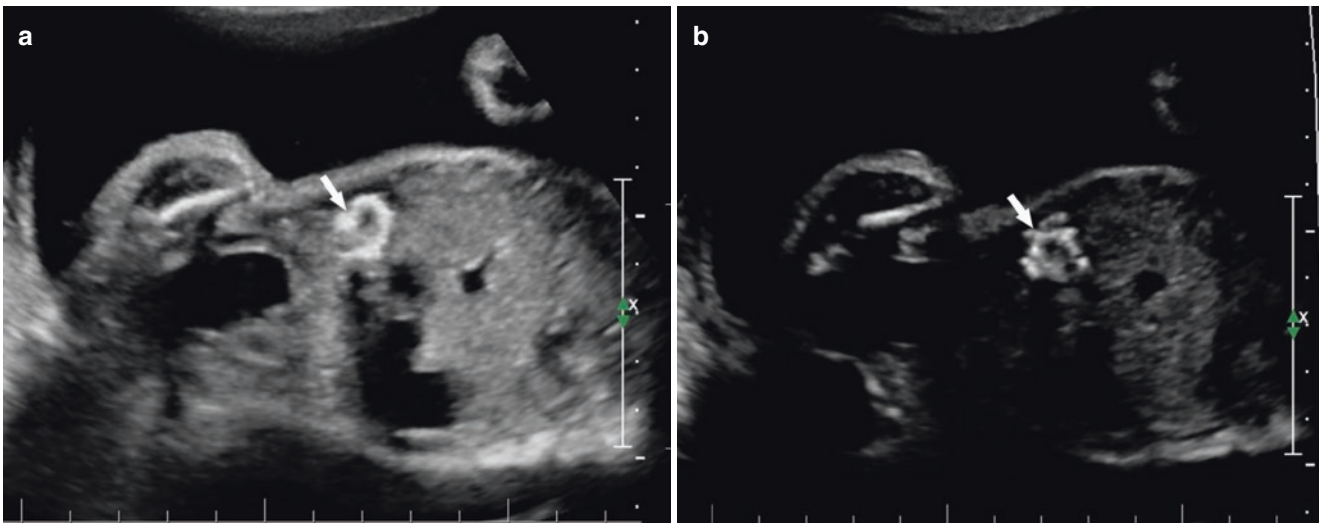

Fig. 2.26 Coronal scan of fetal abdomen showing echogenic bowel (arrow) (**a**) which remains echogenic equal to bone with decrease in the gain (**b**) (Videos 2.14 and 2.15)

2.12 Fetal Large Bowel

Fetal colon becomes visible on sonography in late II trimester and is well seen close to term. It is seen as a hypoechoic tubular structure with haustrations in periphery of fetal abdomen in the usual location of colon. There are redundancies and turns (Fig. 2.27). Occasionally colon may be filled with echogenic meconium near term in normal fetuses (Figs. 2.28, 2.33b, and 2.39a). The diameter of colon shows a large range—up to 18 mm near term. Dilated colon with echogenic meconium balls is a feature of anal atresia (Fig. 2.33b).

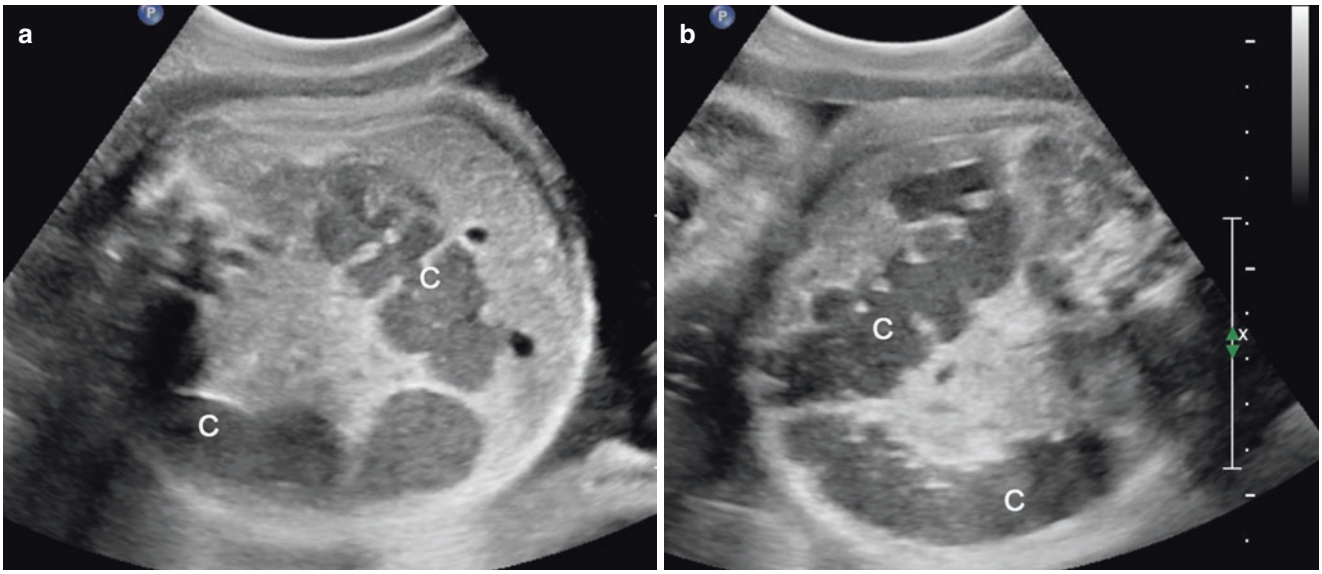

Fig. 2.27 (**a**, **b**) Axial scan of fetal abdomen in third trimester showing the normal fluid distended colon (arrow) along the periphery of abdomen with haustrations and redundancies

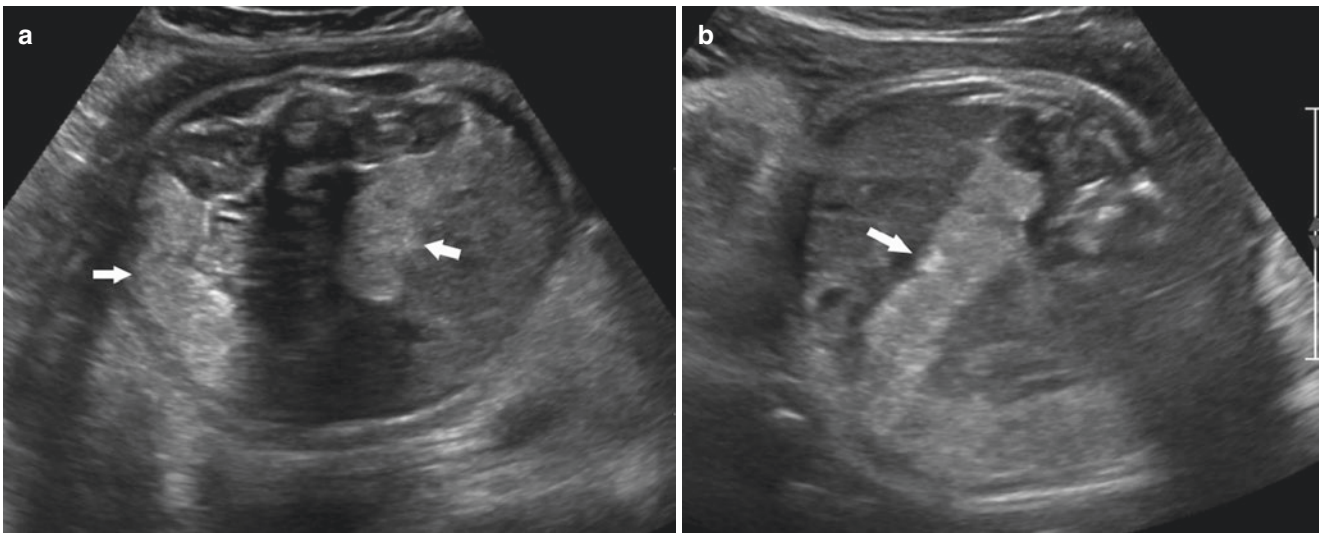

Fig. 2.28 (**a**, **b**) Axial scan of abdomen of 35 weeks fetus shows normal colon filled with echogenic meconium (arrow)

2.13 Anorectal Malformation (ARM)

Anorectal malformation is a group of anomalies with absent anal opening. It is a spectrum of anomalies from minor types to very complex anomaly. It may be a low anorectal malformation in the form of covered anus where the anus is covered by skin only. In high anorectal malformation the rectum is high above the perineum, most of the times complicated by a fistula with bladder, urethra or vagina. The anomaly may be more complex in the form of urorectal septal malformation (URSM) sequence. It may also form part of complex associated anomalies like VACTERL association, caudal dysplasia, Trisomy 18 and 21, OEIS complex or bladder exstrophy complex. Anorectal malformation is seen in about 1 in 5000 live births.

2.13.1 Sonographic Features

Initially diagnosis of ARM was suspected when fetus showed a dilated colon with or without echogenic meconium balls in it (Figs. 2.33b and 2.38a). The sensitivity of the sonography in diagnosis of anorectal malformation was very poor ranging from 0% to 33%. The reasons were (1) the wide range of size of normal large bowel. (2) Difficulty to differentiate the small bowel from large bowel in earlier gestation and (3) the colon is not dilated in many cases of ARM. Hence the diagnosis of anorectal malformation is improved to a great extent by direct visualization of the fetal anus.

2.13.2 Technique of Seeing the Fetal Anus

From the axial scan of pelvis showing the urinary bladder the scan is continued down up to the perineum. The tangential axial scan of perineum is obtained by tilting and rotating the transducer to see the two gluteal regions with the anus in between (Fig. 2.29, Videos 2.16 and 2.17). The anus is seen as an echopoor circle due to the anal muscle complex with an echogenic dot in the center due to the lumen. In this section the ischium should not be seen to confirm that the section is at the correct plane of section of perineum. If the anus is not seen by this technique then diagnosis of anorectal malformation is made (Fig. 2.30, Video 2.18). High frequency probe can be used in doubtful cases to obtain sagittal and coronal scans of fetal pelvis and perineum to see the rectum and anal canal reaching up to the perineal skin (Fig. 2.29d, e). Then scan is extended to look for other associated anomalies. When an anomaly like a spinal defect is seen the fetal anus is looked for to diagnose a complex anomaly like VACTERL association.

2.13.3 Nonvisualized Fetal Anus

The fetal anus is not visualized in anorectal malformation (ARM). The ARM can be isolated or form part of complex associations of which the commonest is URSM sequence.

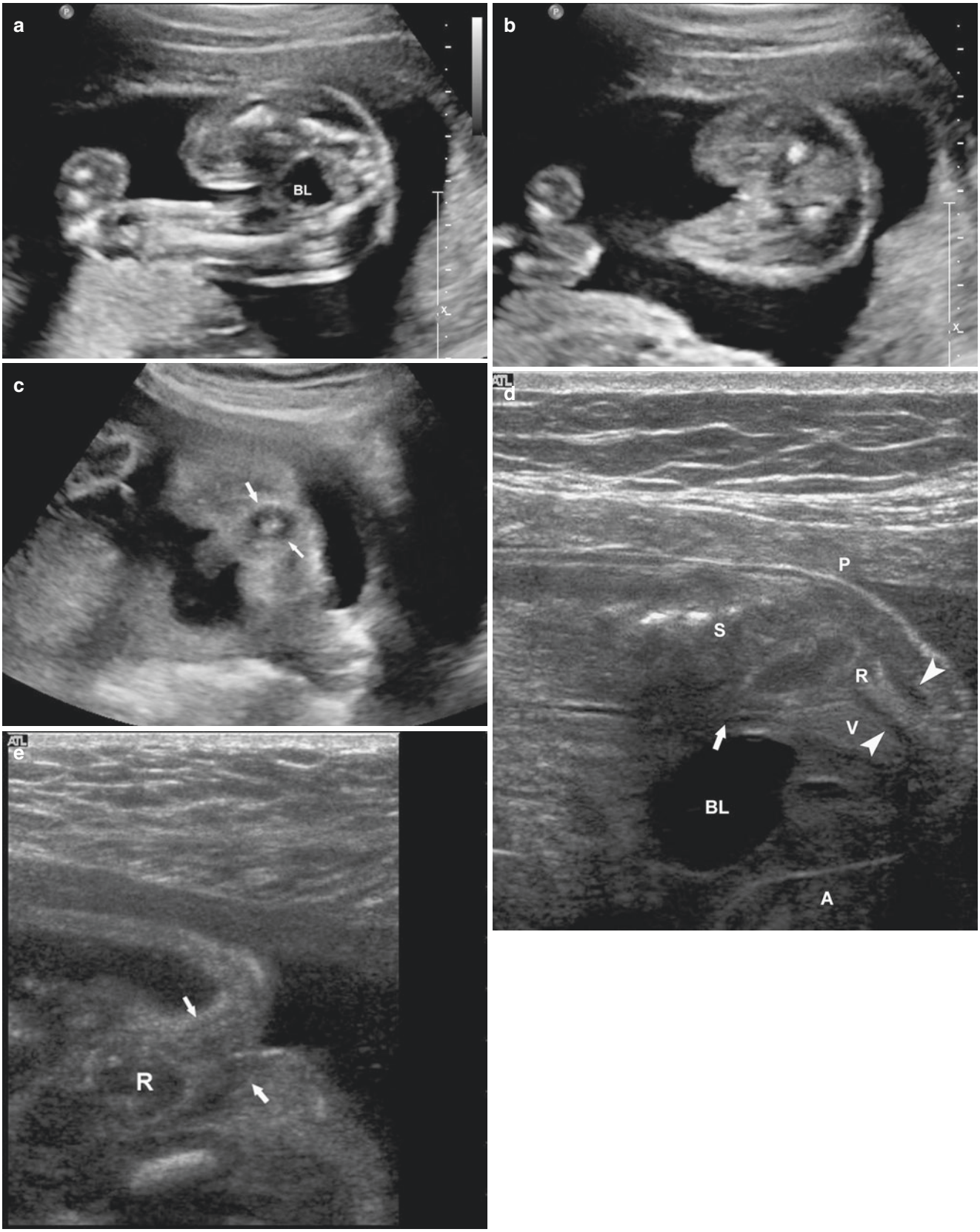

Fig. 2.29 Technique of seeing fetal anus: Transducer is moved down from (**a**) axial section of pelvis through the urinary bladder (BL) and sacral spine to (**b**) the lower pelvis at the level of ischium and then (**c**) the tangential section of the perineum showing the anus (arrows) (Videos 2.15 and 2.16). (**d**) Sagittal High Resolutions scan showing the fetal anus as an echo poor tubular structure with central echogenic stripe (arrow heads). *A* anterior, *BL* urinary bladder, *P* posterior, *R* rectum, *S* sacrum, *V* vagina, *arrow* uterus. (**e**) Coronal High Resolutions scan showing the fetal anus (arrows) and rectum (R)

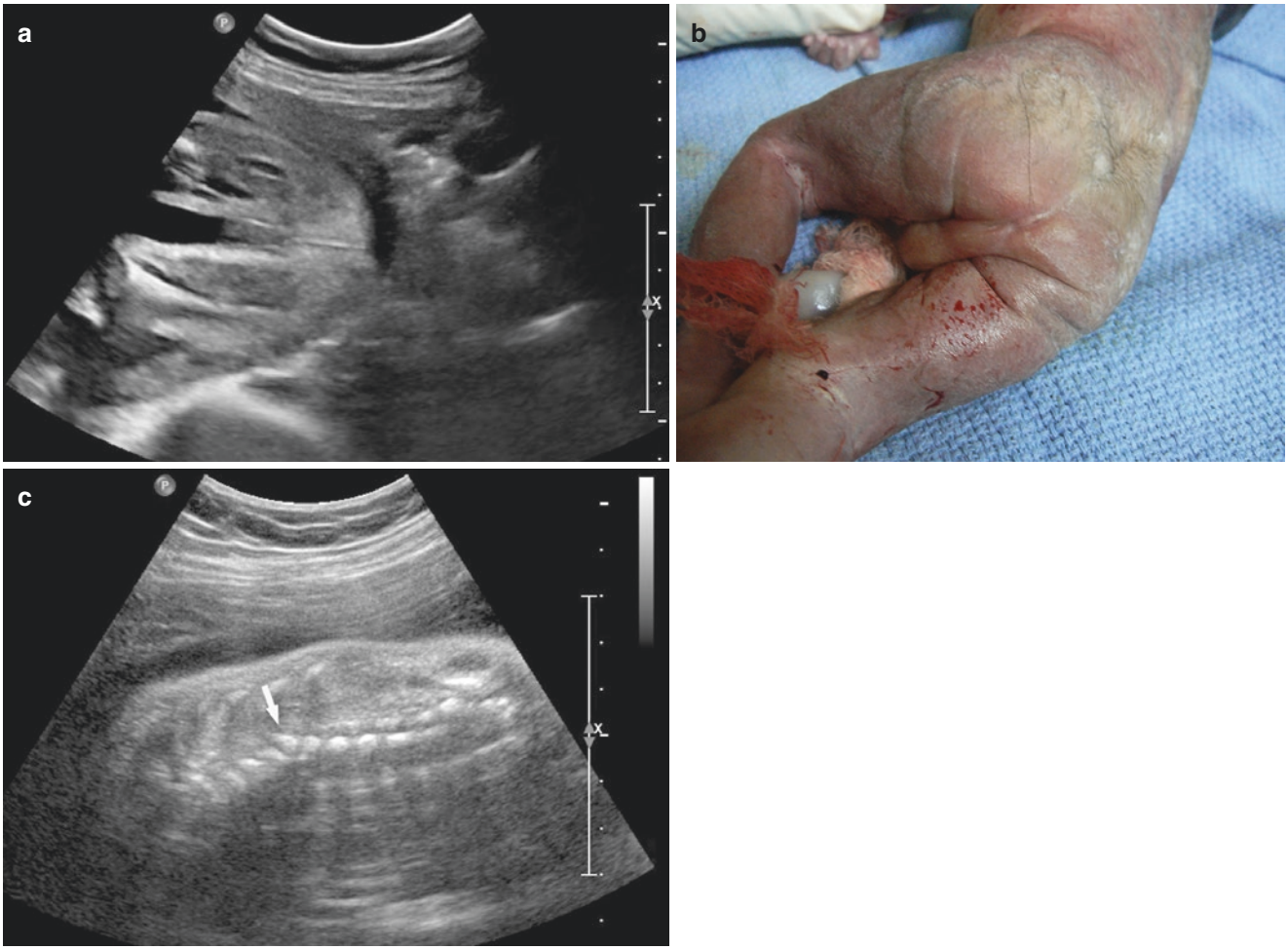

Fig. 2.30 Failure to see the fetal anus in a fetus with VACTERL anomaly. (**a**) Tangential scan of the perineum shows the midline echogenic stripe of the perineum with non-visualized anus (Video 2.17). (**b**) Photograph of the perineum of the abortus shows the anal atresia. (**c**) Coronal scan of the fetal spine showing the hemi vertebra (arrow)

2.14 Urorectal Septal Malformation (URSM) Sequence or Cloacal Malformation

The lower portion of gastrointestinal and the genito-urinary tracts develop from the caudal mesoderm—the primitive cloaca. During 5–7 weeks of gestation the urorectal septum develops and descends down dividing the cloaca into the anterior urogenital sinus and posterior hindgut and fuses with the cloacal membrane. The urorectal septum then breaks down and leaves an open urogenital sinus and rectum. The urogenital sinus differentiates into the urinary and genital tracts. Arrest of this developmental process would lead to URSM, though a precise etiology has not been established. No familial inheritance has been reported. Recent evidence suggests the involvement of homeobox and sonic hedgehog signaling pathways in the pathogenesis of URSM. Genetic cause has not yet been established. The incidence of URSM is reported to be 1 in 50,000–250,000 among live born with a female preponderance.

The following signs would suggest a URSM:

(a) Non-visualization of the anus on a tangential scan of the fetal perineum (Fig. 2.29).
(b) Cystic mass with a fluid-debris level that funnels to the pelvis in a female fetus representing the fluid distended common urogenital sinus is one of the most consistent observations (Fig. 2.31). The fluid-debris level is due to the urine admixed with meconium distending the urogenital sinus of the fetus. Mullerian duplication is noted in 60% of cases with URSM. The incidence increases to 80% in those cases where prenatal diagnosis of septated cystic mass is made, which represents hydrocolpos of duplicated vagina (Fig. 2.32). Hydrocolpos is highly diagnostic of URSM but its absence does not rule out URSM. Hydrocolpos may not be evident in up to 50% of fetuses with URSM.
(c) Renal anomalies are reported in 90% of fetuses with URSM. Bilateral hydronephrosis is the most common, though other anomalies such as renal cystic dysplasia, pelvic kidney, horse-shoe kidney and crossed fused ectopia have also been noted. There may be dilated colon with echogenic balls of meconium (Fig. 2.33).
(d) Presence of echogenic ascites due to the reflux of urine mixed with meconium through fallopian tubes into the peritoneum (Fig. 2.32). Occasionally meconium peritonitis may be visible as peritoneal calcification. Bowel may either be normal in caliber or dilated.
(e) Spinal abnormalities such as hemivertebra or hypoplastic sacrum are frequently associated (Fig. 2.29).
(f) The degree of oligohydramnios depends on the severity and renal involvement. Complete URSM is associated with anhydramnios.

There could be other associated anomalies such as ambiguous genitalia (Fig. 2.31) and single umbilical artery. Antenatal recognition is important since it may provide the couple the option of termination when diagnosis is established before the legal time limits of termination. URSM carries a guarded prognosis. Functional disturbances are often encountered in anorectal, urological and gynecological systems.

Two types of URSM have been described. Complete URSM is characterized by the absence of anal and perineal openings, a smooth perineum and ambiguous genitalia (Fig. 2.34). It is a lethal anomaly and would result in stillbirth and perinatal mortality. Partial URSM is characterized by a single anal or perineal opening that serves a common conduit for gastrointestinal and

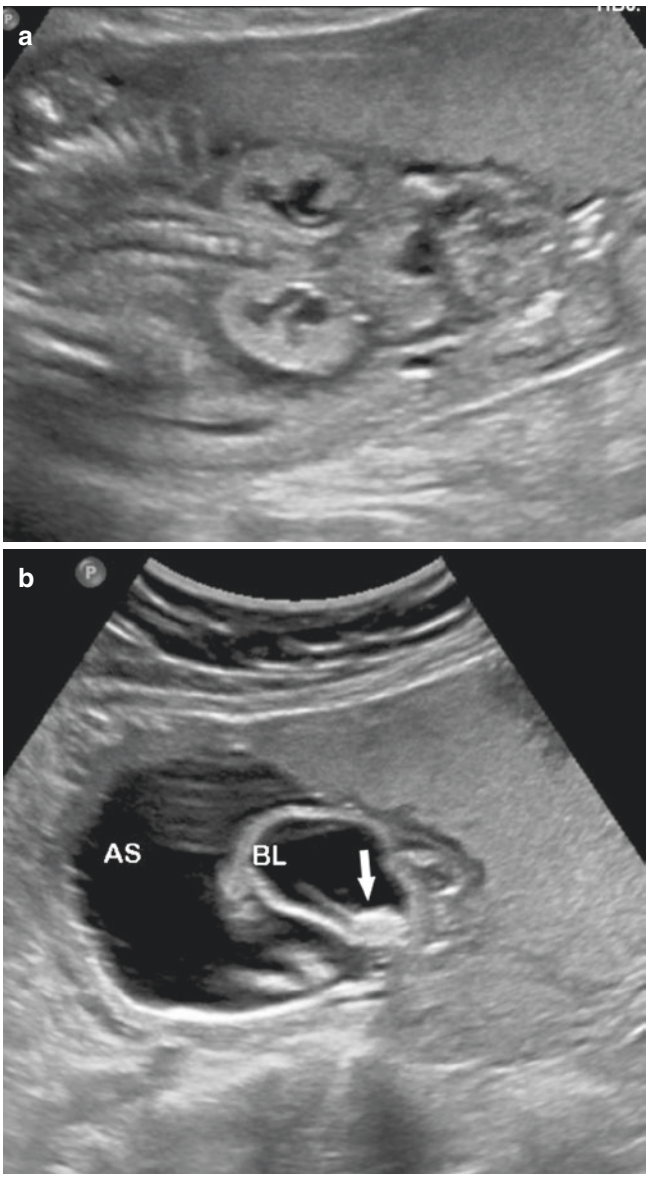

Fig. 2.31 Urorectal Malformation Sequence (URSM): (**a**) Coronal scan of fetal abdomen reveals anhydramnios and bilateral hydronephrosis with echogenic parenchyma. (**b**) Demonstrates ascites and pyriform cystic mass (BL) with debris (arrow)

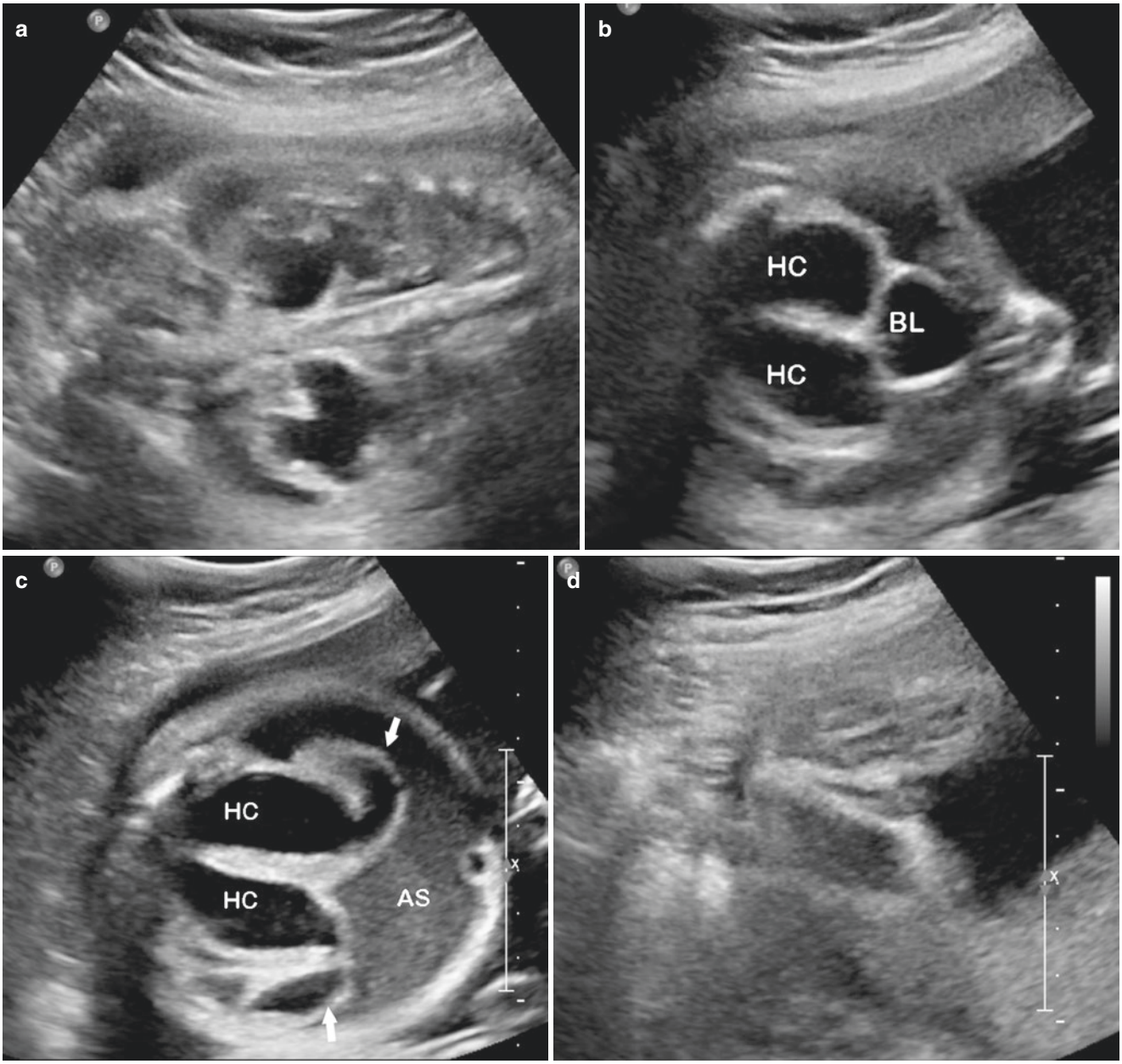

Fig. 2.32 Urorectal Malformation Sequence (URSM): (**a**) Coronal scan shows bilateral hydronephrosis. (**b**) Axial scan of fetal pelvis shows a large septated cystic mass (HC) posterior to urinary bladder (BL). (**c**) Oblique Coronal scan of fetal abdomen demonstrates echogenic ascites (AS) and hydrocolpos (HC) of duplicated vagina with hydrometra of the duplicated uteri (arrows). (**d**) Tangential scan of fetal perineum demonstrates nonvisualised anus

genitourinary tracts (Figs. 2.35 and 2.36). It is a less severe variant. Differentiation of the types is not possible by prenatal ultrasonography. In both types fetal anus will not be seen. The association of URSM with other anomalies such as VACTERL and OEIS complex has been described.

1. OEIS complex/Cloacal anomaly (described later) (Fig. 2.37).
2. VACTERL association denotes the complex combination of anomalies of vertebrae, anus, cardiac, tracheoesophageal, renal and limb anomalies. Vertebral anomalies can vary from simple anomalies like hemivertebra (Fig. 2.29), spinal dysraphism to gross kyphoscoliosis. Anorectal malformation can be low or high, cardiac anomalies can range from ventricular septal defect to complex anomalies. There can be esophageal atresia with or without tracheoesophageal fistula. Renal anomalies can be a spectrum from agenesis, to positional anomalies or complex obstructive lesion. Limb anomaly is usually a radial ray aplasia. When one component anomaly is seen care-

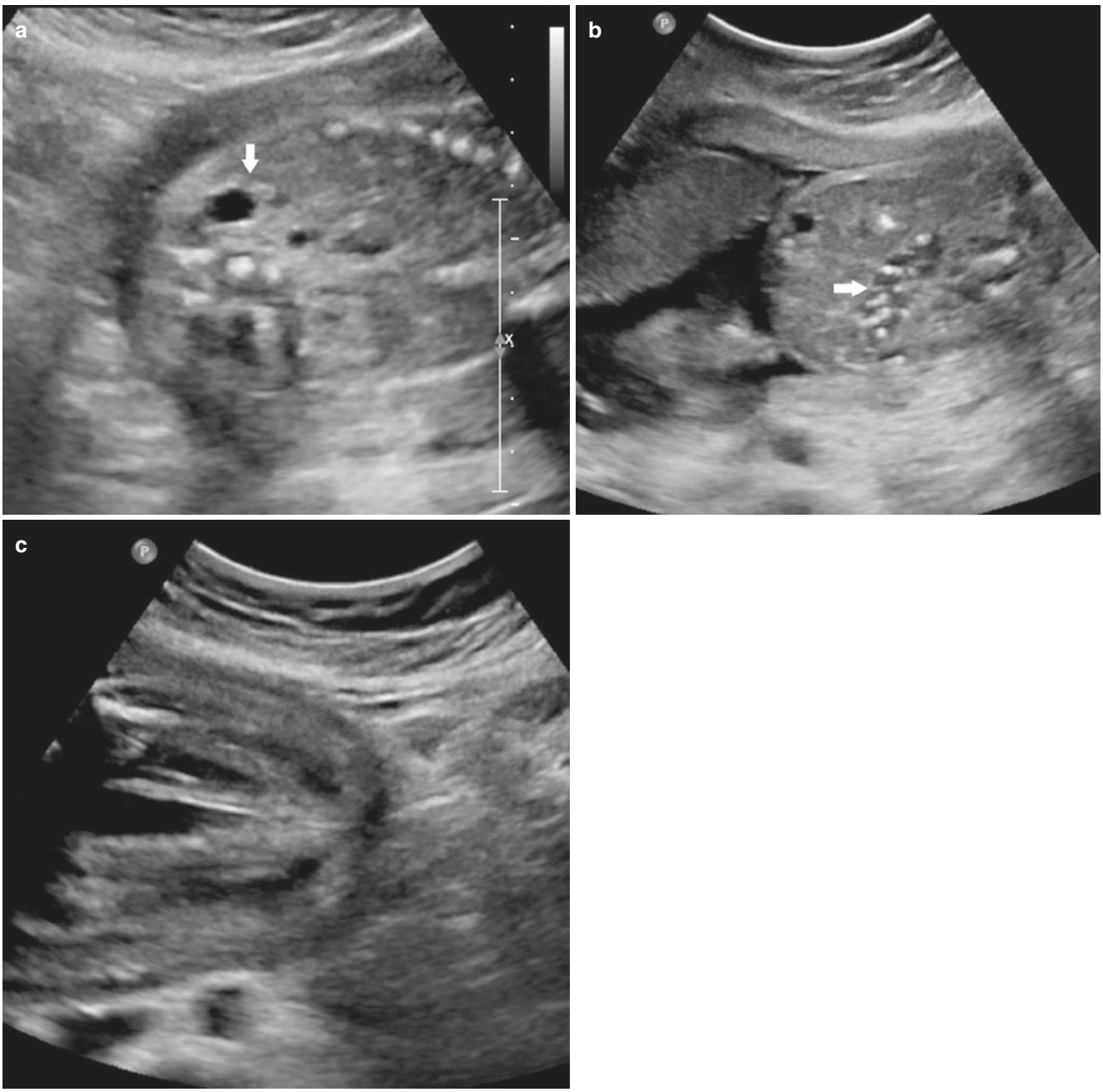

Fig. 2.33 Urorectal Malformation Sequence (URSM): (**a**) Coronal Scan reveals multicystic dysplastic kidney (arrow). (**b**) Axial scan of lower abdomen shows dilated colon with echogenic meconium balls. (**c**) Tangential scan of fetal perineum demonstrates nonvisualized anus

ful search for other components has to be done. When a spinal anomaly or esophageal atresia is seen, looking for the fetal anus helps to categorize if it is isolated or part of VACTERL association.

3. One of the features of anorectal malformation described earlier is dilated colon with echogenic meconium balls in it (Figs. 2.33b and 2.38a). It is now known to be a nonspecific finding because of the large normal range of caliber of colon and echogenic meconium seen as a normal feature towards term. So seeing the fetal anus is crucial to diagnose if it is anorectal malformation or a normal finding (Figs. 2.38 and 2.39).
4. Isolated anorectal malformation can be a low type of covered anus where the anal opening is not seen because of skin covering the anus. Here the anal sphincter complex is normally developed. Hence the fetal anus will be seen on sonography which results in a false negative situation. In high anorectal malformation the rectum stops high above the perineum and so the normal anus is not seen.

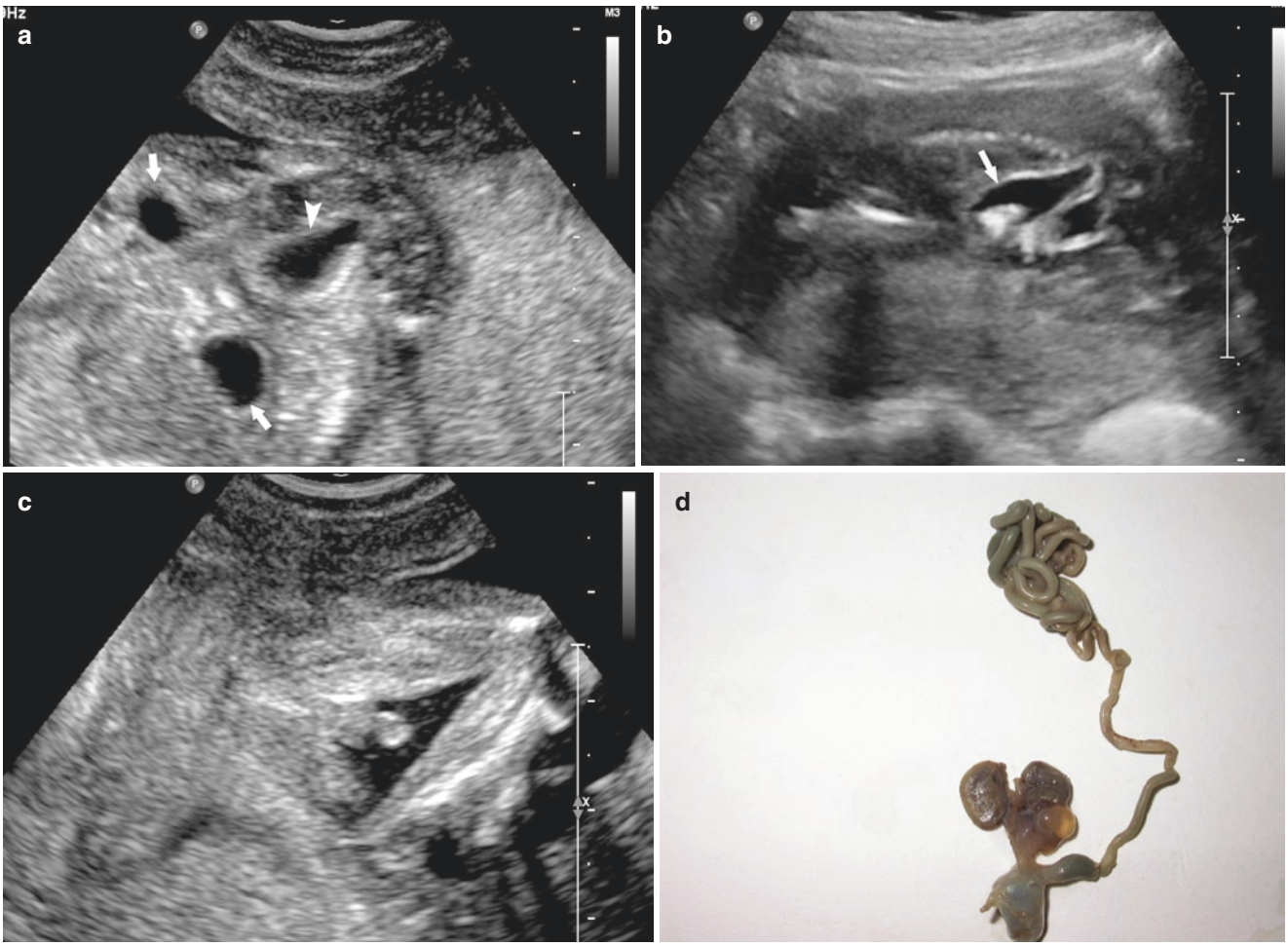

Fig. 2.34 Fetal images of complete URSM sequence. (**a**) Coronal scan of fetal abdomen showing bilateral gross hydronephrosis (arrows) with a thick-walled conical cystic structure (arrow head) in pelvis with oligohydramnios. (**b**) Oblique scan of lower abdomen shows dilated distal colon (arrow) with echogenic calcified meconium. (**c**) Tangential scan of perineum showing nonvisualized anus. (**d**) Autopsy picture showing a common cloacal pouch to which the ureters and rectum are connected

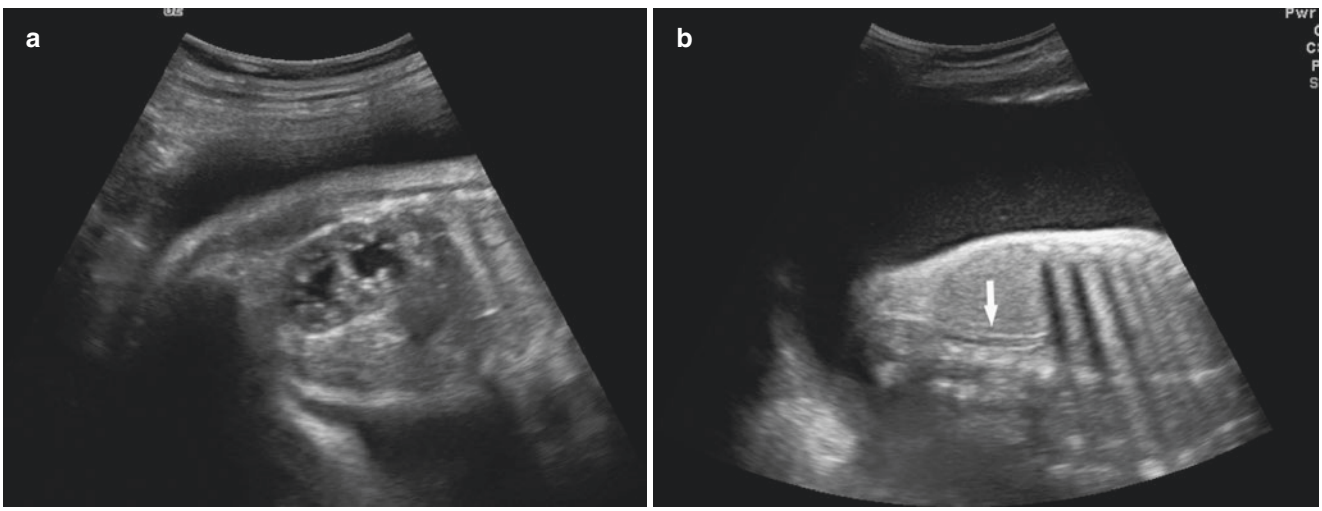

Fig. 2.35 Partial URSM Sequence: Coronal scans of fetal abdomen shows (**a**) gross hydronephrosis of right kidney and (**b**) agenesis of left kidney (arrow). (**c**) Scan of perineum shows nonvisualized anus. (**d**) Photograph of the newborn baby shows anal atresia

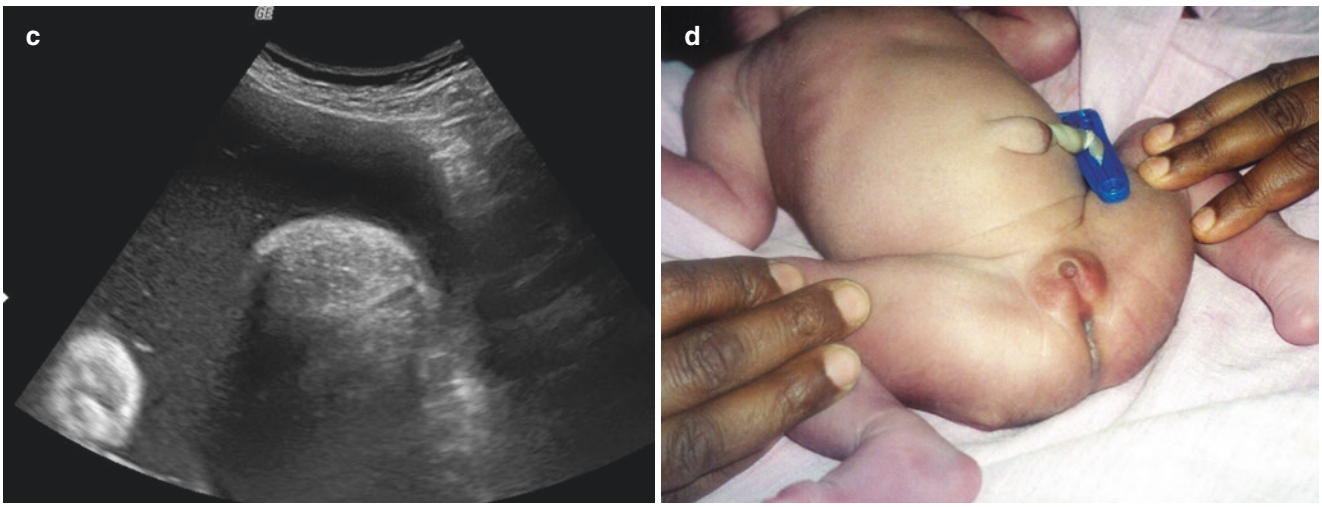

Fig. 2.35 (continued)

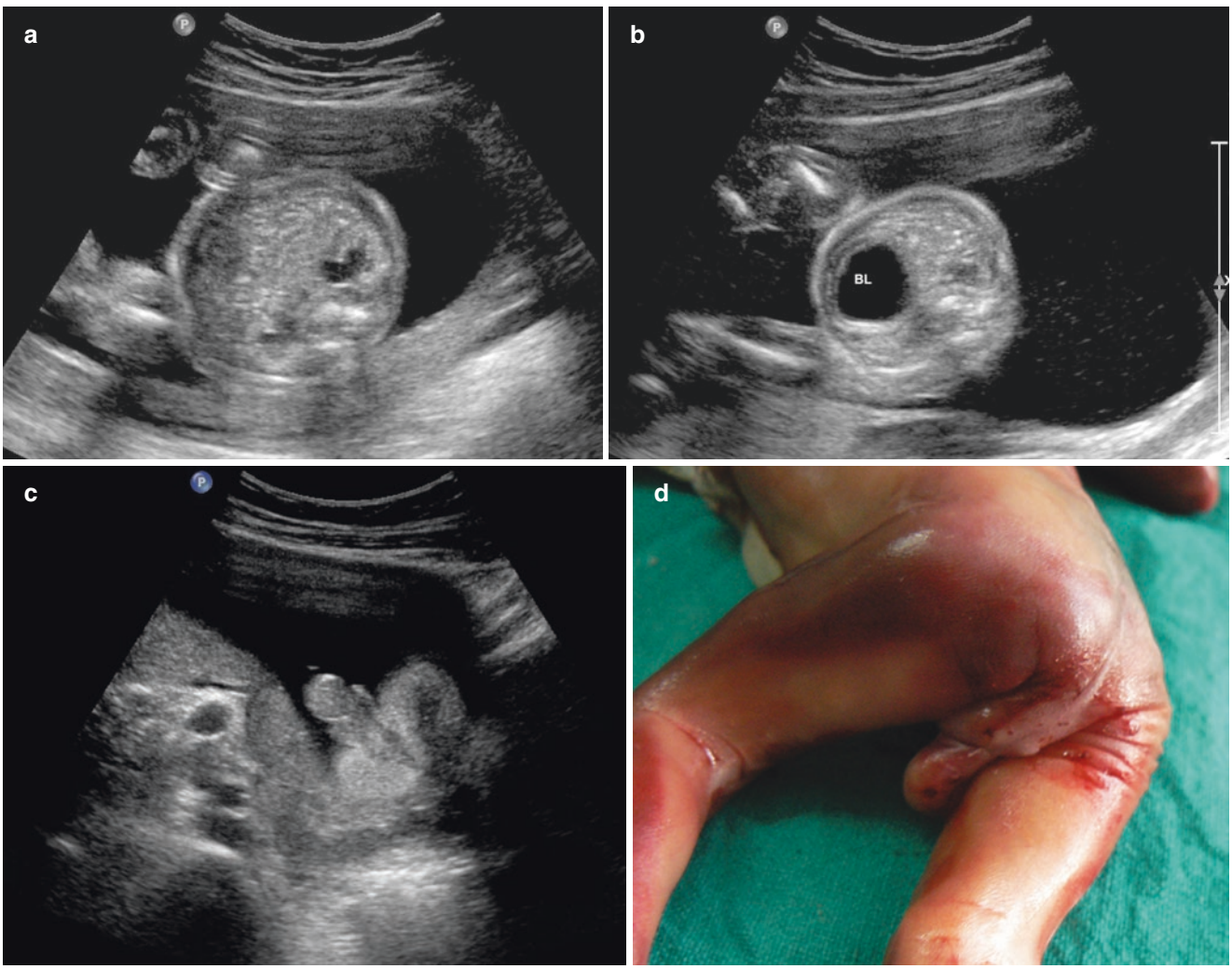

Fig. 2.36 Partial URSM Sequence: (**a**) Axial scan shows bilateral hydronephrosis. (**b**) Scan of pelvis shows urinary bladder (BL). (**c**) Scan of perineum shows an ambiguous genitalia and absent anus. (**d**) Photograph of the abortus confirms the findings

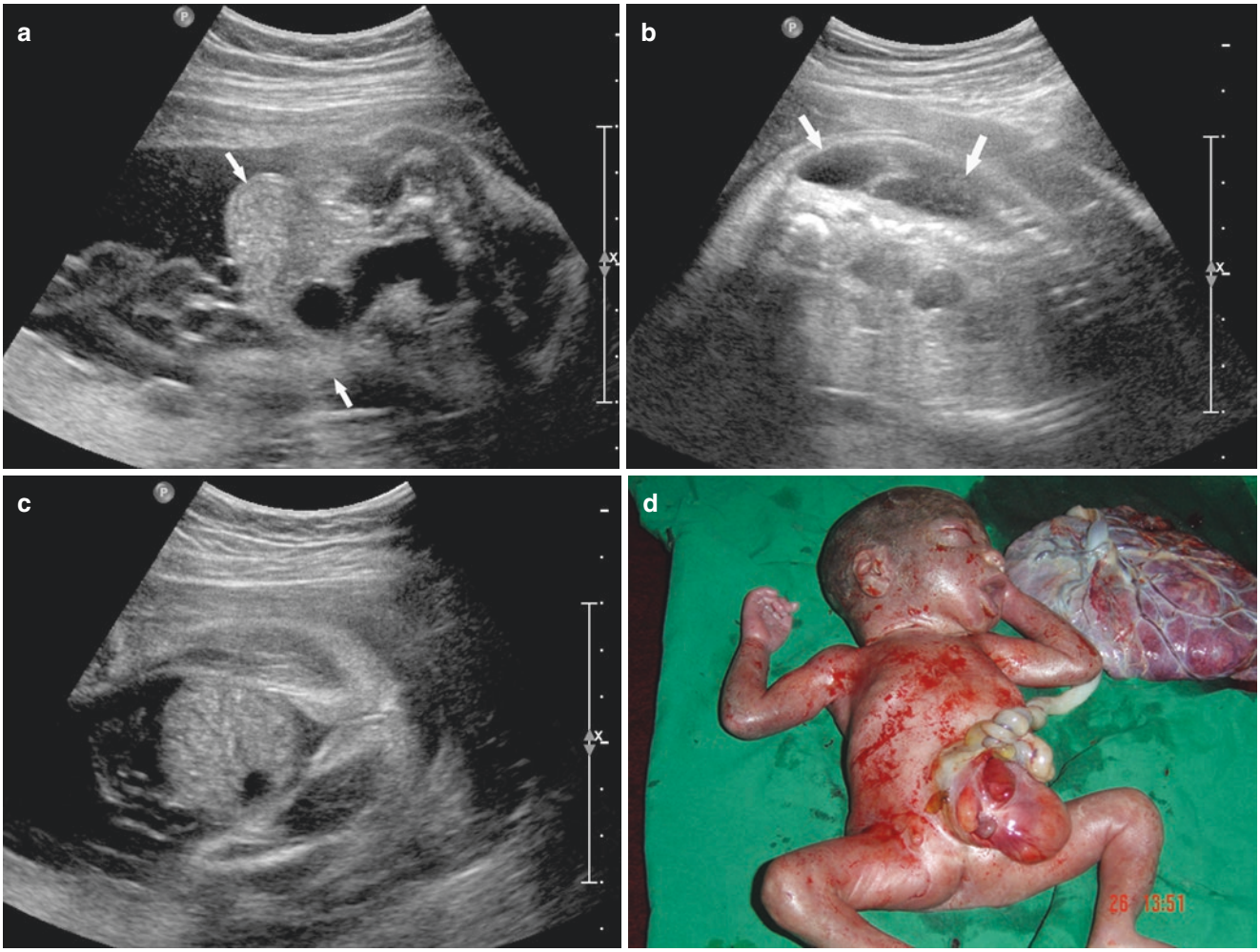

Fig. 2.37 Fetus of OEIS complex. (**a**) Shows the omphalocele (arrows). (**b**) Shows the spinal anomaly with meningocele (arrows). (**c**) Scan of perineum shows absent anus. (**d**) Photo of abortus confirming the features

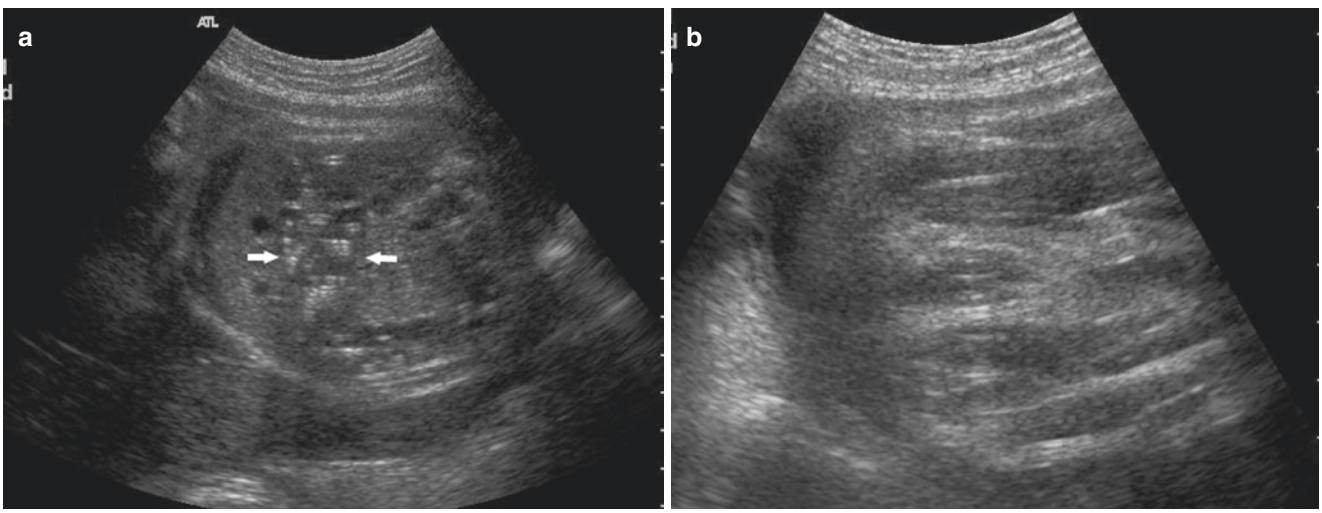

Fig. 2.38 (**a**) Axial section showing the dilated colon with calcified meconium balls (arrows). (**b**) Scan of perineum showing absent anus indicating anal atresia

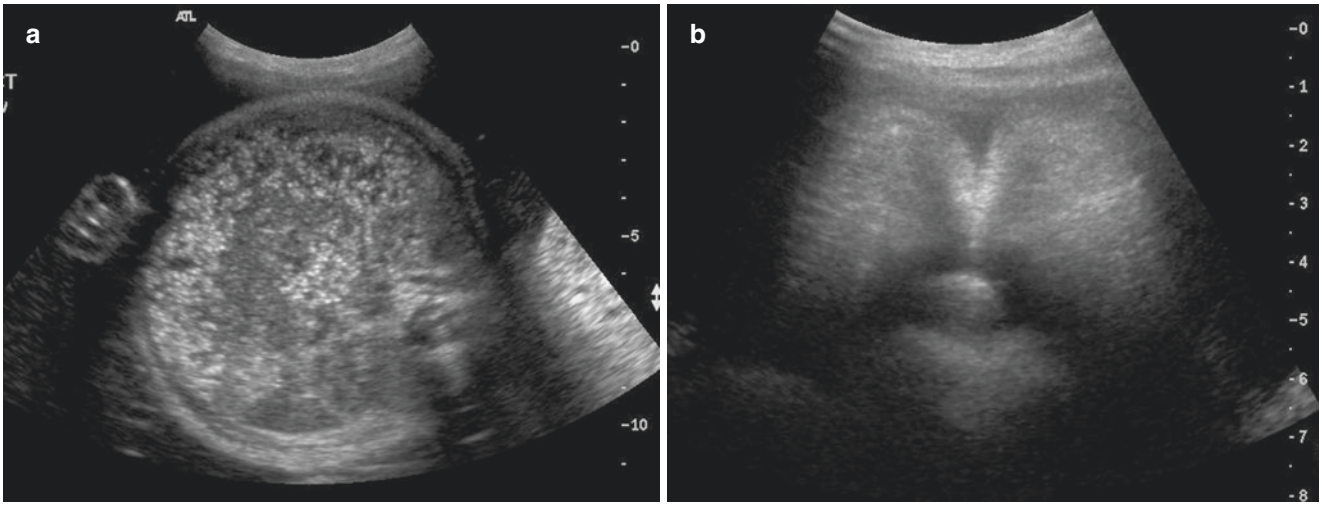

Fig. 2.39 (**a**) Axial scan showing dilated colon with echogenic meconium balls. (**b**) Scan of perineum showing normal anus ruling out anal atresia

Suggested Reading

Escobar LF, Weaver DD, Bixler D, Hodes ME, Mitchell M. Urorectal septum malformation sequence. Report of six cases and embryological analysis. Am J Dis Child. 1987;141(9):1021–4.

Gupta A, Bischoff A, Pena A, Runck LA, Guasch G. The great divide: septation and malformation of the cloaca, and its implications for surgeons. Pediatr Surg Int. 2014;30(11):1089–95.

Vijayaraghavan SB. Antenatal diagnosis of esophageal atresia with tracheoesophageal fistula. J Ultrasound Med. 1996;15:417–9.

Vijayaraghavan SB. Antenatal diagnosis of congenital chloride diarrhoea. Ind J Med Ultrasound. 1998;3 and 4:17–8.

Vijayaraghavan SB, Prema AS, et al. Sonographic depiction of the fetal anus and its utility in the diagnosis of anorectal malformations. J Ultrasound Med. 2011;30(1):37–45.

Fetal Genitourinary Tract Sonography

3

3.1 Introduction

Congenital abnormalities of urinary tract are quite common with an incidence of 1–4 in 1000 pregnancies. Prenatal sonographic diagnosis of fetal urinary tract malformation has proved to be useful in the prevention of serious renal damage in children and young adults. Prenatal diagnosis of urinary tract anomalies requires a systematic ultrasound assessment of fetal kidneys, urinary bladder, amniotic fluid volume and associated anomalies. Urinary tract anomalies may form part of some chromosomal anomalies, syndromes or associations, some of which can be recurrent or inherited. Hence, when urinary tract anomalies are seen in a fetus, associated anomalies have to be searched for in detail and a detailed family history has to be taken. Renal scan is recommended for parents and siblings of fetuses suspected to have certain renal abnormalities (polycystic kidney disease, bilateral renal agenesis/dysgenesis) because it may help to diagnose the type of kidney disease in the fetus.

Electronic Supplementary Material The online version of this chapter (https://doi.org/10.1007/978-981-13-0932-8_3) contains supplementary material, which is available to authorized users.

S. B. Vijayaraghavan, *Atlas of Fetal Imaging*, https://doi.org/10.1007/978-981-13-0932-8_3

3.2 Ultrasound Scanning Technique of Fetal Urinary Tract (Extended Fetal Urosonography)

The fetal kidneys can be seen satisfactorily on sonography from late first trimester (12 weeks onwards). The Endovaginal Sonography (EVS) can be used in first trimester. The kidneys are seen best in coronal scan of the fetal abdomen. They are seen as oval echogenic structures on either side of spine (Fig. 3.1).

In second and third trimester, the ultrasound assessment of kidneys is made on a minimum of two scan planes: axial and coronal. A third longitudinal plane may be necessary in certain situations. The highest frequency transducer that allows adequate penetration of the maternal abdomen should be used. On axial scan, the kidneys are seen as round echopoor structures on either side of fetal spine with a horizontally oriented slit like fluid filled renal pelvis. On longitudinal scan, the kidney appears oval with the adrenal gland located cranially. On coronal scan, the kidneys appear as bean shaped structures on either side of the spine. In second trimester, it appears echopoor (Fig. 3.2).

In the third trimester, the corticomedullary differentiation (CMD) is distinctly is made out. The medullary pyramids are seen as triangular echopoor areas towards the inner aspect of the kidney. Towards term, the medullary pyramids are prominent (Fig. 3.3) and should not be mistaken for dilated calyces.

They can be differentiated on coronal scan, where the dilated calyces will communicate with medially placed renal pelvis while the renal pyramids will remain triangular. In selected situations, high frequency probe can be used to scan the kidneys to look for parenchymal abnormalities like echogenicity, cysts and corticomedullary differentiation (Fig. 3.3d). Urinary bladder is seen as a round echopoor cystic structure in axial scan of the fetal pelvis (Fig. 3.4).

In longitudinal and coronal scan it appears fusiform. When the color box is turned on in oblique scan including cord insertion, the two umbilical arteries are seen skirting the urinary bladder (Fig. 3.4e, f). It exhibits alternate cycles of filling and emptying due to fetal micturition. Hence if fetal urinary bladder is not seen, scan has to be repeated to confirm persistent nonvisualisation. In urinary bladder outflow obstruction, the urinary bladder remains over distended over time. The fetal urinary bladder can be visualized consistently from 12 weeks of gestation (Fig. 3.4a, b). In second trimester endovaginal sonography can be done for better visualization of the kidneys and urinary bladder if the fetus is in breech presentation. In certain situations, fetal perineal sonography and sonographic fetal micturating cystourethrogram (SFMCUG) have to be performed. A midline sagittal section of the fetal pelvis, perineum and external genitalia is obtained (Fig. 3.5) and the same section is observed continuously for the occurrence of fetal micturition.

During micturition, the urinary bladder is seen to contract, the urethra distends slightly with fluid and a urinary stream from the external urethral meatus is observed. The urinary stream can be seen on both gray scale and color Doppler sonography (Fig. 3.6, Videos 3.1 and 3.2).

When micturition is observed, it is stored as a cine loop. This cine loop can then be reviewed either as cine at varying speed or as multiple freeze frames. The same section is also useful to look for ectopic ureteric opening.

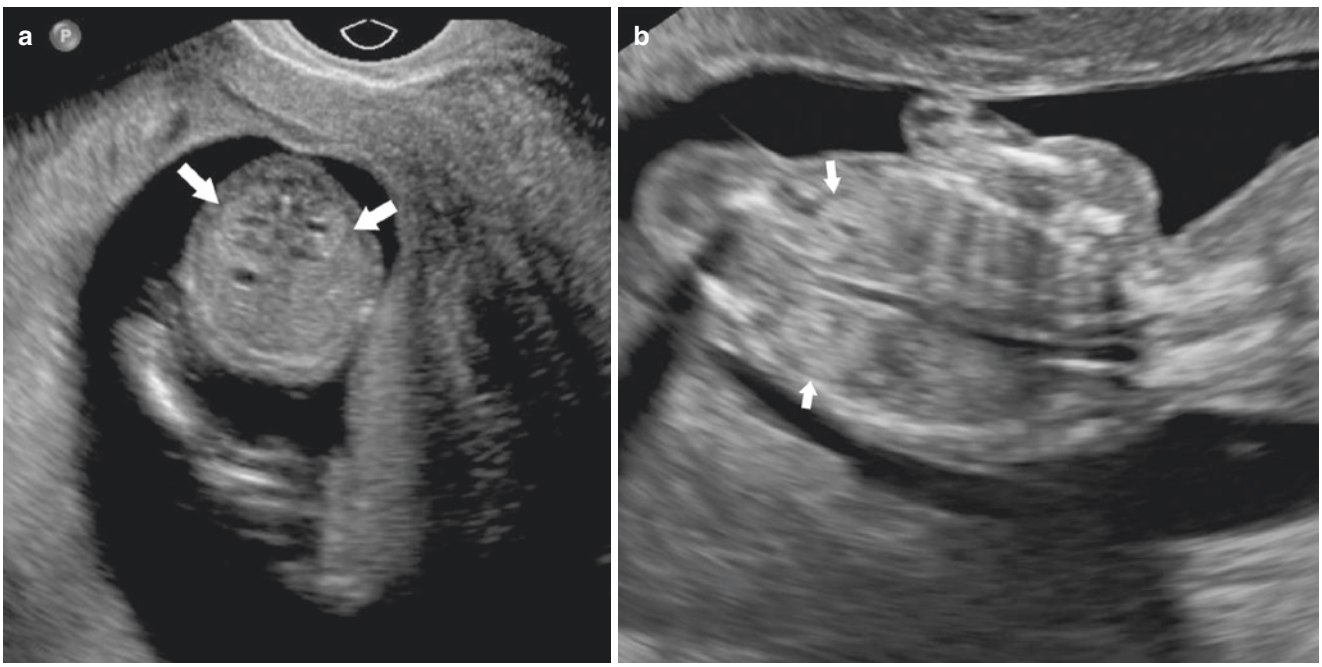

Fig. 3.1 Normal appearance of the kidneys in first trimester: (**a**) Axial and (**b**) coronal planes of the fetal abdomen showing the echogenic kidneys (arrows)

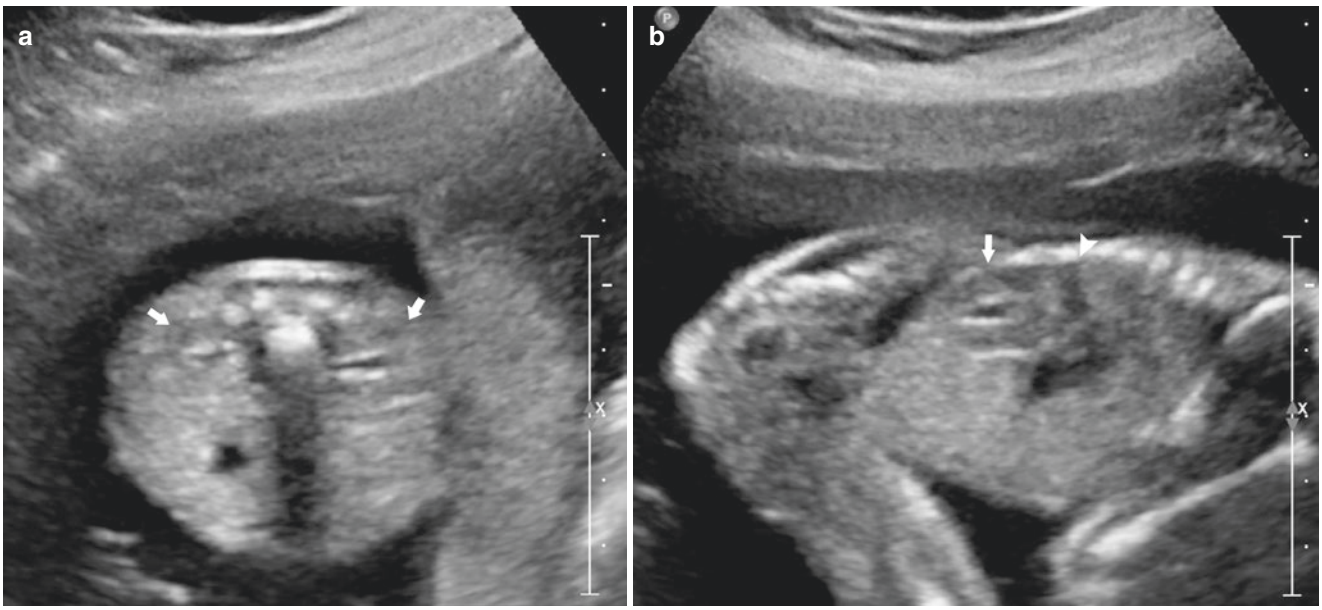

Fig. 3.2 Normal appearance of kidneys in second trimester: (**a**) Axial scan from posterior aspect shows the round echo-poor kidneys (arrows) on either side of the spine with slit like fluid filled renal pelvis in the center. (**b**) Longitudinal scan shows the oval kidney (arrow) with the echo-poor adrenal (arrowhead) above it

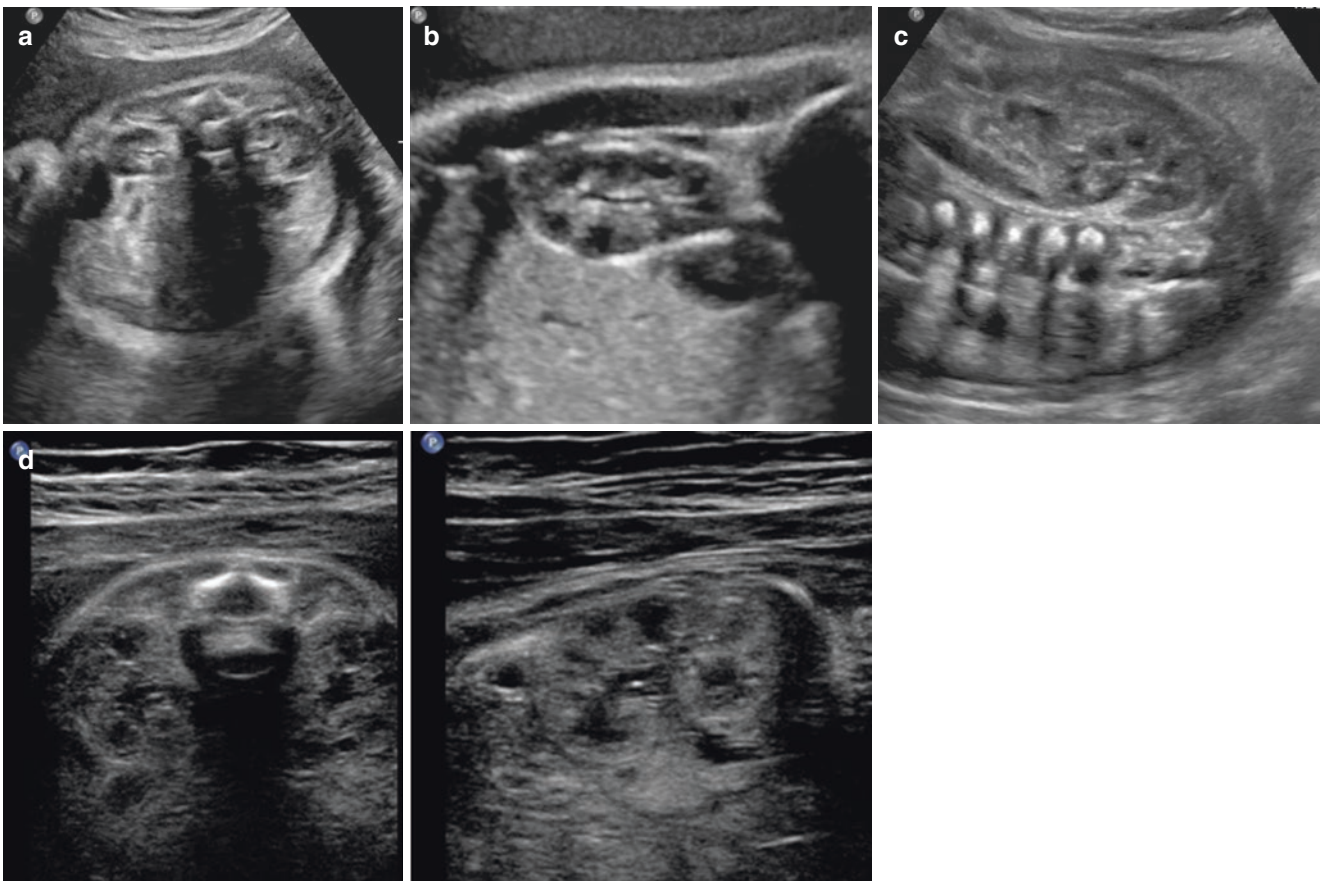

Fig. 3.3 Normal appearance of kidneys in third trimester: (**a**) Axial scan. (**b**) Longitudinal scan shows good cortico-medullary differentiation (CMD) with the echo-poor triangular pyramids on the inner side of the kidney. (**c**) Coronal scan showing the bean shaped kidney. (**d**) High frequency scans of the kidney showing the excellent CMD

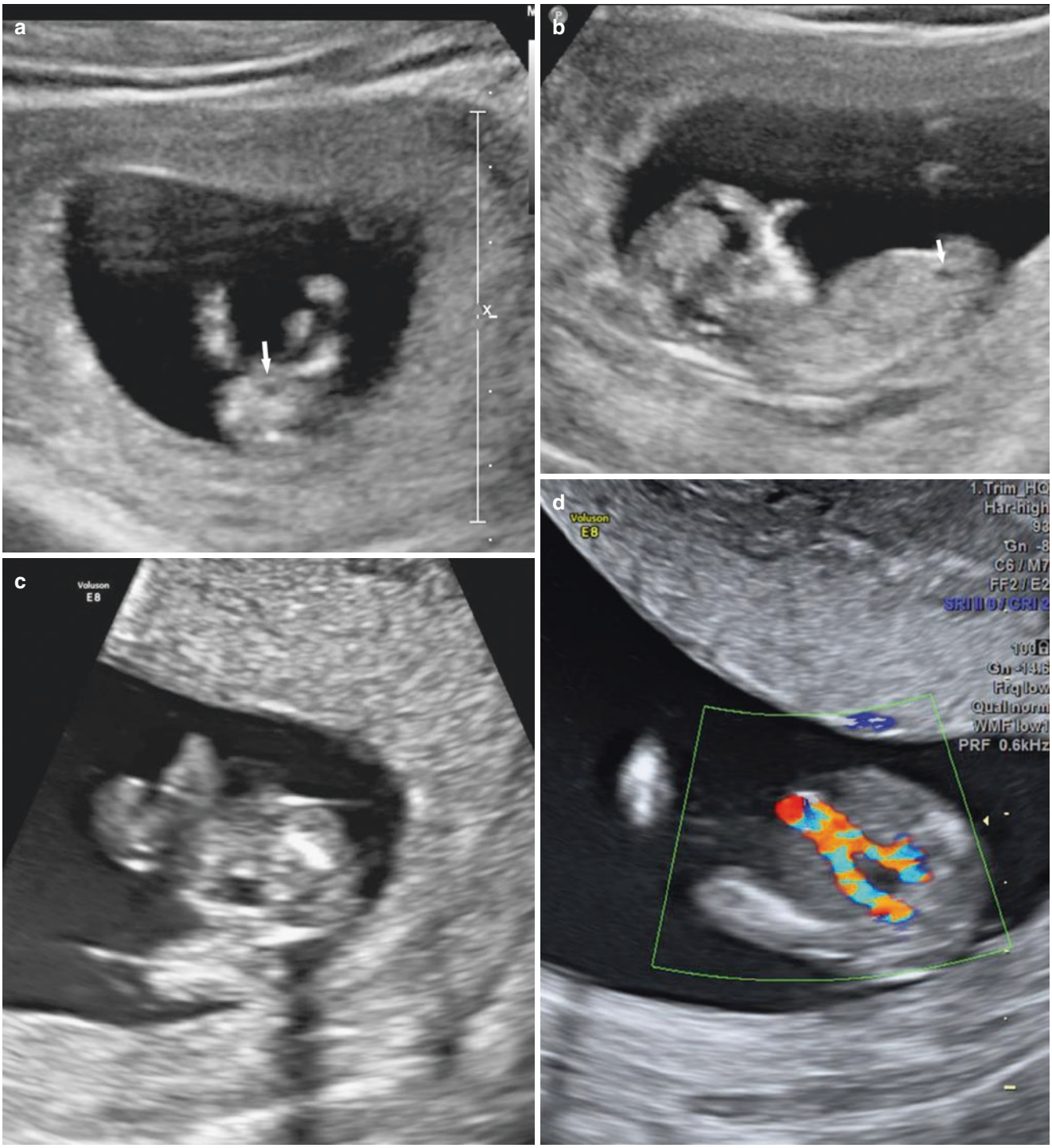

Fig. 3.4 Normal appearance of the urinary bladder at 11 weeks: (**a**) Axial and (**b**) Longitudinal scan of the fetus showing the tiny urinary bladder (arrow). At 13–14 weeks: (**c**) Axial scan and (**d**) Oblique coronal scan with color Doppler showing the umbilical arteries skirting around the urinary bladder. (**e**, **f**) Similar images in second trimester

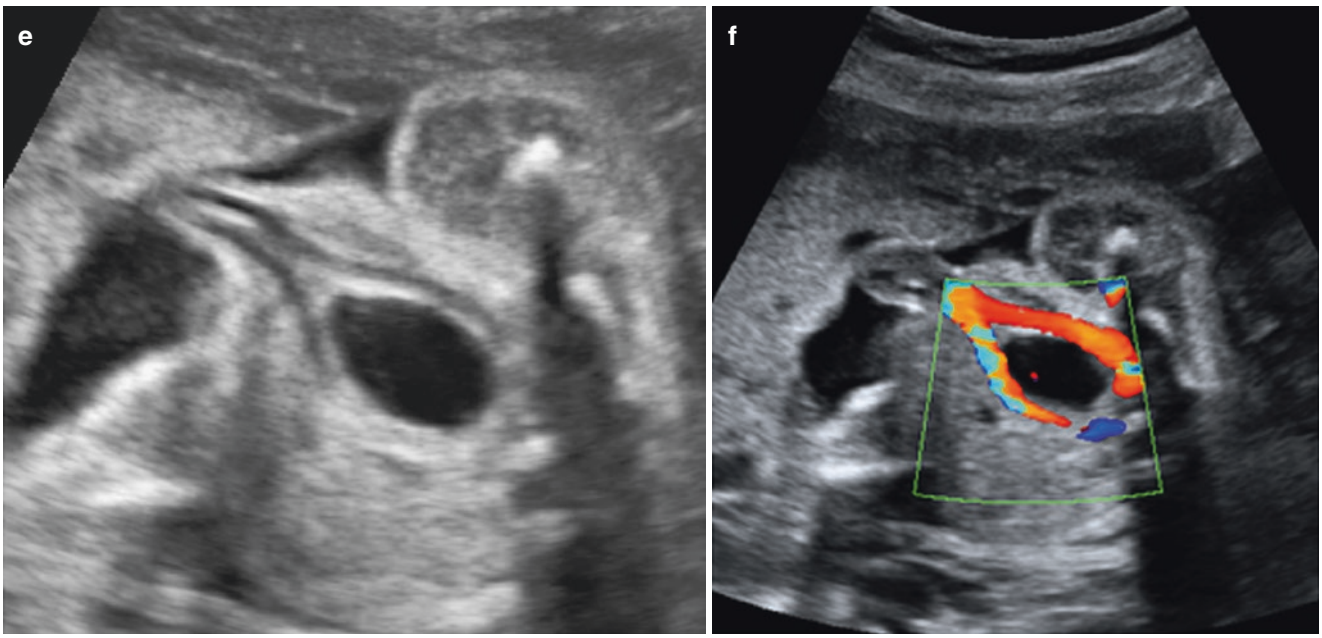

Fig. 3.4 (continued)

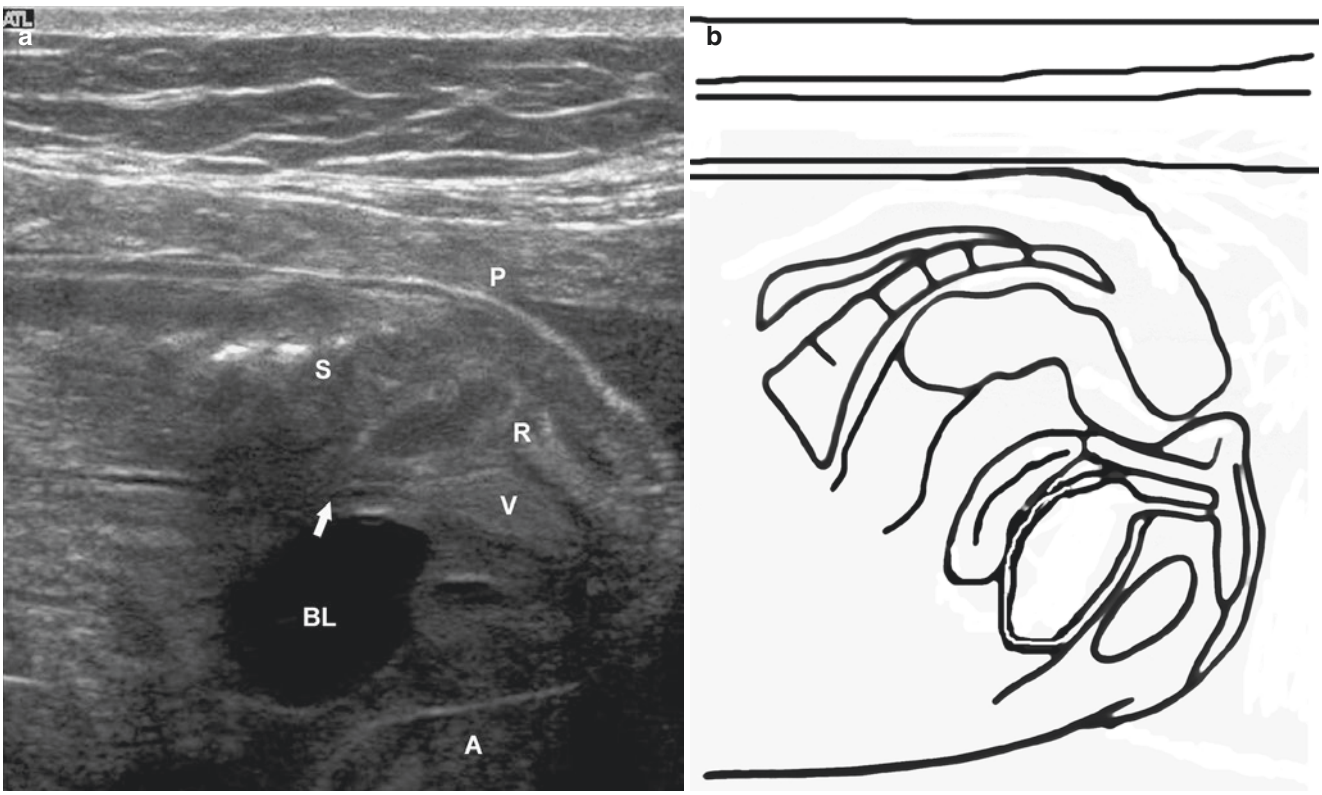

Fig. 3.5 Fetal perineal scan in a female fetus from posterocaudal approach (**a**, **b**) and anterocaudal approach (**c**, **d**) showing the urinary bladder (BL) and urethra anteriorly, vagina (V) and uterus (arrow) in the middle and rectum (R) posteriorly. A indicates anterior, P—posterior and S—sacrum. (**e**, **f**) Fetal perineal scan in a male fetus showing the urinary bladder (BL) and urethra anteriorly and rectum (R) posteriorly. A indicates anterior, P—posterior and SC—scrotum

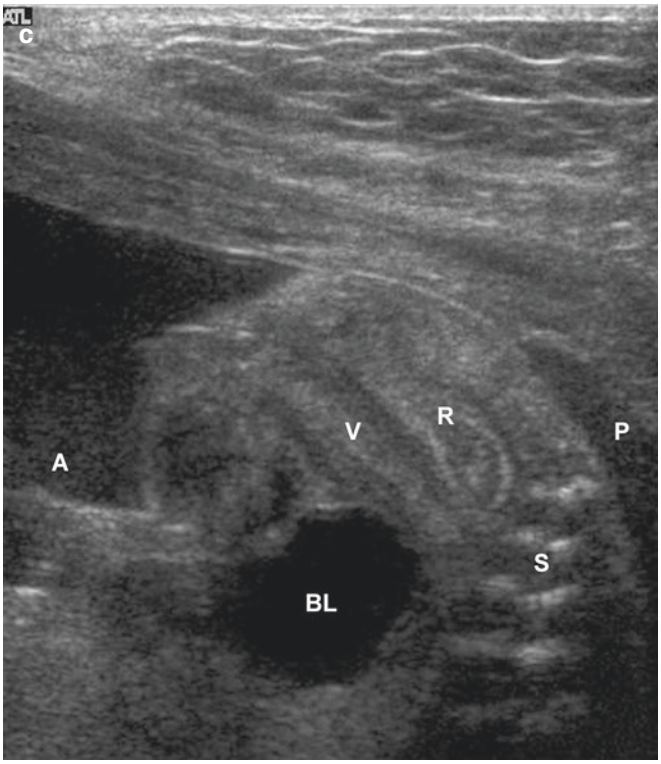

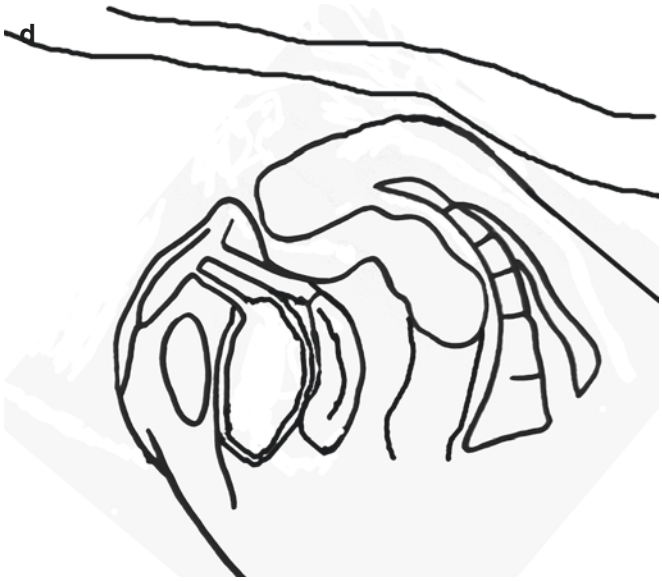

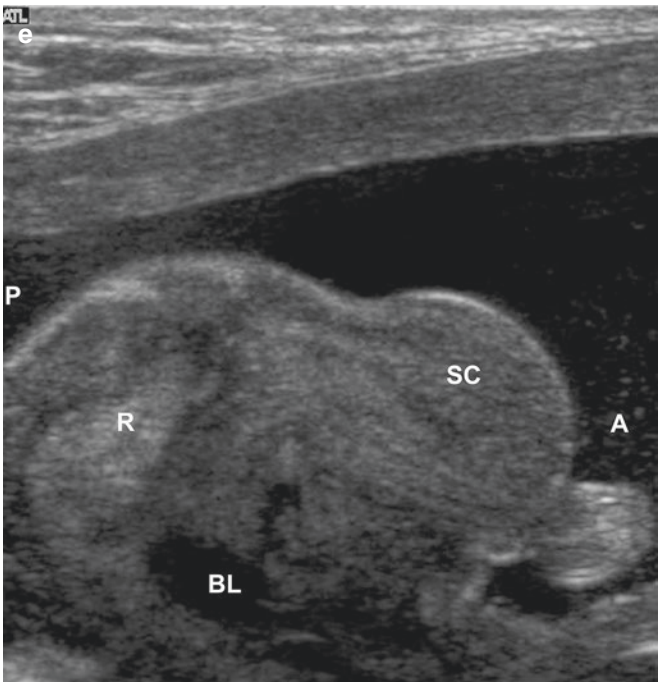

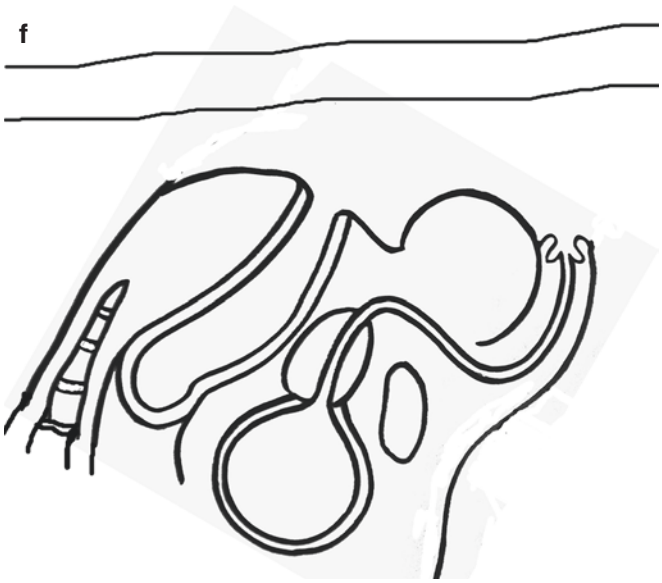

Fig. 3.5 (continued)

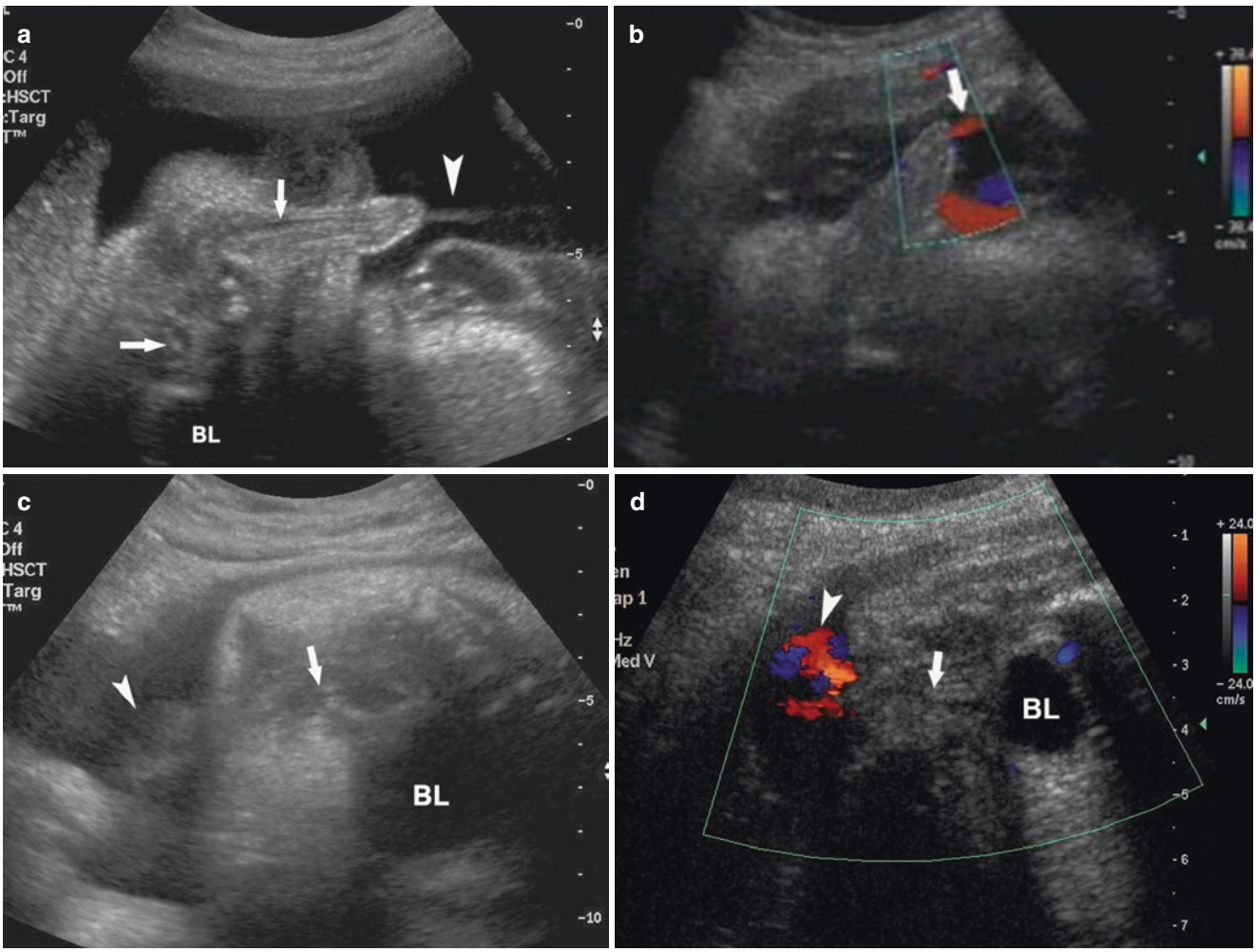

Fig. 3.6 Fetal sonographic Micturating Cystourethrogram (FSMCUG). (**a**) Midline sagittal gray scale image through the fetal pelvis, perineum and the penis during micturition showing the urinary bladder (BL) slightly fluid distended posterior and anterior urethra (arrows) and the urinary stream from the tip of the penis (arrow head) in a fetus with normal urethra (Video 3.1). (**b**) Color Doppler image of the same fetus showing the urinary stream from the tip of the penis. (**c**) Gray scale and (**d**) color Doppler images of micturition in a female fetus showing the urinary bladder (BL) urethra (arrow) and the urinary stream (arrowhead) (Video 3.2)

3.3 Amniotic Fluid and Urinary Tract Anomaly

The fetal urine is the major source of amniotic fluid volume after 16–18 weeks. Hence, there is a close association between the anomalies of urinary tract and amniotic fluid volume. In Barter's syndrome, fetal anemia and recipient in twin to twin transfusion syndrome, there is polyhydramnios due to polyuria. When there is decreased urine output due to urinary tract anomaly or fetal growth restriction (FGR), it will result in oligohydramnios. Decrease in urine output is seen in either urinary bladder outflow obstruction or bilateral renal disease or obstruction. Hence when there is oligohydramnios, the following protocol has to be followed.

1. Premature rupture of membranes (PROM) as the cause of oligohydramnios should be ruled out.
2. Urinary bladder should be looked for. It may be seen and may appear normal. It may appear over distended in urinary bladder outflow obstruction. If urinary bladder is not seen, then the scan has to be repeated at intervals to see if it is not seen persistently.
3. If urinary bladder is not persistently seen, then the renal fossa should be looked for to rule out diseased kidneys or renal agenesis.
4. If the urinary bladder is persistently small, careful scan of the kidneys is to be done. The kidneys may be small (Fig. 3.7). One kidney may be absent with small other kidney (Fig. 3.8). These indicate that there is poor urine output because of decreased renal volume. This condition become manifest around 20–24 weeks when fetal urine becomes the major source of amniotic fluid.
5. If urinary bladder and kidneys are normal then the placenta has to be assessed for hyper maturity. Color Doppler assessment of umbilical artery has to be done to rule in or out placental dysfunction with or without fetal growth restriction.

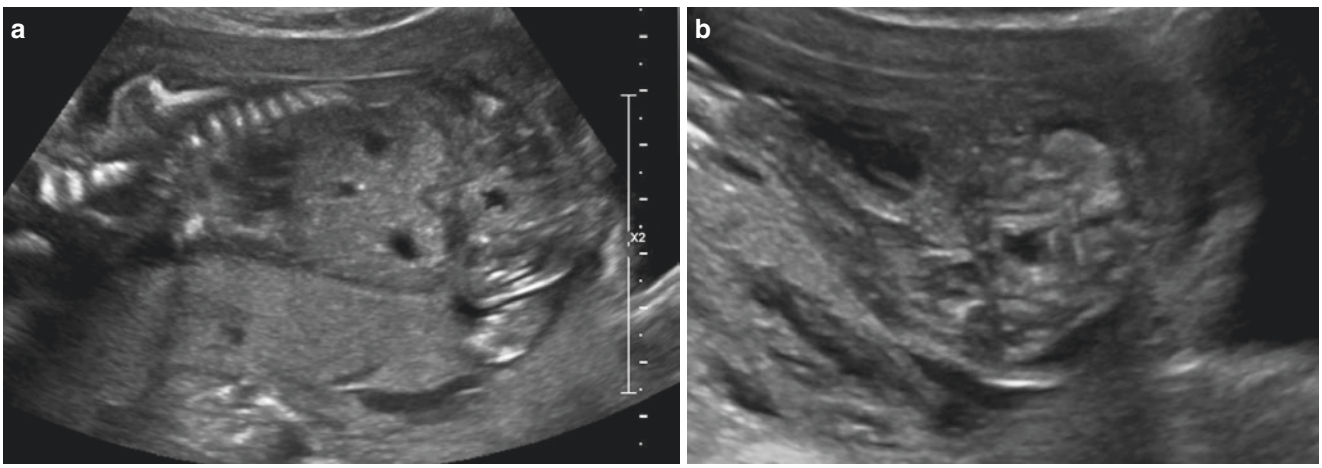

Fig. 3.7 (**a**) Longitudinal scan of gravid uterus at 21 weeks showing oligoamnios. (**b**) Axial scan showing persistently small urinary bladder (**c**) Longitudinal and (**d**) Axial scan of the kidneys showing smaller kidneys for the gestational age

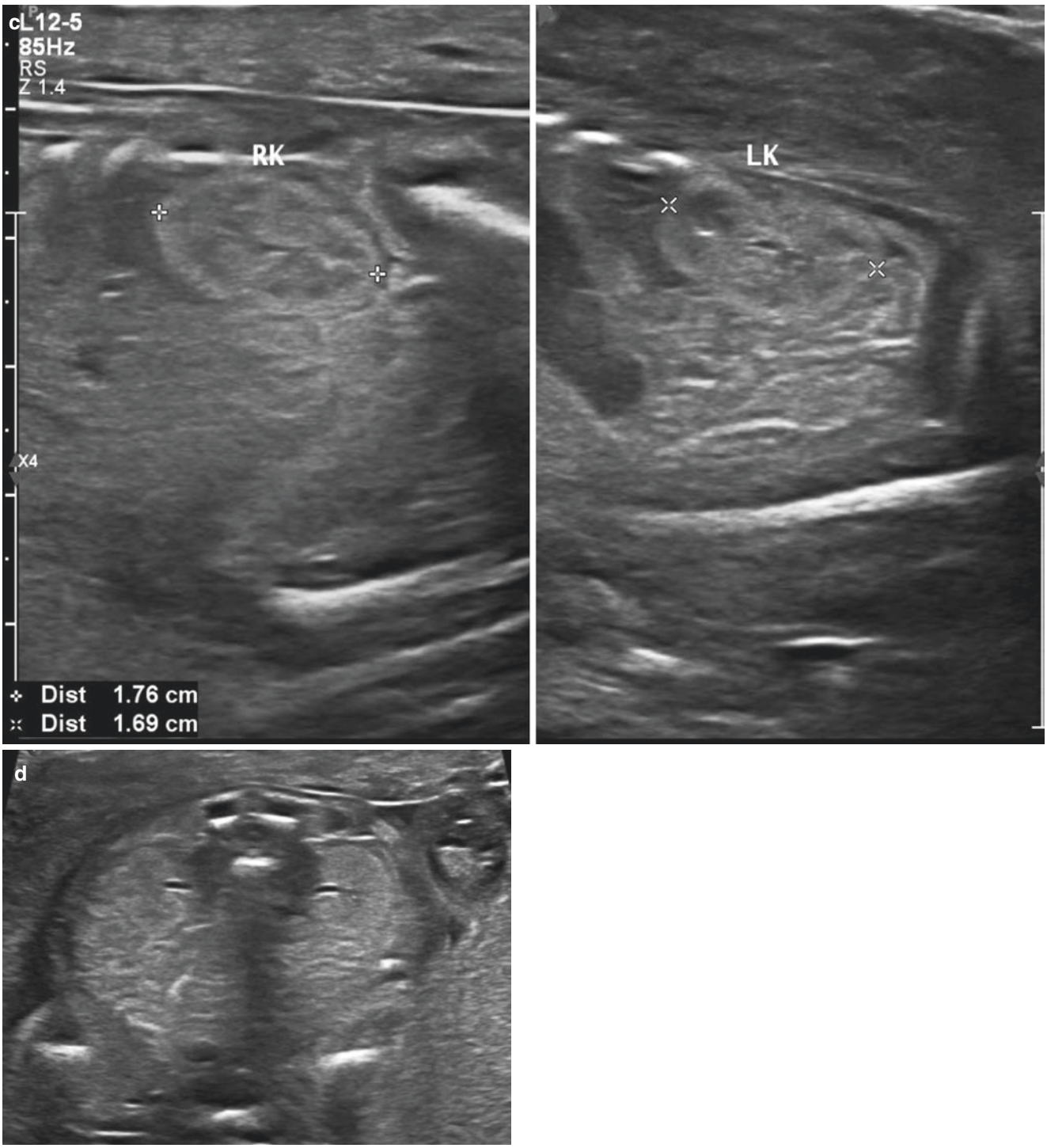

Fig. 3.7 (continued)

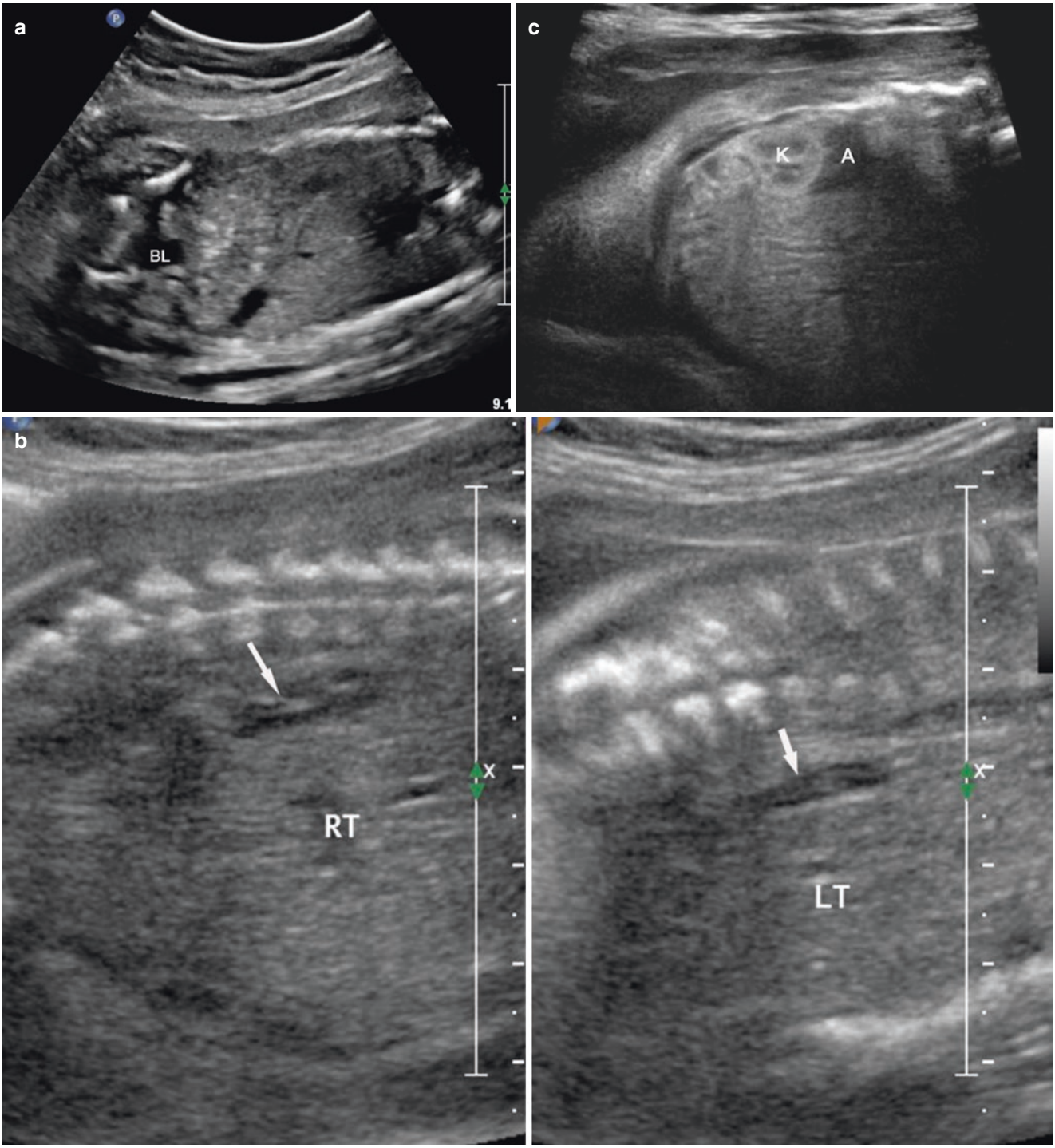

Fig. 3.8 (**a**) Coronal scan of fetal abdomen of a 23 week fetus shows severe oligamnios with small bladder (BL). (**b**) High frequency longitudinal scan of both renal areas showing lying down adrenal sign (arrows). (**c**) Longitudinal scan of right side at a slightly lower level shows a very small right kidney (K) below the adrenal gland (A)

3.4 Urinary Tract Dilatation

Urinary Tract dilatation (UTD) is one of the most common anomalies that can be picked up prenatally. It occurs in 1–2% of all pregnancies. Its prenatal detection helps to manage the condition prior to the development of complications such as urinary tract infection (UTI), calculus formation or renal dysfunction postnatally. In most of the cases (50–70%), the urinary tract dilatation is transient or physiologic without any clinical significance. In the rest, it may be due to obstructive pathology like pelviureteric junction obstruction (10–30%), primary obstructive megaureter (5–15%), posterior urethral valves (1–5%) or vesicoureteric reflux (10–40%). The less common causes can be ectopic ureter, duplex collecting system, and urethral atresia or prune belly syndrome. The etiology may not be defined before birth in all cases and is diagnosed postnatally with imaging which includes ultrasound and micturating cystourethrogram (MCUG). Urinary tract dilatation is a dynamic process fluctuating over time and with varying conditions like degree of distension of urinary bladder prenatally and hydration and patient position postnatally. Hence, urinary tract dilatation can present as a spectrum of severity—for example, not all cases of posterior urethral valves present with severe urinary tract dilatation (Figs. 3.49–3.53).

In 2014, a multidisciplinary consensus on the classification of prenatal and postnatal urinary tract dilatation has been published by Nguyen HT et al, where a statement of unified description of urinary tract dilatation with consistent terminology and standardized scheme for the perinatal evaluation of these patients has been put forth. This system is designed to be used in cases of isolated urinary tract dilatation and not to be applied to unique situations or anomalous kidneys. The statement recommends the consistent use of the term "urinary tract dilatation". The ideal technique for anteroposterior renal pelvic diameter (APRPD) measurement is based on images of the kidney obtained with the fetus in an anterior-posterior plane. For optimal visualization of the fetal kidneys, and measurement of the AP diameter of renal pelvis dilatation, the spine should be demonstrated at the 12 or 6 o'clock positions. In addition, the measurement should be taken at the maximal diameter of intrarenal pelvis dilatation (Fig. 3.9) rather than that of the extrarenal pelvis dilatation.

Additional sonographic features to be evaluated are: (1) calyceal dilatation; (2) parenchymal thickness by subjective assessment; (3) parenchymal appearance—(a) echogenicity assessed subjectively by comparison with liver and spleen, (b) presence or absence of cortical cyst, (c) corticomedullary differentiation; (4) ureteric dilatation; (5) abnormalities of urinary bladder like wall thickness, over distension, presence of ureterocele or dilated urethra and (6) oligohydramnios.

The renal pelvis is considered normal if the APRPD is <4 mm at <28 weeks gestation, <7 mm at ≥28 weeks and <10 mm postnatally without calyceal dilatation, normal parenchyma, nonvisualized ureter and normal urinary bladder. Above these threshold measurements, it is diagnosed as urinary tract dilatation (UTD). In antenatal period, the UTD is classified into two groups—a low risk group of UTD A1 with low risk for postnatal uropathy and an increased risk group of UTD A2–3 with increased risk for postnatal uropathy.

In fetuses of UTD A1, the APRPD is 4 to <7 mm at <28 weeks (Fig. 3.10a, b) and 7 to <10 mm at ≥28 weeks (Fig. 3.10c, d) with normal renal parenchyma, nonvisualized or undilated ureter, normal urinary bladder with normal amniotic fluid volume. They may have central calyceal dilatation. In fetuses with UTD A2–3, the APRPD is ≥7 mm at <28 weeks (Fig. 3.11a, b) and ≥ 10 mm at ≥28 weeks (Fig. 3.11c, d) or any one of the following findings: dilatation of peripheral calyces (Fig. 3.11e, f), abnormal parenchymal thickness or appearance (Fig. 3.11g, h), dilated ureter (Fig. 3.11i) an abnormal urinary bladder or oligohydramnios.

Based on the UTD classification system, a follow up management scheme has been proposed. For UTD A1 diagnosed before 32 weeks, a follow up prenatal ultrasound is recommended at ≥32 weeks. If the ultrasound at ≥32 weeks reveals resolution of the UTD with normal renal parenchyma, bladder and ureters, no further prenatal or postnatal follow up is necessary. If there is persistent UTD A1 or UTD A2–3, evaluation after birth is recommended. Postnatal evaluation should include two ultrasound evaluations: the first at >48 h but less than 1 month after birth; and the second 1–6 months later. In fetuses considered at increased risk for postnatal uropathy (UTD A2–3), a follow up prenatal ultrasound is recommended within 4–6 weeks of the initial diagnosis of urinary tract dilatation. Where there is substantial risk for surgery or renal dysfunction, prenatal consultation with a specialist is recommended. After birth, a follow up ultrasound is recommended at >48 h of life to avoid a false negative appearance due to neonatal dehydration. Follow up should be performed earlier for obstructive uropathy, such as suspected posterior urethral valve (as suggested by the finding of a thick walled bladder with persistent dilatation and a fusiform appearance and/or posterior urethral dilatation on prenatal ultrasound) or for bilateral conditions. Worsening findings on serial prenatal or postnatal ultrasound are associated with increased risk for genitourinary pathology. UTD is most often transient and associated with an increased risk of Trisomy 21 anomaly warranting a detailed ultrasound and correlation with aneuploidy screening protocols.

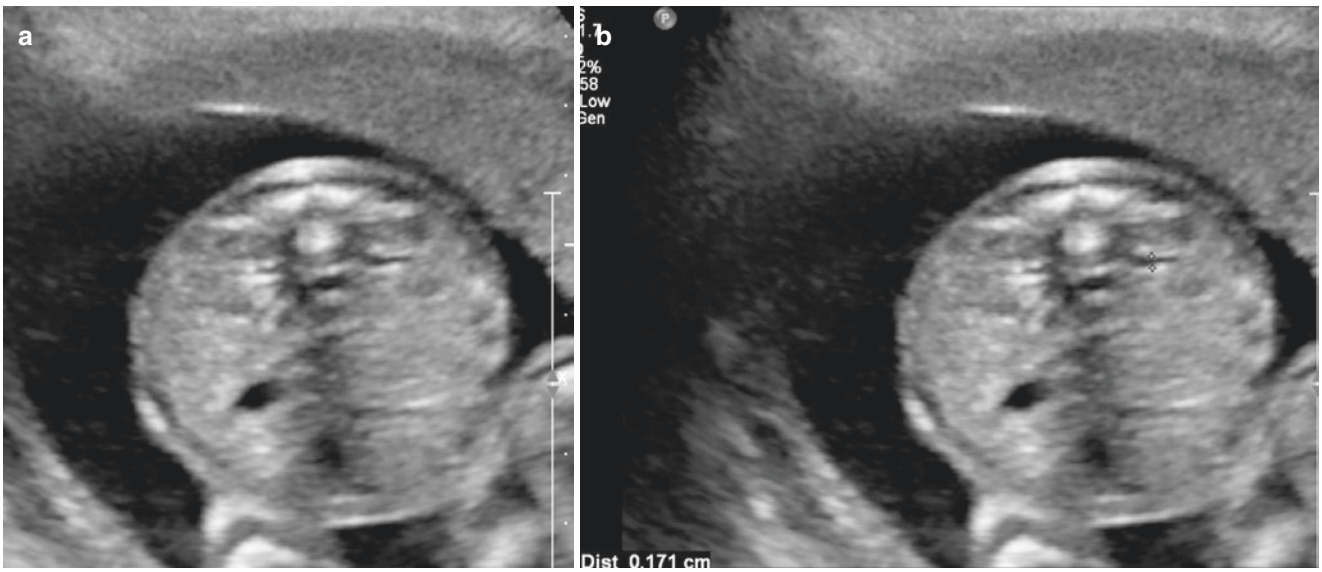

Fig. 3.9 Technique of measurement of APRPD: Axial scan of fetal abdomen demonstrates the fetal spine at 12 o'clock position (**a**) and placement of calipers for the measurement (**b**)

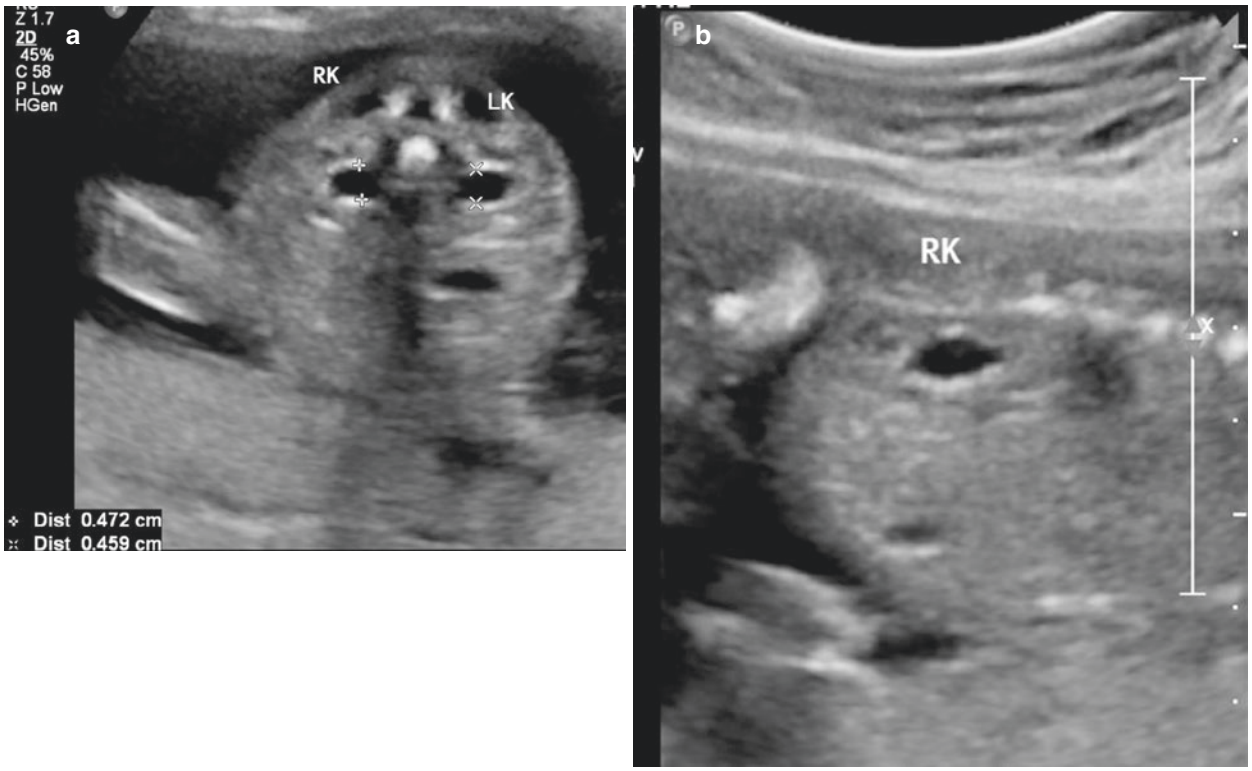

Fig. 3.10 Ultrasound appearance of UTD A1: Fetal kidneys at 21 weeks of gestation: (**a**) Transverse scan showing APRPD measuring less than 7 mm which is within the UTD A1 range. (**b**) Sagittal scan demonstrates normal parenchyma and no peripheral calyceal dilatation. (**c**, **d**) Fetal kidneys at 35 weeks: (**c**) Transverse scan shows APRPD of less than 10 mm which is within the UTD A1 range for this gestational age. (**d**) Sagittal scan demonstrates normal parenchyma and no peripheral calyceal dilatation

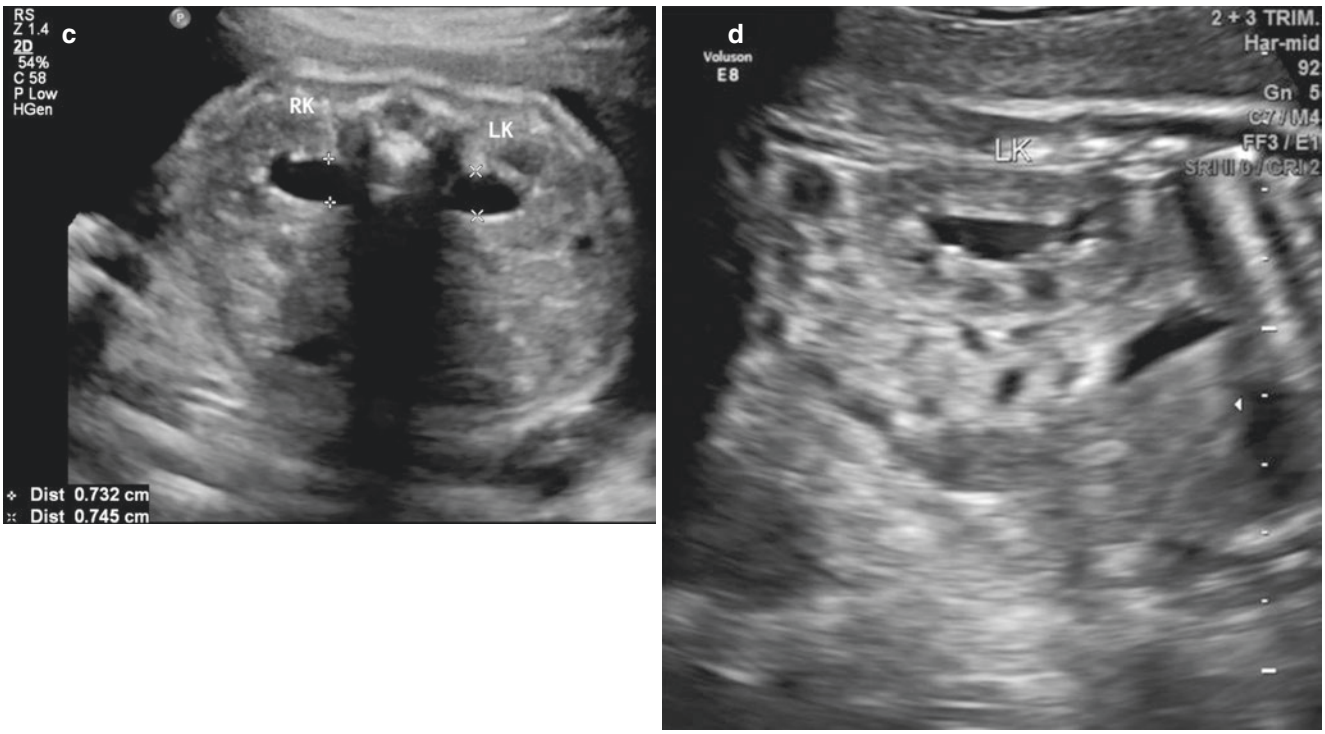

Fig. 3.10 (continued)

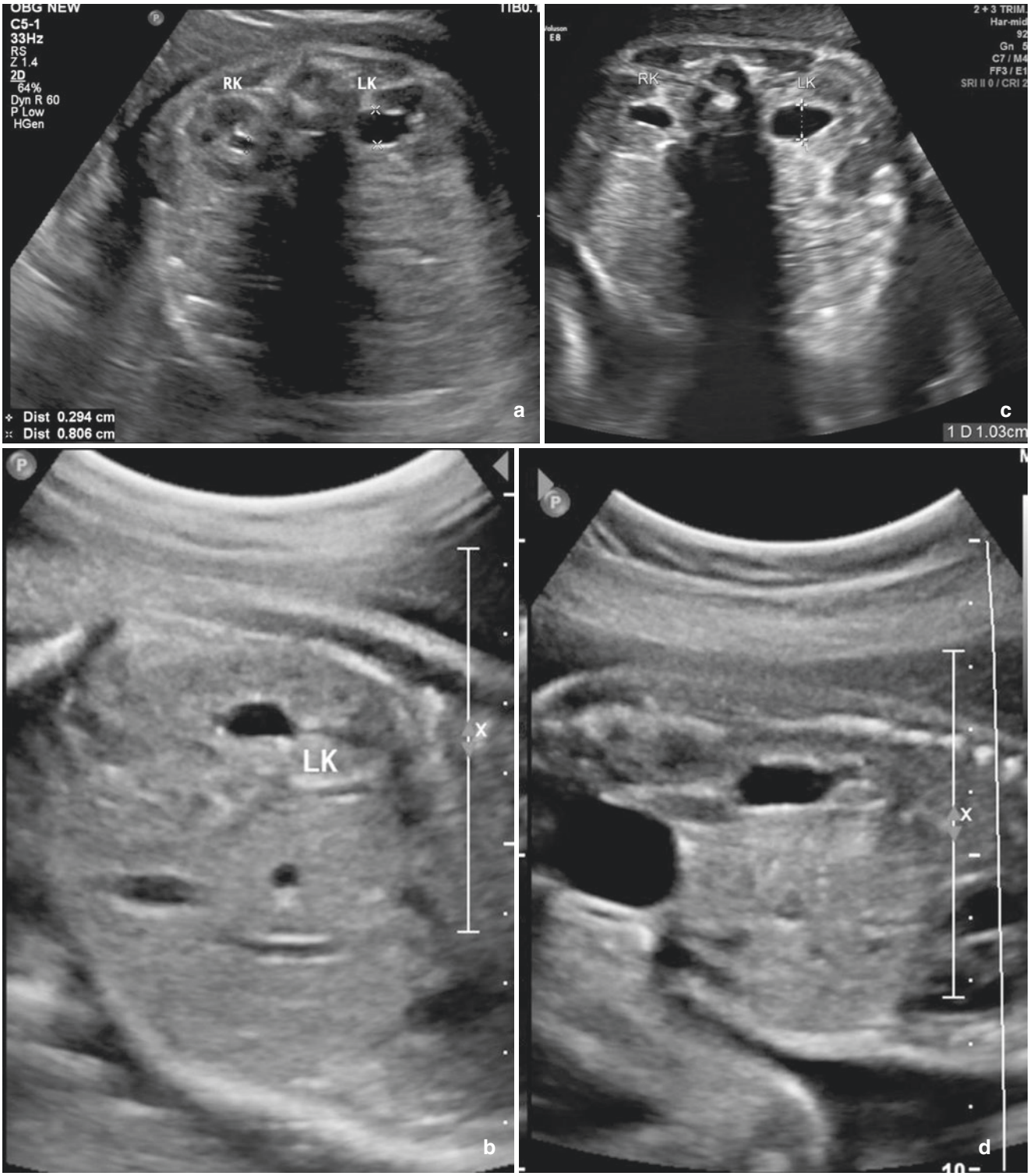

Fig. 3.11 Ultrasound appearance of UTD A2–3: (**a**, **b**) Fetal kidneys at 23 weeks gestation: (**a**) Transverse plane demonstrates an APRPD of more than 7 mm in left kidney (LK) that is in the UTD A2–3 range. (**b**) Sagittal scan showing normal parenchyma. (**c**, **d**) Fetal kidneys at 33 weeks: (**c**) Transverse scan shows APRPD of more than 10 mm which is in range of UTD A2–3 range. (**d**) Sagittal scan shows normal parenchyma (**e**, **f**). Fetus of 37 weeks: (**e**) Axial scan shows APRPD of less than 10 mm but (**f**) Coronal scan showing peripheral calyceal dilatation putting this in UTDA-2–3 group. (**g**, **h**) Fetus at 25 weeks showing APRPD of less than 7 mm but demonstrates abnormal echogenic parenchyma leading to classification of UTD A2–3 group. (**i**) Oblique scan demonstrates dilated ureter leading to classification of UTD A2–3 group

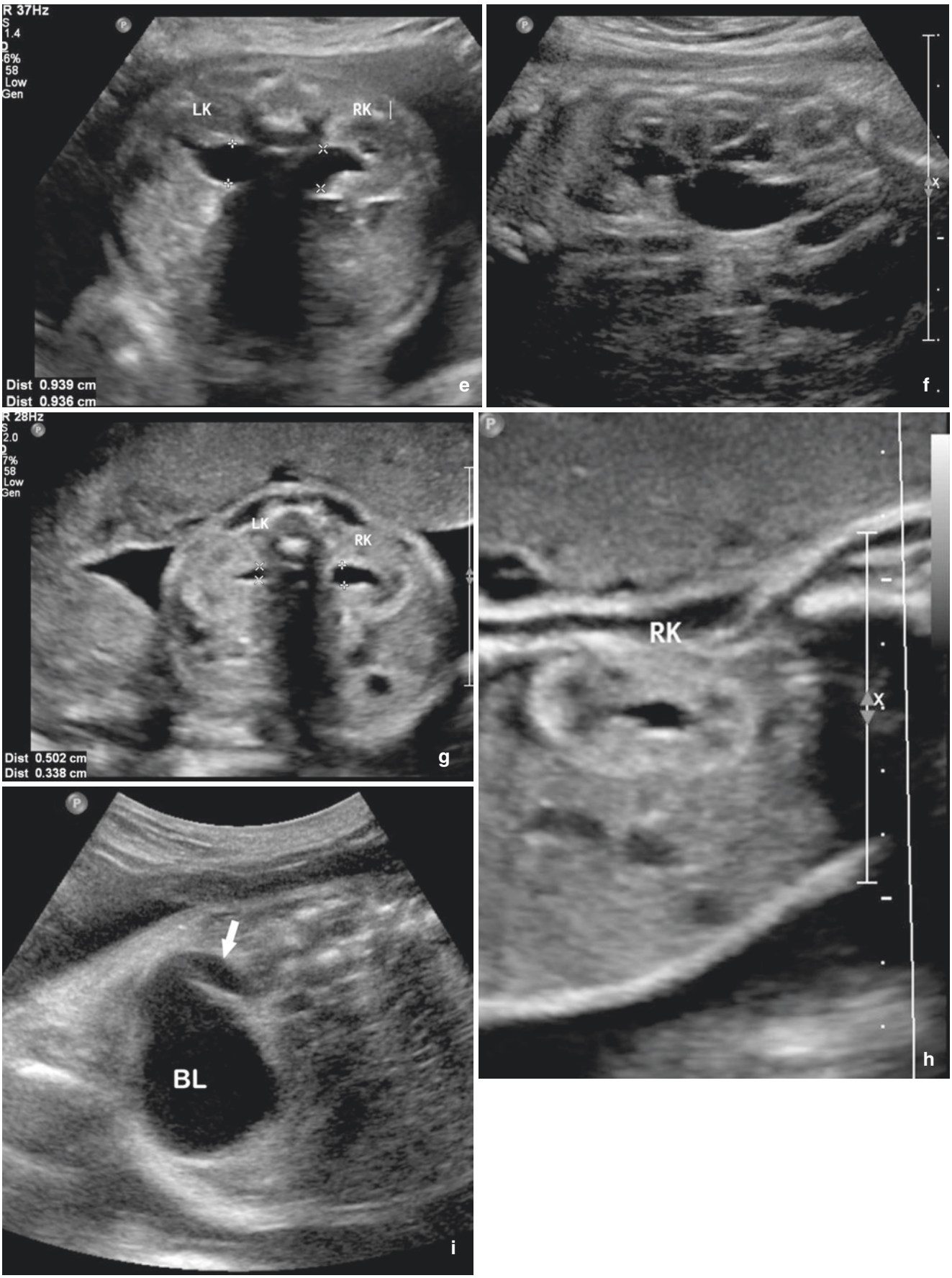

Fig. 3.11 (continued)

3.5 Cystic Renal Disease

Two main sonographic features lead to the suspicion of renal cystic disease in a fetus: cysts and renal hyperechogenicity. Cysts can occur anywhere in the kidney and can occur in one or both kidneys. Increased echogenicity can be visualized in the entire kidney, only the cortex, or only the medulla. There are no objective criteria for comparison of echogenicity up to 32 weeks. At later gestational ages, hyperechogenicity is confirmed when the renal cortex appears hyperechoic compared to liver and spleen.

In their article, Imaging and classification of congenital cystic renal diseases, Avni FE et al describe a decision tree approach once renal cystic disease is suspected. The basis of approach is a detailed sonographic analysis in addition to assessment of clinical data and the familial history. A detailed ultrasound examination includes renal size, defining the echogenicity of the cortex (hypoechoic, isoechoic or hyperechoic) and medulla (hypoechoic, hyperechoic) assessing the corticomedullary differentiation (CMD) (preserved, absent, reversed), evaluating cysts (number, size, location), calcifications and assessing the pelvicalyceal system. Whenever cystic kidneys are suspected, it is useful to perform a sonographic examination of the parents to check for unknown familial disease.

3.5.1 Decision Tree Approach to Renal Cystic Disease

See Fig. 3.12.

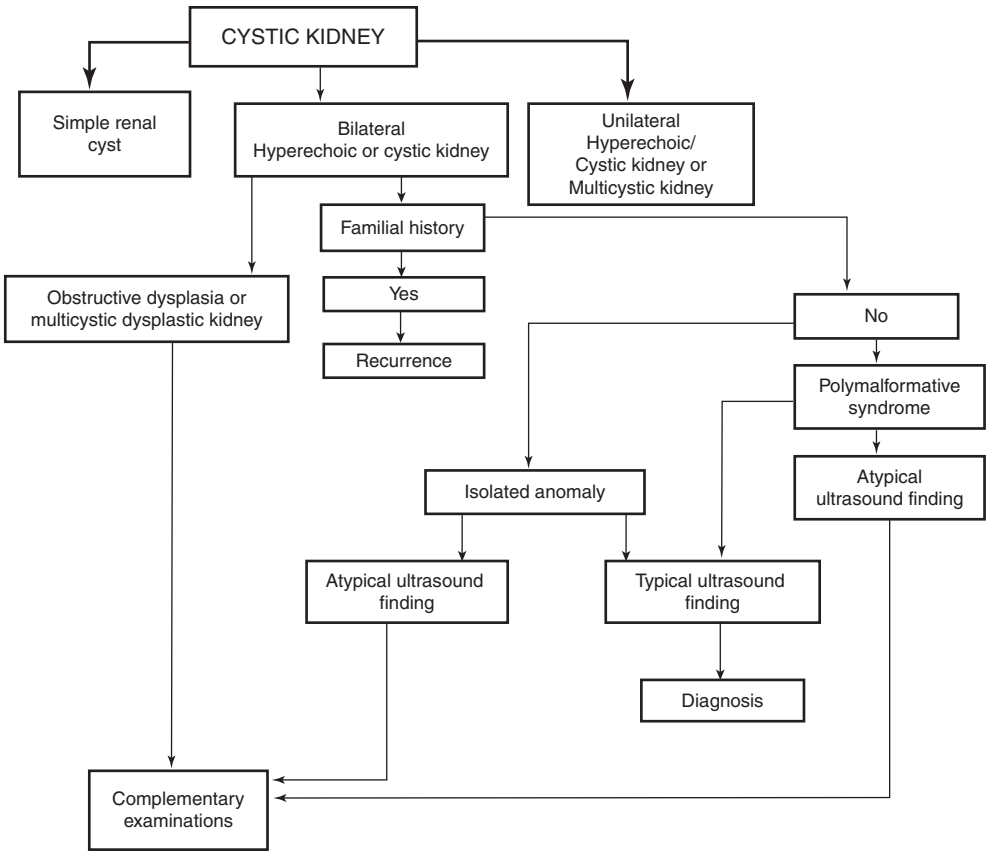

Fig. 3.12 Decision tree approach to cystic renal disease (Modified from the article by Avni FE et al)

3.5.2 Obstructive Dysplasia of Kidneys

- One of common causes of hyperechoic cortex with or without cysts is obstructive dysplasia. It can be unilateral or bilateral. The kidneys can be of variable size with hyperechoic normal or thinned irregular cortex, absent CMD and with or without cysts (Fig. 3.13). The pelvicalyceal system will be dilated.

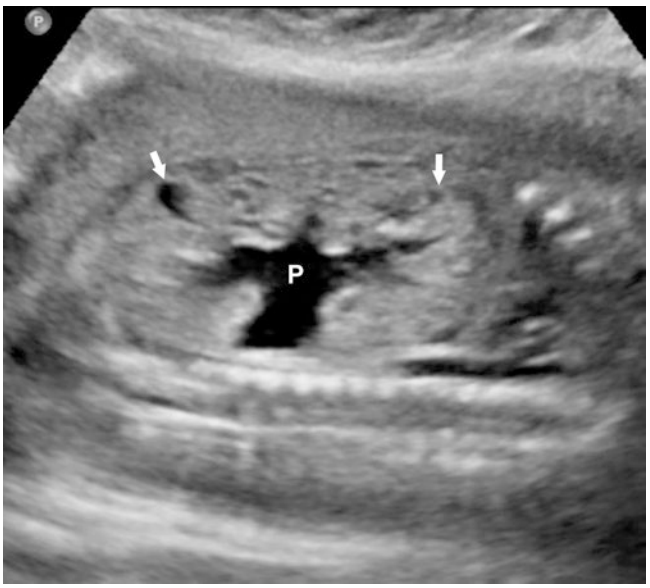

Fig. 3.13 Renal dysplasia with obstruction: Longitudinal scan of the kidney shows echogenic parenchyma without CMD and with small cysts (arrows). The collecting system (P) is dilated

3.5.3 Multicystic Dysplasia (MCD) of Kidney

- The second diagnosis to be considered is multicystic dysplasia of kidneys. There are multiple cysts of variable size without connections between them in the renal fossa with no or little parenchyma (Fig. 3.14).
- They can be unilateral or bilateral (Fig. 3.15), involving the segmental upper or lower poles of duplex kidney (Fig. 3.16), one moiety of horseshoe kidney (Fig. 3.17) or affect an ectopic kidney (Fig. 3.18).
- It is due to an abnormal development or associated with a significant percentage of cases with early obstruction. It may form part of some syndromes like Brachio-otorenal syndrome, cerebrorenodigital syndrome or VACTERL association. It can be associated with genital malformations both in girls (hemi uterus or uterine agenesis) and in boys (absent testis, seminal vesicle agenesis or cyst). The cysts can involute during pregnancy or after birth. The appearance of multicystic kidney may show some variations. One pattern shows peripheral small cysts and a large central cyst. This mimics hydronephrosis due to pelviureteric junction obstruction (Fig. 3.19).

The differentiating features are: the peripheral cysts do not communicate with the central cyst; the varying size of peripheral cysts and absence of renal parenchyma. Multicystic kidney is a nonfunctioning kidney. If it is bilateral, there will be anhydramnios and is not compatible with postnatal life.

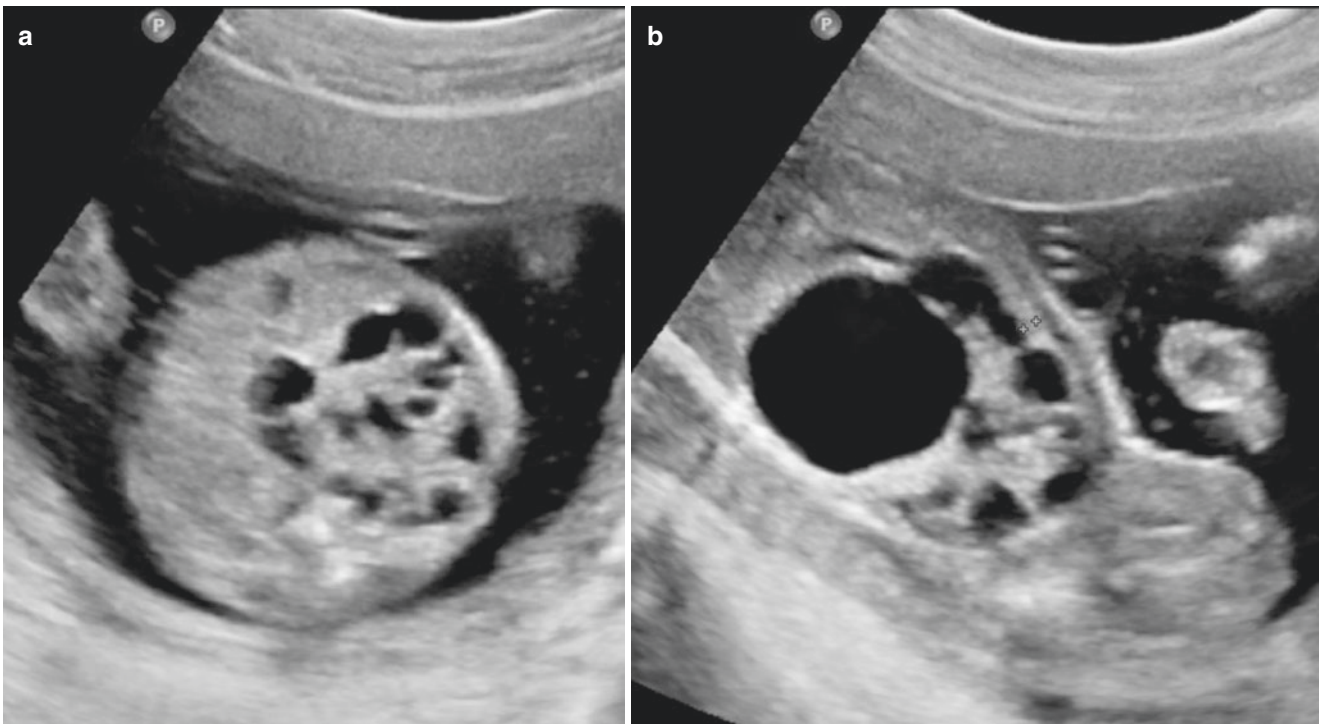

Fig. 3.14 Multicystic dysplasia: (**a**) Axial and (**b**) Longitudinal scan of the renal fossa showing multiple cysts of varying size without connection between them and without normal parenchyma

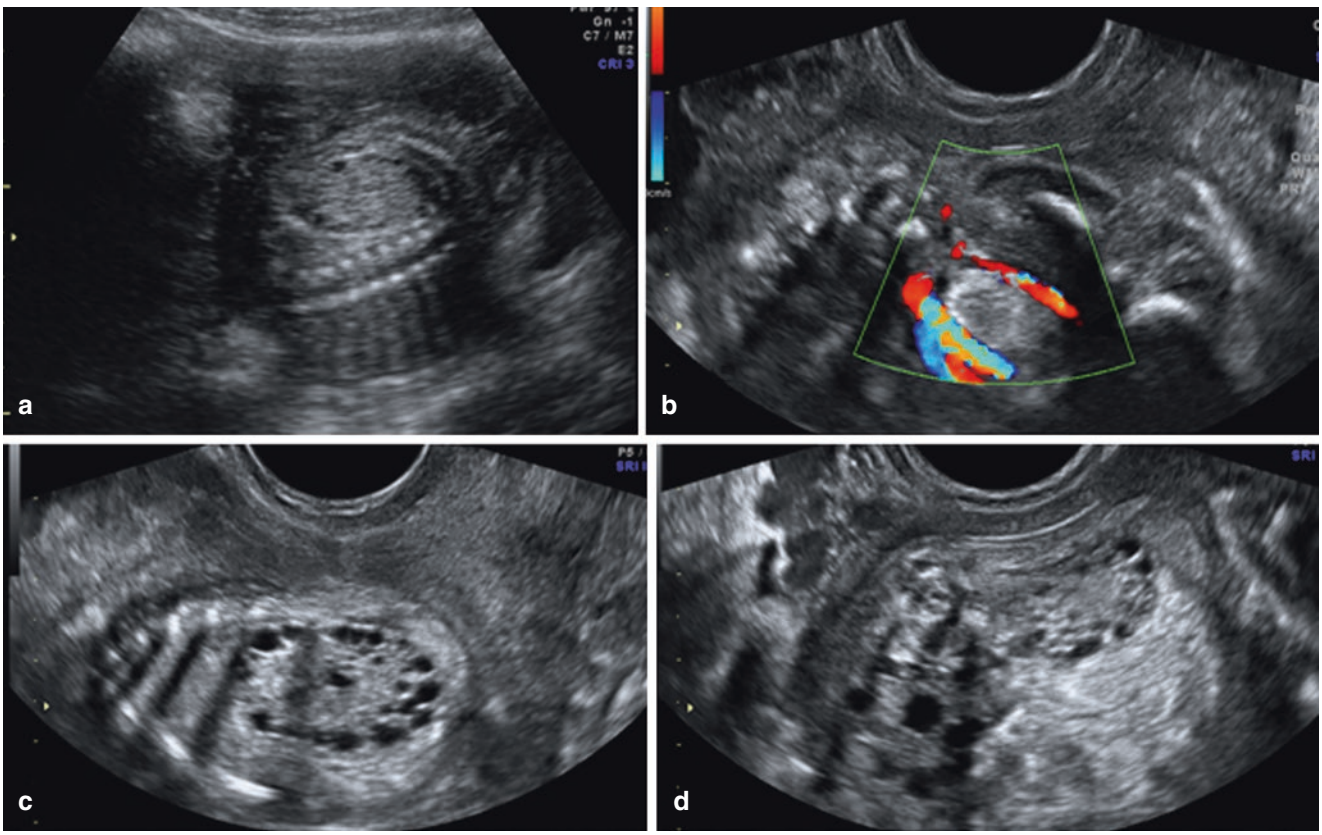

Fig. 3.15 Bilateral multicystic dysplasia: (**a**) Transabdominal Sonography of a 19 weeks fetus in breech presentation shows anhydramnios with apparently normal kidney. Endovaginal Sonography of (**b**) Pelvis showing the nonvisualized urinary bladder between the umbilical arteries. (**c**) Longitudinal scan of one kidney showing the typical appearance of MCD and (**d**) axial scan demonstrating MCD of both kidneys, explaining the anhydramnios

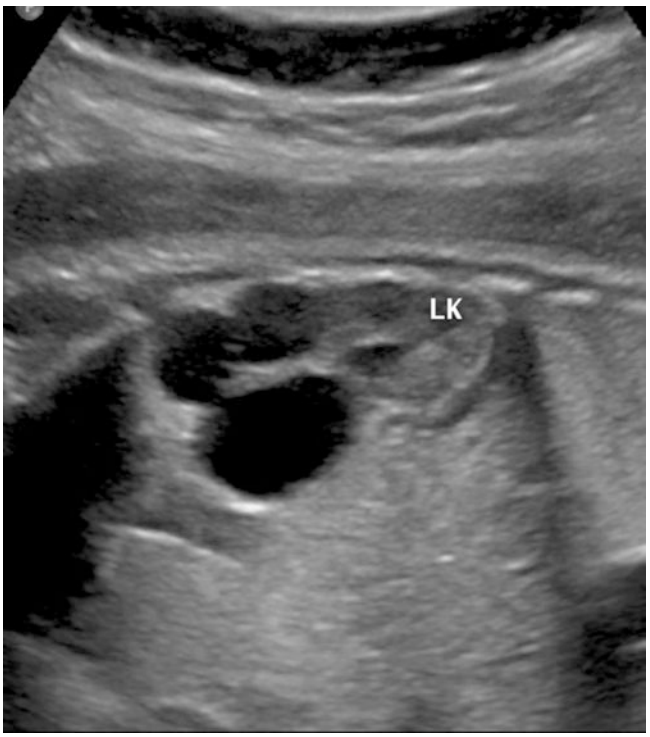

Fig. 3.16 Segmental multicystic dysplasia: Longitudinal scan of the kidney showing the MCD of lower half of the kidney. The upper half (LK) appears normal

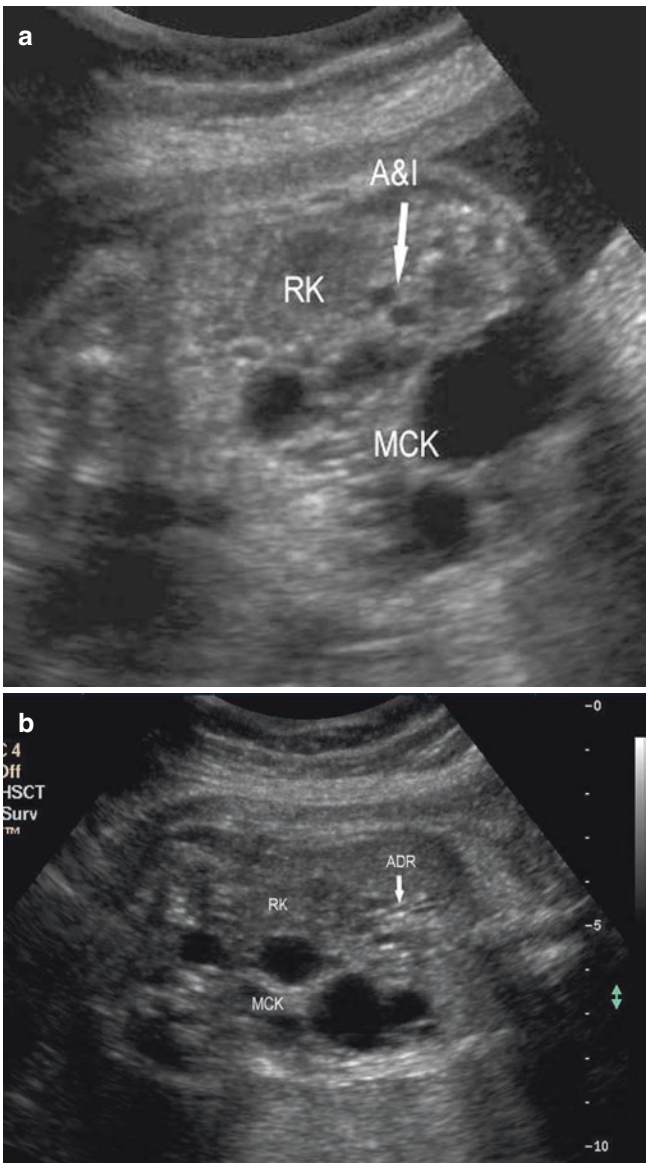

Fig. 3.17 Horseshoe kidney with multicystic dysplasia of one moiety: (**a**) Axial and (**b**) Coronal scan of the fetal abdomen demonstrating the Horseshoe kidney with isthmus anterior to the aorta and inferior vena cava (arrow A&I) with multicystic dysplasia (MCK) of the left moiety and isthmus with normal lower placed right kidney (RK) and elongated right adrenal (ADR) above the right kidney

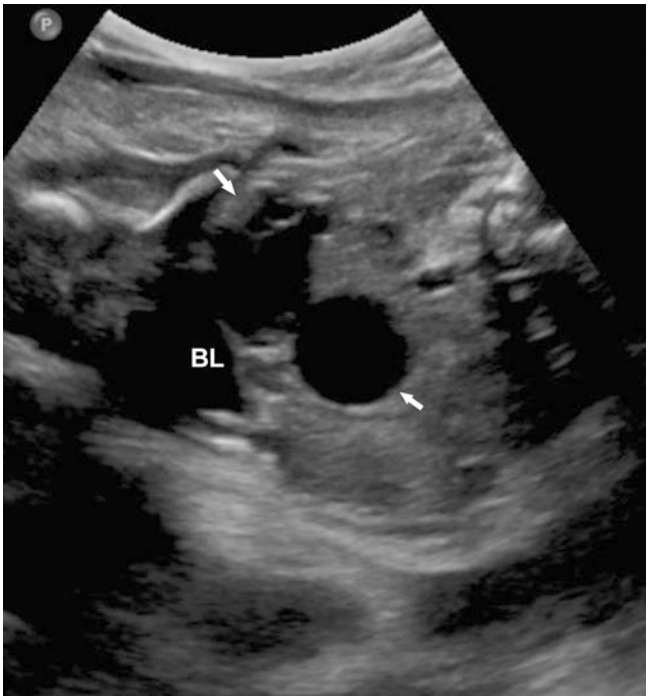

Fig. 3.18 Multicystic dysplasia of ectopic pelvic kidney: Transverse scan of fetal pelvis showing the multicystic dysplasia of ectopic presacral kidney (arrows) posterior to urinary bladder (BL)

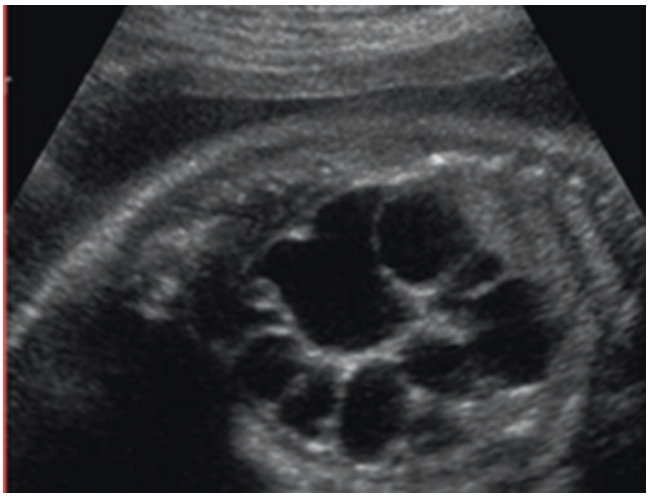

Fig. 3.19 Coronal scan of multicystic dysplastic kidney demonstrating the variant appearance of the central and medial large cyst with peripheral cysts mimicking hydronephrosis due to pelviureteric junction obstruction. Differentiating features are varying size of peripheral cysts, lack of connection with the larger central cyst and absent parenchyma

3.5.4 Simple Renal Cyst

- Simple renal cyst is very rare in the fetuses. It is seen as a well-defined unilocular anechoic lesion with thin smooth walls and clear fluid (Fig. 3.20).

  Hydronephrosis of one of the moieties in duplex kidney is to be ruled out by looking for continuity with ureter on coronal scan (Fig. 3.47a).

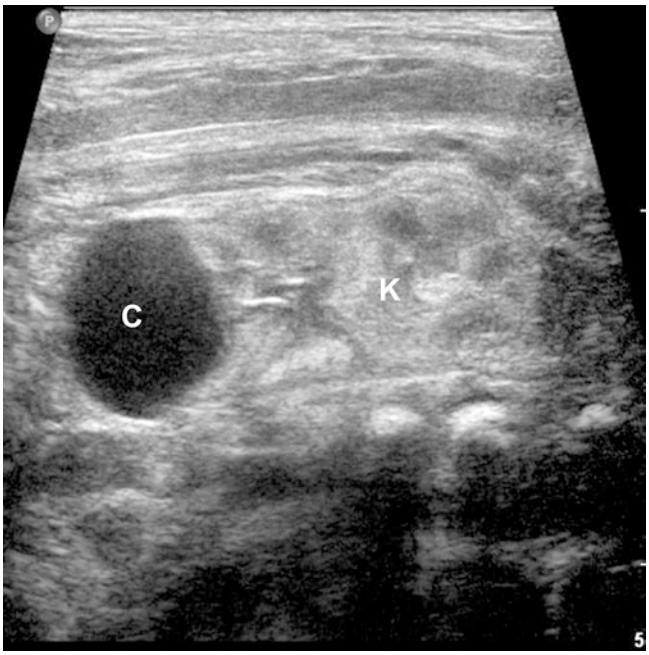

Fig. 3.20 Simple renal cyst [C] seen in a longitudinal scan of the kidney (K) seen as a well-defined round anechoic lesion with thin smooth walls and clear fluid in the lower pole

3.5.5 Inherited Renal Cystic Disease

- Knowledge of familial history is essential. If there is familial history of renal cystic disease, fetus with abnormal kidneys suggests recurrence of the disease. If there is no familial history, the fetuses could be categorized into two groups:
  - Isolated renal finding.
  - Those associated with other organ malformations.

Both categories of fetuses can be further divided into those with typical ultrasound patterns suggestive of specific diagnoses and those with atypical ultrasound patterns.

- A typical pattern means all sonographic features such as a typical pattern of cysts (size, location, number), appearance of the parenchyma (echogenicity, CMD), and renal size that leads to a straight-forward specific diagnosis (isolated or associated with other malformations) like Autosomal Recessive Polycystic kidney disease (ARPKD). Nonspecific or atypical pattern means that no significant features are present that lead to a specific diagnosis and needs an approach with differential diagnosis tables. In rare cases, supplementary examinations, such as genetic studies and MRI may be necessary to reach the diagnosis.
- Typical ultrasound patterns can be seen both as isolated findings and as polymalformative syndromes. Although the ultrasound findings are typical of these conditions, they need a genetic confirmation.

Autosomal Recessive Polycystic Kidney Disease (ARPKD)

ARPKD is the most common childhood ciliopathy with incidence of 1/20,000 live births. It is caused by mutation in the PKHD 1 gene. The extent of ARPKD can be variable and evolve over time. They are seen as a spectrum, depending on the time of manifestation and severity, as fetal, infantile and juvenile. Fetal type presents in second trimester as oligohydramnios. Both the kidneys are markedly enlarged (>4SD) and echogenic, filling almost the entire abdomen and even bulging out. There is no CMD with or without evident cysts (Fig. 3.21).

The hyperechogenicity is due to the multiple interfaces of the dilated renal tubules. High frequency scan will show numerous tiny linear cysts. The urinary bladder will not be seen. The infantile type has similar features but manifests in the third trimester. The kidneys are seen as very large and echogenic with hyperechoic medullary pyramids and oligohydramnios. The rare less severe juvenile type, presents as slightly enlarged kidneys with enlarged echogenic pyramids (reverse CMD) (Fig. 3.22), normal urinary bladder and normal amniotic fluid volume. The children with this type develop hepatic fibrosis in their later childhood.

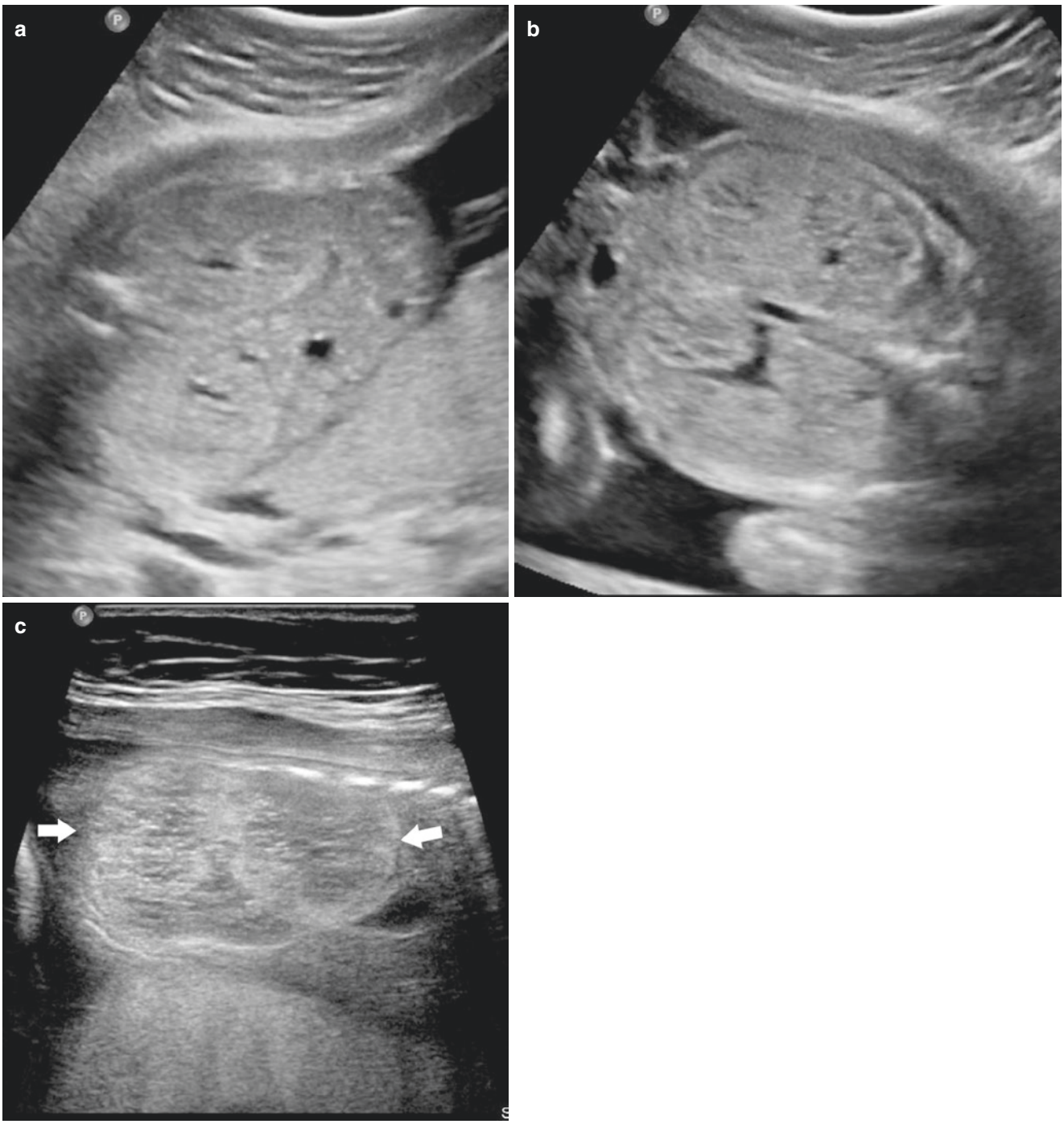

Fig. 3.21 Autosomal recessive polycystic kidney: (**a**) Axial and (**b**) Coronal scan of the fetal abdomen demonstrating the markedly enlarged hyperechoic kidneys without CMD. There is oligohydramnios. (**c**) High frequency scan of the kidney (arrows) shows tiny linear cysts in medulla

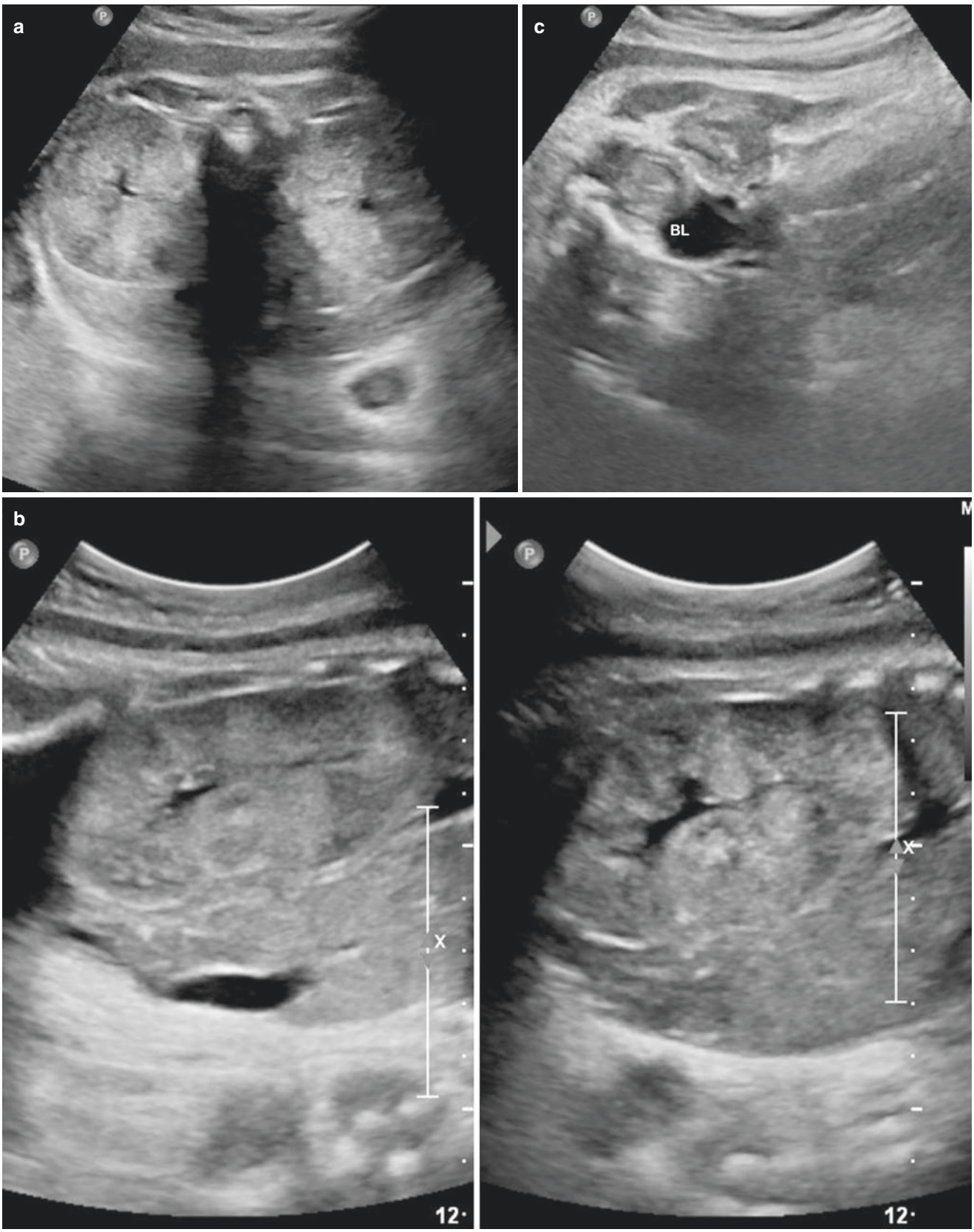

Fig. 3.22 Juvenile Autosomal recessive polycystic kidney in fetus of 35 weeks: (**a**) Axial and (**b**) Longitudinal scan demonstrating enlarged kidneys with enlarged echogenic pyramids (reverse CMD). (**c**) shows normal urinary bladder (BL)

Glomerulocystic Kidney Disease (GCKD)

Fetus shows diffusely hyperechoic and enlarged (+2SD) kidneys without CMD but with multiple sub capsular cysts and additional cortical cysts (Fig. 3.23).

The cysts develop in utero or postnatally. This condition has autosomal dominant transmission. The same pattern is seen in autosomal dominant polycystic kidney disease (ADPKD). The appearance should lead to scan of parents. The same pattern can be seen in HNF1B/TCF2 gene mutation. Besides producing renal cysts, TCF2 mutations express various other renal anomalies (renal agenesis, hypoplasia, horseshoe kidney, cystic dysplasia) and genital malformation. Because several TCF2 mutations can occur, the ultrasound findings of disease vary. Cysts can develop in the cortex (sub capsular), at the corticomedullary junction, or in the medulla. Detectable cysts can develop in utero or after birth. The cysts can be very large (more than several centimeters). TCF2 mutations can be confirmed only with knowledge of a familial history or results of genetic studies.

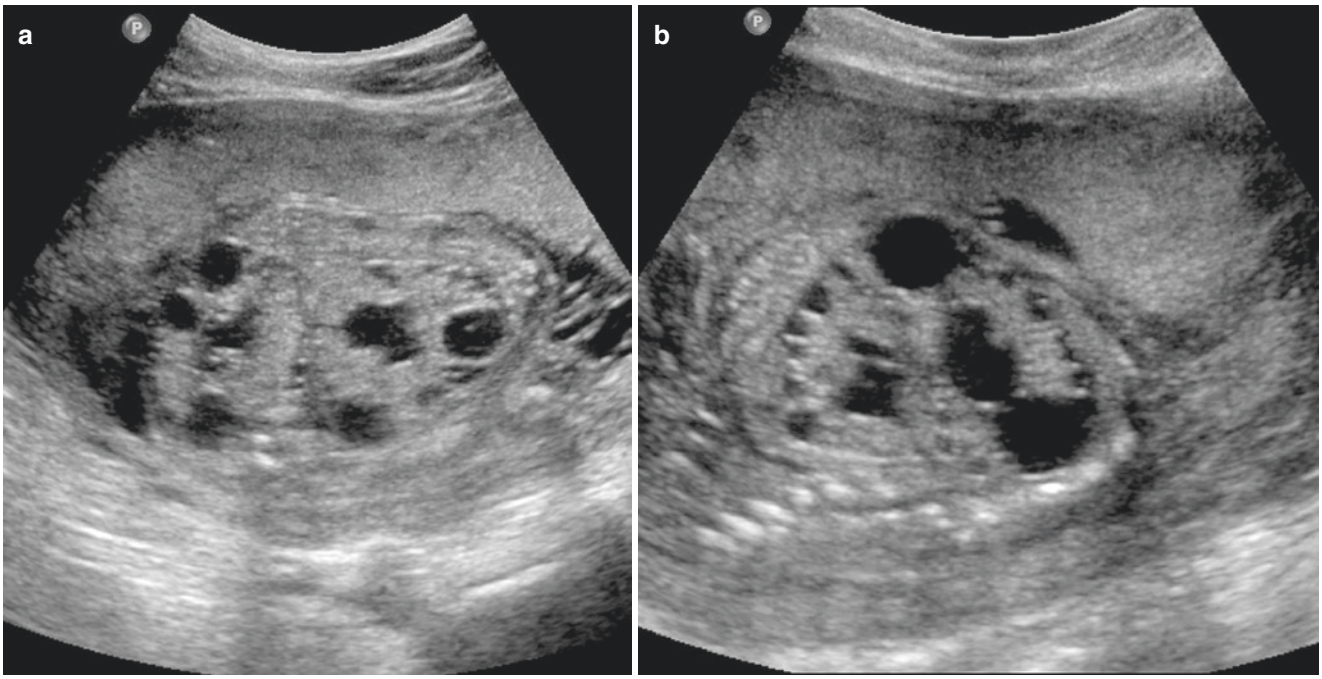

Fig. 3.23 Glomerulo cystic kidney disease: (**a**) Axial and (**b**) Longitudinal scans revealing enlarged hyperechoic kidneys without CMD with multiple cysts, some of them are subscapular

Autosomal Dominant Polycystic Kidney Disease (ADPKD)

ADPKD affects about 1/1000 people. It is an important differential diagnosis of hyperechoic kidneys with increased CMD due to hyperechoic cortex with cortical cysts (Fig. 3.24).

ADPKD affects the kidneys, liver, pancreas and macro vessels. Two mutations have been recognized PKD1 and PKD2. PKD1 causes more renal disease. PKD2 causes extrarenal manifestations such as intracranial aneurysm. Only the renal involvement can be detected in utero, as renal cysts. The clue to the diagnosis is a familial history or detection of yet unknown familial disease with renal ultrasound of the parents and grandparents. ADPKD can resemble GCKD appearance.

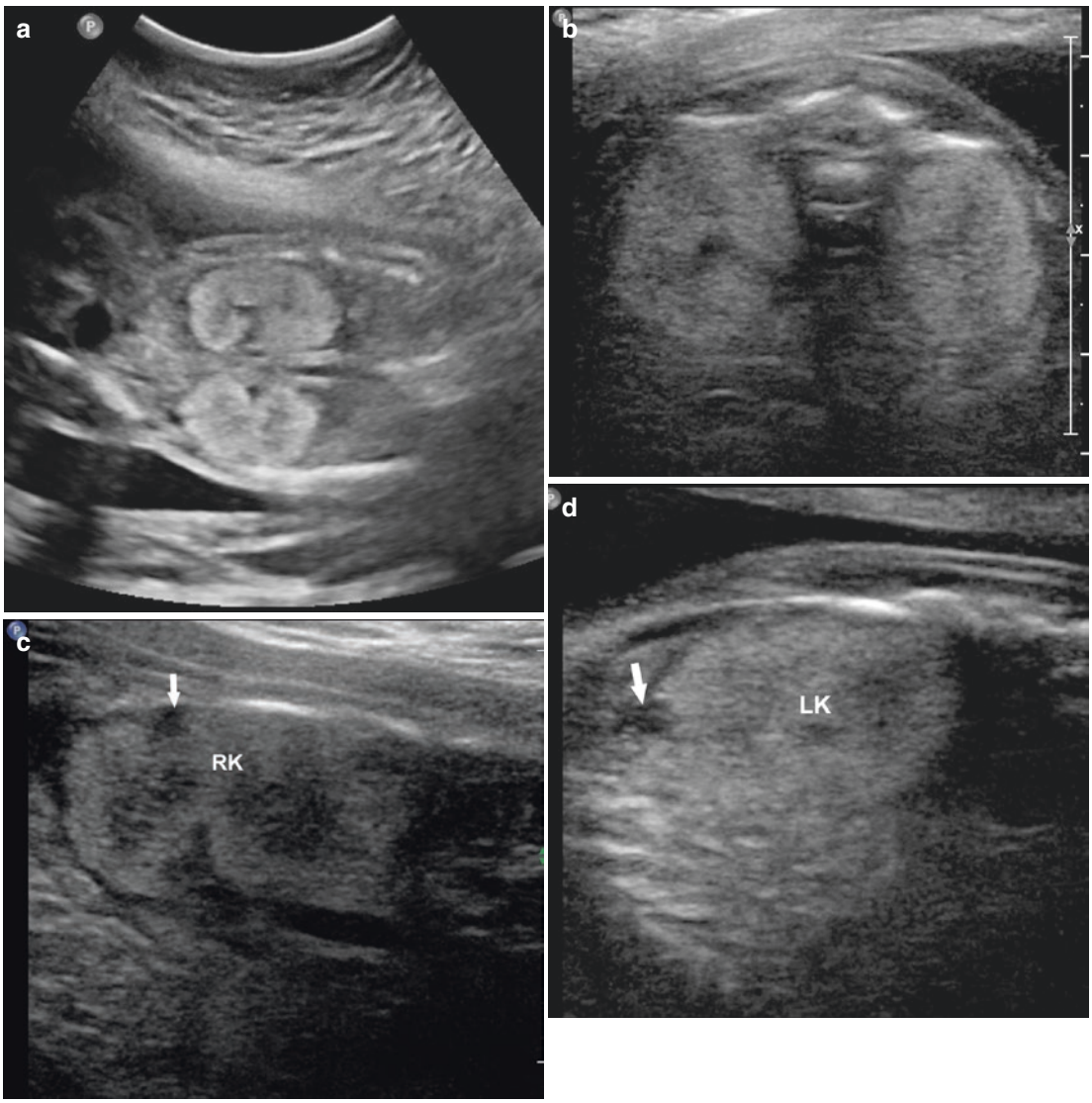

Fig. 3.24 Autosomal dominant polycystic kidney: (**a**) Coronal scan demonstrating bilateral enlarged hyperechoic kidneys with increased CMD. High frequency axial (**b**) and longitudinal (**c**, **d**) scan demonstrating the small cortical cysts (*arrow*) in both kidneys

Nephronophthisis

Nephronophthisis shows the fourth typical pattern where the kidneys are hyperechoic, normal sized or small and without CMD with renal cysts at the corticomedullary junction (Fig. 3.25).

It is a group with autosomal recessive inheritance. It can be diagnosed at any age. The same pattern can be seen in various syndromes.

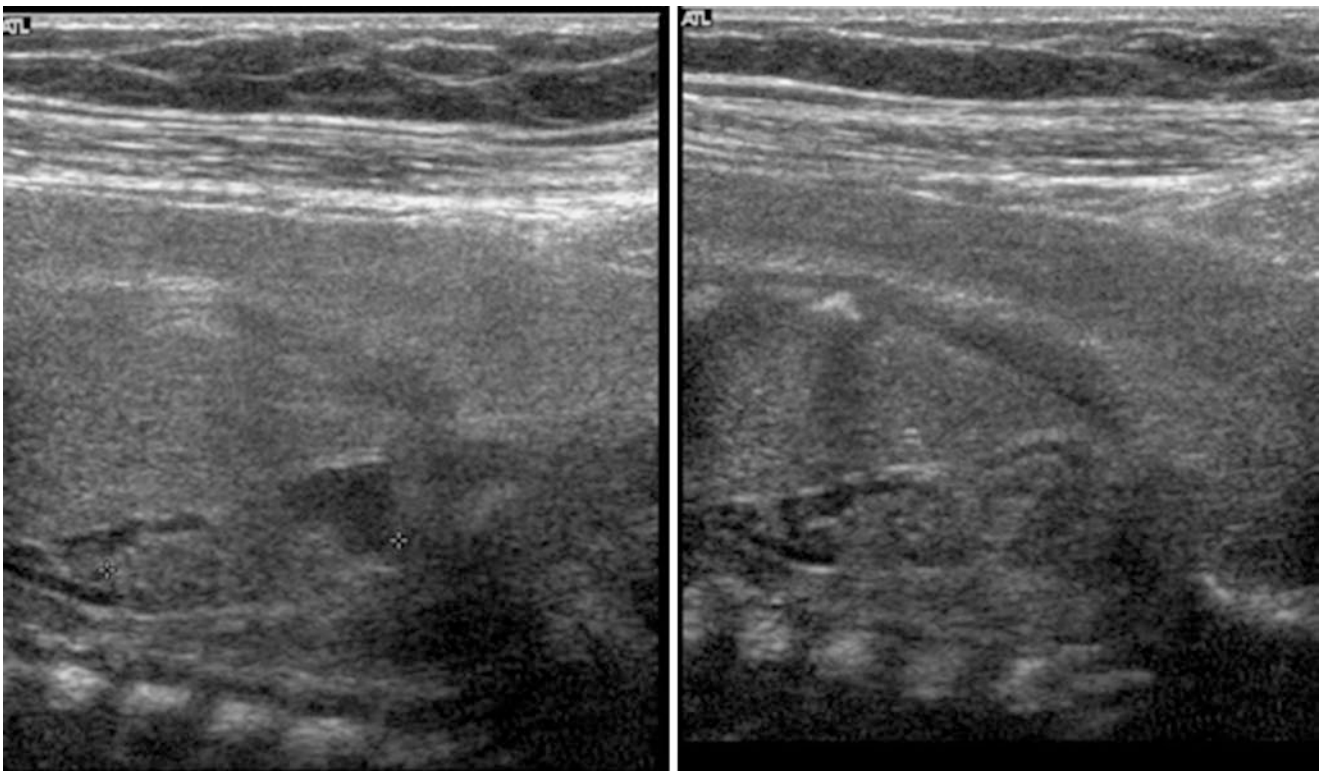

Fig. 3.25 Nephronophthisis: High frequency scan of the kidneys reveal small echogenic kidneys with cysts

3.5.6 Renal Anomalies with Typical Ultrasound Pattern as Part of Polymalformative Syndromes

Renal cystic disease may be seen as part of some syndromes. When there are renal anomalies, complete survey of the fetus has to be performed to detect associated malformation in other organ systems. The association between renal cystic disease and malformations of other systems is found to be characteristic of a syndrome or association. In Bardet-Biedl syndrome (BBS), renal changes of markedly enlarged (>4SD) diffusely hyperechoic kidneys with loss of CMD are associated with postaxial polydactyly, hypogonadism, obesity and retinitis. It is an autosomal recessive genetically heterogeneous ciliopathy. The renal changes and polydactyly are seen prenatally (Fig. 3.26).

Meckel-Gruber Syndrome is another autosomal recessive syndrome in which the kidneys are markedly enlarged (4SD) with enlarged hypoechoic medulla containing cysts associated with postaxial polydactyly and anomalies of central nervous system, more commonly encephalocele (Fig. 3.27).

The Meckel Gruber Syndrome develops early and may be diagnosed in first trimester and renal medullary changes are more profound compared to BBS. The combinations of renal, hepatic and pancreatic dysplasia (RHPD) also known as Ivemark II syndrome, is very rare and uniformly fatal. The patterns of renal, hepatic and pancreatic involvement were indistinguishable from those reported in several other syndromes, including Jeune Asphyxiating Thoracic Dystrophy (JATD) and Ellis-Van Creveld syndrome (EVC). In the MIM system, RHPD is described along with autosomal recessive polycystic kidney disease. Renal hepatic pancreatic dysplasia (Ivemark II Syndrome) shows renal cystic changes of glomerulocystic or medullary dysplasia type, hepatic dysplasia in the form of dilated bile ducts and pancreatic cysts (Fig. 3.28).

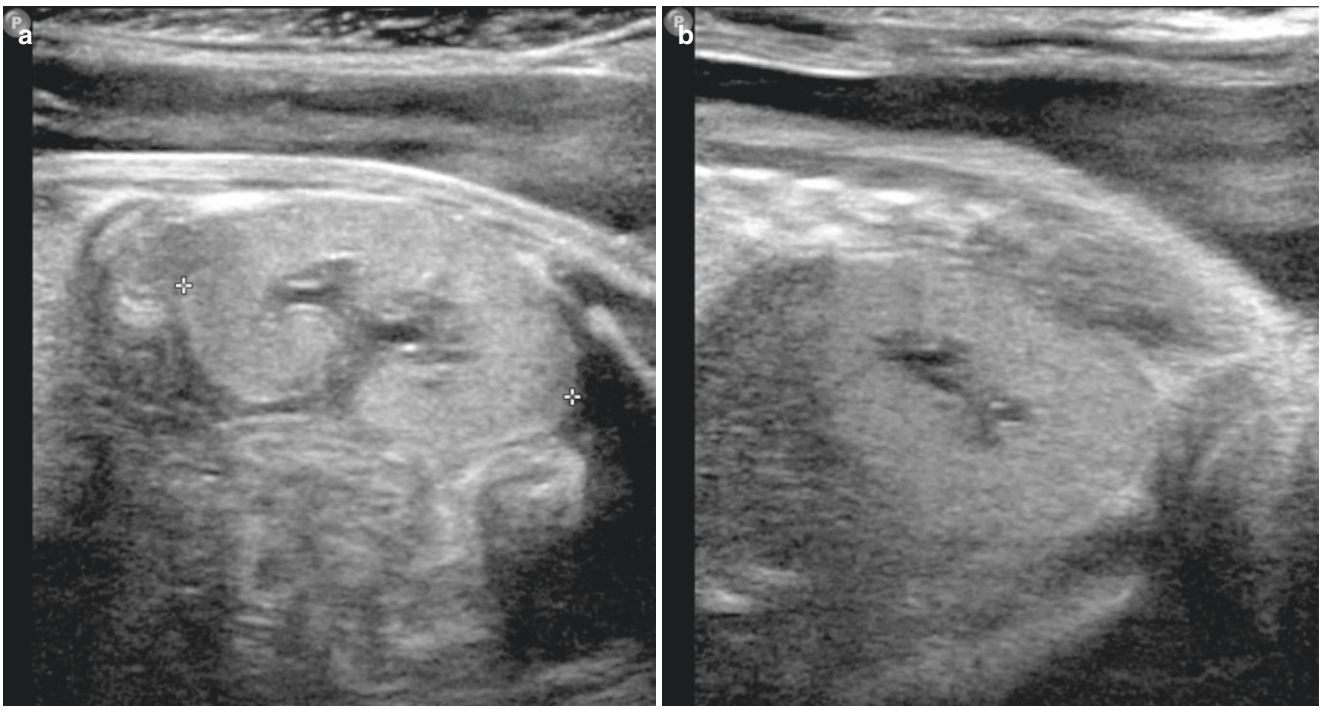

Fig. 3.26 Bardet–Biedl syndrome: High frequency longitudinal scan of the kidneys (**a**, **b**) demonstrating enlarged hyperechoic kidneys without CMD with polydactyly of foot (**c**) and hand (**d**)

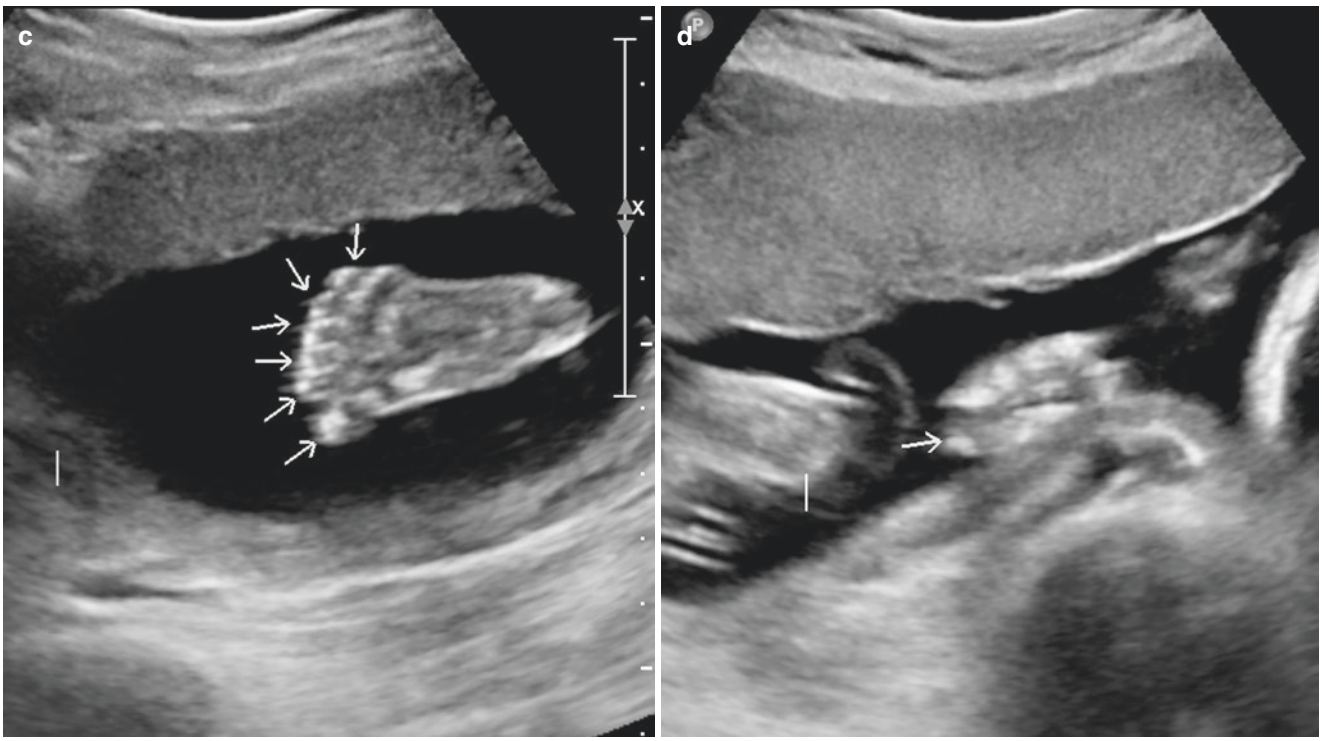

Fig. 3.26 (continued)

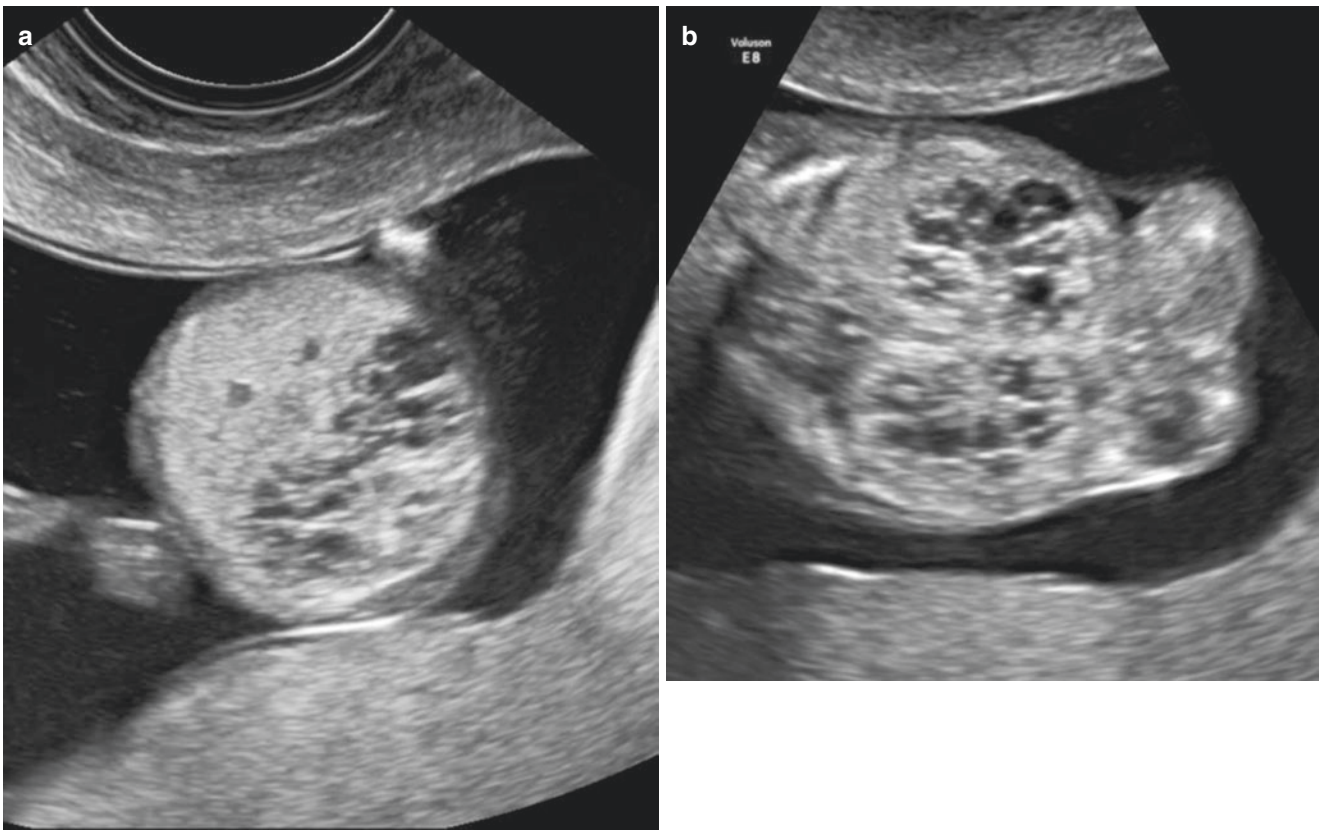

Fig. 3.27 Meckel-Gruber system: (**a**) Axial and (**b**) Coronal scan demonstrating the bilateral markedly enlarged kidneys with enlarged hypoechoic medulla containing cysts associated with (**c**) encephalocele (pointing fingers) and polydactyly of foot (**d**) and hand (**e**)

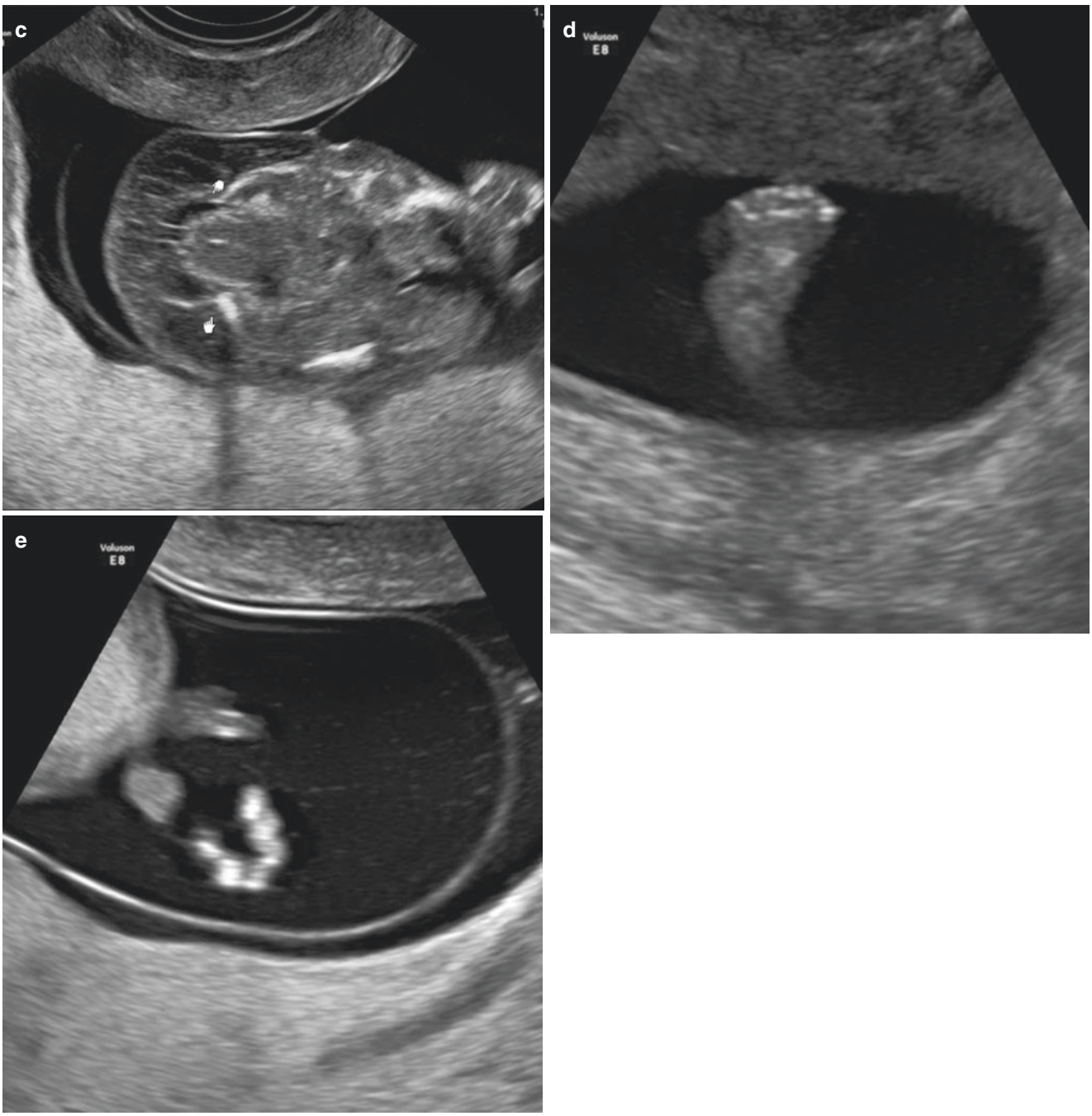

Fig. 3.27 (continued)

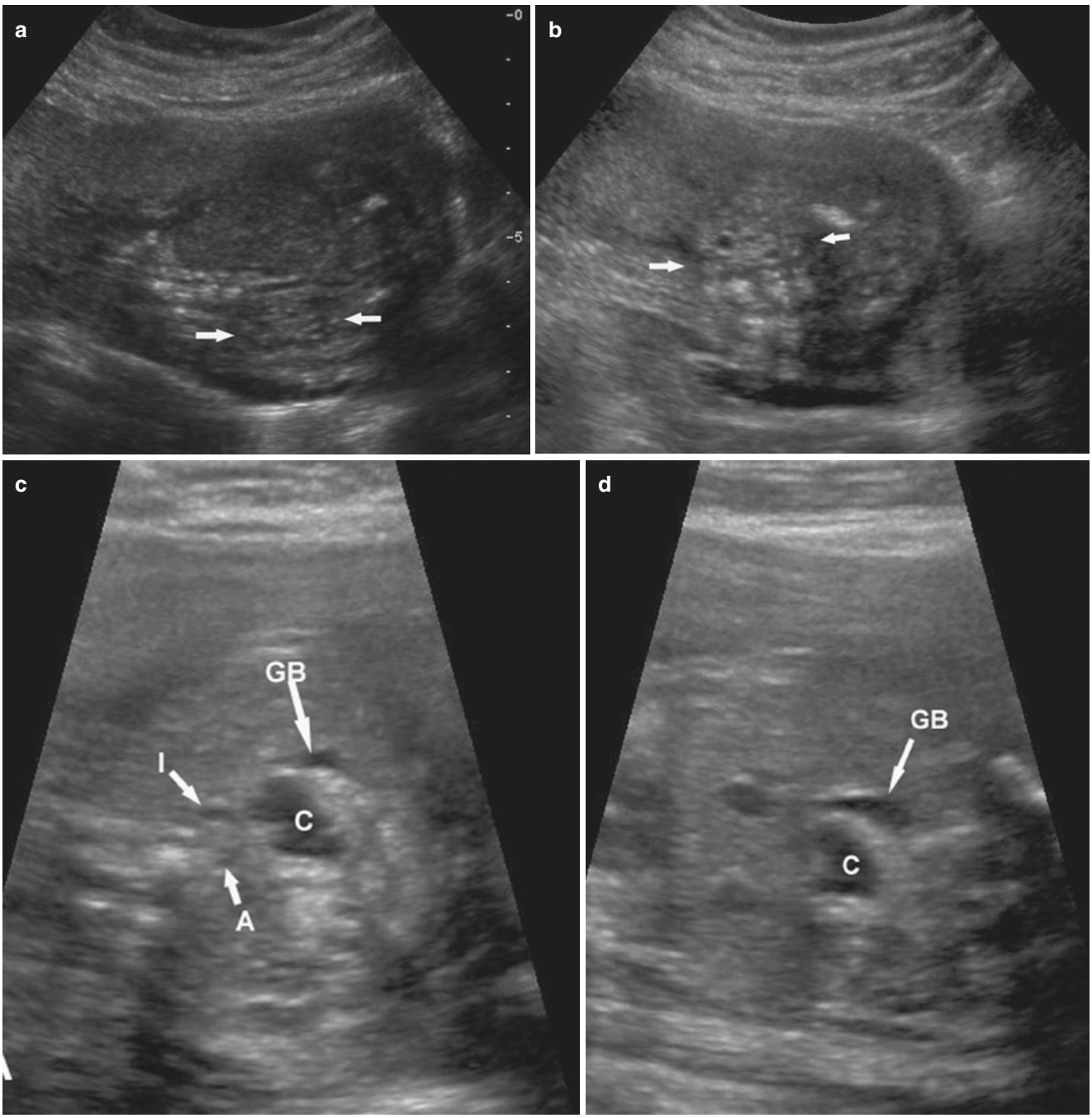

Fig. 3.28 Renal Hepatic Pancreatic Dysplasia: Longitudinal scan of the kidneys (arrows) showing multiple cysts in them. (**a**) Left Kidney. (**b**) Right Kidney. Transverse (**c**) and longitudinal (**d**) scans of upper abdomen showing the pancreatic cyst (C). *A* Aorta, *GB* Gall bladder, *I* Inferior vena cava. (**e**) Transverse scan of liver showing dilated right and left hepatic ducts (arrow) anterior to right and left branches of the portal vein. (**f**) Color Doppler scan of same section confirms blood flow in portal vein. (**g**) Autopsy picture of bilateral multicystic kidneys. (**h**) Autopsy picture of cut section of pancreas showing the irregular cyst in head of the pancreas

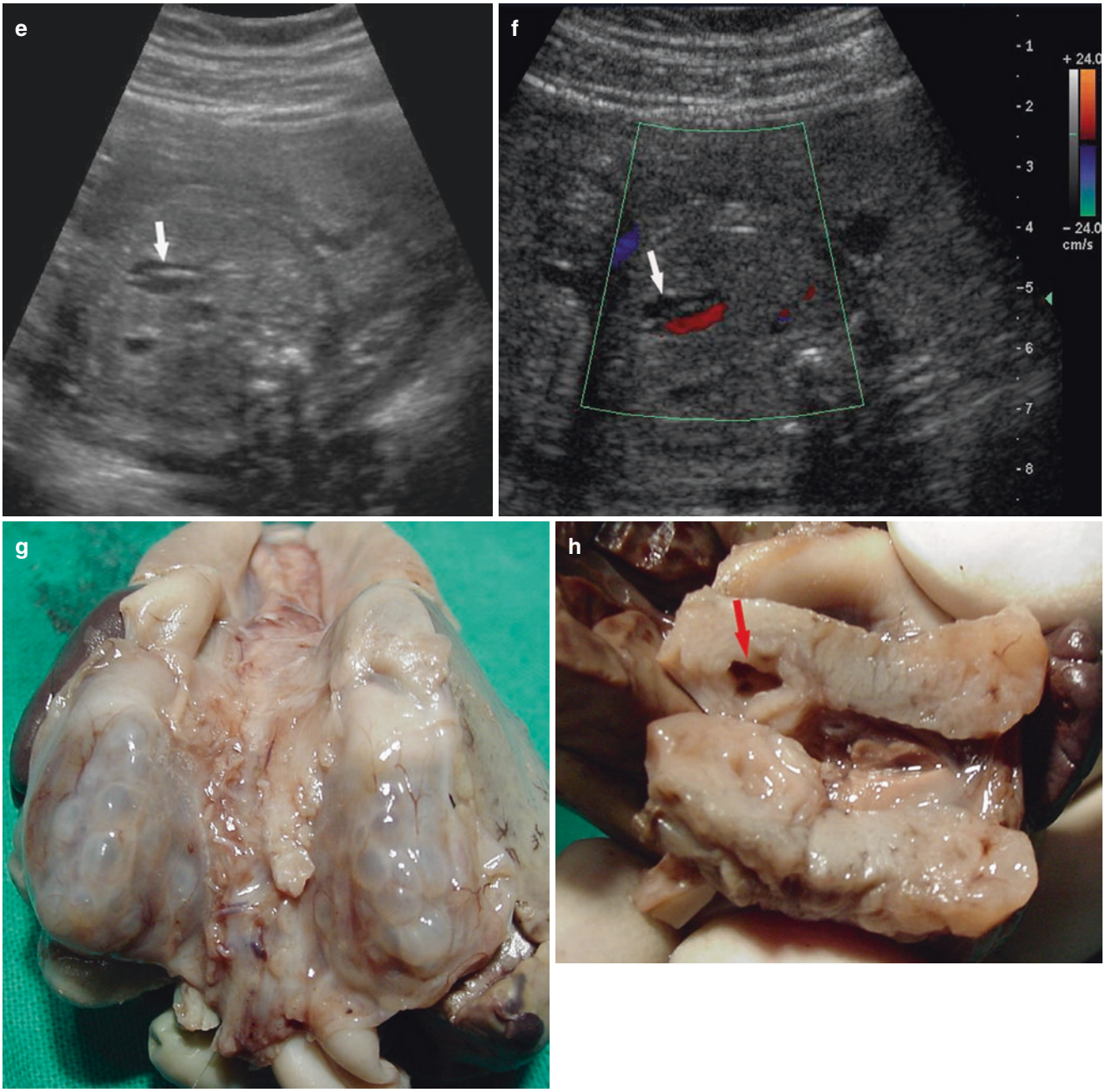

Fig. 3.28 (continued)

3.6 Renal Anomalies with Atypical Ultrasound Pattern

1. Simple renal cyst.
2. Bilateral echogenic kidneys.

The incidence of this finding on prenatal sonography is increasing and becoming a challenge in differential diagnosis. The conditions which can present with this feature are as follows:

(a) Renal cystic disease which has been discussed earlier.
(b) Cytomegalo virus (CMV) infection: In CMV infection, the kidneys are either normal in size or slightly enlarged and echogenic. The corticomedullary differentiation is present (Fig. 3.29). The urinary bladder and amniotic fluid volume are normal. The other markers of CMV infection may be seen.
(c) Nephrotic syndrome—Finnish type.
(d) Medullary Nephrocalcinosis (Fig. 3.30).
(e) Some trisomy.
(f) Transient finding in normal fetuses: Echogenic kidneys of normal size, normal urinary bladder and normal amniotic fluid volume have good outcome and are usually normal.

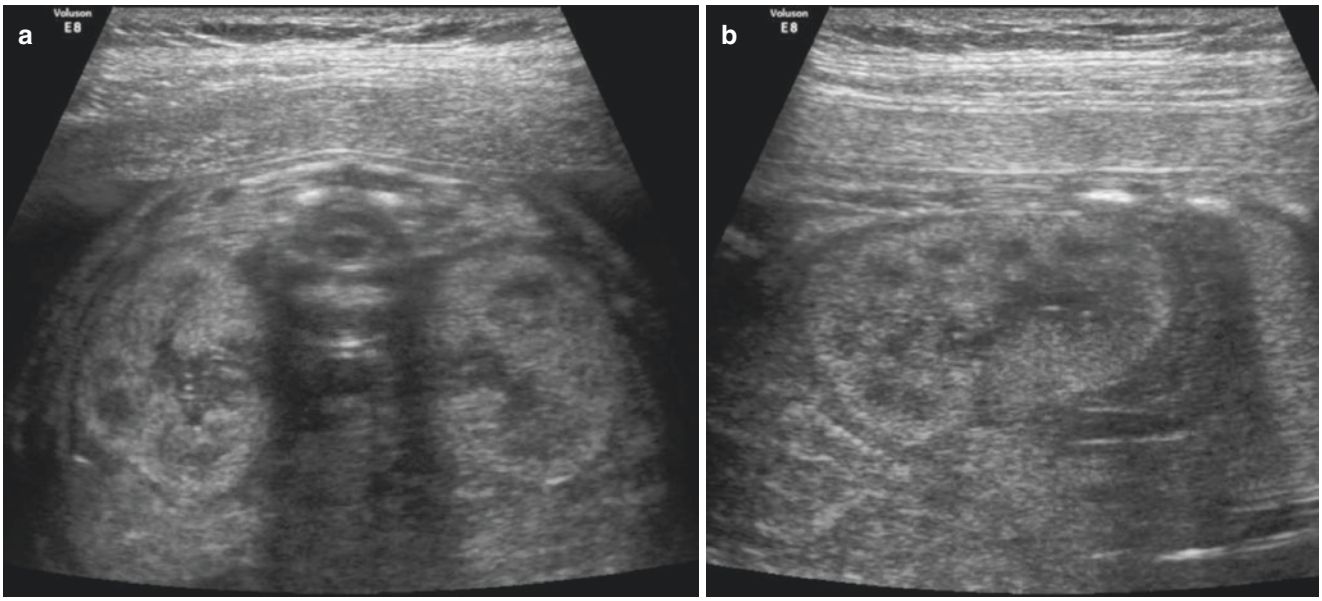

Fig. 3.29 Cystomegalo virus (CMV) infection: High frequency (**a**) Axial and (**b**) longitudinal scan, demonstrating slightly enlarged echogenic kidneys with preserved CMD

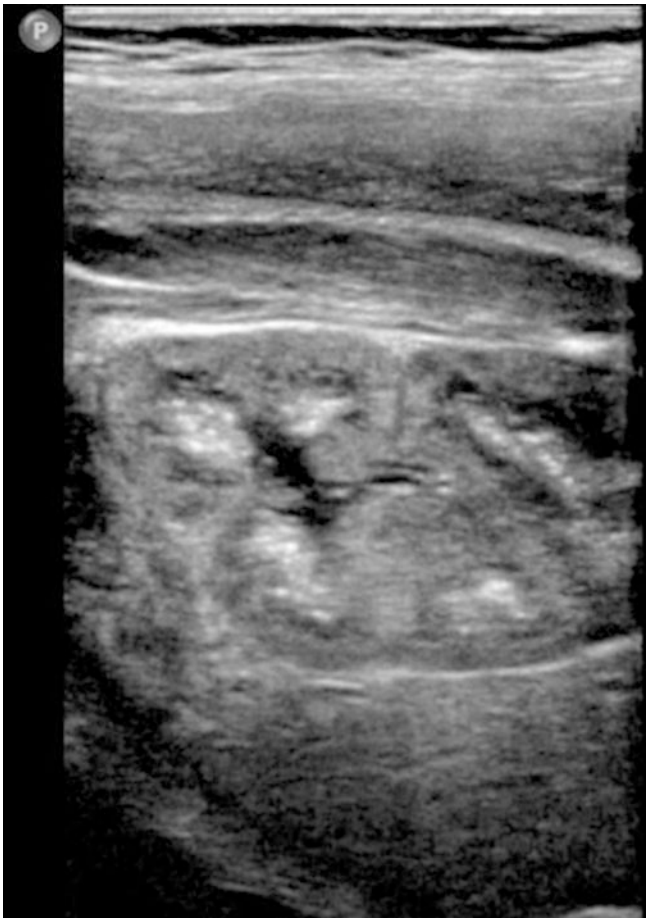

Fig. 3.30 Medullary nephrocalcinosis: Longitudinal high frequency scan of the kidney shows bunches of small calcifications in the medullary pyramids

3.7 Nonvisualized Kidney

3.7.1 Unilateral Nonvisualized Kidney

On axial scan, one kidney may not be seen. A coronal or sagittal scan will confirm the same by showing elongated adrenal gland replacing the kidney (lying down adrenal sign). Rest of the fetal abdomen should be evaluated to look for an ectopic kidney. Unilateral nonvisualized kidney may be due to:

1. Unilateral renal agenesis: Unilateral renal agenesis is due to failure of development of ureteric bud. It is three to four times more common than bilateral renal agenesis (1 in 1000 new born). The kidney is absent and an ectopic kidney is not seen (Fig. 3.31).

   The contralateral kidney can be enlarged due to compensatory hypertrophy and there is higher incidence of renal abnormalities like vesicoureteric reflux. Unilateral renal agenesis can be the main sign of many nonchromosomal syndromes the risk being 20–25%. The most common are Fraser syndrome and VACTERL association. The risk of chromosomal anomaly is low (<1%).
2. Unilateral ectopic kidney: The incidence of renal ectopia varies between 1:500 and 1:1200. The ectopic kidney may be, low lumbar or presacral (Fig. 3.32) in position. There is possibility of crossed renal ectopia with or without fusion where the ectopic kidney is located on the opposite side of the abdomen relative to its ureteral insertion into the bladder (Fig. 3.33). Crossed fused ectopia can have obstructive features. Ectopic kidney is identified by the morphology and the fluid filled renal pelvis in the center.

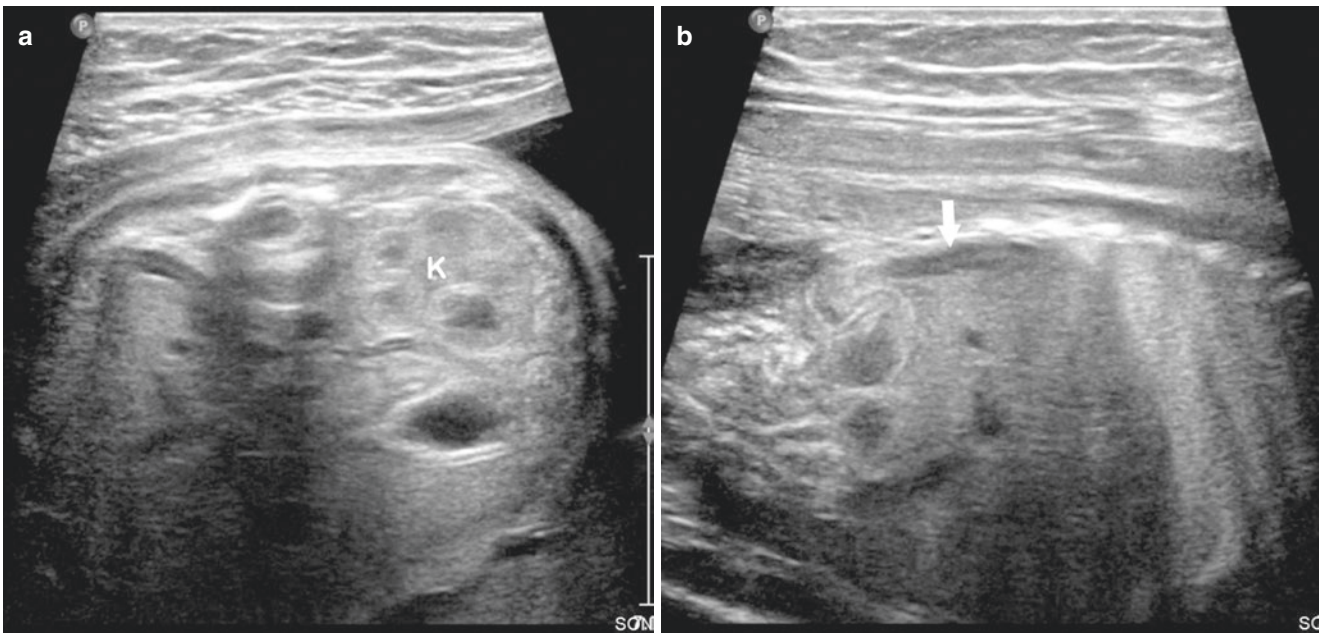

Fig. 3.31 Unilateral Renal Agenesis: (**a**) Axial scan revealing the normal kidney (K) on one side and nonvisualized kidney on opposite side. (**b**) Longitudinal scan demonstrating the elongated adrenal (arrow) of lying down adrenal sign

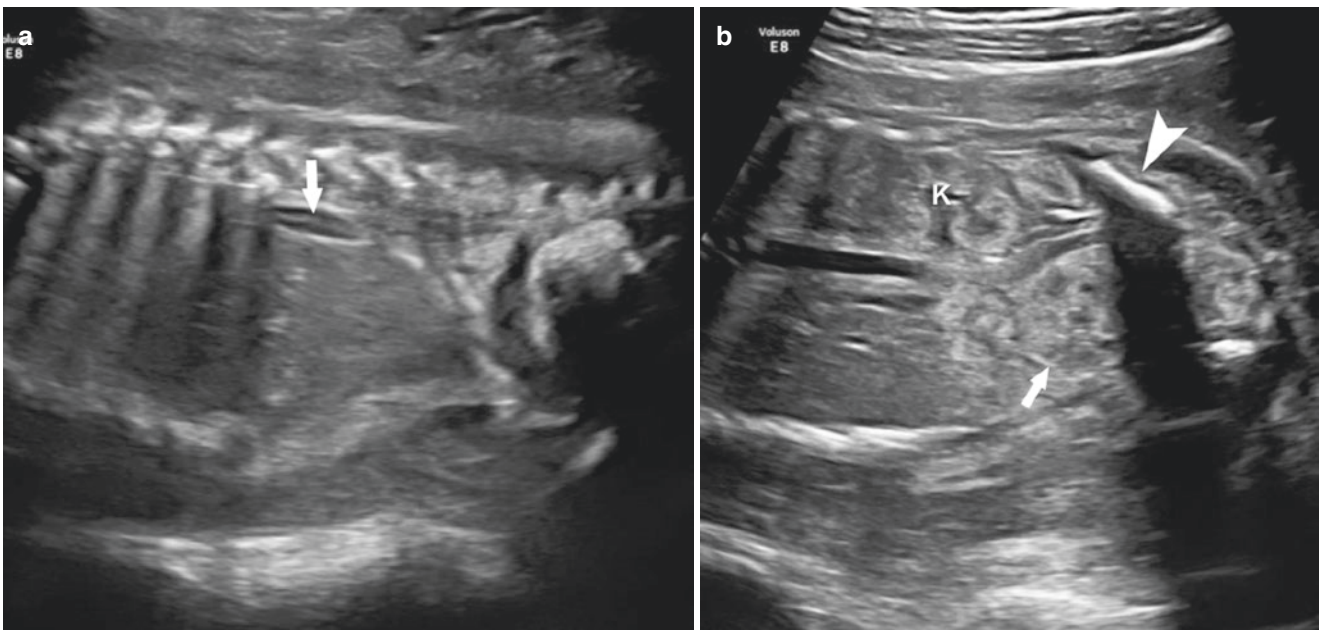

Fig. 3.32 Ectopic presacral kidney: (**a**) Longitudinal scan of renal area showing the lying down adrenal sign (arrow). (**b**) Coronal scan of the fetal abdomen and pelvis behind the urinary bladder demonstrates the normally located kidney (K) and ectopic kidney in the pelvis (arrow). Arrowhead indicates iliac bone

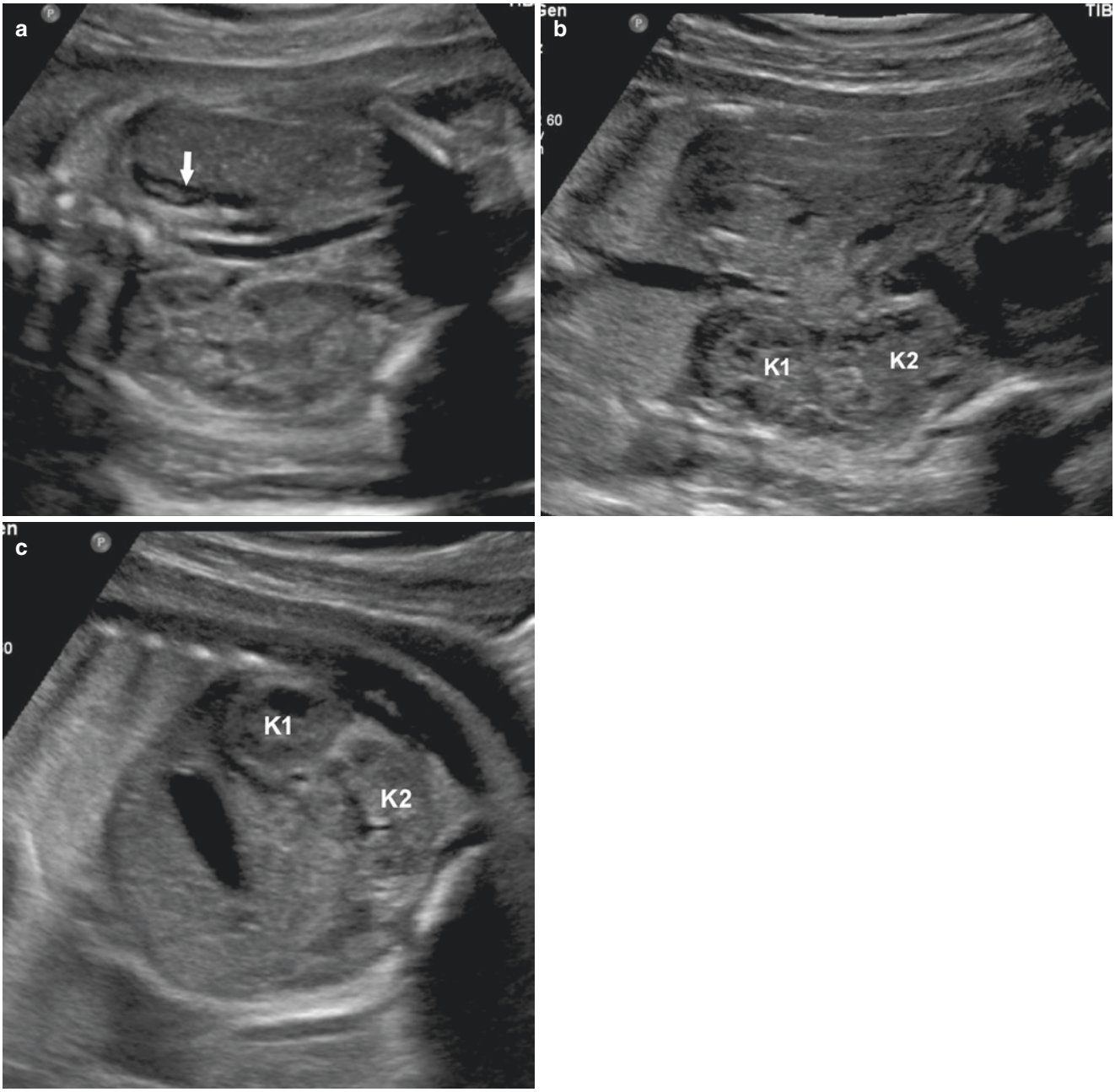

Fig. 3.33 Crossed Renal Ectopia: Coronal Scans of fetal abdomen showing the lying down adrenal sign (arrow) on one side (**a**) and both kidneys (K1 and K2) on the other side with fusion (**b**). (**c**) Oblique scan in another fetus shows crossed renal ectopia without fusion

3.7.2 Bilateral Nonvisualized Kidneys

When both kidneys are not seen in the renal fossa, it may be due to bilateral renal agenesis and bilateral ectopic kidneys.

1. Bilateral renal agenesis (BRA): It is a lethal congenital anomaly with an incidence of 1 in 4000 births. The ureteric bud fails to develop, nephrons do not form, and no urine is produced. The sonographic signs are anhydramnios and nonvisualisation of kidneys and bladder (Fig. 3.34a). The lying down adrenal sign helps to confirm that the kidneys have not developed in the flank. The bowel or adrenal glands can be mistaken for kidneys. The image quality will be poor due to oligohydramnios. High resolution scan using linear probe can be used to visualize the renal fossa better. If the fetus is in breech presentation, transvaginal scan can be used to visualize the renal fossa. Color Doppler study can be used to diagnose absent renal arteries and to confirm that the urinary bladder is not seen between the two umbilical arteries (Fig. 3.34b). If there is single umbilical artery along with bilateral renal agenesis and it is arising from abdominal aorta instead of iliac artery, it is aberrant vitelline artery. In such a situation sirenomelia has to be ruled out which is discussed subsequently. BRA may be a component of caudal dysplasia.
2. Bilateral ectopic kidneys: When both kidneys are not seen in the renal fossa but the bladder is seen, then the kidneys may be located ectopically in the pelvis close to bladder or iliac wing (Fig. 3.35). It may not be possible always to see the two ectopic kidneys separately, to differentiate from unilateral ectopic kidney on one side and unilateral renal agenesis on the other side. The amniotic fluid volume is normal in bilateral ectopic kidneys or when at least one kidney is present.

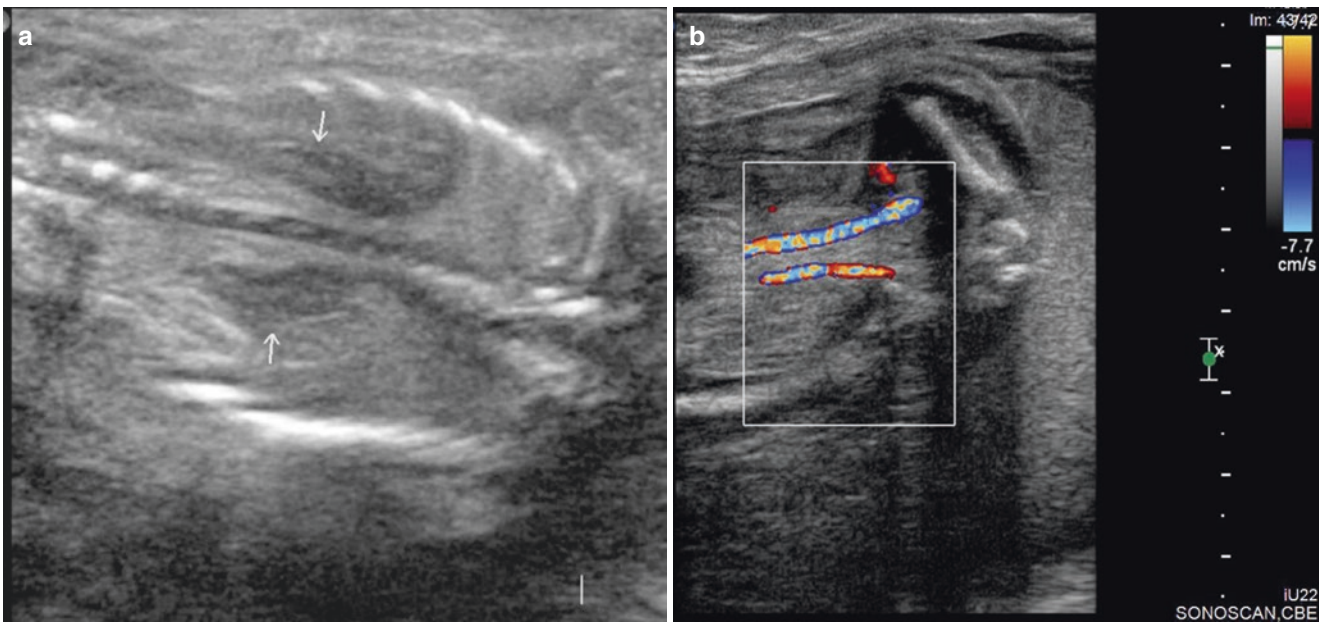

Fig. 3.34 Bilateral Renal Agenesis: (**a**) Coronal Scan of the fetal trunk demonstrates anhydramnios and bilateral lying down adrenal sign (*arrows*). (**b**) CDS of pelvis revealing the nonvisualized urinary bladder between the two umbilical arteries diagnostic of bilateral renal agenesis

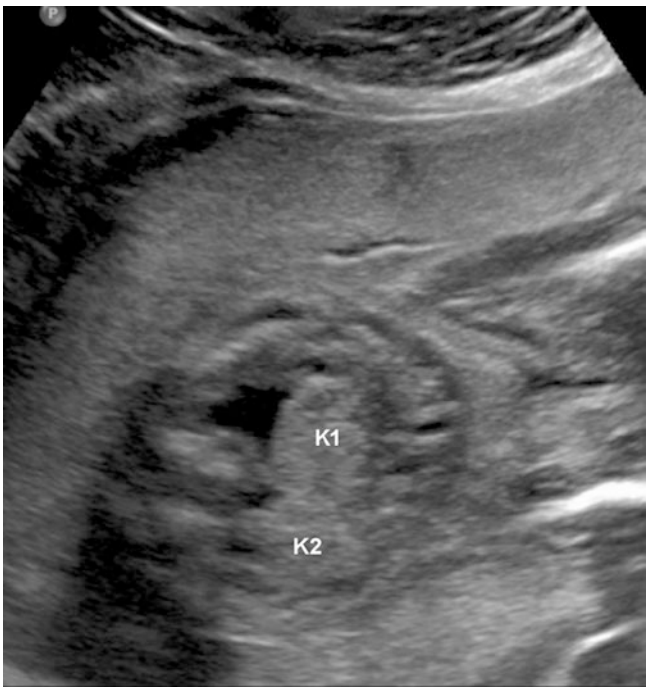

Fig. 3.35 Bilateral Ectopic Kidneys: Oblique scan of fetal pelvis demonstrating both kidneys (K1 and K2) located ectopically in the pelvis

3.8 Unilateral Smaller Kidney

Unilateral smaller kidney may be due to horseshoe kidney, congenital hypoplasia or vesicoureteric reflux. Horseshoe kidney occurs in 1 in 400–500 births. The inferior poles of the kidneys are fused. It is considered when one kidney is smaller (Fig. 3.36a) or when the orientation of the renal pelvis is anteroposterior instead of the normal horizontally placed pelvis (Fig. 3.36c). Transverse and coronal scan will demonstrate the bridge of renal tissue (isthmus) connecting the lower poles of both kidneys (Fig. 3.36b).

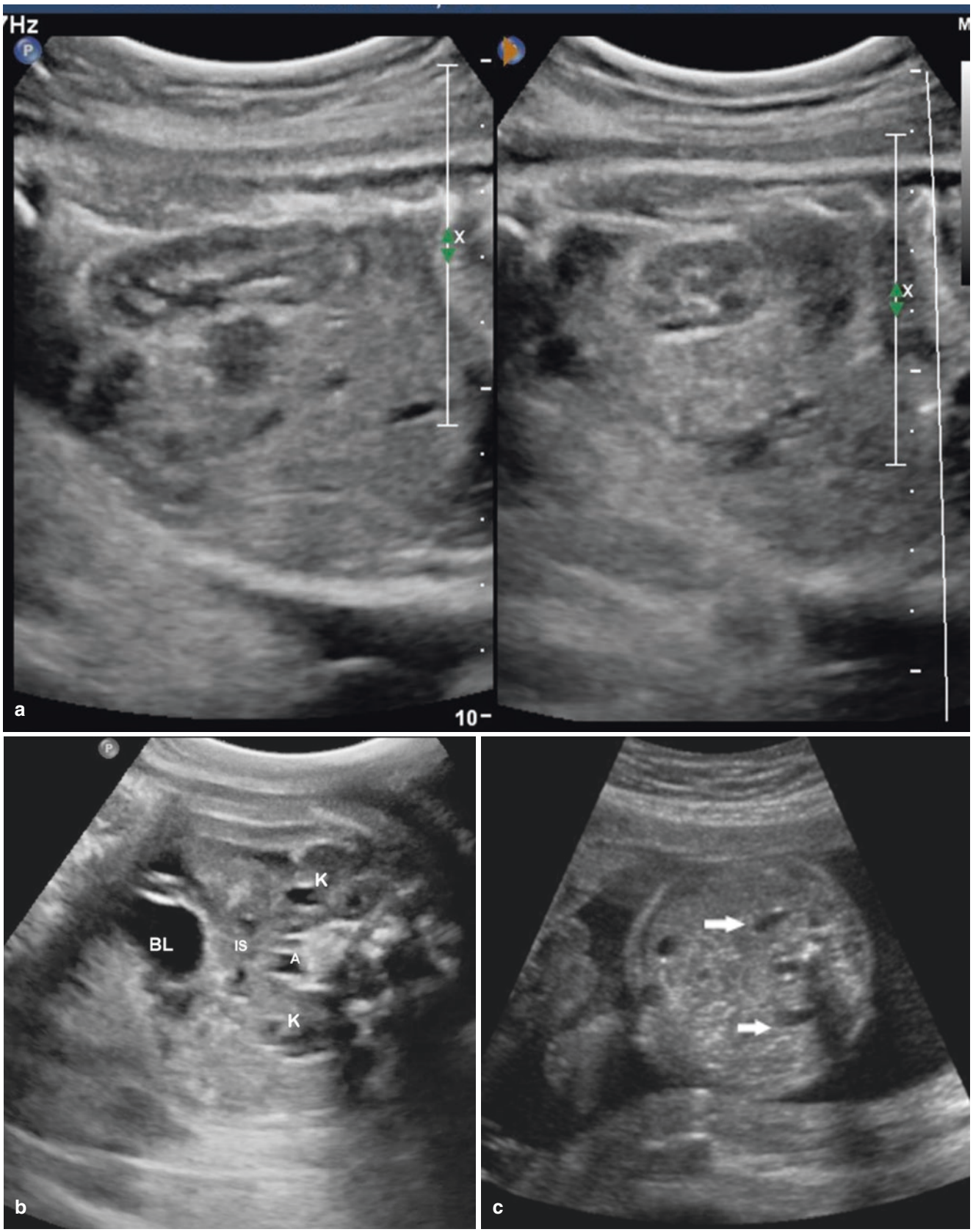

Fig. 3.36 Horseshoe Kidney—(**a**) Longitudinal scans of the kidneys reveal a smaller kidney on one side. (**b**) Oblique coronal scan demonstrates the isthmus (IS) anterior to aorta (A) connecting the two kidneys (K). BL—urinary bladder. (**c**) Axial scan of another fetus with horseshoe kidney shows the anteroposterior orientation of the renal pelvis of both kidneys (*arrows*)

3.9 Hydronephrosis

Pelviureteric junction (PUJ) obstruction: Here there is functional obstruction at PUJ resulting in hydronephrosis. It is more common in males and is more often unilateral. There is dilatation of calyces and pelvis. On coronal scan, the peripheral dilated calyces communicate with the medial larger renal pelvis. The ureter and bladder are not dilated (Fig. 3.37a).

The prognosis is dependent on parenchymal thickness (Fig. 3.37b), hyperechogenic parenchyma with or without cysts (Fig. 3.37c), anteroposterior diameter of renal pelvis (Fig. 3.37d) and whether the renal pelvis is intrarenal or extrarenal. In intrarenal pelvis (Fig. 3.38), the parenchymal atrophy is seen early as the pressure is extended to the parenchyma, while in extrarenal pelvis, the renal pelvis can reach enormous proportion with good preservation of the parenchyma (Fig. 3.39).

When the pelviureteric junction obstruction is bilateral (Fig. 3.40), the prognosis depends upon the severity, duration of obstruction and on amniotic fluid volume.

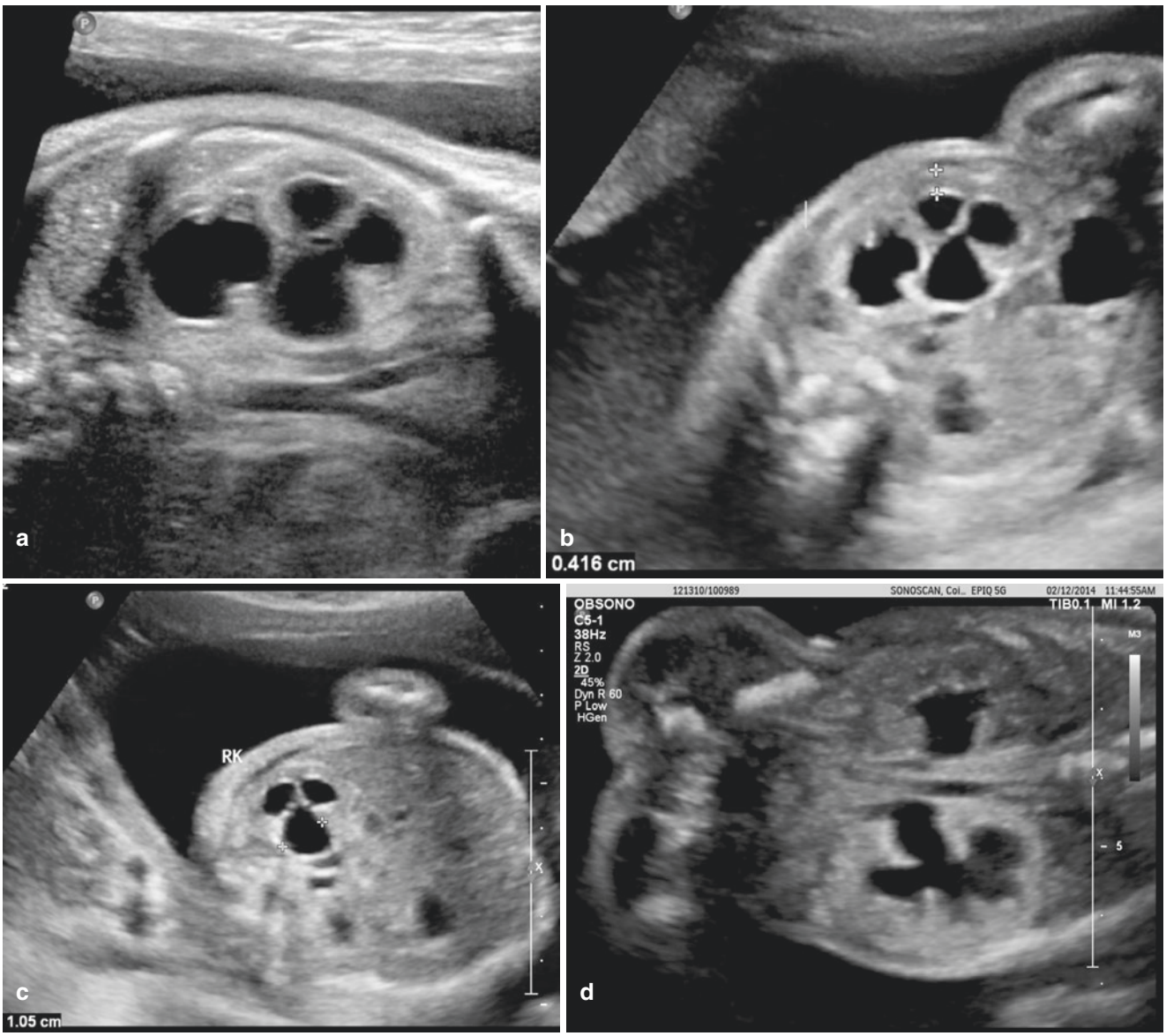

Fig. 3.37 Pelviureteric junction (PUJ) obstruction: (**a**) Coronal scan of the kidney shows the peripheral symmetrically dilated calyces communicating with the dilated pelvis. The ureter is not dilated. Images showing thin parenchyma (**b**), echogenic parenchyma (**c**) in PUJ Obstruction (**d**) and measurement of APD

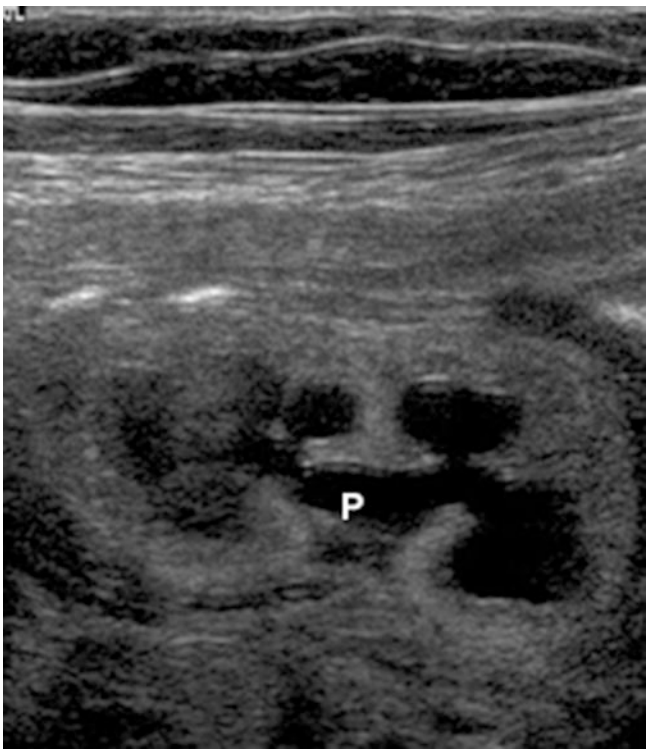

Fig. 3.38 Coronal scan of a kidney with pelviureteric junction obstruction demonstrating a slightly dilated intrarenal pelvis (P) with echogenic parenchyma indicating dysplasia

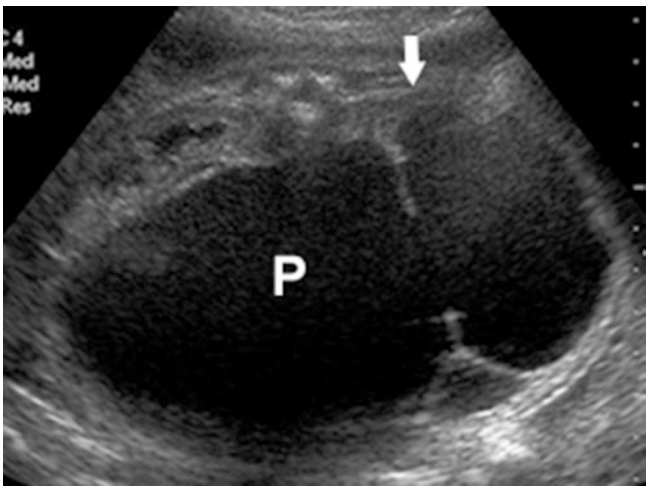

Fig. 3.39 Axial scan demonstrating a grossly dilated extra renal pelvis (P) filling most of the abdomen with well-preserved renal parenchyma (arrow)

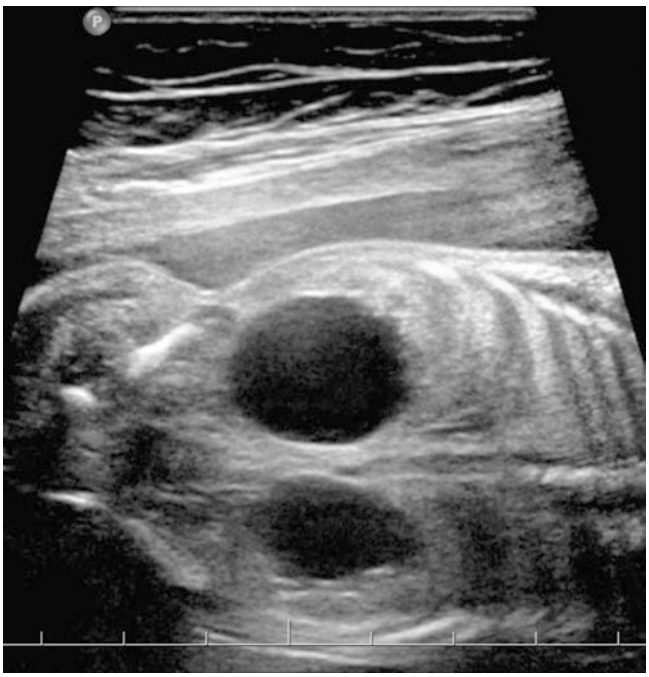

Fig. 3.40 Coronal scan of fetal abdomen demonstrating bilateral pelviureteric junction obstruction

3.10 Hydroureteronephrosis

There is dilatation of calyces, pelvis and ureter. It may be unilateral and bilateral. The level of obstruction varies.

3.10.1 Unilateral Hydroureteronephrosis

Mid ureteric obstruction is due to ureteric valve. It is seen as a cystic dilatation of the proximal ureter with hydronephrosis. The renal pelvis is connected to the cystically dilated upper ureter (Fig. 3.41).

This has to be differentiated from retroperitoneal lymph cyst which is multiseptated and displaces the kidney without hydronephrosis. When the ureteric dilatation is seen up to urinary bladder (Fig. 3.42) the causes may be:

1. Primary obstructive mega ureter.
2. Vesicoureteric reflux.
3. Ureterocele.
4. Ectopic ureteric opening.

In the fetus the primary obstructive mega ureter and vesicoureteric reflux cannot be usually differentiated. Occasionally in vesicoureteric reflux, the kidney is smaller and the collecting system shows intermittent dilatation, varying grades of dilatation over time or ureteric hyperperistalsis (Fig. 3.43, Video 3.3).

Vesicoureteric reflux can be associated with duplex collecting system with hydroureteronephrosis of lower moiety. Ureterocele is seen as a thin-walled cystic structure within the urinary bladder (Fig. 3.44).

It is seen well when the bladder is partially full and can be overlooked when the bladder is empty or well distended. It is more often associated with duplex collecting system with hydroureteronephrosis of the upper moiety. Ureterocele collapses and distends overtime and hence it may not be obvious all the time.

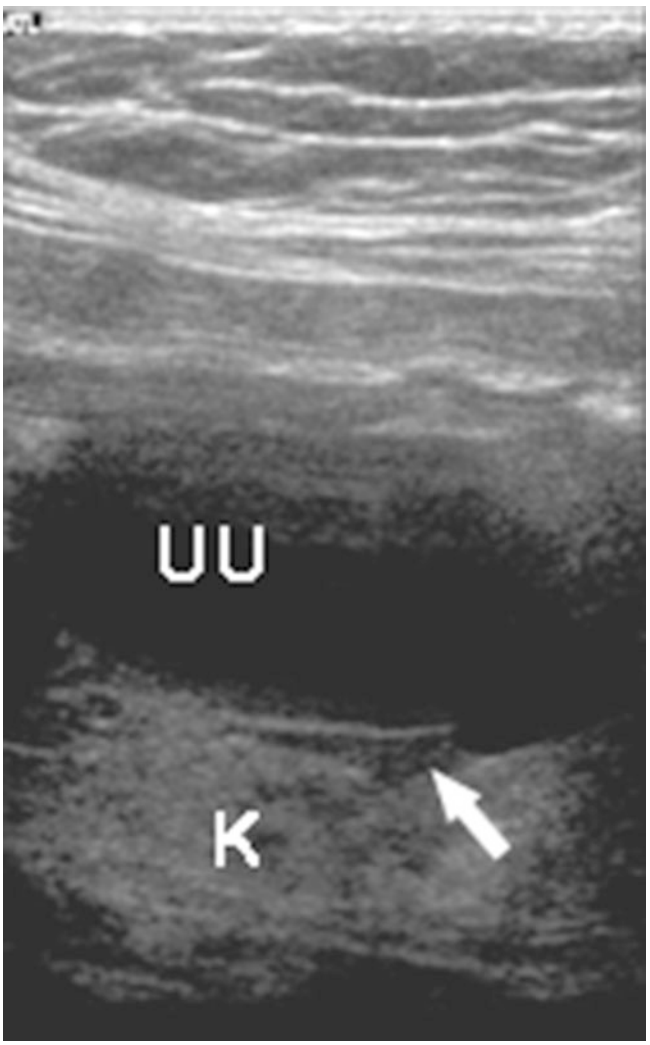

Fig. 3.41 Ureteric Valve: Longitudinal scan showing the cystic dilatation of the upper ureter (UU) continuous with the slightly dilated renal pelvis (arrow). K indicates the kidney

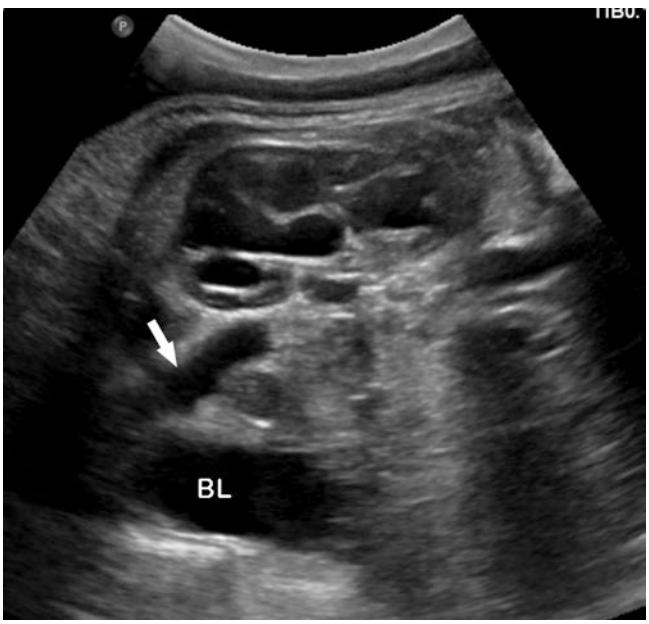

Fig. 3.42 Hydroureteronephrosis: Oblique coronal scan demonstrating hydronephrosis of the kidney and dilated ureter (arrow) up to urinary bladder (BL)

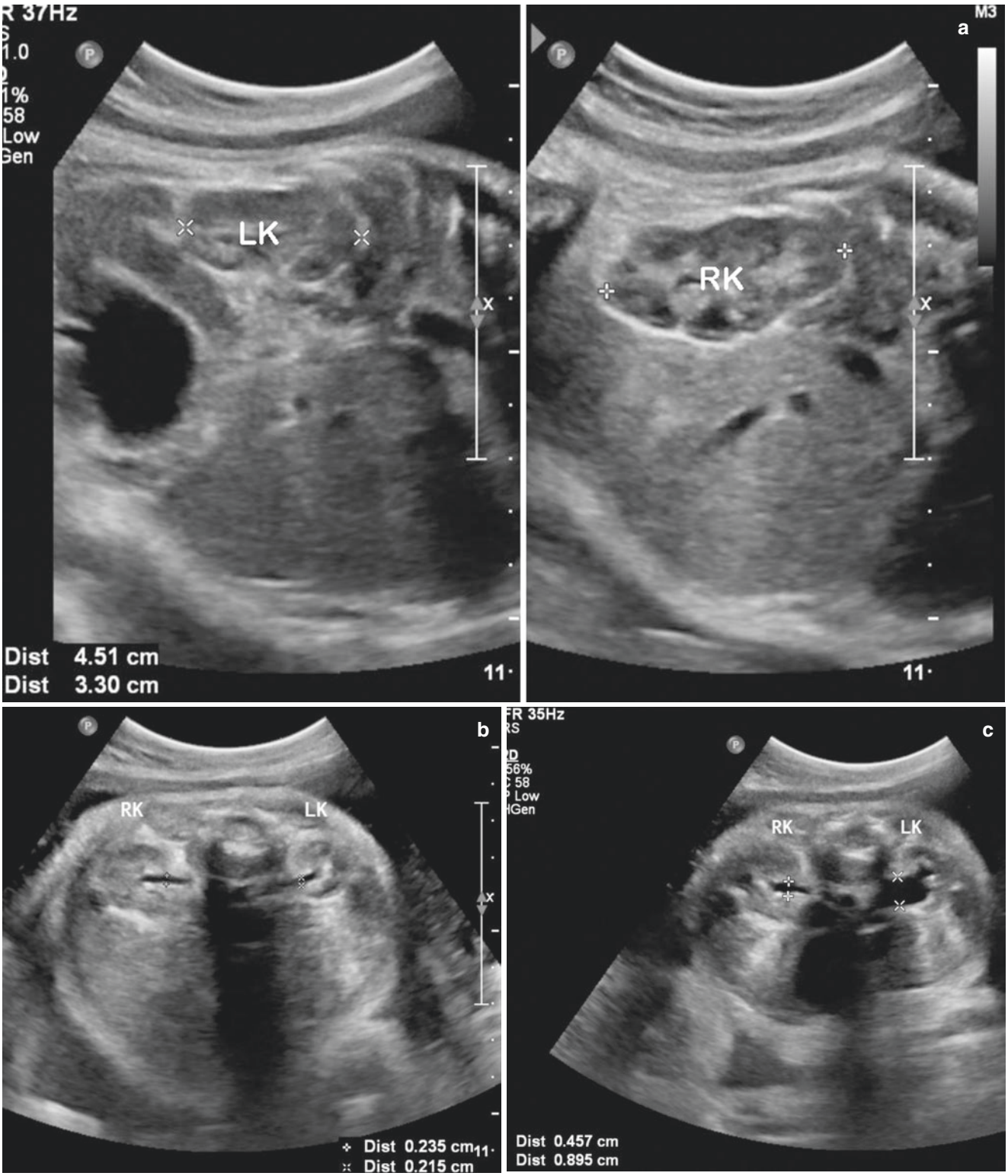

Fig. 3.43 Vesicoureteric Reflux: (**a**) Longitudinal scans showing the smaller left kidney (LK) compared to normal right kidney (RK). Axial scan at two different times shows normal left renal pelvis in (**b**) and dilated left renal pelvis in (**c**). (**d**) Oblique scan shows dilated left ureter (arrow). It showed hyper peristalsis. (**e**) Postnatal MCU shows the grade III Vesicoureteric Reflux on left side

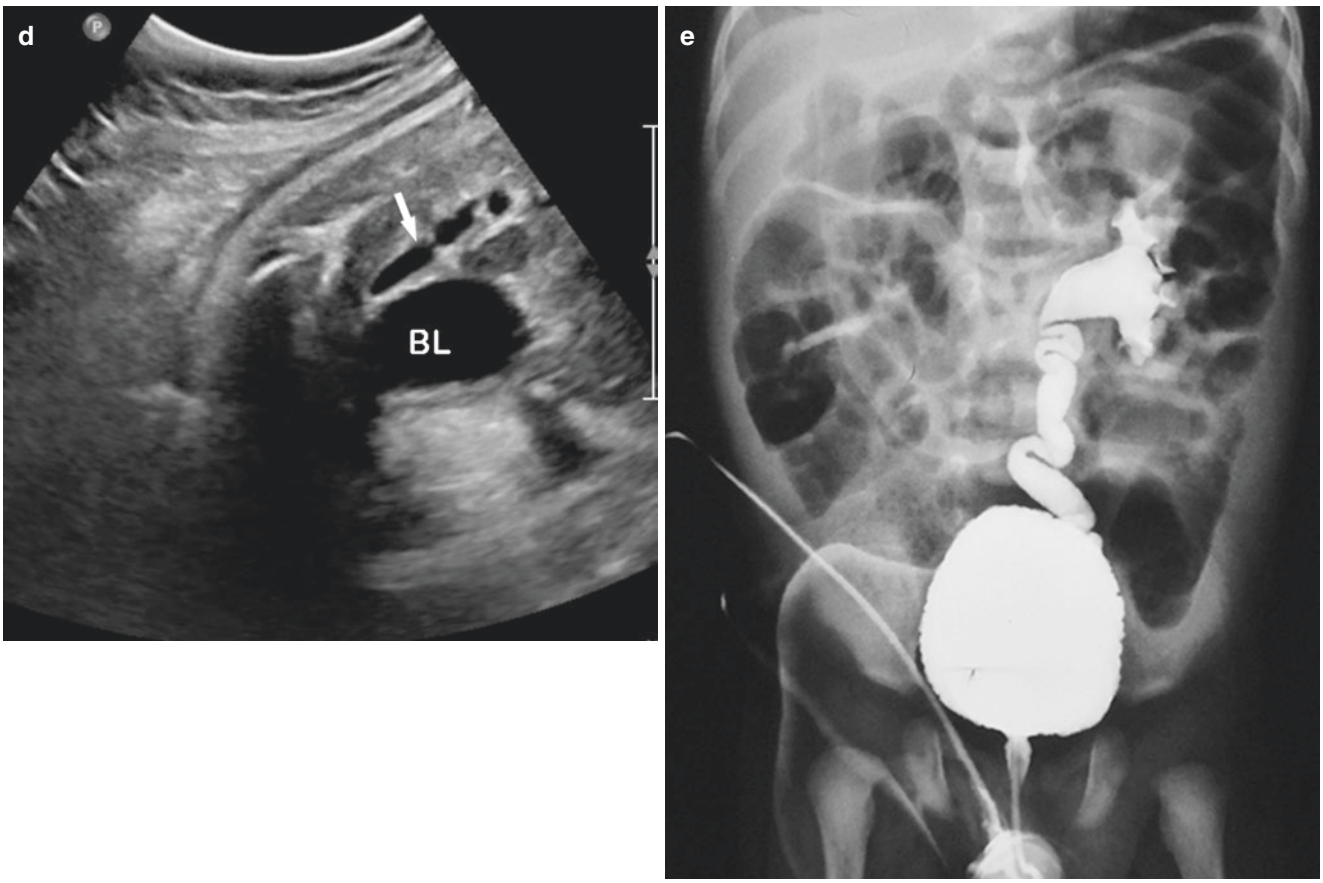

Fig. 3.43 (continued)

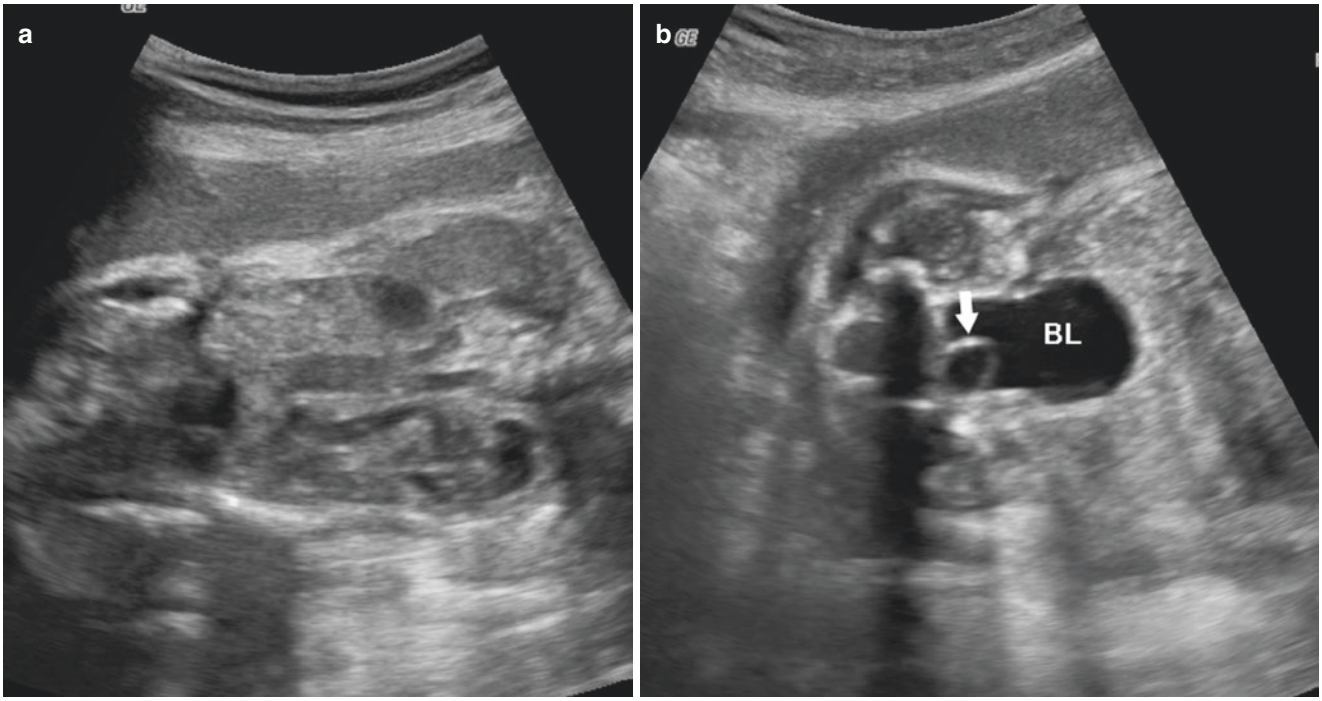

Fig. 3.44 Ureterocele: (**a**) Coronal scan reveals hydroureteronephrosis. (**b**) Coronal scan of fetal pelvis demonstrates the ureterocele (arrow) within the urinary bladder (BL)

3.10.2 Ectopic Ureteric Opening

The incidence of ureteric anomalies at autopsy is 2–3%. Ureteric ectopia is more common in females (70–90%) and is usually associated with duplication (80–90%). In both sexes, the most common site of an ectopic opening of the ureter is into the urethra. Other sites are the seminal vesicle, ejaculatory duct and vas deferens in males and the vagina and uterus in females. During normal development, the ureteric buds are incorporated into the urogenital sinus. This is followed by caudal movement of the mesonephric duct and cranial migration of the ureter, with the mesodermal tissue between them differentiating into the bladder neck and trigone. In ureteric ectopia, separation of the two orifices and cranial migration of the ureter do not occur. If it is bilateral, because of lack of appropriate stimuli, there is deficient development of the bladder neck and trigone. Associated anomalies in males are agenesis or dysplasia of the kidney and agenesis or cysts of the seminal vesicles. In females, there can be uterine anomalies and duplication or atresia of the vagina. In case of ectopic ureteric opening, the dilated ureter is seen to extend low in the pelvis beyond the urinary bladder, indicating an ectopic opening below the urinary bladder (Fig. 3.45a) which is seen better on fetal perineal sonography (Fig. 3.45b, c).

On fetal perineal sonography real-time visualization of the continuity of ureteric peristalsis as a distension of the urethra, although rare, can confirm an ectopic ureteric opening into the urethra (Video 3.4). It is associated with duplex collecting system with hydroureteronephrosis of the upper moiety.

In hydronephrosis, the appearance of renal parenchyma is useful in predicting the prognosis of the function of that kidney. The echogenic parenchyma indicates dysplasia. There may be peripheral tiny cysts in obstructive dysplasia of the kidney.

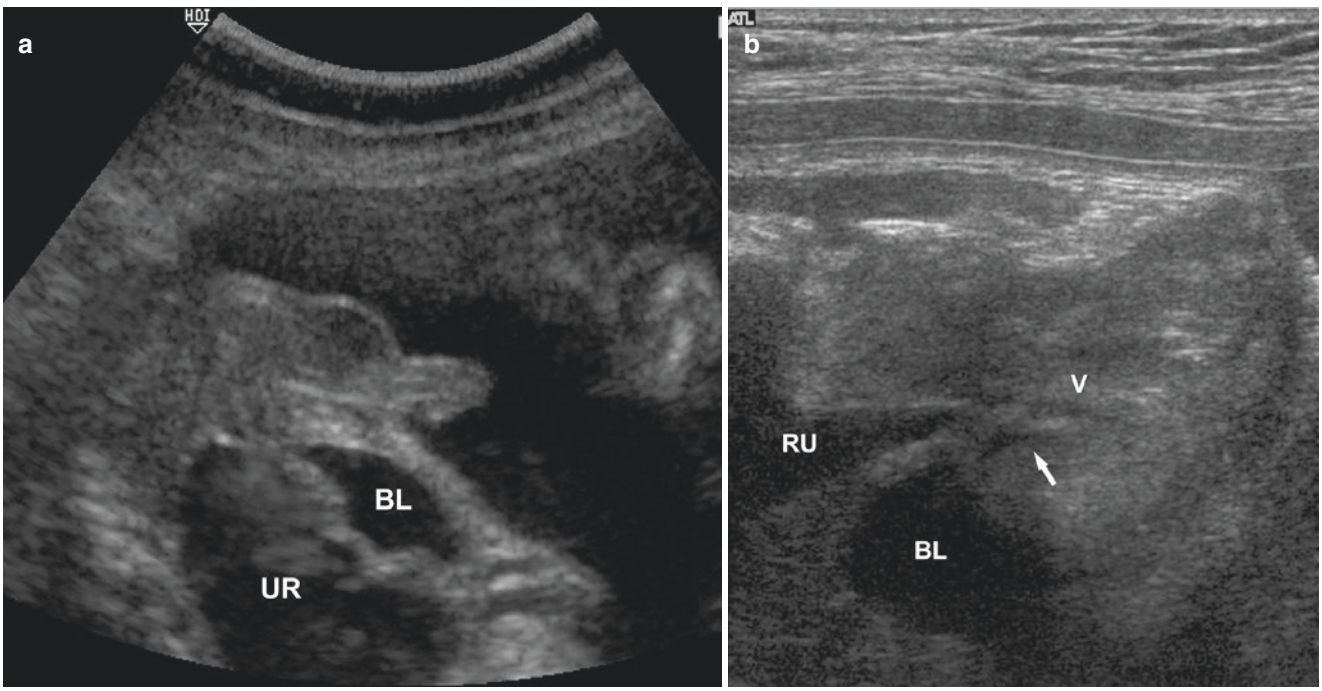

Fig. 3.45 Ectopic Ureteric Opening: (**a**) Sagittal scan of fetal pelvis demonstrating the grossly dilated ureter (UR) extending beyond the urinary bladder (BL). Parasagittal perineal scan of the fetus with bilateral ectopic ureteric opening showing distal ends of the right ureter (UR) in (**b**) and the left ureter (UR) in (**c**), extending beyond the urinary bladder (BL) and opening into urethra (arrow). V indicates Vagina

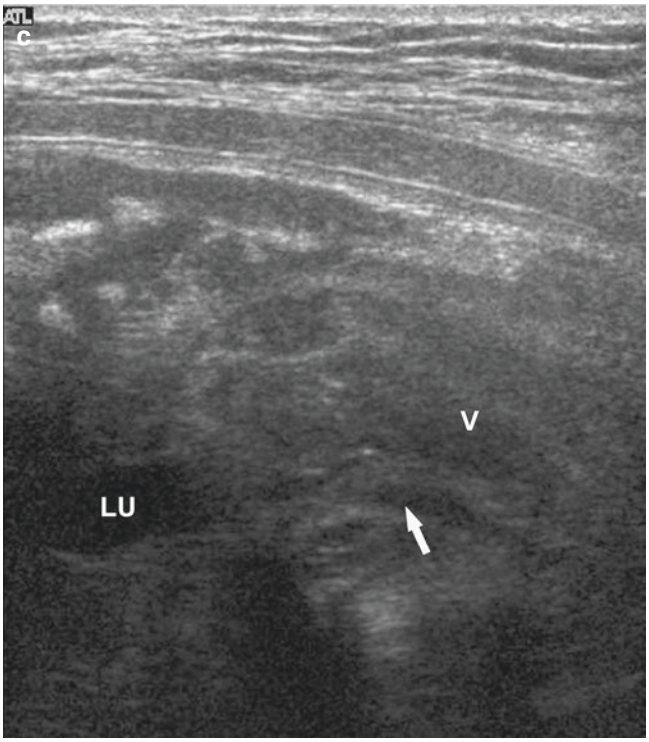

Fig. 3.45 (continued)

3.10.3 Duplex Collecting System of Kidneys

Duplication of the collecting system results from division of the metanephric diverticulum or ureteric bud. They can be seen prenatally if one or both of the moieties are dilated. The two ureters may join together anywhere along their course or they may open separately into the urinary bladder or at ectopic location.

The dilatation of the upper moiety is due to ureterocele (Fig. 3.46) or ectopic ureteric opening (Fig. 3.47) and dilatation of lower moiety is due to pelviureteric junction obstruction (Fig. 3.48) or vesicoureteric reflux.

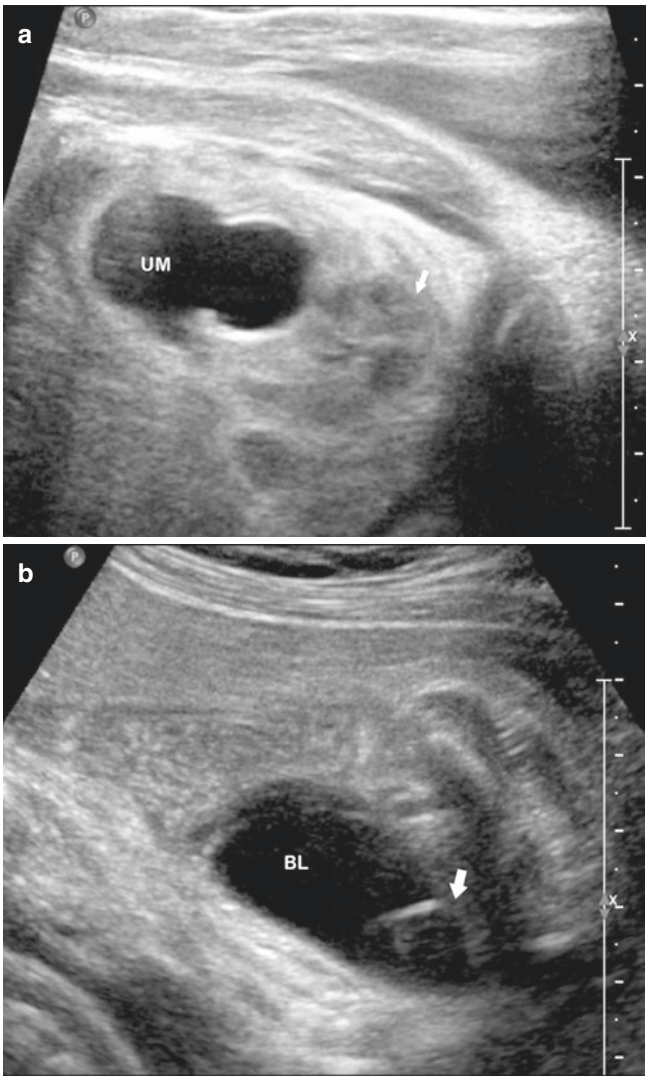

Fig. 3.46 Duplex collecting system: (**a**) Longitudinal scan of the kidney shows duplex collecting system with hydronephrosis of upper moiety (UM) due to (**b**) ureterocele (arrow) in urinary bladder (BL)

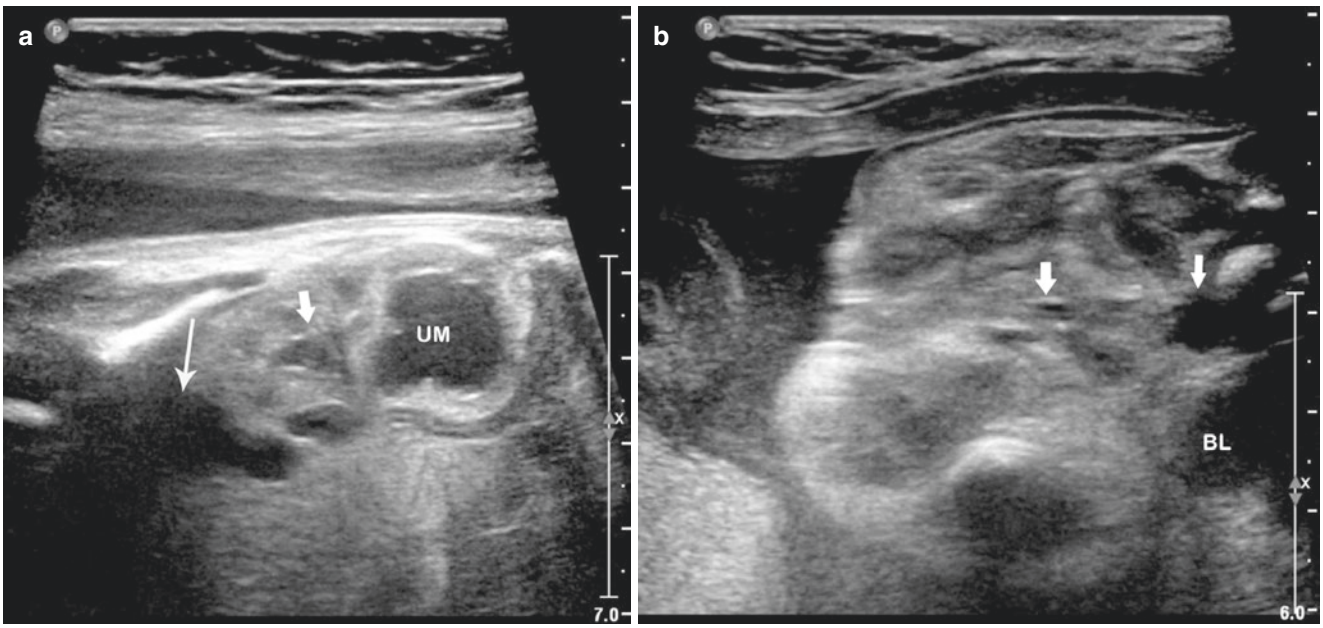

Fig. 3.47 Duplex collecting system: (**a**) Longitudinal scan of the kidney shows duplex collecting system with hydroureteronephrosis of upper moiety (UM) and normal lower moiety (arrow). Thin arrow points the dilated ureter. (**b**) Fetal parasagittal perineal scan demonstrates the dilated upper moiety ureter (arrow) opening into the vagina

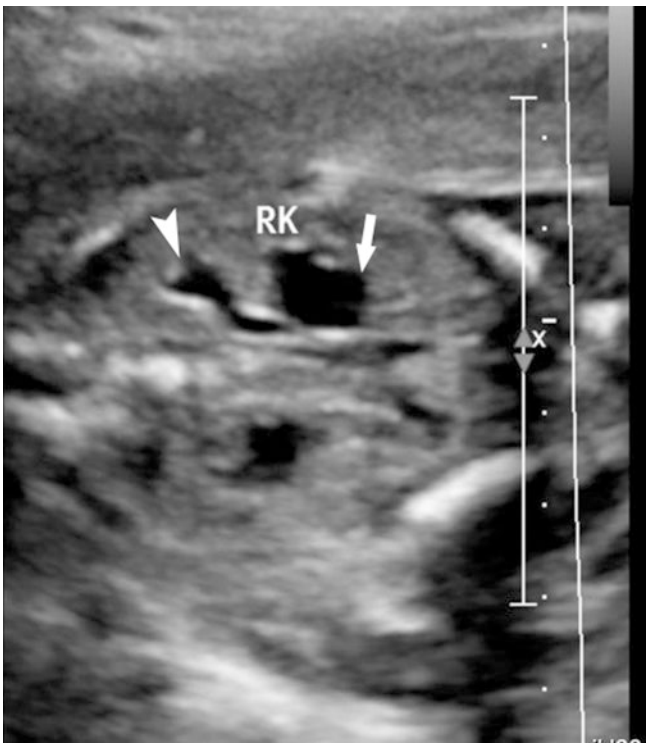

Fig. 3.48 Duplex collecting system: Coronal scan of the right kidney demonstrates duplex collecting system with normal upper moiety (arrowhead). There is hydronephrosis of the lower moiety (arrow)

3.10.4 Bilateral Hydroureteronephrosis

When bilateral hydroureteronephrosis is seen, the cause is either bilateral occurrence of conditions described for unilateral hydroureteronephrosis, where the urinary bladder can be normal or urinary bladder outflow obstruction. In urinary bladder outflow obstruction, the urinary bladder is over distended with thick walls. The walls may be trabeculated (Fig. 3.49c, d).

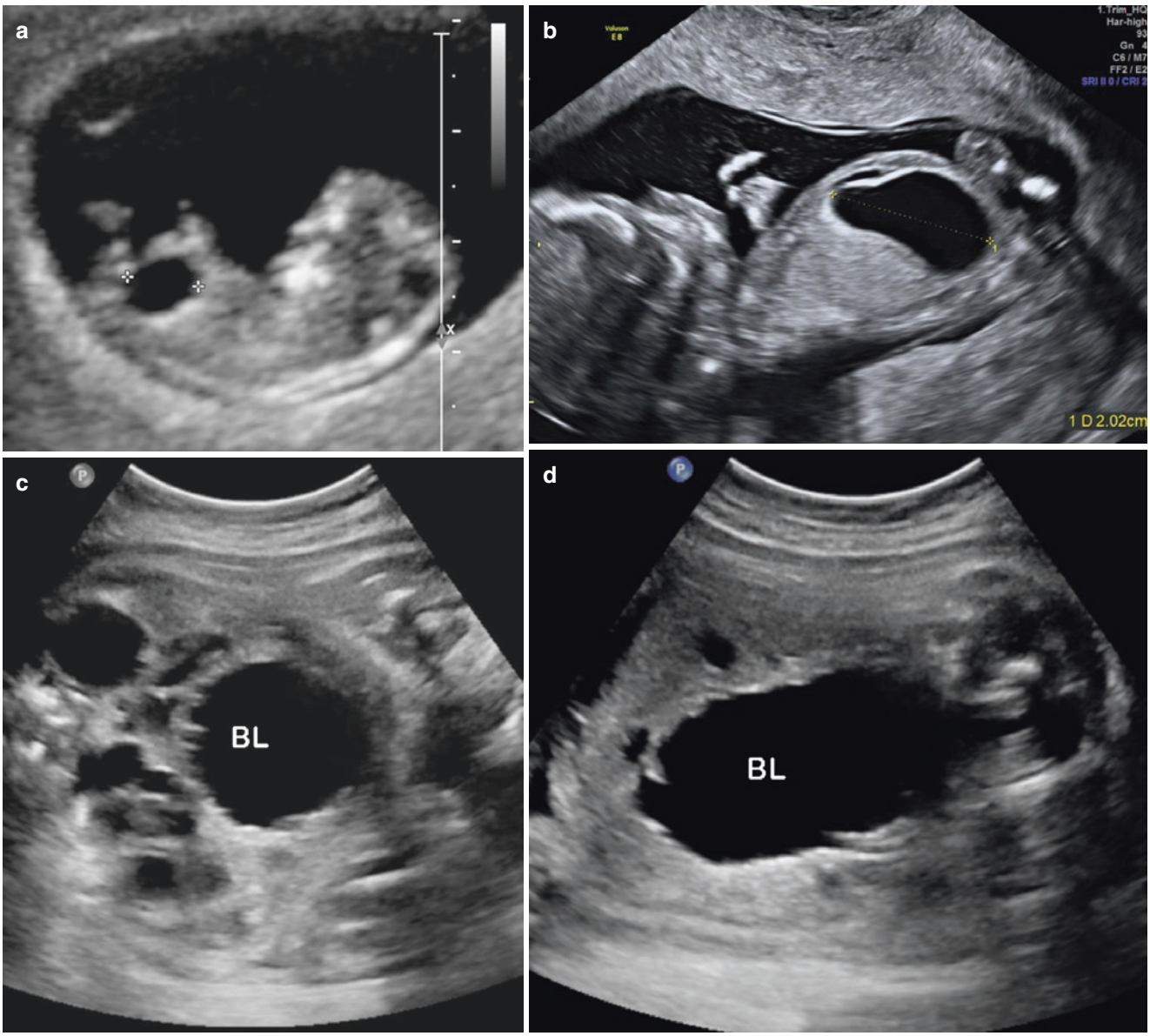

Fig. 3.49 Megacystis: Ist trimester: Longitudinal scan of the fetus shows megacystis with (**a**) longitudinal diameter of the bladder between 7 to 15 mm, a marker for aneuploidy and (**b**) above 15 mm indicating obstruction. II and III trimester: (**c**) Axial and (**d**) Coronal scan of pelvis showing over distended and trabeculated urinary bladder (BL) indicating urinary bladder outflow obstruction

3.11 Megacystis or Dilated Urinary Bladder

A dilated urinary bladder may be due to obstructive or non-obstructive conditions. There is a definite measurement cut off in the first trimester to define dilated bladder. Beyond first trimester, there is no agreement on measurement cut off to define it. Megacystis is diagnosed if longitudinal diameter of urinary bladder is 7 mm or more in first trimester (11–14 weeks) (Fig. 3.49a, b). In 11–14 weeks fetuses with a longitudinal diameter of urinary bladder between 7 and 15 mm, 23% of them have a chromosomal anomaly which has to be ruled out. It resolves in 90% of the fetuses. In the fetuses with longitudinal bladder diameter of more than 15 mm, risk of aneuploidy is only 10%. Fetuses in this group invariably progress to obstructive uropathy. The urinary bladder is normally distensible with cycles of micturition. So it will be seen in varying degrees of distension during the time of scan. Assessment of dilatation of urinary bladder after 14–15 weeks is subjective and hence correlation with associated findings such as thickness and echogenicity or trabeculation of its walls (Fig. 3.49c, d), or presence of hydronephrosis indicating obstruction is necessary. Rarely there may be patent urachus extending from the urinary bladder to umbilicus in case of urinary bladder outflow obstruction. There may be allantoic cyst in the umbilical cord.

3.11.1 Urethral Atresia

The onset of obstruction is early. So the dilatation of urinary bladder is gross, almost filling the abdomen and may protrude anteriorly. Usually there is bilateral hydronephrosis with or without parenchymal dysplasia. The urethra is not dilated. The amniotic fluid volume may be normal before 18 weeks but there will be marked oligohydramnios or anhydramnios beyond this gestation (Fig. 3.50).

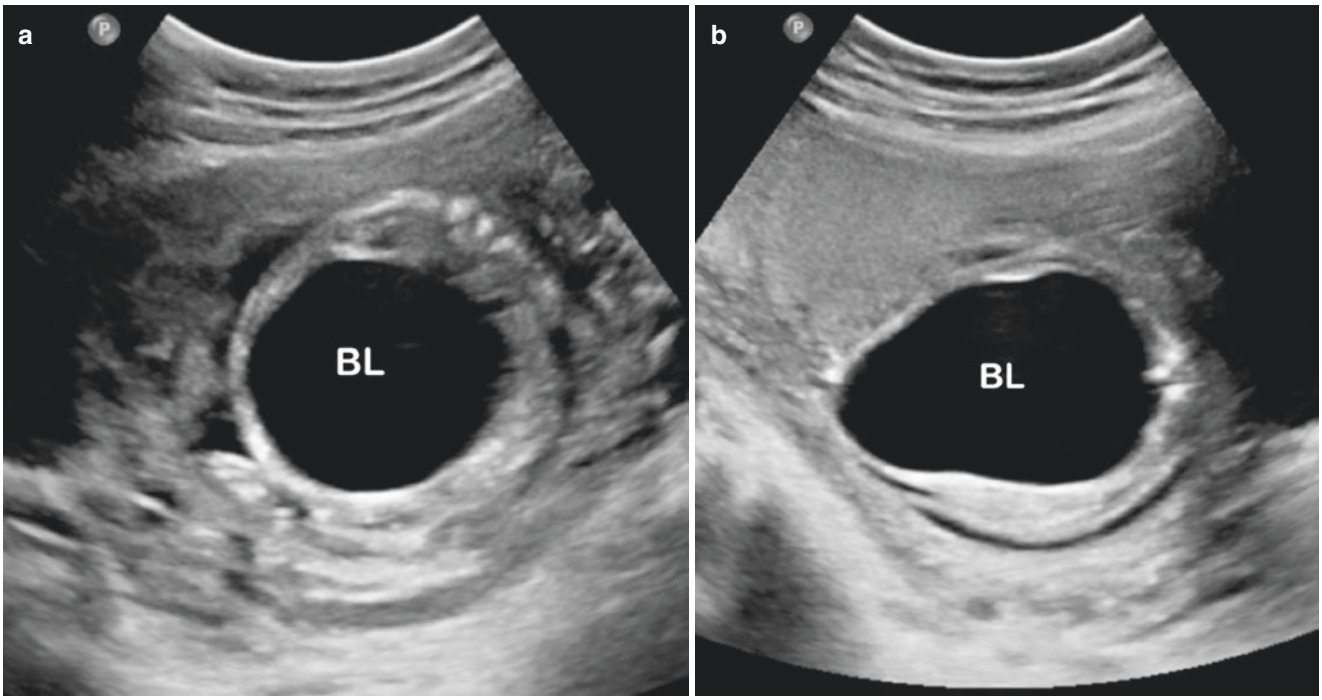

Fig. 3.50 Urethral atresia: Axial (**a**) and coronal (**b**) scan of fetal pelvis reveals the markedly over distended urinary bladder (BL) with anhydramnios

3.11.2 Posterior Urethral Valves

These are valves in posterior urethra in male fetuses causing varying degree of urinary bladder outflow obstruction. The prenatal sonographic findings are variable in degree of severity and time of manifestation from first to third trimester. The common presentation is with oligohydramnios. There is bilateral hydroureteronephrosis of varying degree (Figs. 3.51 and 3.52).

The urinary bladder is over distended with thick echogenic walls. The posterior urethra is dilated with a key-hole appearance on coronal scan (Fig. 3.51). In severe form, the renal parenchyma is echogenic with or without small peripheral cysts indicating obstructive dysplasia (Fig. 3.52). There may be perinephric urinoma due to rupture of a calyx (Fig. 3.53) or urinary ascites due to a breach in the wall of in urinary bladder (Fig. 3.54). The signs of bad prognosis are oligohydramnios, early manifestation, dysplastic parenchyma, perinephric urinoma and ascites. Sometimes, the posterior urethra is not dilated in resting state. It dilates only during fetal micturition. Hence when suspected a sonographic fetal micturating cystourethrogram (SFMCUG) is to be done. When fetus micturates, the posterior urethra dilates in posterior urethral valves (Fig. 3.55, Video 3.5).

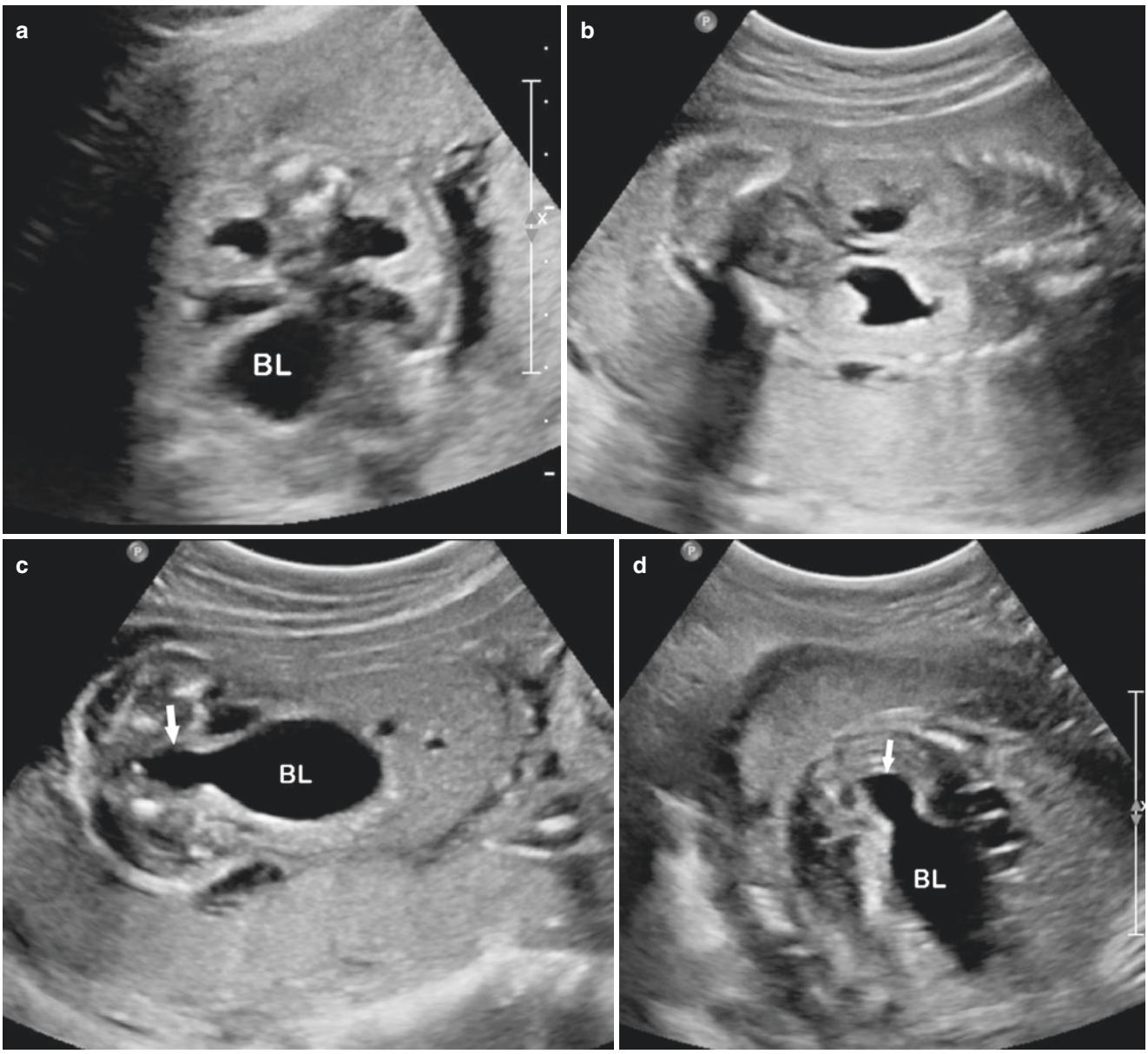

Fig. 3.51 Posterior urethral valves: (**a**) Axial and (**b**) coronal scans showing bilateral hydronephrosis and dilated urinary bladder (BL). (**c**) Coronal scan of the fetal pelvis shows the characteristic key hole appearance of dilated urinary bladder (BL) and the posterior urethra (arrow). (**d**) Sagittal scan of fetal pelvis and perineum demonstrates the cephalocaudal orientation of the dilated posterior urethra (arrow) stopping at root of penis

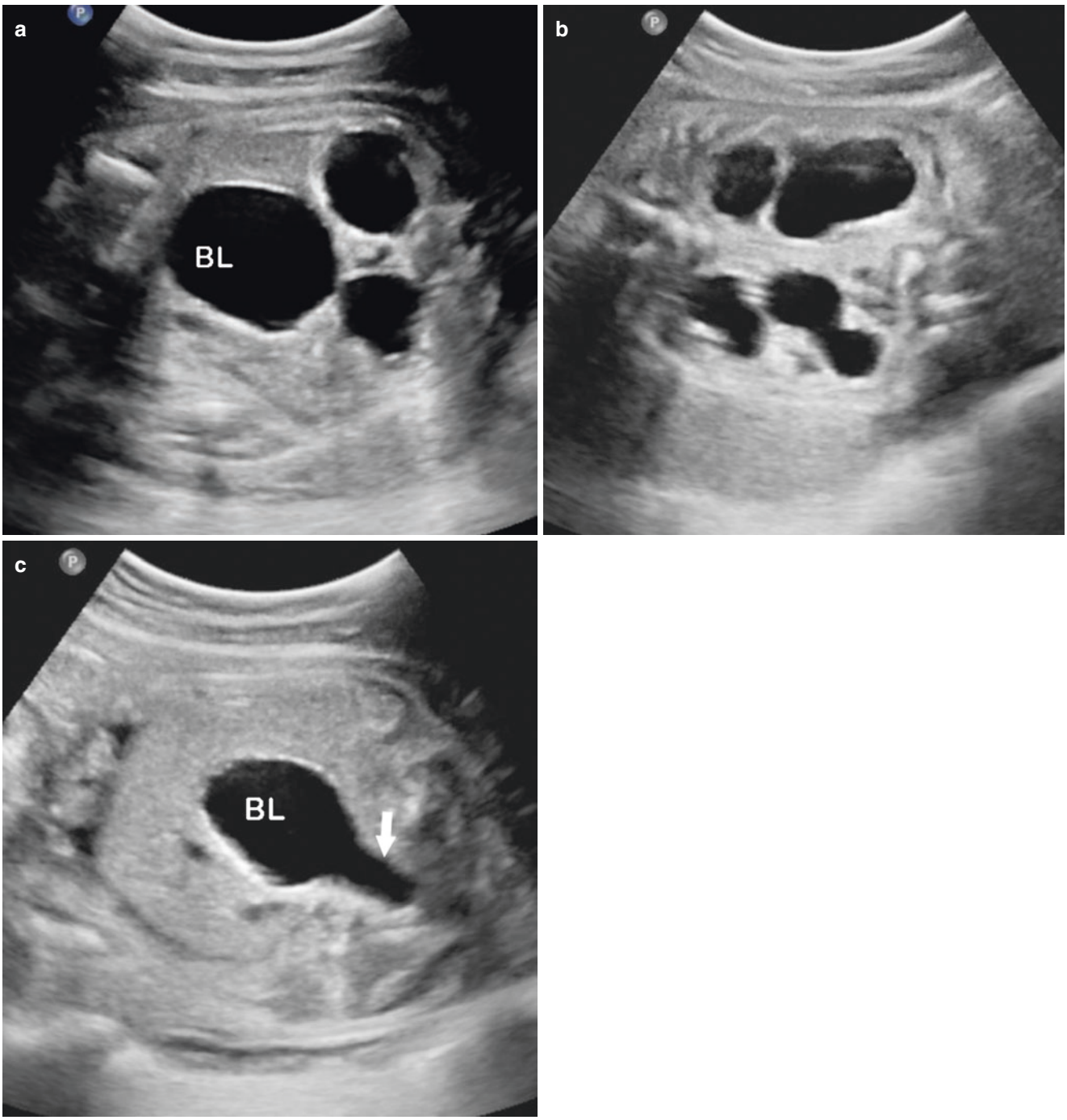

Fig. 3.52 Posterior urethral valve: (**a**) Axial scan showing the gross bilateral hydronephrosis and dilated urinary bladder (BL). (**b**) Coronal scan of the kidneys showing bilateral gross hydronephrosis with thin echogenic parenchyma. (**c**) Coronal scan revealing the dilated urinary bladder (BL) and posterior urethra (arrow)

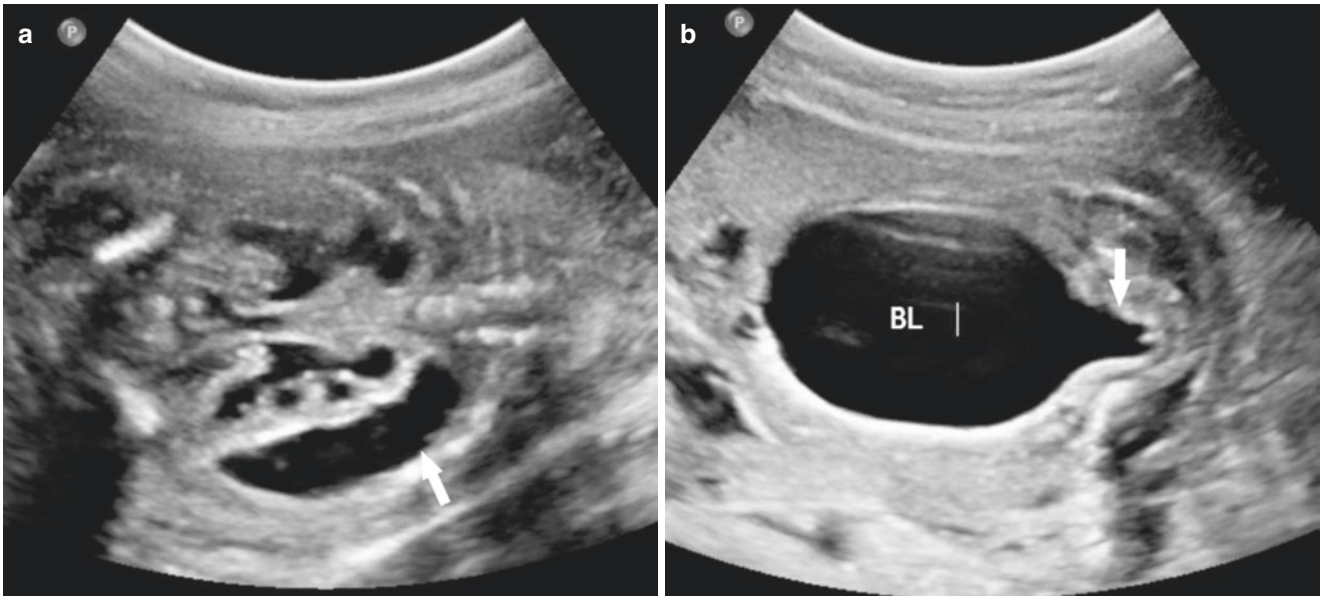

Fig. 3.53 Urinoma: (**a**) Coronal scan of the kidneys shows bilateral hydronephrosis with a large perinephric urinoma on one side (arrows). (**b**) Coronal scan of dilated urinary bladder (BL) and posterior urethra (arrow head)

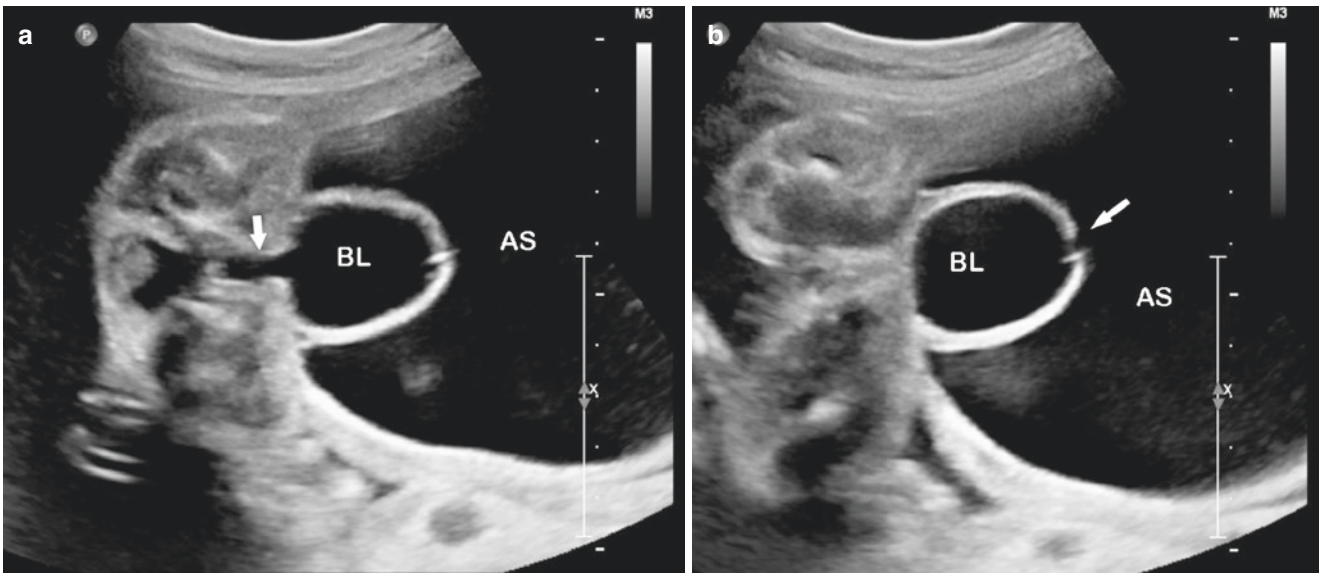

Fig. 3.54 Urinary ascites: Coronal scan of fetal pelvis demonstrating dilated urinary bladder (BL), ascites and dilated posterior urethra (arrow) in (**a**) and breach in urinary bladder (arrow) in (**b**)

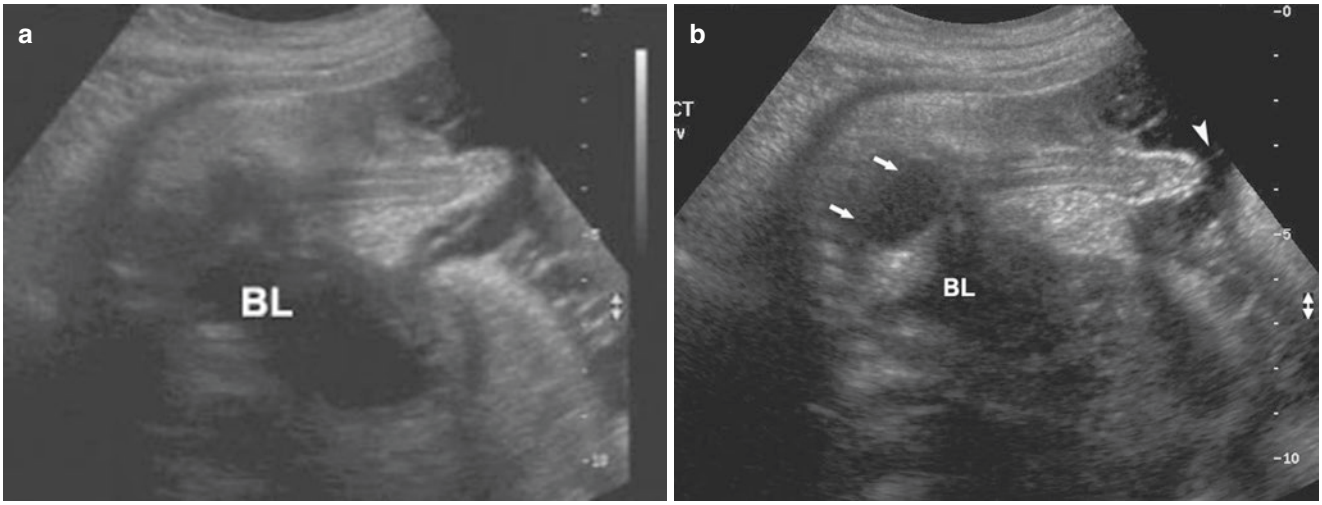

Fig. 3.55 PUV: Fetal SMCUG: Sagittal scan of fetal perineum and pelvis revealing nondilated posterior urethra in resting state (**a**) and dilated posterior urethra (arrows) during fetal micturition (**b**). Arrow head demonstrates the stream of urine from tip of penis (Video 3.5)

3.11.3 Anterior Urethral Valves

This is a very rare condition, where there is obstruction to anterior or penile urethra in male fetuses. It is not clear if the obstruction is due to valves or a small diverticulum which fills up during micturition and obstructs the urethra. On prenatal ultrasound the findings of kidneys and urinary bladder are similar to posterior urethral valves. SFMCUG is necessary for the diagnosis as the anterior urethra is seen to distend only during fetal micturition. The differentiation between posterior and anterior urethral valves is possible only on mid sagittal scan of fetal pelvis showing the urinary bladder and urethra during fetal micturition. In posterior urethral valves the dilated posterior urethra is cephalo caudal in orientation (Fig. 3.55) whereas in anterior urethral valve the dilatation extends to the horizontal portion of urethra up to mid shaft of penis (Fig. 3.56, Video 3.6).

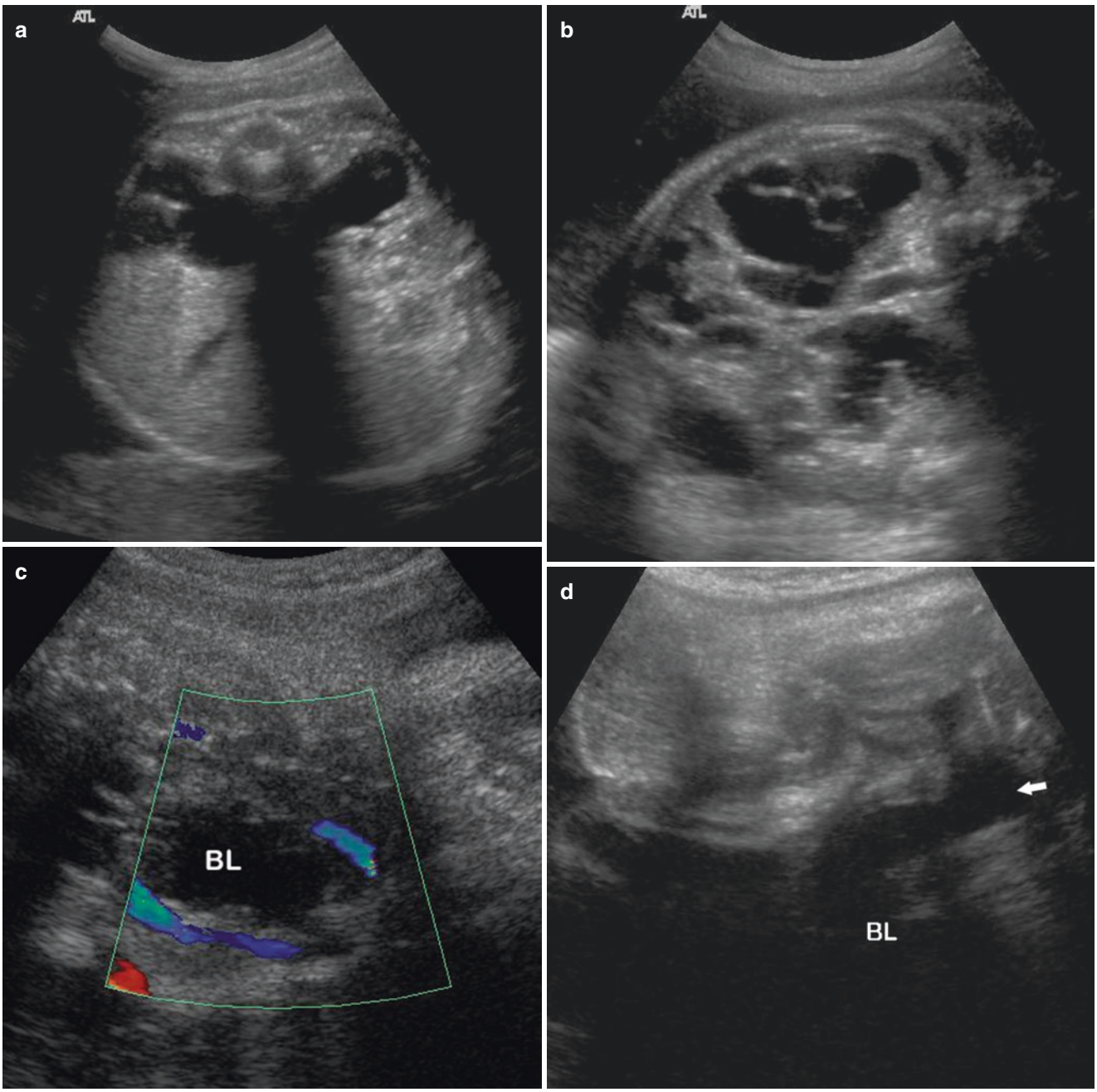

Fig. 3.56 Anterior urethral valves: (**a**) Axial scan shows bilateral hydronephrosis. (**b**) Coronal scan demonstrates bilateral hydronephrosis and dilated ureters. (**c**) Coronal scan of fetal pelvis shows dilated thick-walled urinary bladder (BL) between the umbilical arteries. (**d**) Fetal perineal scan showing the dilated posterior urethra (arrow). The anterior urethra is not dilated. (**e**) Fetal SMCUG with fetal micturition: The anterior urethra (arrowhead) is dilated up to mid shaft of penis (Video 3.6)

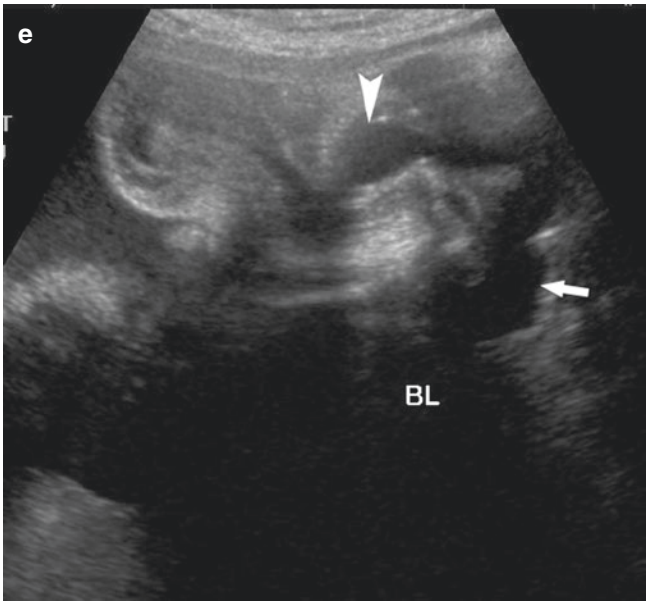

Fig. 3.56 (continued)

3.11.4 Anterior Urethral Atresia

Embryologically, most of the male urethra develops from the endoderm of the urogenital sinus. The distal part of the male urethra is derived from the glandular plate which grows inwards from the tip of the glans penis to meet the urethra derived from the urogenital sinus. Then it canalizes. When there is failure of canalization of the distal ectodermal origin of the urethra it results in anterior urethral atresia. The prenatal onset and sonographic features are similar to urethral atresia except that the fluid distended urethra is seen up to the tip of penis (Fig. 3.57). This can be mistaken for a vessel in a loop of umbilical cord, particularly when there is anhydramnios, which can be ruled out by color Doppler study.

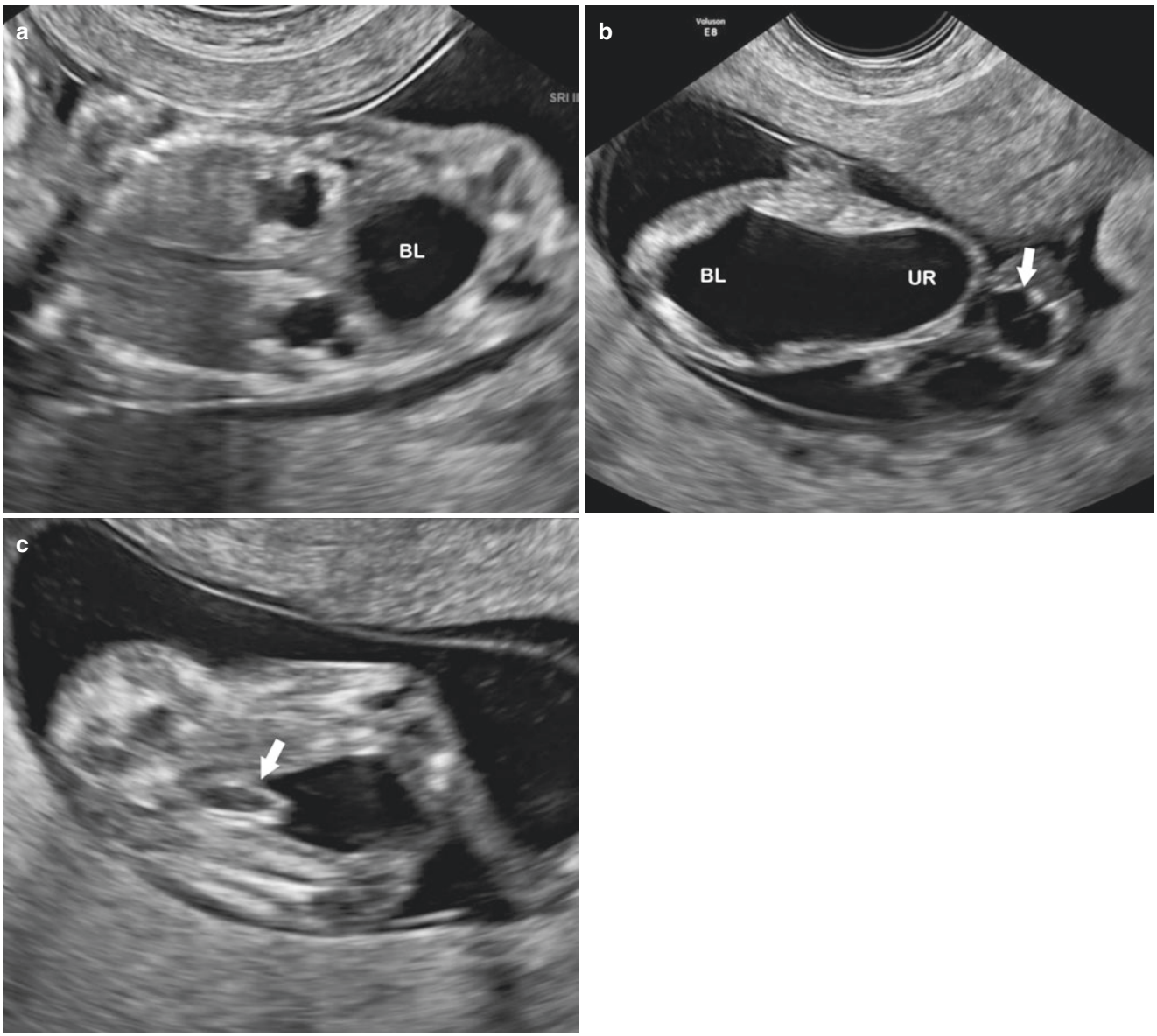

Fig. 3.57 Anterior urethral atresia: (**a**) Coronal scan of fetal abdomen showing the bilateral hydronephrosis (arrows) and dilated urinary bladder (BL). (**b**) Oblique coronal scan of the fetal pelvis and cord insertion showing megacystis (BL), dilated urachus (UR) and allantoic cyst in the umbilical cord (*arrow*). (**c**) Scan of fetal perineum shows the penis with dilated anterior urethra (arrow) up to tip of penis

3.11.5 Megacystis Microcolon Intestinal Hypoperistalsis Syndrome (MMIHS)

Megacystis microcolon-intestinal hypoperistalsis syndrome or Berdon syndrome, is a rare congenital autosomal recessive condition that is characterized by nonobstructive bladder distention, hydronephrosis, hydroureter, intestinal hypoperistalsis and microcolon. The intestines are poorly developed, stenotic or atretic. In these cases, the amniotic fluid volume is normal or increased. Megacystis-microcolon-hypoperistalsis syndrome has a 4:1 female to male ratio. On Sonography, there is megacystis with mild hydronephrosis with normal or increased amniotic fluid volume (Fig. 3.58).

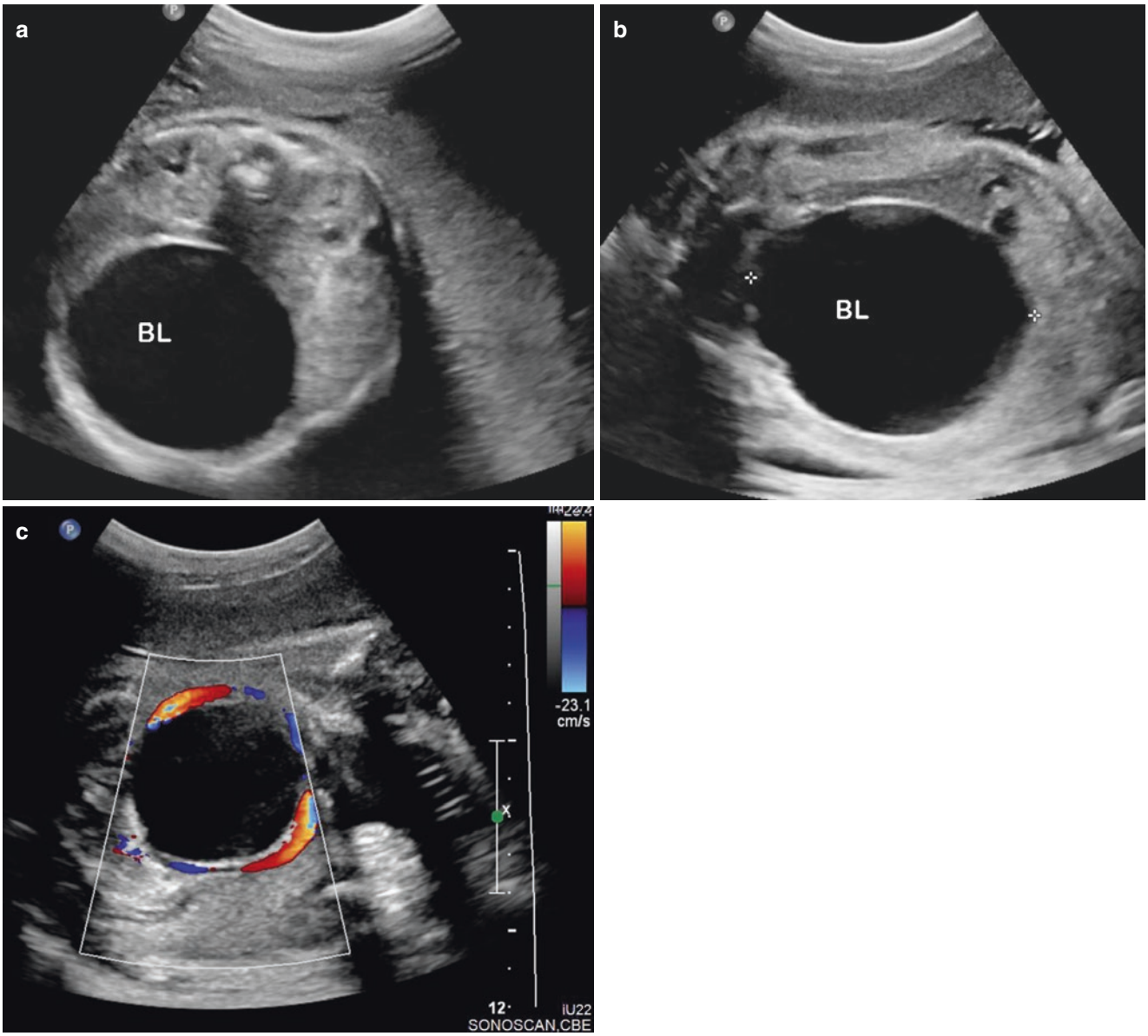

Fig. 3.58 Megacystis Microcolon Intestinal Hypoperistalsis: (**a**) Axial scan showing normal kidneys and overdistended urinary bladder (BL). (**b**) Coronal scan of overdistended urinary bladder. (**c**) Color Doppler study showing umbilical arteries skirting the urinary bladder. There was Polyhydramnios. BL—urinary bladder

3.11.6 Megacystis Megaureter Complex

This is an association of large capacity thin walled urinary bladder and bilateral hydroureteronephrosis due to massive vesicoureteric reflux. The amniotic fluid volume is normal (Fig. 3.59). There may be hyperperistalsis of ureters. SFMCUG will reveal that the urethra and micturition are normal ruling out urinary bladder outflow obstruction (Fig. 3.59d, Video 3.7). This condition is due to bilateral gross vesicoureteric reflux.

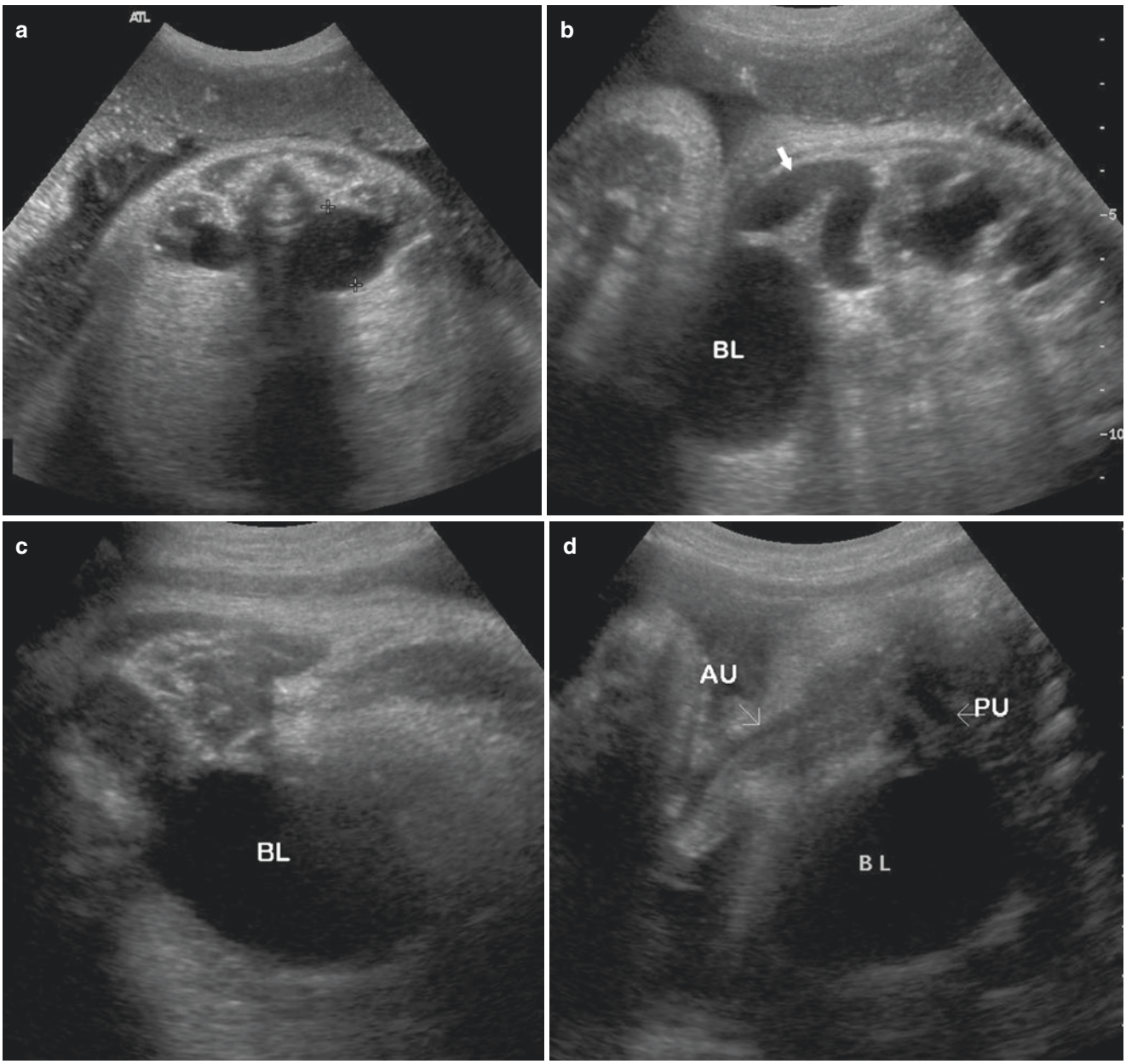

Fig. 3.59 Megacystis megaureter complex: (**a**) Axial scan shows bilateral hydronephrosis. (**b**) Oblique scan shows dilated tortuous ureter (arrow). (**c**) Coronal scan of fetal pelvis showing the megacystis. (**d**) Fetal SMCUG shows slightly distended normal urethra. BL—urinary bladder, AU—anterior urethra, PU—posterior urethra. Postnatal MCU revealed bilateral gross vesicoureteric Reflux (Video 3.7)

3.11.7 Prune Belly Syndrome

Prune Belly Syndrome is a very rare congenital condition where there is aplasia of the detrusor muscles resulting in grossly dilated urinary bladder which stretches the anterior abdominal wall leading to secondary atrophy of the muscles of abdominal wall. About 97% of cases occur in male fetuses. Postnatally when the urinary bladder collapses the abdominal wall reveals wrinkles resembling the prune fruit. On prenatal scan, there is grossly over distended urinary bladder with bulging thin anterior abdominal wall. The thin anterior abdominal wall differentiates this condition from urethral atresia where the abdominal wall is thick (Figs. 3.57 and 3.60).

Rarely there may be transient megacystis and normal amniotic fluid volume in third trimester without any other associated features. Postnatally these newborns do well spontaneously or with an indwelling catheter of a few days.

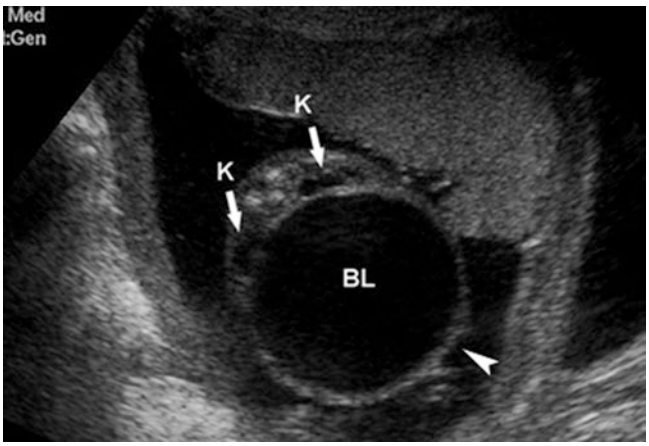

Fig. 3.60 Prune Belly syndrome: Axial scan of fetal abdomen demonstrating bilateral hydronephrosis (arrows) and markedly overdistended urinary bladder (BL) completely filling the abdomen and bulging the anterior abdominal wall. The combined urinary bladder wall and anterior abdominal wall is extremely thin (arrowhead). There is Oligohydramnios

3.12 Nonvisualized Urinary Bladder

When urinary bladder is not visualized, scan should be repeated a few times, since it may be physiological due to emptying cycles of fetal micturition. Nonvisualized urinary bladder is confirmed by the narrow space between the umbilical arteries on color Doppler study (Figs. 3.34b and 3.53d). If there is persistent nonvisualisation, amniotic fluid volume has to be assessed. Nonvisualized urinary bladder with oligohydramnios/anhydramnios should lead to imaging of the fetal kidneys. The pathological conditions causing this may be bilateral renal agenesis, bilateral severe obstruction or bilateral cystic renal diseases which have been discussed already. The urinary bladder is persistently nonvisualized in rare conditions of renal tubular dysgenesis (RTD) and exstrophy of urinary bladder which is discussed later.

3.12.1 Renal Tubular Dysgenesis

RTD is a rare autosomal recessive condition with severe disorder of renal tubular development characterized by early onset and persistent fetal anuria leading to severe oligohydramnios. The disease is genetically heterogenous and linked to mutation in the genes encoding any of the components of the renin angiotensin system (RAS). It can manifest as early as 20–22 weeks with oligohydramnios. Ultrasound shows normal kidneys or mild hyperechogenicity with or without poor cortico medullary differentiation (CMD). There is moderate oligohydramnios with nonvisualised urinary bladder (Fig. 3.61). Chronic oligohydramnios leads to Potter sequence. Fetuses may die in utero. The diagnosis is by histopathology of the kidneys.

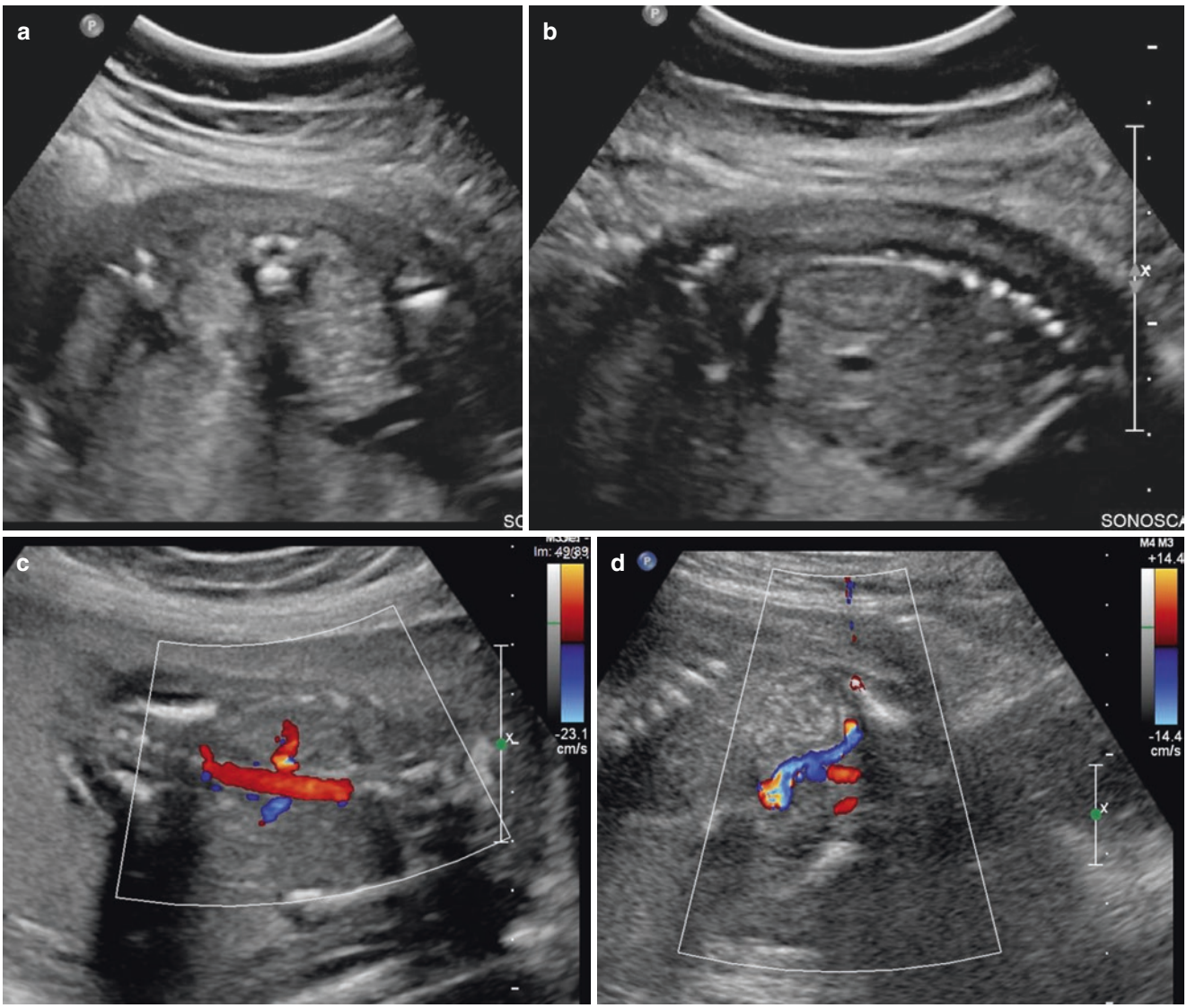

Fig. 3.61 Renal Tubal Dysgenesis: (**a**) Axial and (**b**) Longitudinal scans showing normal appearing kidneys. (**c**) Color Doppler Study shows normal renal arteries. (**d**) Coronal scan of fetus show absent urinary bladder between the umbilical arteries indicating non-functioning kidneys

3.13 Duplication of Urinary Bladder

Duplication of urinary bladder can be partial or complete. Partial duplication is seen as a sagittal incomplete septum from fundus of urinary bladder. It is usually associated with ambiguous genitalia (Fig. 3.62). Complete duplication of the urinary bladder and urethra is extremely uncommon and is more frequent in males. In complete bladder duplication a septum divides the two bladders and orientation of the septum is variable. A sagittal septum is more common. Each bladder receives a ureter of its ipsilateral kidney and is drained by its own urethra lying side by side. Associated anomalies are more common in children with the sagittal type of duplication. In more than 50% of cases there is also duplication of the hindgut. About 90% may demonstrate duplication of the genital tract. In males there may be duplication of the penis with bifid scrotum. In females duplication of the vagina and/or uterus is present. Various hypotheses have been proposed as an embryological explanation for duplication of urinary bladder. Complete duplication of urinary bladder and urethra presents as two cysts in pelvis in between the two umbilical arteries. The two urinary bladders will show emptying independent of each other (Fig. 3.63). There will be varying degrees of duplication of external genitalia, internal genital organs and midgut.

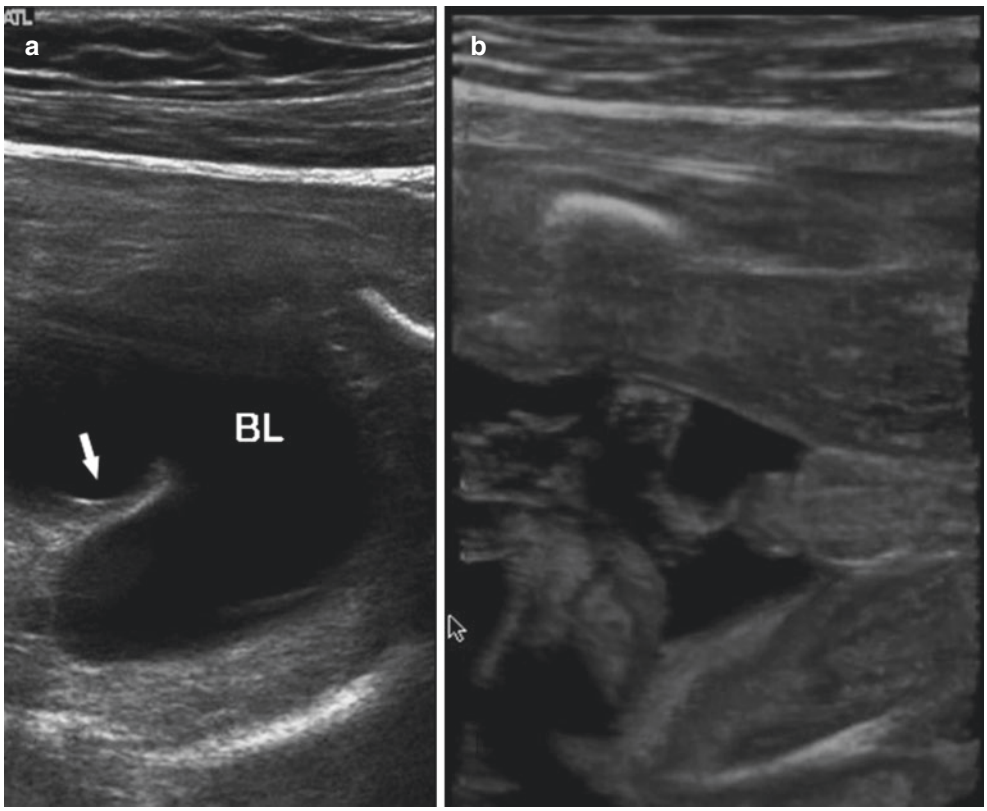

Fig. 3.62 Partial duplication of urinary bladder: (**a**) Coronal scan of fetal pelvis showing the partially septated (arrow) urinary bladder (BL). (**b**) Scan of perineum demonstrating the ambiguous genitalia

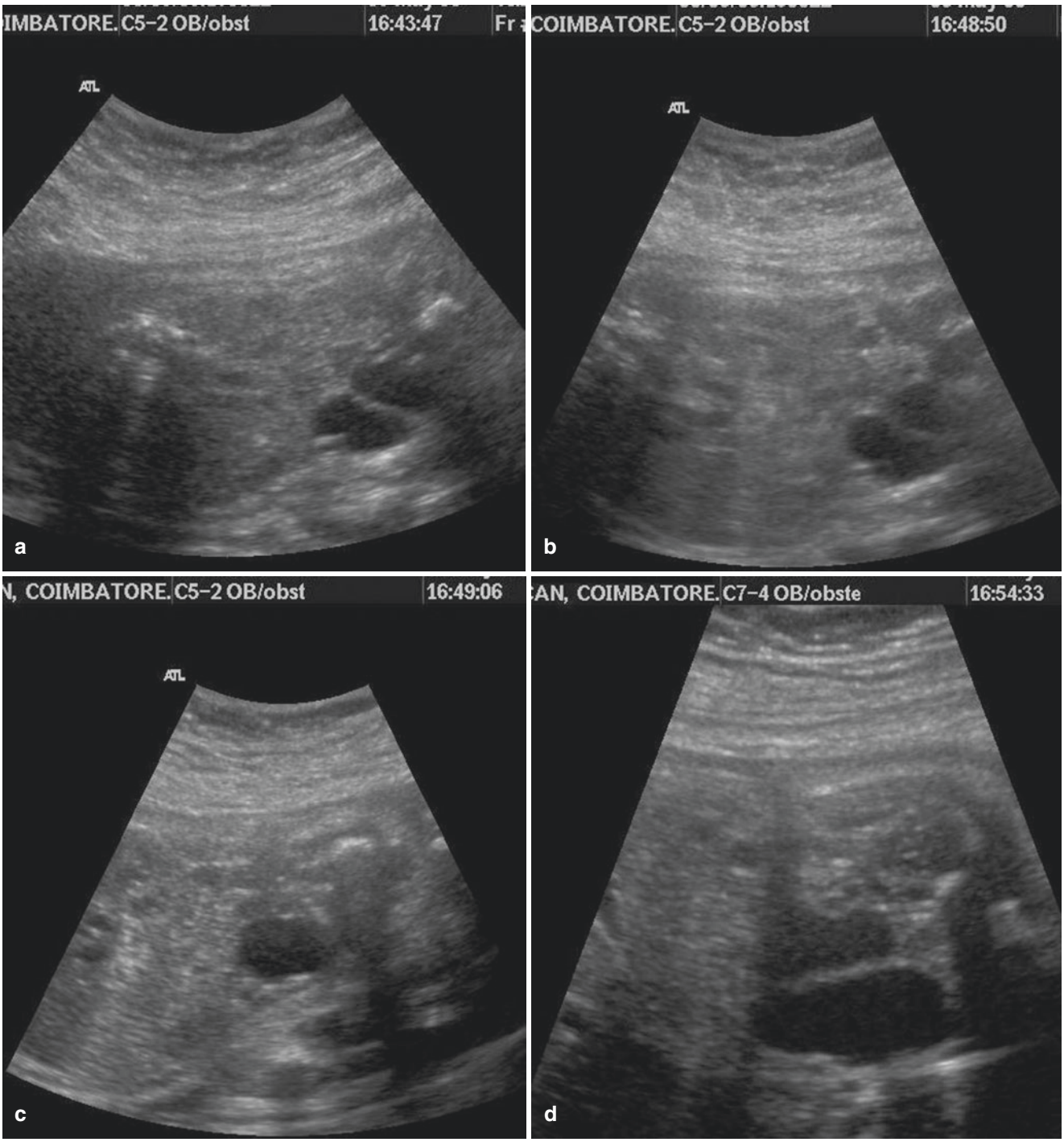

Fig. 3.63 Complete duplication of urinary bladder: Serial coronal scans of fetal pelvis showing two urinary bladders emptying independent of each other. (**a**) Both bladders appear full. (**b**) Scan 5 min after first image shows partially contracted left bladder. (**c**) Scan 16 s after (**b**) showing left bladder completely emptied and right bladder alone is seen. (**d**). Scan 5 min after (**c**) showing partially full left bladder and a full right bladder. (**e**) Scan 1 min after (**d**) showing partially emptied right bladder. (**f**) Scan of fetal perineum shows the two vulvae (arrows). (**g**) Postnatal transverse scan of pelvis of the newborn confirms the two bladders (BL1 and BL2) and also shows the two uteri (U1 and U2) posterior to them. (**h**) Postnatal photograph confirms the two vulvae and two anal openings

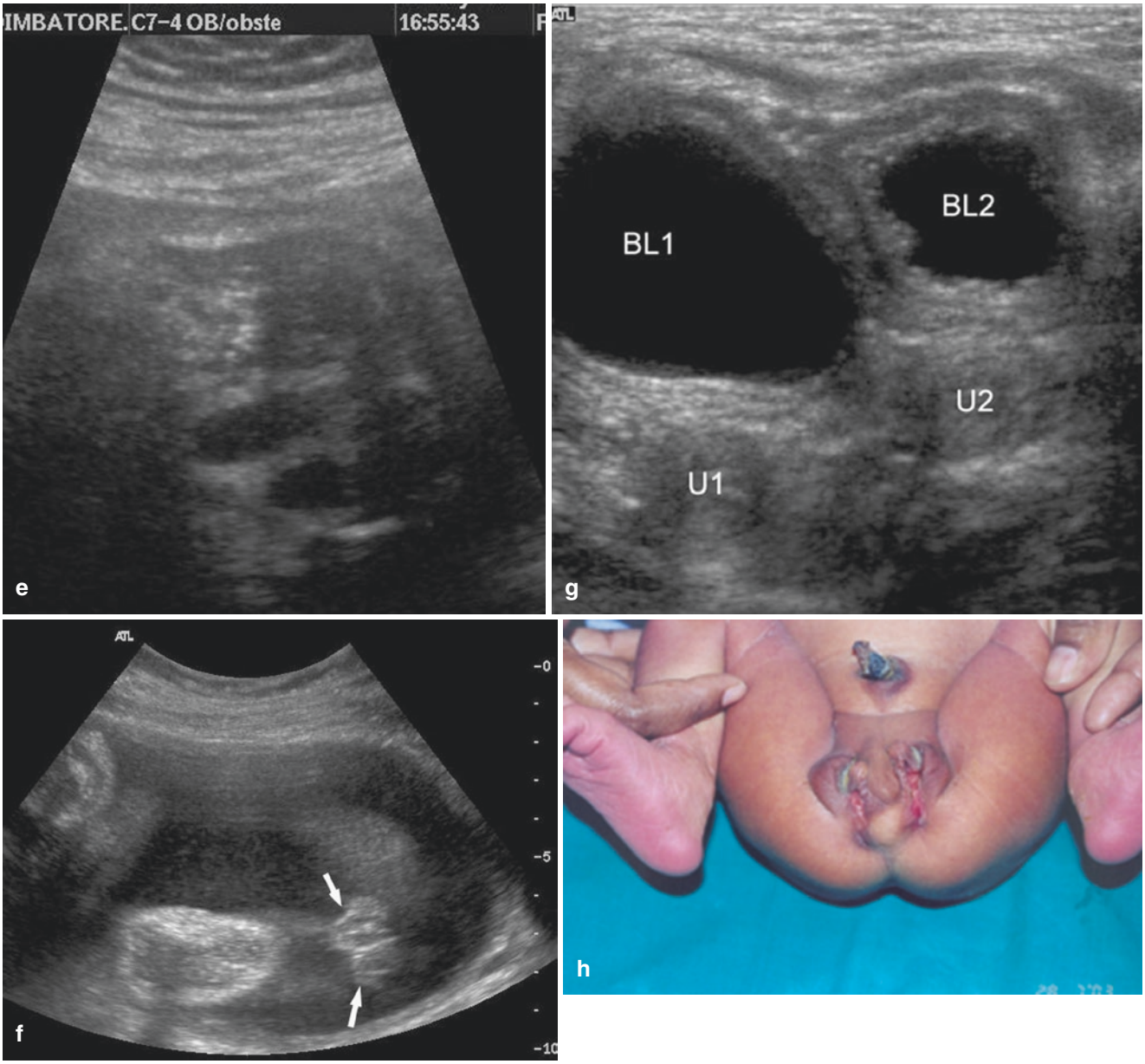

Fig. 3.63 (continued)

3.14 Megalourethra

Megalourethra is a rare form of functional lower urinary tract obstructive uropathy characterized by a congenital deficiency of the mesodermal tissues of the phallus leading to a fusiform, or scaphoid dilatation of penile urethra. There is no obstruction to the flow of urine. It may be isolated or associated with proximal urinary tract dilatation and oligohydramnios. In megalourethra, urinary tract dilatation develops as a result of urinary stasis in the dilated penile urethra, which lacks adequate support and balloons during fetal micturition, thus causing passive obstruction of urinary flow. This functional obstruction may also act as a valve like flap mechanism in some cases, producing intermittent mechanical obstruction to the urine stream through the glandular urethra. Although severe narrowing of the meatus may cause complete anatomic urethral obstruction, no true anatomic obstructive defect has been identified in cases of megalourethra. The confident prenatal diagnosis of megalourethra is established by the documentation of scaphoid dilatation of the penile urethra (Fig. 3.64).

Color Doppler sonography is also used to rule out the presence of a loop or cyst of the umbilical cord, which can be mistaken as the dilated urethra. The differential diagnosis of the condition is anterior urethral atresia, where there is total obstruction with obstructive signs and severe oligohydramnios or anhydramnios. The dilated anterior urethra is tubular in anterior urethral atresia (Fig. 3.57) in contrast to the scaphoid dilatation in megalourethra.

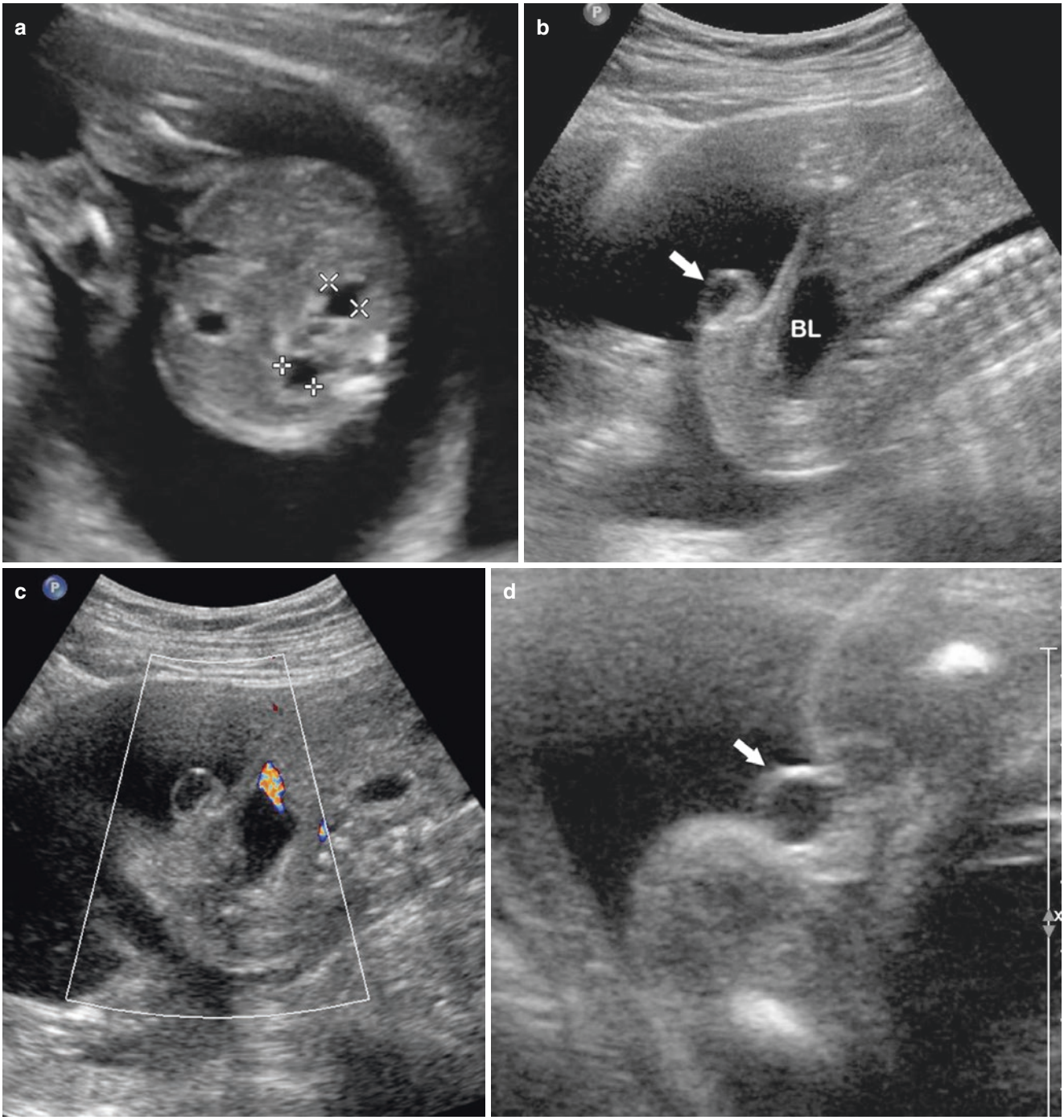

Fig. 3.64 Megalourethra: (**a**) Axial scan of the fetal abdomen showing bilateral mild hydronephrosis. (**b**) Sagittal scan of the lower abdomen and perineum demonstrates the urinary bladder (BL) and scaphoid dilation of the penile urethra (arrow). (**c**) Color Doppler image shows absent flow in the urethra. (**d**) High frequency transverse scan of the penis demonstrates the dilated penile urethra (arrow) and absent corpus spongiosum

3.15 Sirenomelia

Sirenomelia sequence is a rare incidence of 1:60,000 births with a lethal pattern of congenital anomalies characterized by a number of hallmark skeletal anomalies including fusion of the lower extremities or a single lower limb with single or two femora, bilateral renal agenesis or dysgenesis with absent or hypoplastic renal arteries, oligohydramnios and the presence of aberrant vasculature. Two separate systems of classification of sirenomelia have been proposed, one based on the number of feet and the other according to the fused bones. The pattern of sonographic anomalies that characterize sirenomelia, especially the single or fused lower limbs, often go undetected prenatally as ultrasonographic exploration of the fetus is hindered by the severe oligohydramnios or anhydramnios that occurs as a result of the bilateral renal agenesis. When sirenomelia is suspected, it is confirmed by the features of a single stout femur (Fig. 3.65).

When there are two femora, the diagnosis is facilitated by color Doppler to pick up vascular malformation and by high resolution scan. The most dominant vascular feature of sirenomelia is the presence of an aberrant umbilical artery derived from a persistent vitelline artery. The vascular steal theory describes this feature as the pathogenic mechanism that causes sirenomelia, attributing the lower limb abnormalities to hypoperfusion secondary to blood shunting into the dominant vitelline vessels and away from the absent or hypoplastic iliac arteries. The prenatal use of color Doppler imaging in the presence of oligohydramnios is threefold. First, it can be used to confirm the presence of bilateral renal agenesis when gray-scale images fail to detect the presence of renal tissue, especially when the adrenal glands take on a discoid configuration. Second, the caliber and patency of the aorta can be assessed in addition to the presence of normal umbilical arteries in fetuses with bilateral renal agenesis, not associated with sirenomelia. Third, it can detect both the origin of the aberrant vitelline artery in the fetal abdomen and the absence of the normal intimated relationship between the umbilical arteries and the side walls of the bladder (Fig. 3.66).

In some types of sirenomelia, there are two femora with soft tissue fusion. High resolution sonography is useful to diagnose this type by revealing the continuous fused soft tissues around the two femora, when it is suspected in the fetus with features of bilateral renal agenesis and aberrant vitelline artery (Fig. 3.66). The rarest form of sirenomelia is one where the soft tissue fusion is incomplete with a pterygium or web like band of fusion on posterior aspect of the lower limbs extending from the perineum to the foot with the knees in fixed flexion (Fig. 3.67).

In contrast to the diagnosis in second trimester, sirenomelia can be diagnosed with ease in first trimester. This is made possible because oligohydramnios is usually less severe in the first trimester on account of the smaller contribution of fetal urinary excretion to the amount of amniotic fluid, allowing clearer lower limb imaging by ultrasound (Fig. 3.68).

Visualization of lower extremity anomalies consistent with sirenomelia sequence has been noted as early as 9 weeks of gestation.

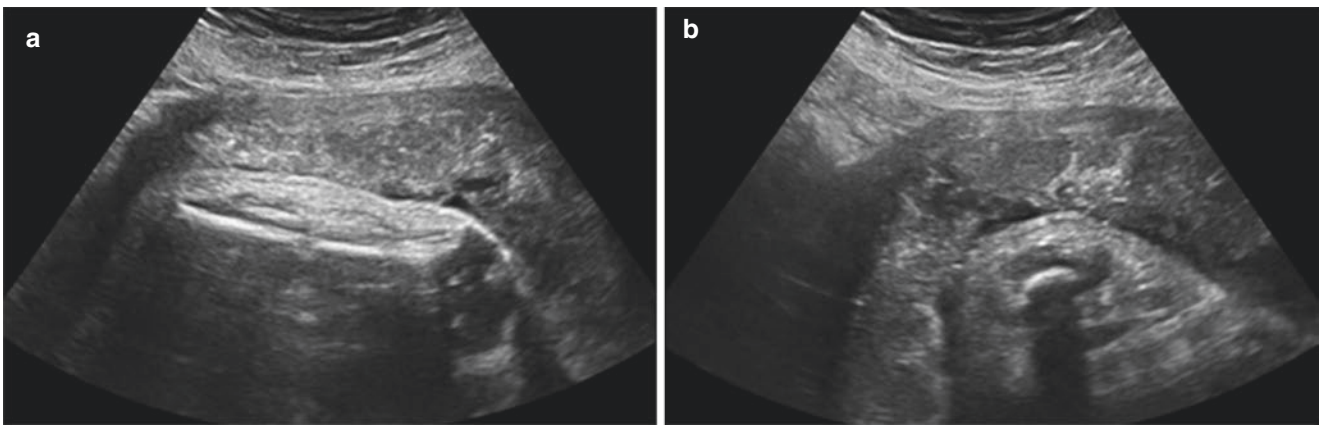

Fig. 3.65 Sirenomelia: (**a**) Longitudinal and (**b**) axial scan of the single stout femur in a fetus with bilateral renal agenesis, single umbilical artery and anhydramnios, characteristic of sirenomelia

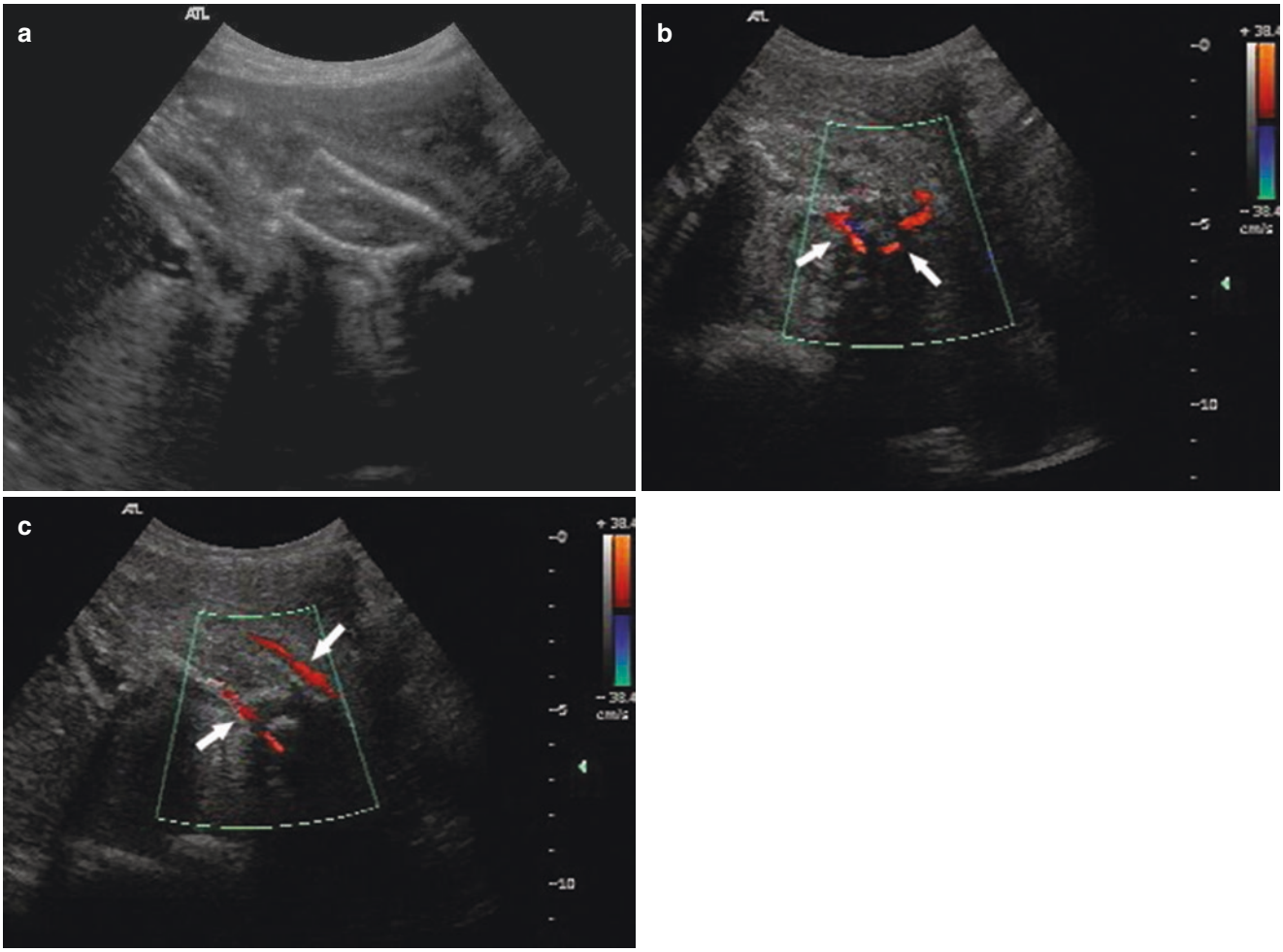

Fig. 3.66 Sirenomelia: (**a**) Ultrasound image of the coronal plane of the thigh showing the two separate femora. Color Doppler images showing (**b**) the two iliac arteries (arrows) in the pelvis and (**c**) the femoral arteries (arrows) in the thigh. High resolution transverse scans through the upper thigh (**d**) and the lower thigh (**e**) depicting the continuous skin line (arrowheads) over both the femora (arrows). (**f**) Picture of the abortus revealing sirenomelia

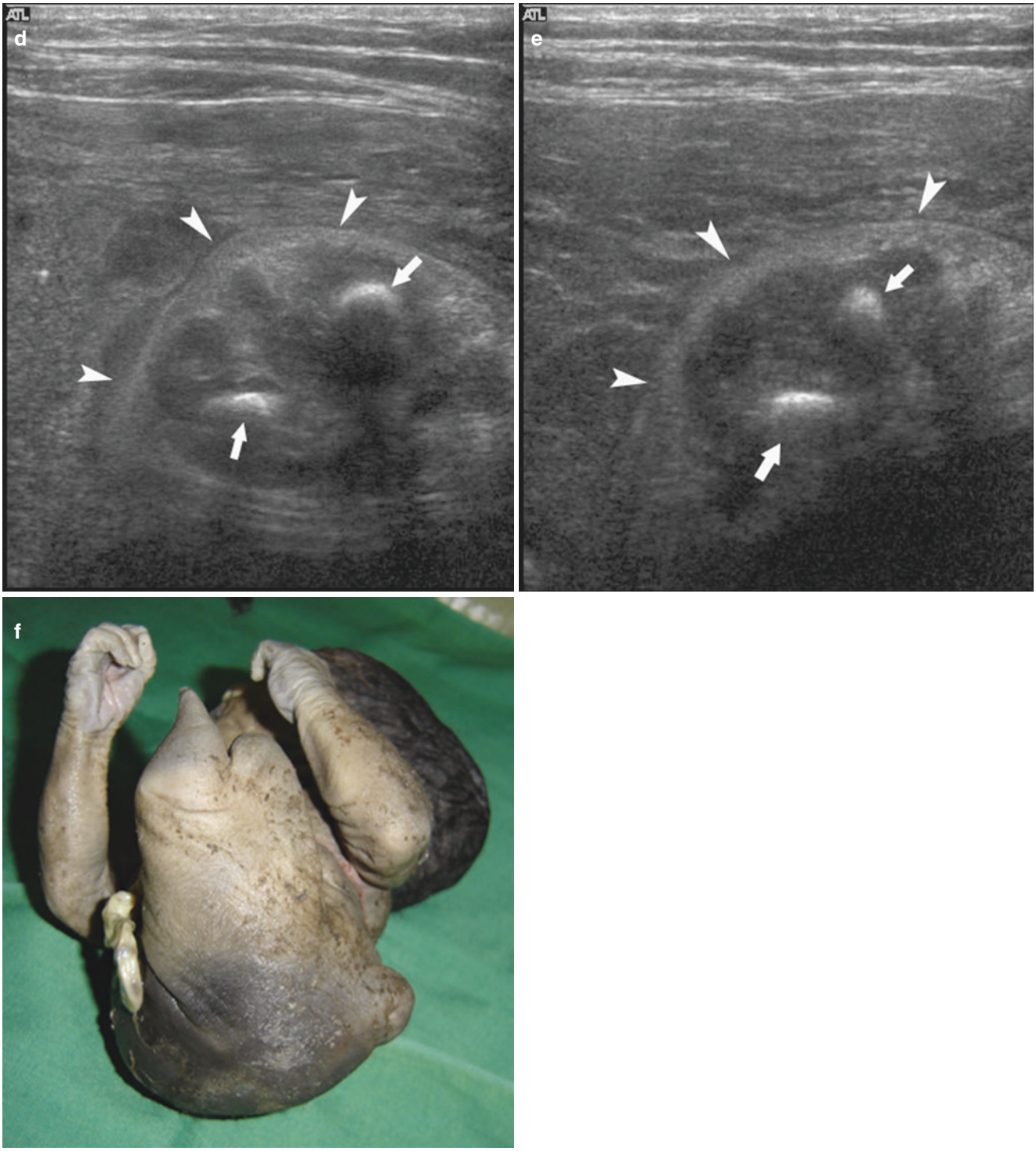

Fig. 3.66 (continued)

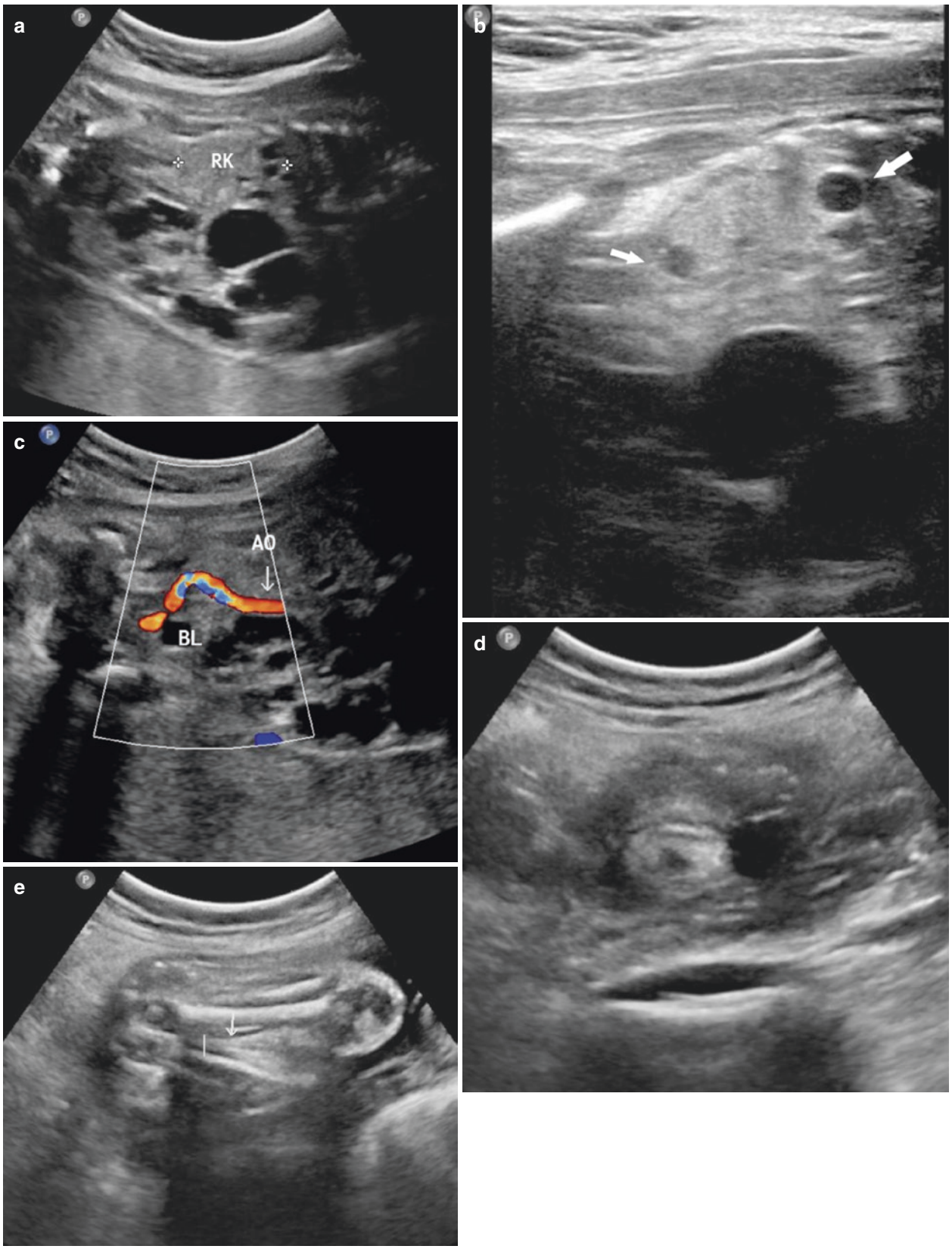

Fig. 3.67 Sirenomelia: (**a**) Coronal scan demonstrating the multicystic dysplasia of both kidneys with anhydramnios. (**b**) High frequency scan of right kidney demonstrating the multicystic dysplasia, (**c**) Color Doppler study revealing the aberrant vitelline artery arising from the aorta (AO). BL—Urinary bladder. (**d**) Scan of perineum showing the nonvisualised anus. (**e**) Coronal scan of thigh shows the soft tissue fusion along the proximal aspect. (**f**) Web like fused soft tissue (arrow) along posterior aspect of thighs and legs extending from perineum to the feet. (**g**, **h**) Photographs of the abortus demonstrating the soft tissue fusion and flat fused gluteal region with absent anal opening

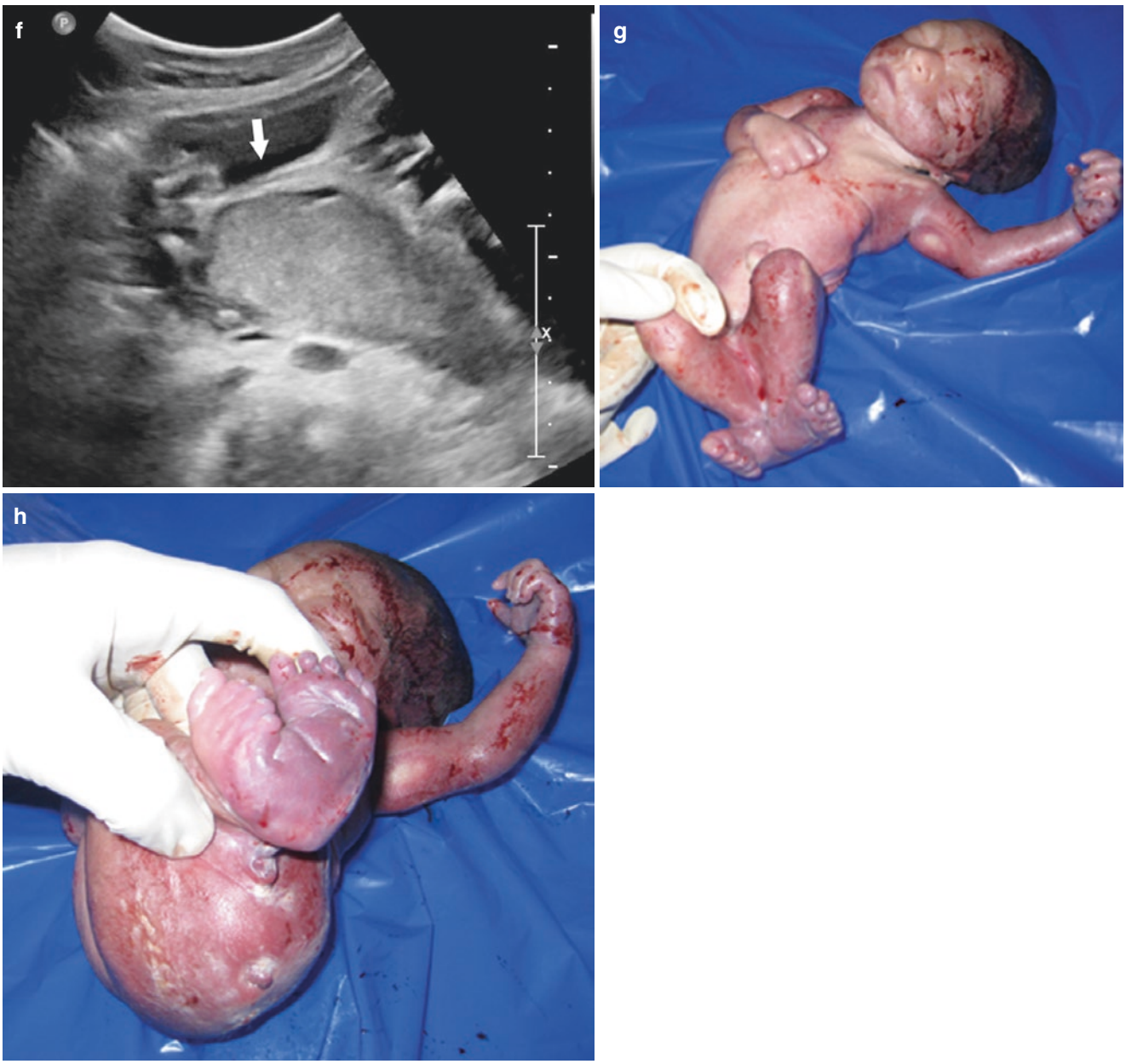

Fig. 3.67 (continued)

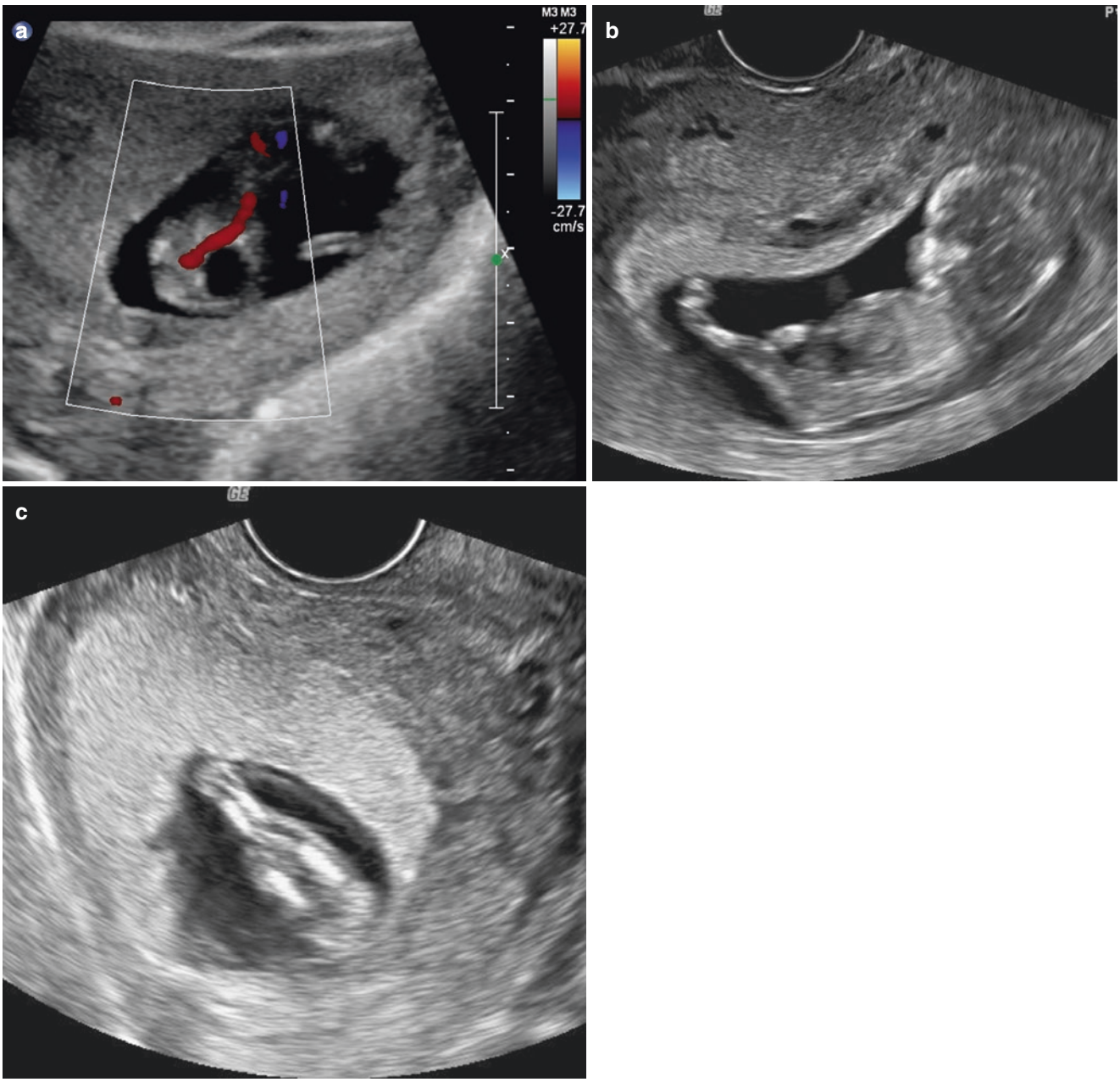

Fig. 3.68 Sirenomelia in first trimester: (**a**) Color Doppler study showing the aberrant vitelline artery. (**b**) Longitudinal scan of the fetus shows the characteristic fixed posture of the fused lower limb. (**c**) Coronal scan of the fused lower limbs easily demonstrated because of adequate amniotic fluid in first trimester

Suggested Reading

Avni FE, Garel C, Cassart M, D'Haene N, Hall M, Riccabona M. Imaging and classification of congenital cystic renal diseases. AJR Am J Roentgenol. 2012;198(5):1004–13.

Boopathy Vijayaraghavan S. Sonography of fetal micturition. Ultrasound Obstet Gynecol. 2004;24(6):659–63.

Boopathy Vijayaraghavan S, Kamalam M, et al. Prenatal sonographic appearance of congenital bile duct dilatation associated with renal-hepatic-pancreatic dysplasia. Ultrasound Obstet Gynecol. 2004;23(6):609–11.

Nguyen HT, Benson CB, Bromley B, Campbell JB, Chow J, Coleman B, Cooper C, Crino J, Darge K, Herndon CD, et al. Multidisciplinary consensus on the classification of prenatal and postnatal urinary tract dilation (UTD classification system). J Pediatr Urol. 2014;10(6):982–98.

Osborne NG, Bonilla-Musoles F, Machado LE, Raga F, Bonilla F Jr, Ruiz F, Perez Guardia CM, Ahluwalia B. Fetal megacystis: differential diagnosis. J Ultrasound Med. 2011;30(6):833–41.

Vijayaraghavan SB. Fetal perineal sonography in the diagnosis of ectopic ureteric opening. Ultrasound Obstet Gynecol. 2007;29(3):347–51.

Vijayaraghavan SB, Amudha AP. High-resolution sonographic diagnosis of sirenomelia. J Ultrasound Med. 2006;25(4):555–7.

Vijayaraghavan SB, Nirmala AB. Complete duplication of urinary bladder and urethra: prenatal sonographic features. Ultrasound Obstet Gynecol. 2004;24(4):464–6.

Masses and Fluid Collection in Fetal Abdomen

4

Mass lesions in fetal abdomen are rare occurrences and may be solid or cystic. They can be differentiated and narrowed down by an algorithm given below:

4.1 Confirmation

The lesion seen had to be confirmed that it is an abnormal mass and not a normal appearance. This is particularly so in a cystic lesion. A Coronal scan of abdomen shows three normal cystic structures namely—stomach bubble, gall bladder and urinary bladder. If an additional cystic mass is seen it has to be evaluated further.

Electronic Supplementary Material The online version of this chapter (https://doi.org/10.1007/978-981-13-0932-8_4) contains supplementary material, which is available to authorized users.

S. B. Vijayaraghavan, *Atlas of Fetal Imaging*, https://doi.org/10.1007/978-981-13-0932-8_4

4.1.1 Organ or Plane of Origin Is Determined by the Following Features

(a) Intraorgan appearance—the mass may be seen to be well within a large organ like liver, spleen or kidney (Figs. 4.1 and 4.2).
(b) Beak sign: A lesion arising from an organ compresses and stretches the normal parenchyma of the organ as a beak over the mass confirming its origin from that organ (Figs. 4.3 and 4.4).
(c) Reverse beak sign: A definite indentation or groove between the mass and an adjacent organ confirms that it is not arising from the organ (Fig. 4.5).
(d) Continuity: If the lesion is not separable from an organ by a visible interphase between them, the mass may be arising from the organ (Fig. 4.20). Continuity of a cyst with a vessel will indicate vascular origin like umbilical vein varix (Fig. 4.6), with dilated bile ducts will indicate a choledochal cyst (Fig. 4.5) and with ureter or renal pelvis will indicate ureteric origin (Fig. 4.14).
(e) Displacement of an organ by the mass confirms that the mass is in the same plane as the organ. Example—Urinoma (Fig. 4.7) and neuroblastoma (Fig. 4.23c) and retroperitoneal lymphangioma (Fig. 4.13).
(f) Colour Doppler is useful to diagnose the origin of a mass by seeing the origin of supplying vessels form the organ (Fig. 4.20). It is also useful to determine the plane of the mass separated by the vessels (Fig. 4.3). It also confirms vascular origin in case of umbilical vein varix (Fig. 4.6).
(g) Fetal gender can narrow down the organ of the mass like ovary or hydrocolpos.
(h) Rarely, it may not be possible to identify the organ of organ but the plane of origin may be determined by looking at the tissue planes and movements.
(i) Shape or pattern of the mass—On coronal scan of renal area hydronephrosis has a characteristic pattern with dilated peripheral calyces communicating with the medial central renal pelvis. A triangular cystic mass above the kidney is likely an adrenal cyst.
(j) Temporal change is useful to diagnose certain conditions like adrenal hemorrhage (Fig. 4.24) or hemorrhagic cyst.

4.1.2 Characterization

The mass can be solid, cystic or heterogeneous. Cystic masses are more common than solid masses. The conditions to be considered will be different for solid and cystic mass and so they will be described separately. Presence of calcification will point to a teratoma.

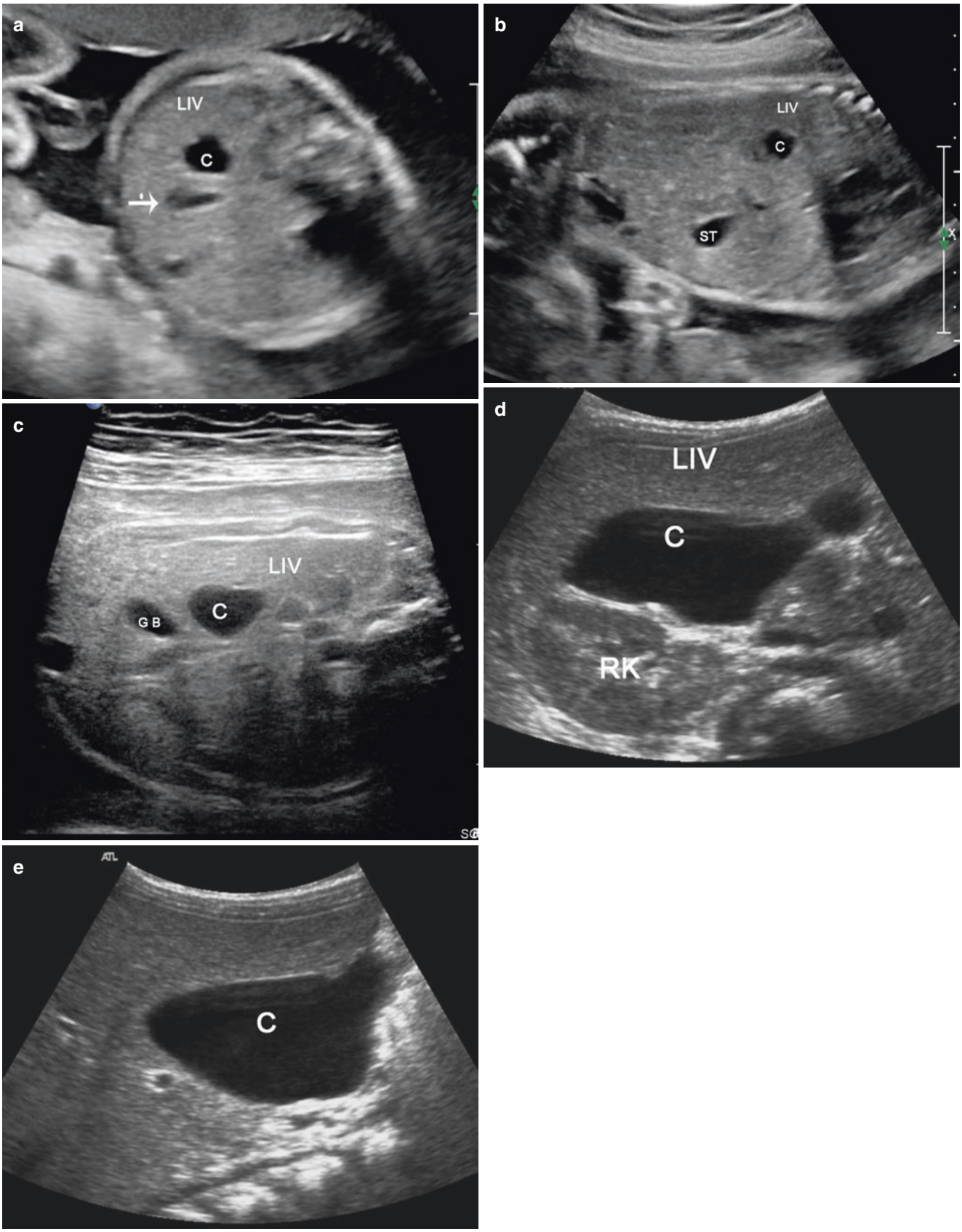

Fig. 4.1 Liver cyst: (**a**) Axial and (**b**) Coronal scan of fetal abdomen showing the cyst (C) within the liver (LIV) with Intraorgan sign. Arrow points to gall bladder. (**c**) High frequency scan showing the cyst in the liver (LIV). Postnatal axial (**d**) and Sagittal (**e**) scan of new born showing the cyst (C) in posterior part of right lobe of liver (LIV). RK—Right kidney

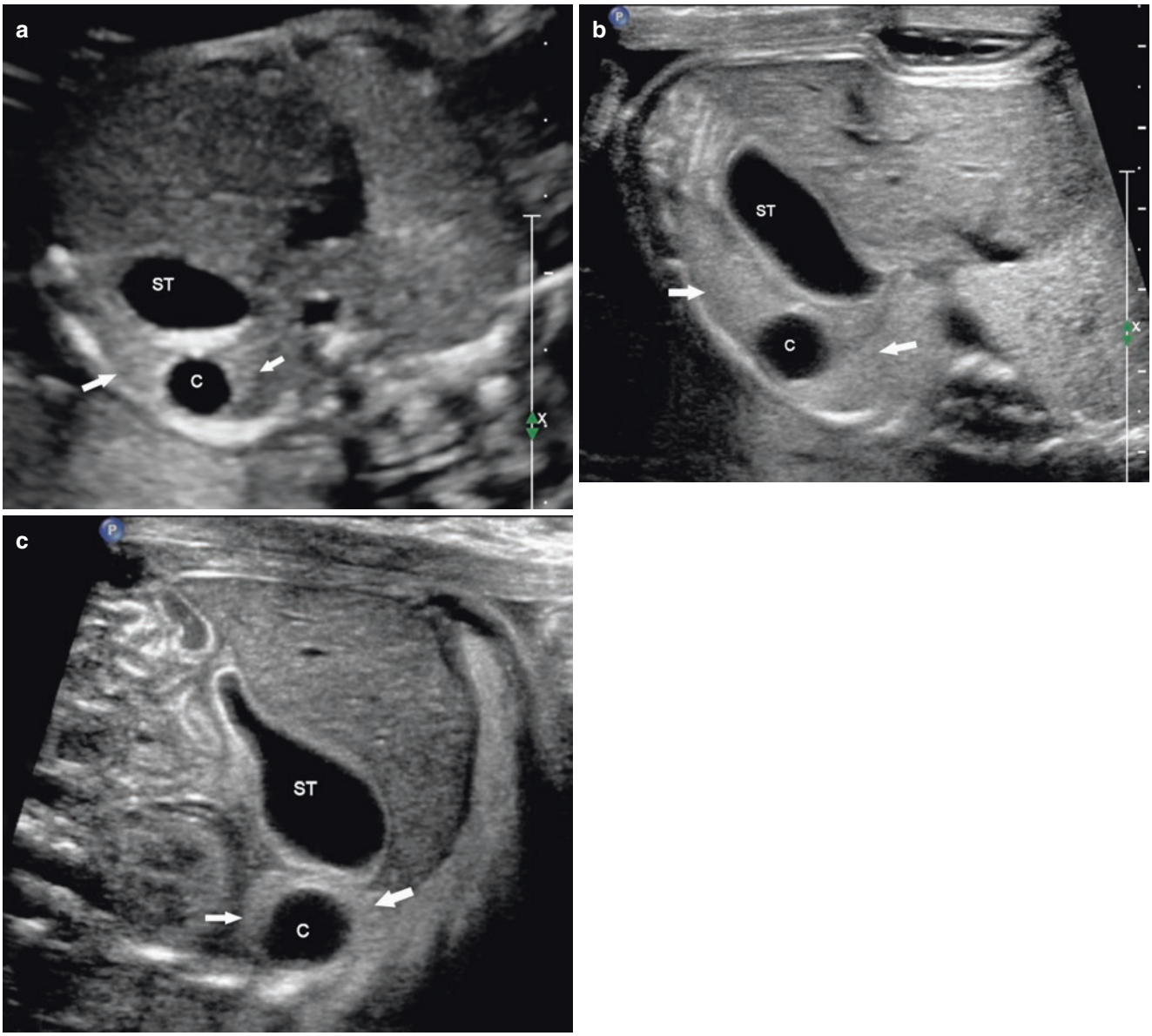

Fig. 4.2 Splenic cyst: (**a**) Axial scan of fetal upper abdomen showing the cyst (C) in spleen posterior to stomach (ST). High frequency axial (**b**) and longitudinal (**c**) scans showing the cyst (C) in spleen (arrows) with the intraorgan sign. (**d**) Colour Doppler image showing the splaying of splenic artery branches by the cyst confirming its location in spleen

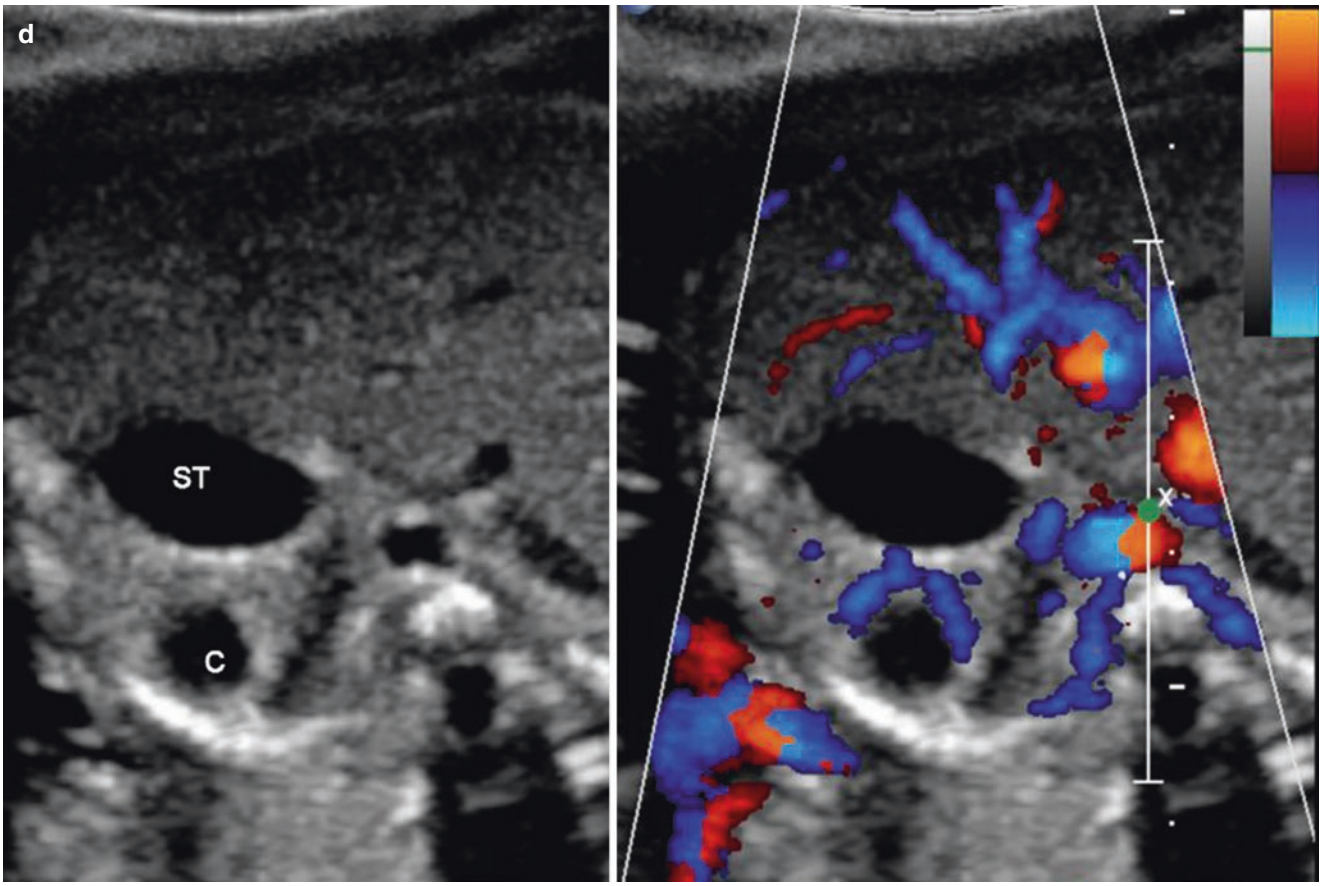

Fig. 4.2 (continued)

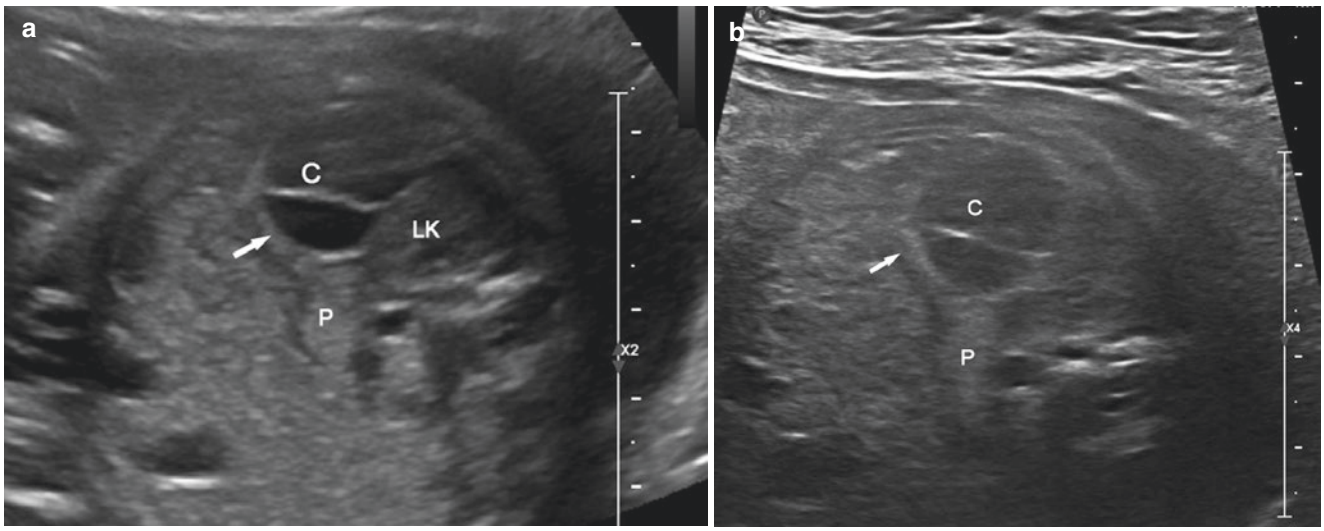

Fig. 4.3 Pancreatic cyst (**a**) Axial scan of fetal upper abdomen showing a septated cyst (C) in tail of echogenic pancreas (P) anterior to left kidney (LK) with beak sign (arrow). (**b**) High frequency scan showing the beak sign better. (**c**) Colour Doppler image shows the cyst (C) anterior to splenic vessels (arrow) and spleen (SP) confirming the plane of the cyst in pancreas

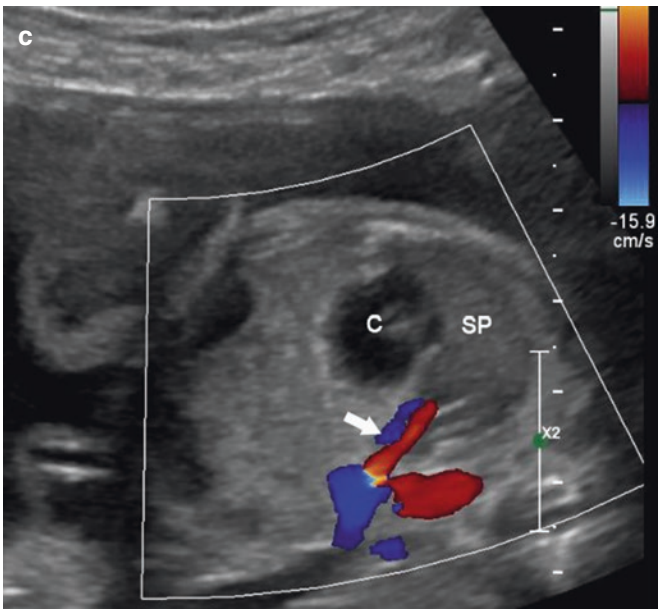

Fig. 4.3 (continued)

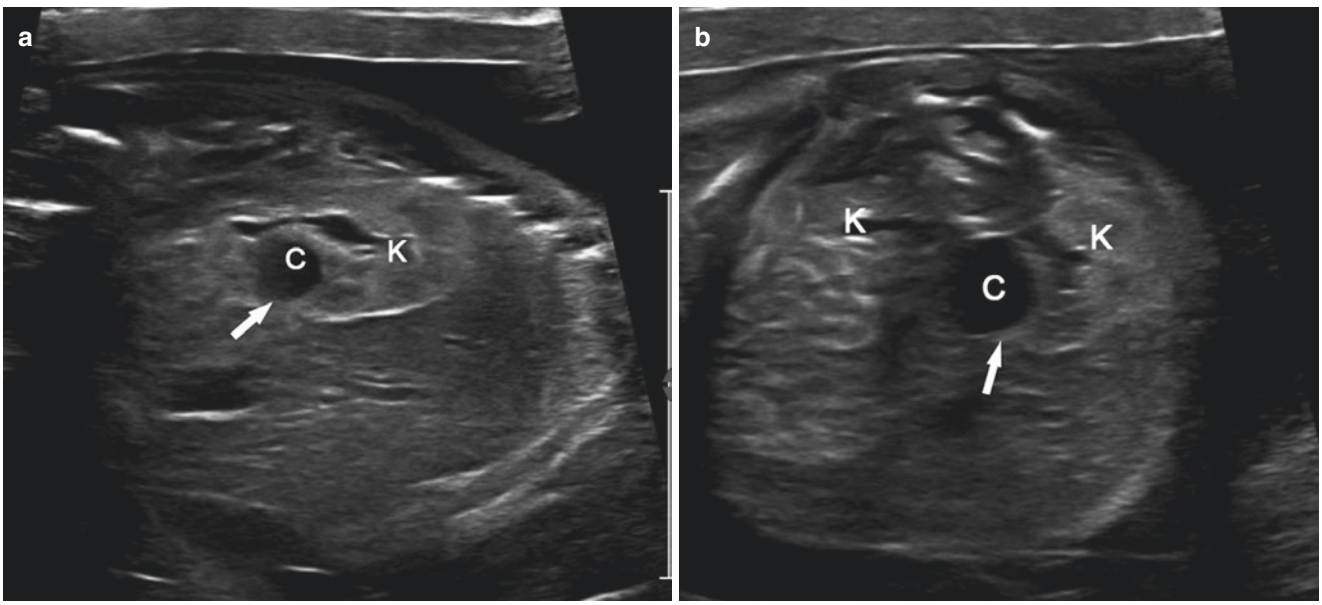

Fig. 4.4 Renal cyst: High frequency axial (**a**) and longitudinal (**b**) scan of kidney showing a cyst (C) in anteromedial parenchyma of the kidney with the beak sign (arrow)

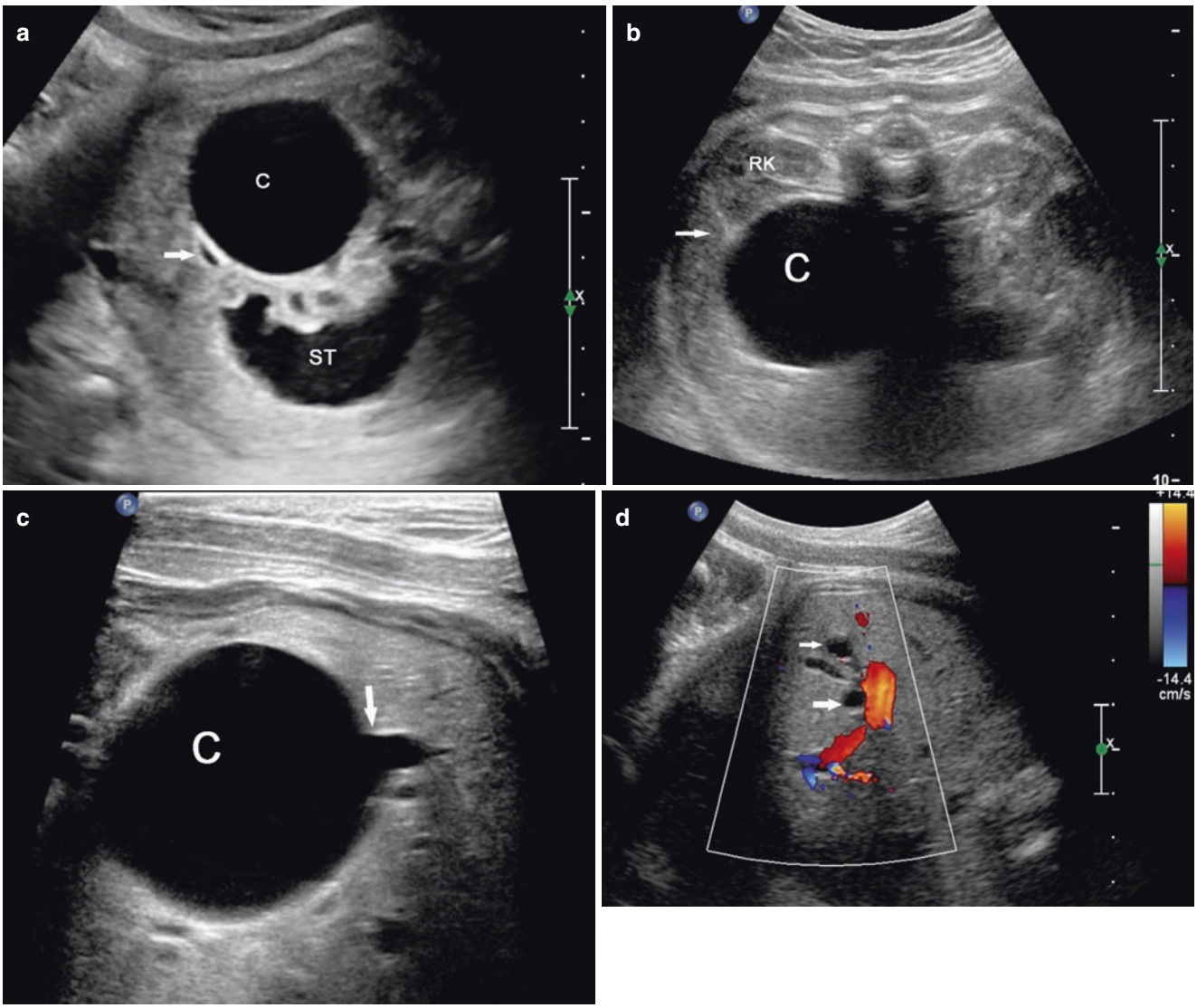

Fig. 4.5 Choledochal cyst: (**a**) Axial scan of fetal upper abdomen showing the cyst (C) in right upper abdomen posterior to the compressed and stretched duodenal cap (arrow) indicating the cyst within the C - loop of duodenum. (**b**) Axial scan just below the previous scan showing the cyst (C) anterior to right kidney (RK) with the groove in between—the reverse beak sign showing that it is not arising from the kidney. (**c**) Coronal scan showing the continuity of the cyst (C) with dilated hepatic duct (arrow) confirming a choledochal cyst. (**d**) Colour Doppler image of a section through the hilum of liver shows dilated hepatic ducts with absent flow (arrow) anterior to color filled branches of portal vein

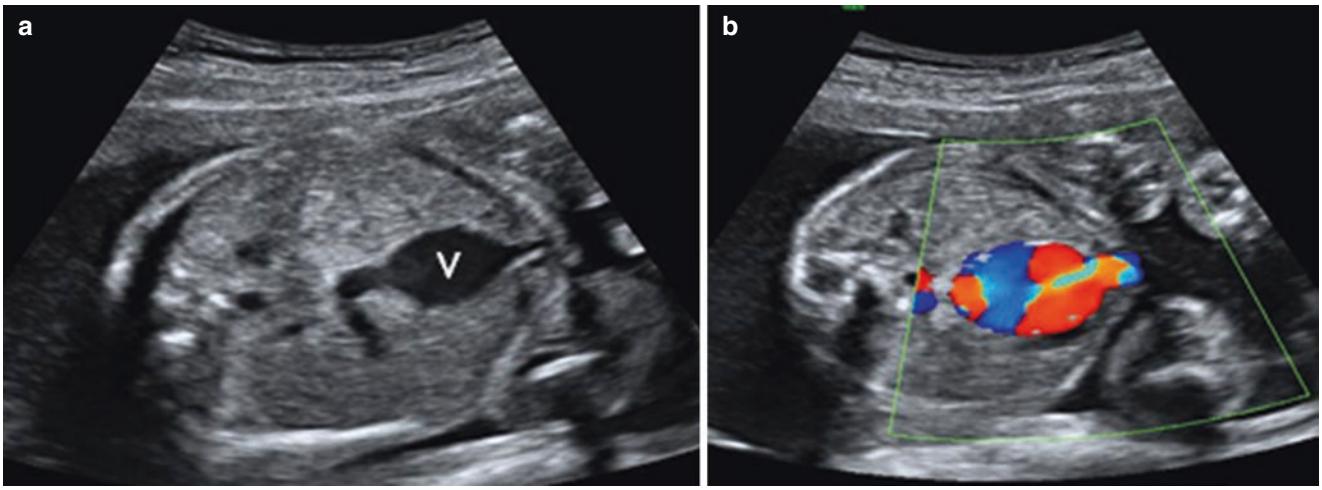

Fig. 4.6 Umbilical vein varix: (**a**) Axial scan of fetal abdomen showing an anteroposteriorly oriented oval cystic mass (V) continuous with the left branch of portal vein confirming that it is umbilical vein varix. (**b**) Colour Doppler image showing circular flow in the cyst confirming the vascular origin

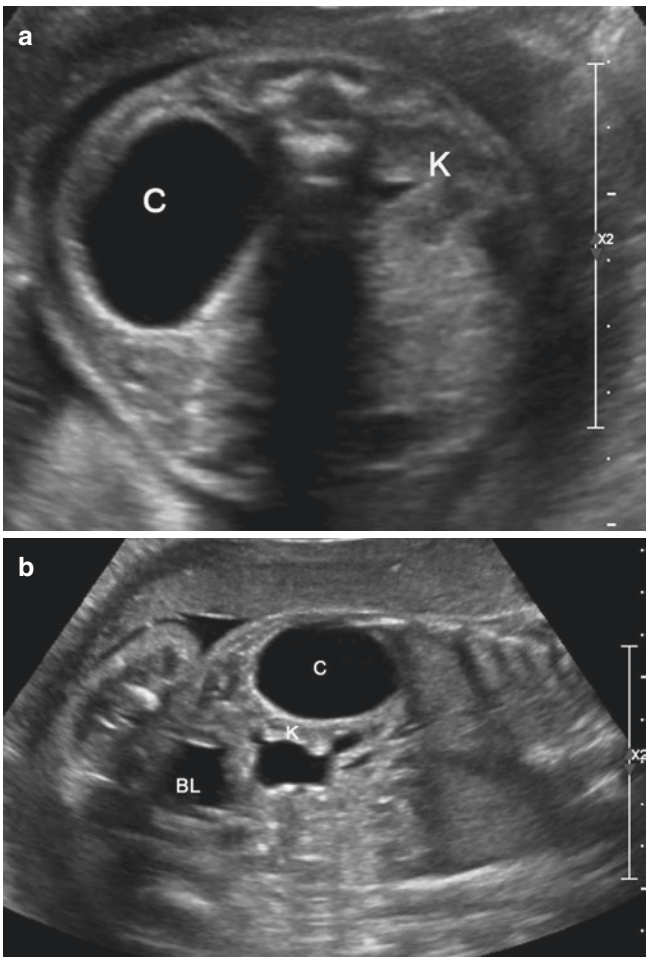

Fig. 4.7 Urinoma: (**a**) Axial scan of the fetal abdomen showing normal right kidney (RK) and a large cyst in left renal area. (**b**) Coronal scan shows the cyst (C) displacing the hydronephrotic left kidney (LK) medially and compressing it confirming that it is in the same plane as the kidney and hence a urinoma

4.2 Fetal Abdominal Cysts

4.2.1 Ultrasound Imaging Approach

The cause of fetal abdominal cysts is determined by looking for the following sonographic features:

(a) Incidence: In female fetuses the commonest cyst is an ovarian cyst. So in female fetuses the diagnosis has to be ovarian cyst unless there are other features against this diagnosis.
(b) Location: A cyst in lower abdomen by the side of urinary bladder is more likely to be ovarian origin (Fig. 4.8) while a cyst in right upper quadrant is more likely to be a choledochal cyst (Fig. 4.5). Changing location of a cyst at different time of scan or on follow up will indicate a mesenteric or bowel duplication cyst since they are in the freely mobile mesentery. Whereas a fixed cyst is more likely to be in retroperitoneum like an adrenal cyst (Fig. 4.22) or renal cyst (Fig. 4.4). A cyst in midline posterior to urinary bladder in a female fetus is suggestive of hydrocolpos (Figs. 4.15 and 4.16).
(c) Cyst morphology: Unilocular cyst can be ovarian or mesenteric origin but a septum in the cyst will point to an ovarian cyst (Fig. 4.8b). Lymphangioma is usually multiseptated (Figs. 4.15 and 4.16). Fat or calcification in a cyst will indicate teratoma (Fig. 4.10). Heterogeneous appearance (Figs. 4.9 and 4.11) or fluid level (Fig. 4.8c) will be seen in a complicated cyst.
(d) Tension/Shape of the cyst: Round shape indicates a cyst under tension like an ovarian cyst. Flaccid cysts are oval or tubular as seen in duplication (Fig. 2.18) or lymph cysts.
(e) Wall of cyst: A thin smooth wall is seen in ovarian or mesenteric cysts. The wall is thick with two discrete layers in duplication cyst (Figs. 2.16, 2.17, and 2.18).
(f) Continuity of the cyst with a vein indicates a vascular origin like umbilical vein varix (Fig. 4.6) or with dilated biliary radicles is diagnostic of a choledochal cyst (Fig. 4.5), with ureter/renal pelvis is suggestive of a cystic dilatation of ureter (Fig. 4.14) and with urinary bladder in urachal cyst (Fig. 4.17).
(g) Peristalsis observed in a cyst is diagnostic of a duplication cyst as this feature is not seen in any other cyst (Figs. 2.17 and 2.18, Videos 2.7 and 2.8). Peristalsis of bowel within a mesenteric lymphangioma is useful in diagnosis (Fig. 4.12, Video 4.1).
(h) Temporal change: The size of a cyst can change in follow up scan—ovarian cysts normally decrease in size and may disappear whereas the duplication or mesenteric cysts usually remain the same in size and appearance. Cysts like choledochal cysts increase in size. Adrenal hemorrhage or hemorrhage into an ovarian cyst show characteristic change over time clinching the diagnosis (Fig. 4.22).
(i) Fetal Micturition—Observation of fetal micturition in the form of contraction of urinary bladder is useful in confirming the urinary bladder when two cysts are seen in fetal pelvis like ovarian cyst (Fig. 4.8), vesical diverticulum (Fig. 4.18), duplication of urinary bladder (Fig. 3.61) and hydrocolpos (Figs. 4.15 and 4.16).

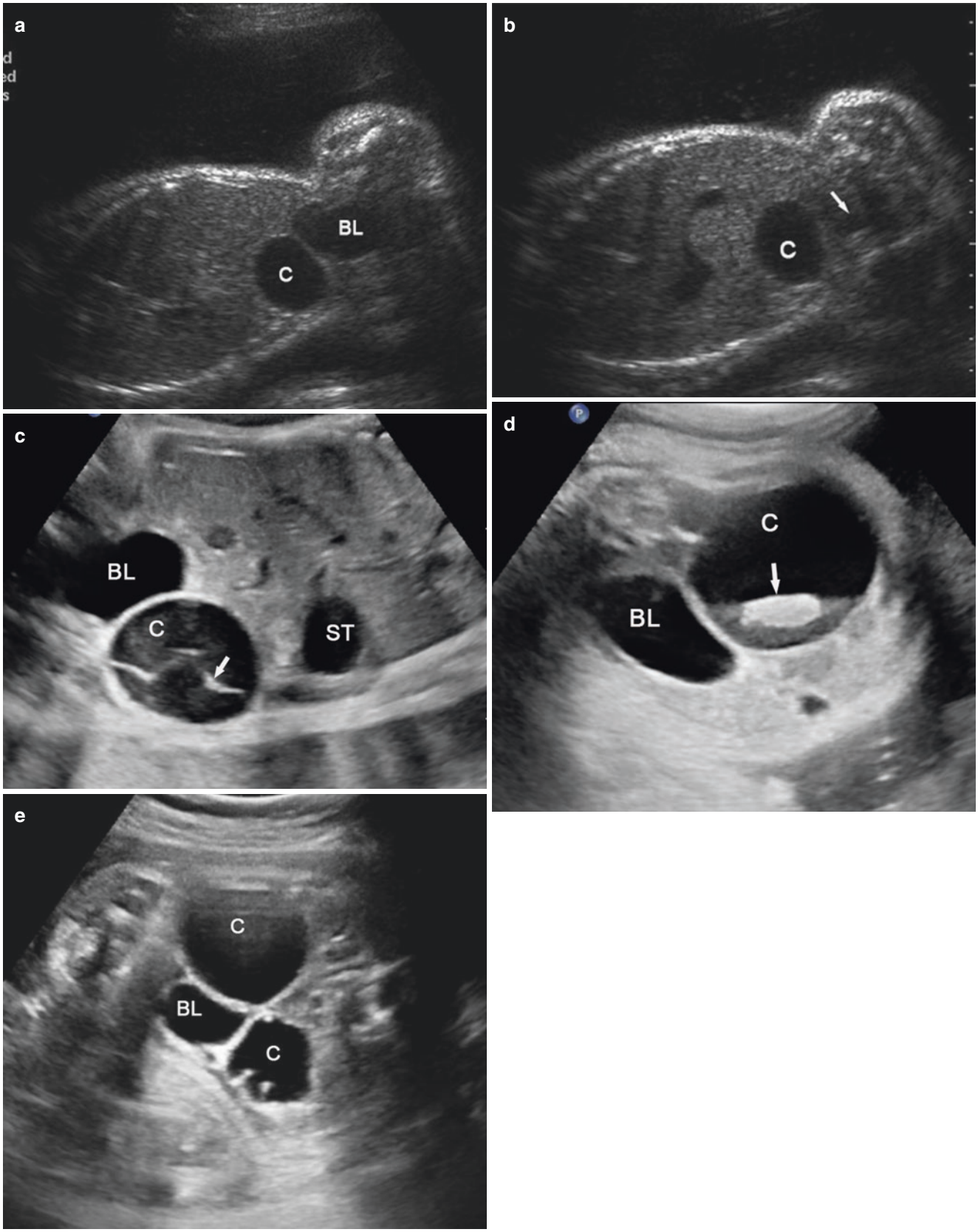

Fig. 4.8 Ovarian cyst: Coronal scan of fetal lower abdomen showing (**a**) Unilocular ovarian cyst (C) by the side of urinary bladder (BL). (**b**) Scan after fetal micturition shows that the bladder has contracted (arrow) while the ovarian cyst (C) remains. (**c**) Septated cyst is in favor of ovarian cyst. (**d**) Ovarian cyst (C) with fluid level (arrow). (**e**) Bilateral ovarian cysts (C) on either side of bladder (BL)

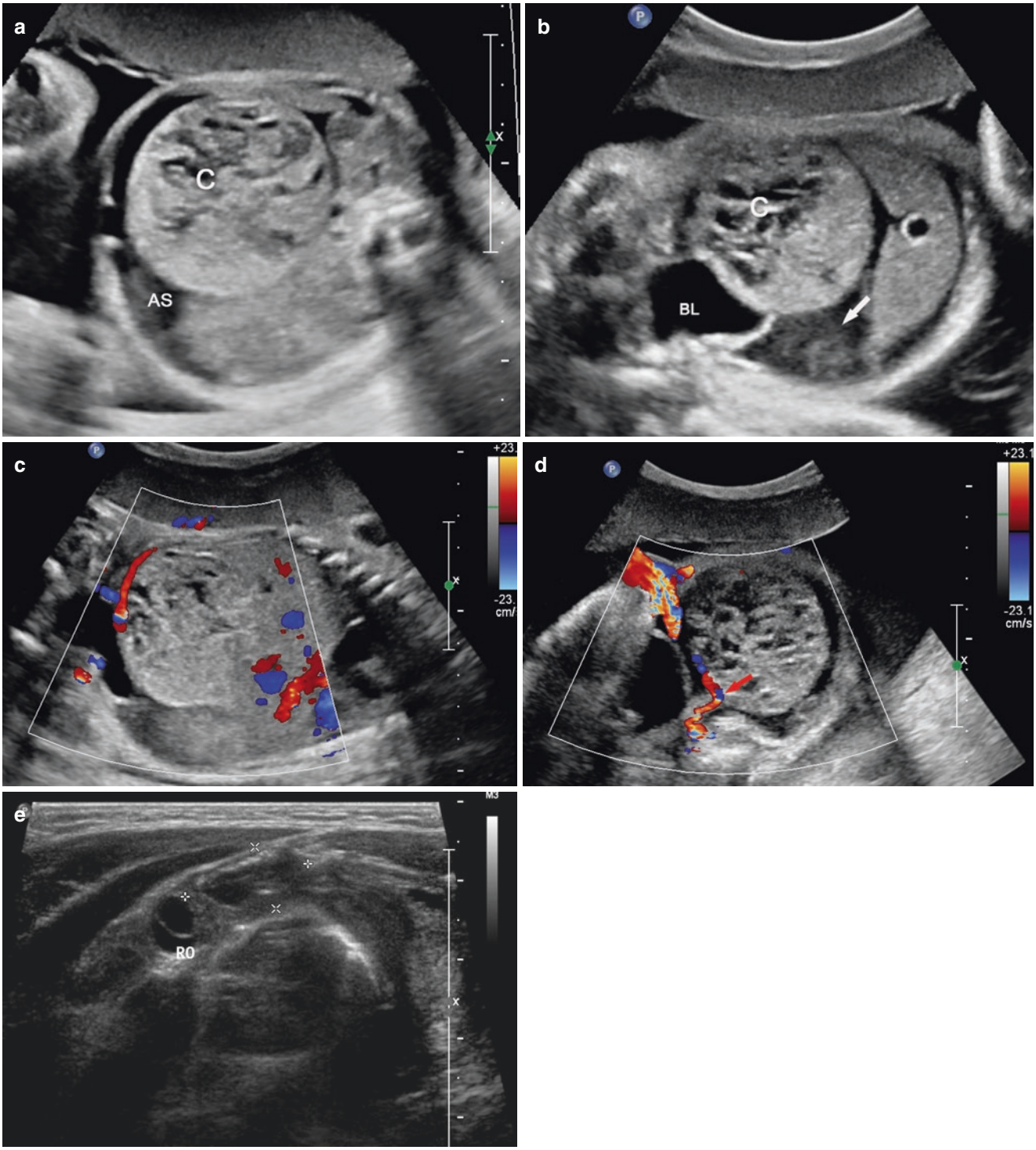

Fig. 4.9 Hemorrhagic ovarian cyst: (**a**) Axial and (**b**) Coronal scan of fetal abdomen showing ascites (As) with debris (arrow) and a heterogeneous ovarian cyst (C) by the side of bladder (BL). (**c**, **d**) Colour Doppler images showing flow in the periphery of the mass and supply vessel arising from the iliac artery confirming a hemorrhagic ovarian cyst. (**e**) Postnatal scan showing the ovary with collapsed cyst

4.2.2 Ovarian Cyst

It is seen classically as a unilocular round or oval cyst in lower abdomen close to urinary bladder in a female fetus. The cyst wall is thin and smooth with clear fluid (Fig. 4.8). The septum inside is diagnostic of an ovarian cyst (Fig. 4.8c). Usually it does not show change in location but occasionally it may do so when its pedicle is long. Most of the ovarian cysts decrease in size or disappear in follow up scan. Rarely ovarian cyst may shows calcification suggestive of cystic teratoma (Fig. 4.10). Ovarian cyst can undergo a complication of hemorrhage or torsion, when the cyst will appear heterogeneous (Figs. 4.9 and 4.11). Heterogeneous appearance may include thick walls, multiple septations, internal echoes and fluid level (Fig. 4.8d) or solid and cystic appearance. When it is heterogeneous due to hemorrhage there is absence of flow on color Doppler study within the cyst but flow may be seen in supplying vessel and in the wall. On follow up scan hemorrhagic cyst will show change in morphology or totally disappear (Fig. 4.9). In torsion the pedicle may sever, with the cyst seen in a location far from the previous location (Fig. 4.11). Rarely ovarian cysts may be bilateral (Fig. 4.8e).

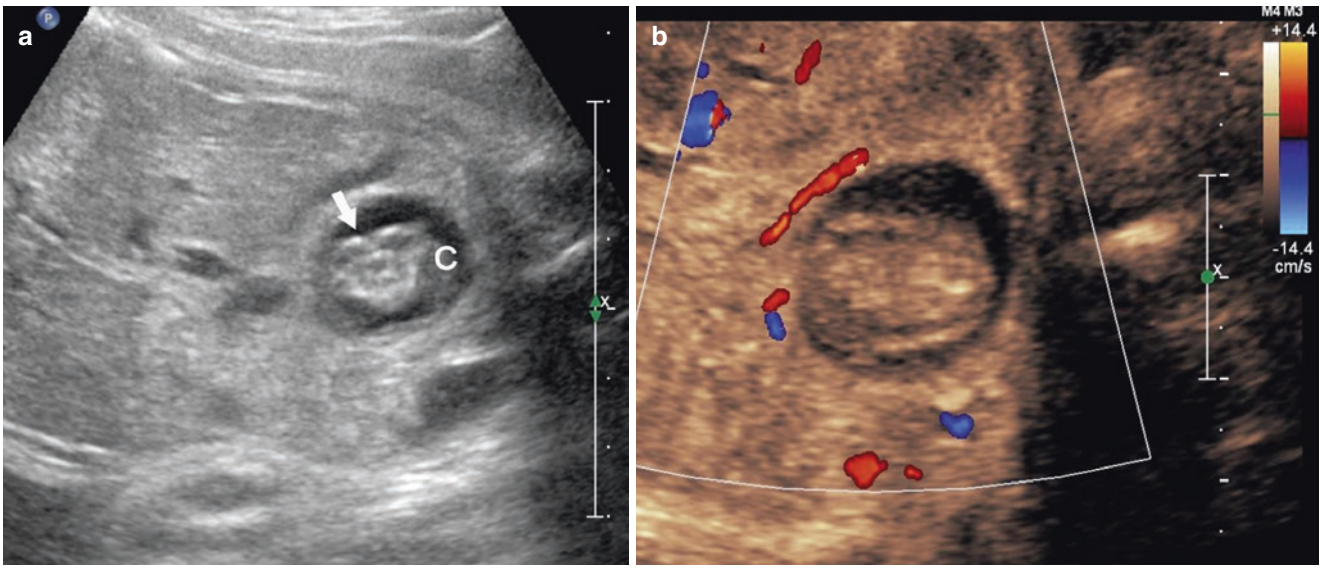

Fig. 4.10 Cystic Teratoma of ovary: (**a**) Coronal Scan of fetal lower abdomen showing a thick-walled cyst with solid area and calcification (arrow). (**b**) Colour Doppler scan shows no flow in the mass

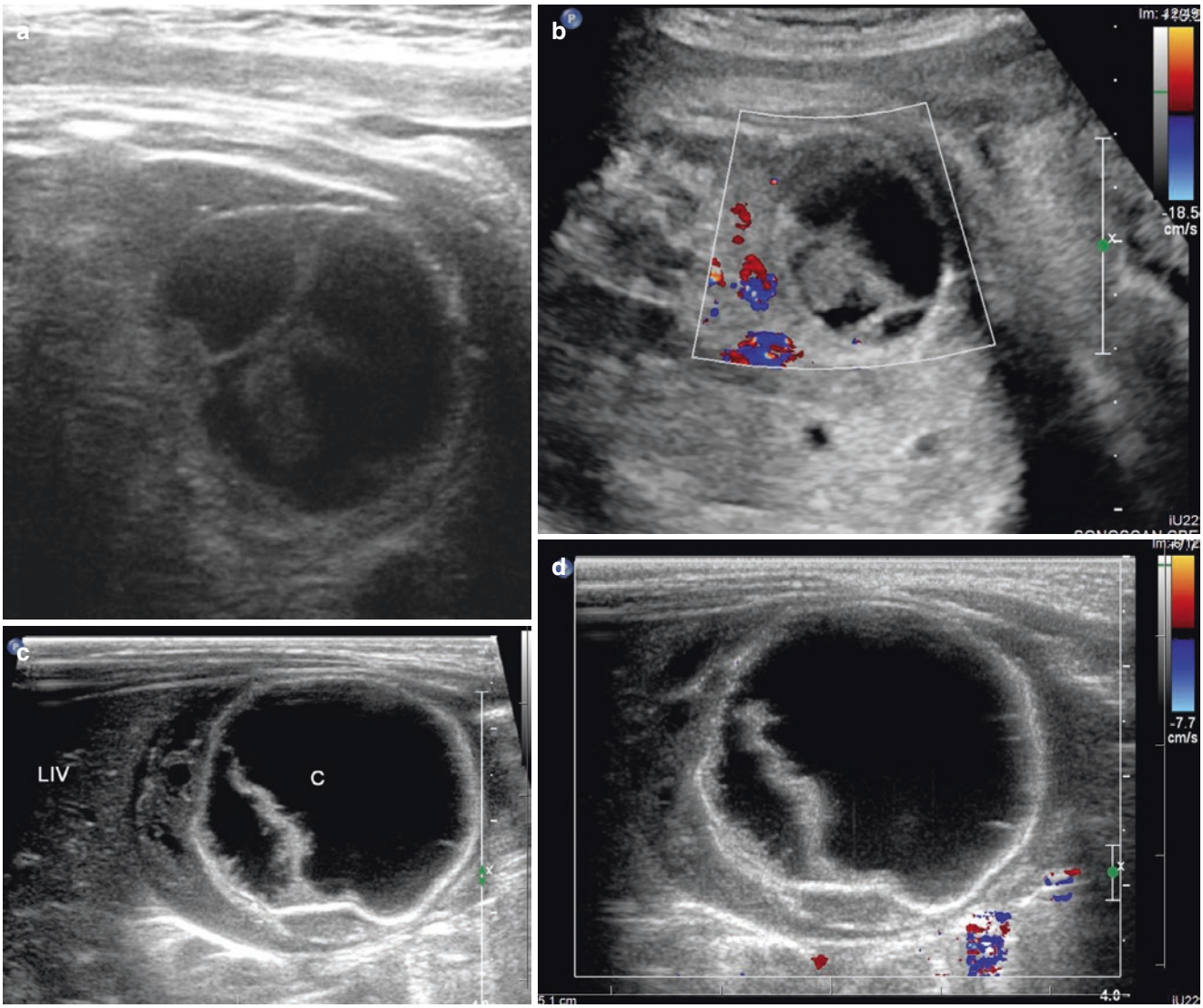

Fig. 4.11 Ovarian cyst with torsion: (**a**) High frequency scan showing an ovarian cyst with thick walls and septa. (**b**) Colour Doppler showing absence of flow in the walls and septa. (**c**, **d**) Postnatal scan showing the thick-walled cyst (C) with thick septa below the liver (Liv) indicating severed pedicle showing no flow on Colour Doppler

4.2.3 Mesenteric Lymphangioma

Mesenteric lymphangioma is seen as a multiseptated cyst in central abdomen mimicking small bowel obstruction. Absence of peristalsis in the cysts and peristalsis of a small bowel loop in the center of the cyst will confirm the diagnosis (Fig. 4.12, Video 4.1). It may show change in location on follow up scan.

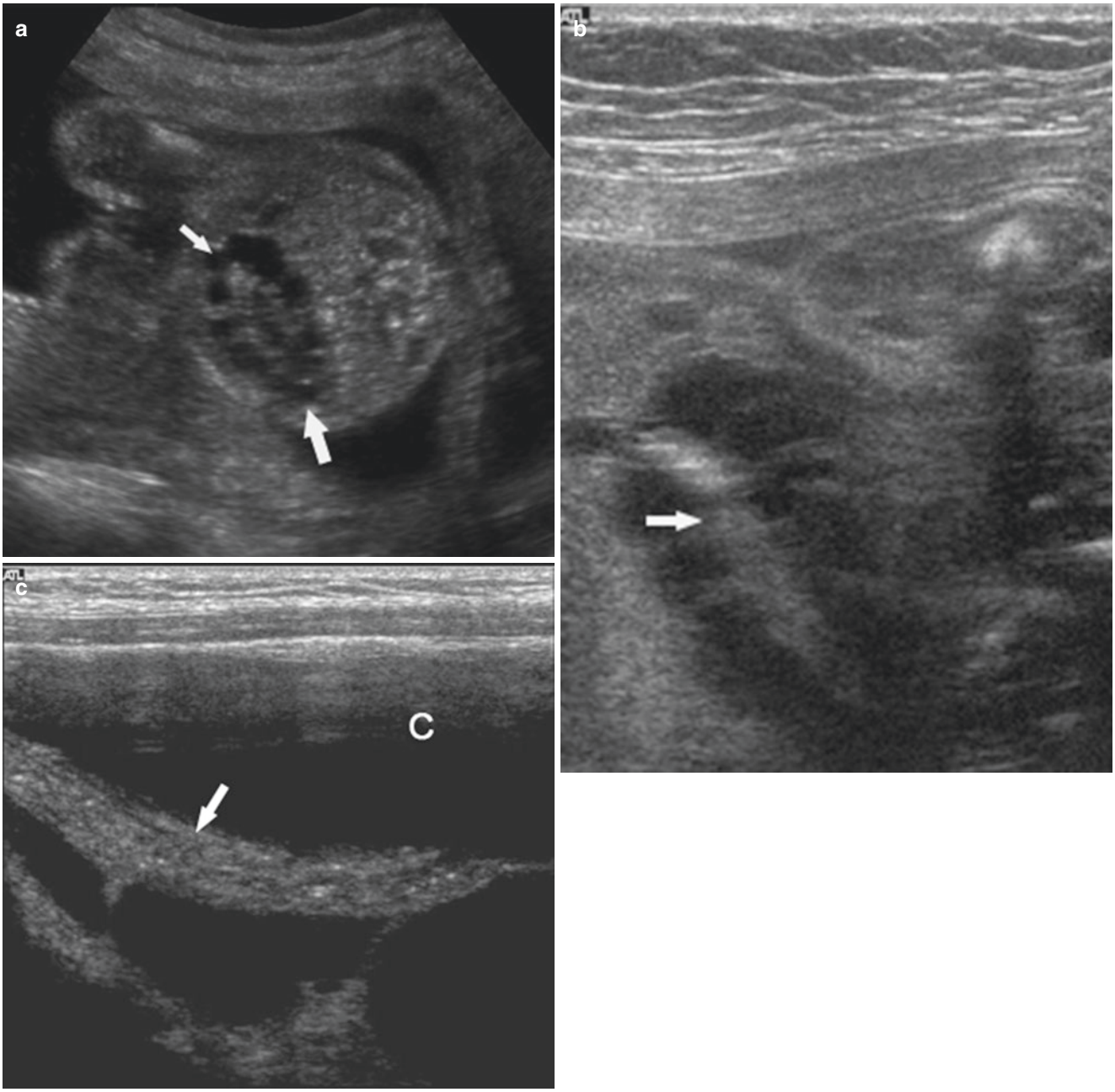

Fig. 4.12 Mesenteric lymphangioma: (**a**) Axial scan of fetal mid abdomen showing a multiseptated cystic mass (arrow) mimicking dilated bowels. (**b**) High frequency image showing a bowel loop (arrow) coursing through the cyst confirmed by peristalsis (video 4.1) and absence of peristalsis in the cysts. (**c**) Postnatal scan confirming the septated mesenteric cyst with a bowel loop coursing through it

4.2.4 Gastrointestinal Duplication Cysts

GI duplication cysts have been discussed earlier.

4.2.5 Choledochal Cyst

Choledochal is seen as an oval cyst in right upper quadrant with a fixed location. Features which help in diagnosis are continuity with dilated biliary ducts, location of cyst posterior to gall bladder/portal vein/duodenal cap and extension into the head of pancreas (Fig. 4.5).

4.2.6 Liver or Splenic Cysts

Liver or splenic cysts are rare. They are seen as round or oval cyst with thin smooth walls and clear fluid within the organ (Figs. 4.1 and 4.2).

4.2.7 Retroperitoneal Lymphangioma

Retroperitoneal lymphangioma is seen as a fixed multiseptated flaccid cyst in posterior aspect of fetal abdomen. Extension of the cyst across tissue planes or a second cyst in a different location is useful in confirming the diagnosis (Fig. 4.13).

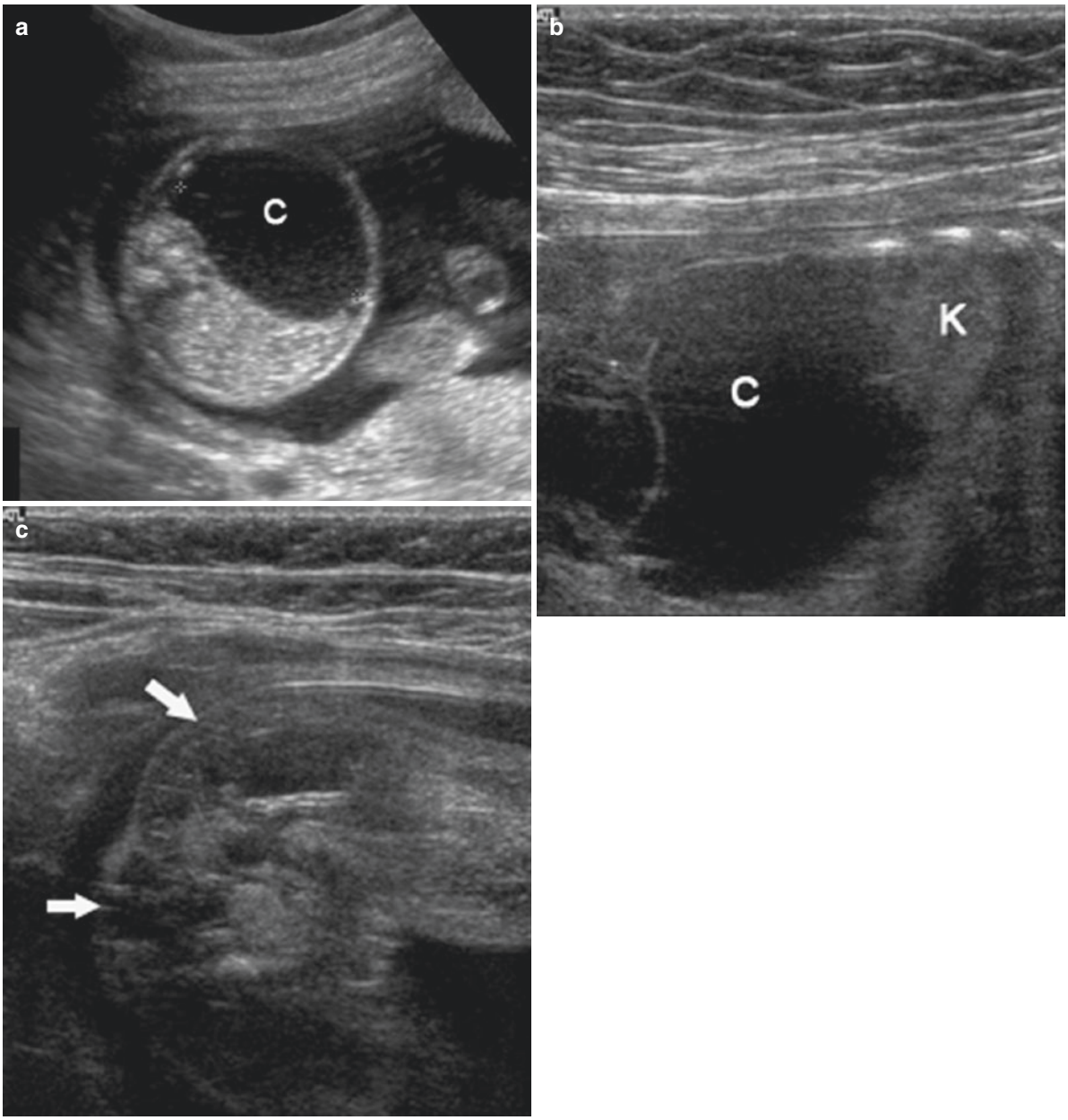

Fig. 4.13 Retroperitoneal lymphangioma: (**a**) Axial scan of fetal abdomen showing a large cyst (C) in renal area. (**b**) High frequency coronal scan shows the normal kidney (K) displaced by the septated cyst indicating its location in retroperitoneum. (**c**) Axial scan of gluteal region shows septated cysts in both gluteal regions confirming that they are lymphangiomas

4.2.8 Cystic Lesions of Urinary Tract

Cystic lesions connected to urinary tract namely renal cyst, hydronephrosis, ectopic kidney with hydroureteronephrosis, vesical diverticulum, duplication of urinary bladder have been discussed elsewhere. A cystic dilatation of upper ureter due to ureteric valve or aganglionosis is seen as a cyst in renal area. On high frequency scan the cyst is seen to communicate with the renal pelvis of a normal kidney confirming the diagnosis (Fig. 4.14).

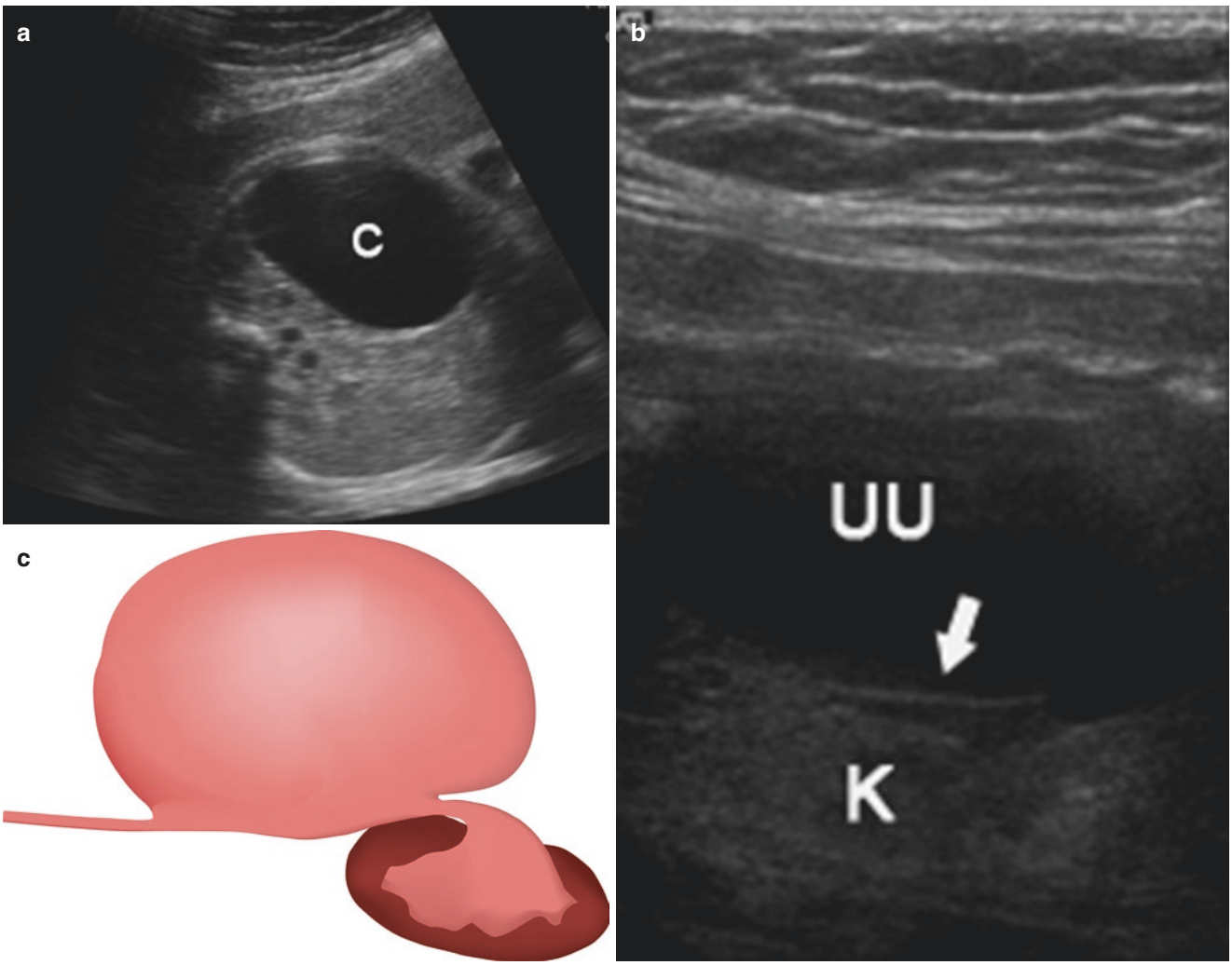

Fig. 4.14 Cystic dilatation of upper ureter: (**a**) Axial scan of fetal abdomen showing a large cyst (C) in renal area. (**b**) High frequency coronal scan shows that the cyst is continuous with the slightly dilated renal pelvis and the kidney (K) is normal. (**c**) Schematic diagram of the cystic dilatation of the upper ureter due to ureteric valve or aganglionosis

4.2.9 Hydrocolpos

Hydrocolpos is seen as an oval cyst in midline of pelvis of a female fetus posterior to urinary bladder. There may be debris in it. Occasionally hydrometra may be seen on the cephalic side (Fig. 4.15). Hydrocolpos may be due to imperforate hymen or vaginal atresia. In imperforate hymen the bulging hymen may be seen at the introitus (Fig. 4.16). Hydrocolpos may be isolated or may be seen as part of URSM sequence or syndromes like McKuisk Kaufman syndrome where there will be associated polydactyly or VACTERL association.

4.2.10 Meconium Cyst

Meconium cyst is discussed elsewhere.

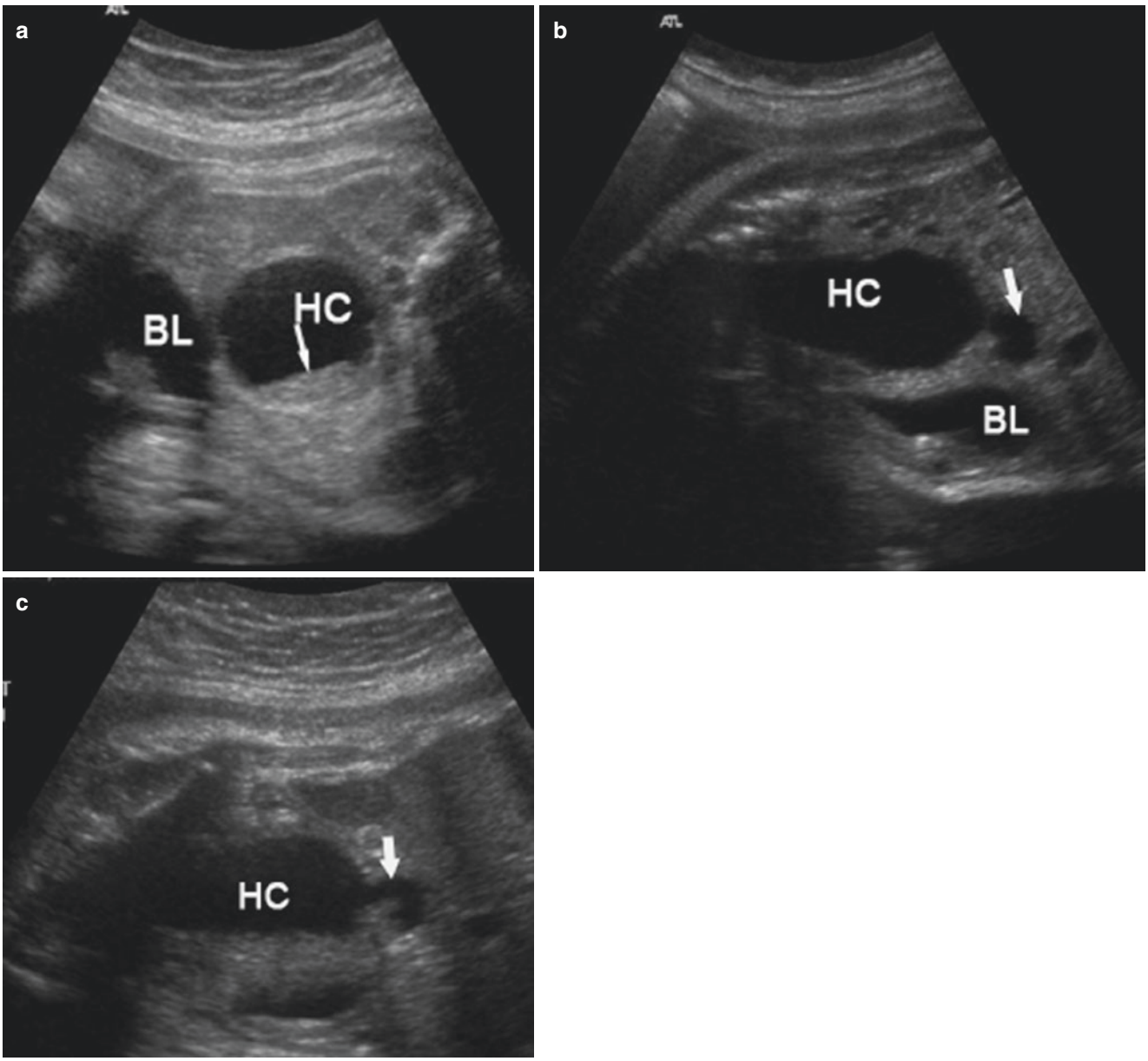

Fig. 4.15 Hydrocolpos: (**a**) Axial scan of pelvis of a female fetus showing a cyst (HC) with debris (arrow) in midline posterior to the urinary bladder (BL). Sagittal scan of fetal pelvis from posterior aspect with full bladder (**b**) and after fetal micturition (**c**) showing the pyriform shape of the cyst (HC) with cephalic hydrometra (arrow) confirming the diagnosis

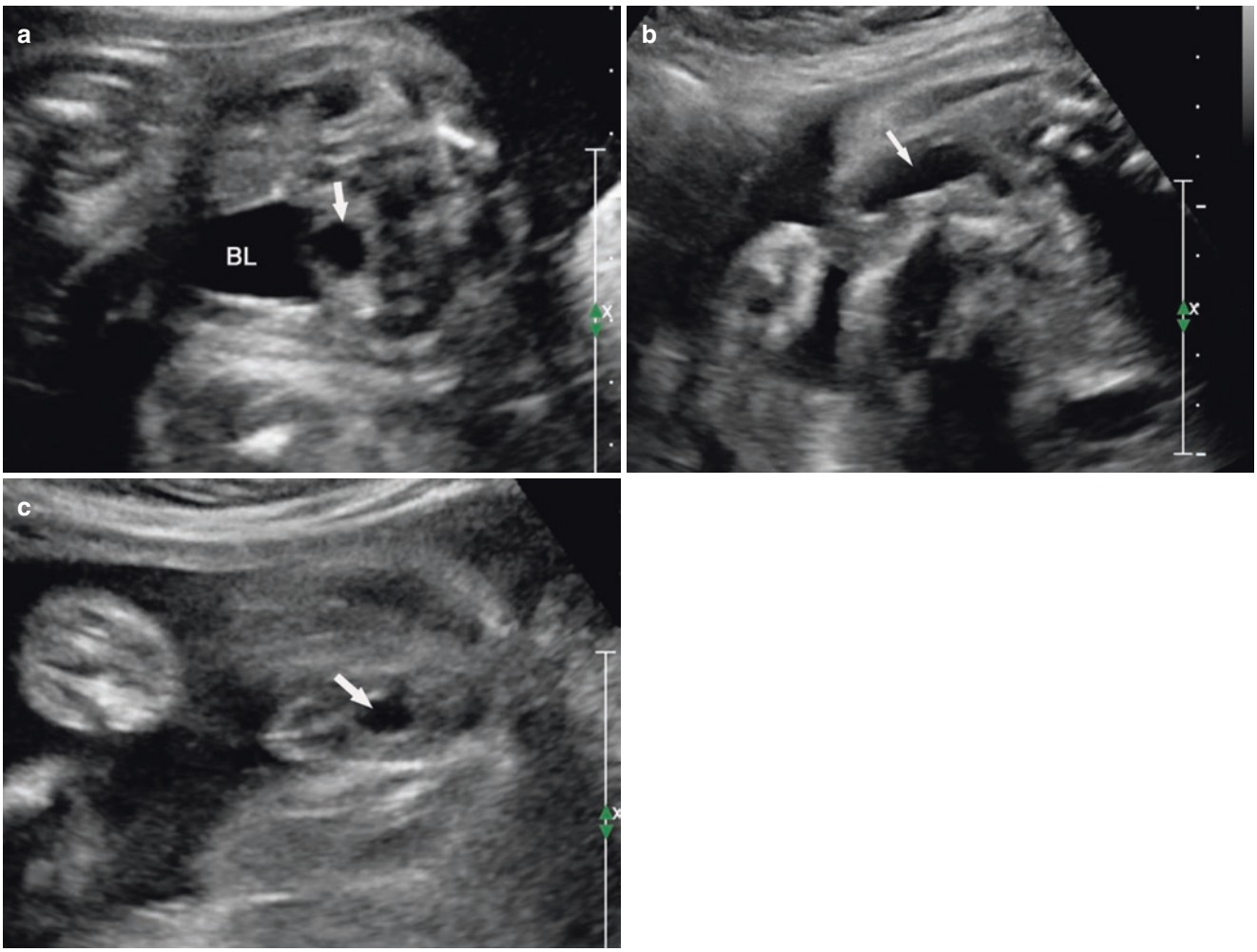

Fig. 4.16 Hydrocolpos due to imperforate hymen: (**a**) Axial scan of fetal pelvis shows a cyst (arrow) posterior to urinary bladder (BL). (**b**) Sagittal scan of pelvis shows the fluid distended tubular vagina. (**c**) Tangential scan of fetal perineum shows the cystic mass in the introitus (arrow) due to the bulging hymen

4.2.11 Urachal Cyst

Urachal cyst is seen as a pyriform cyst in midline between umbilicus and urinary bladder, usually communicating with bladder. Most of the times it is seen in a case of urinary bladder outflow obstruction. It may be continuous with or associated with an allantoic cyst in the fetal cord insertion (Figs. 4.17 and Fig. 3.55).

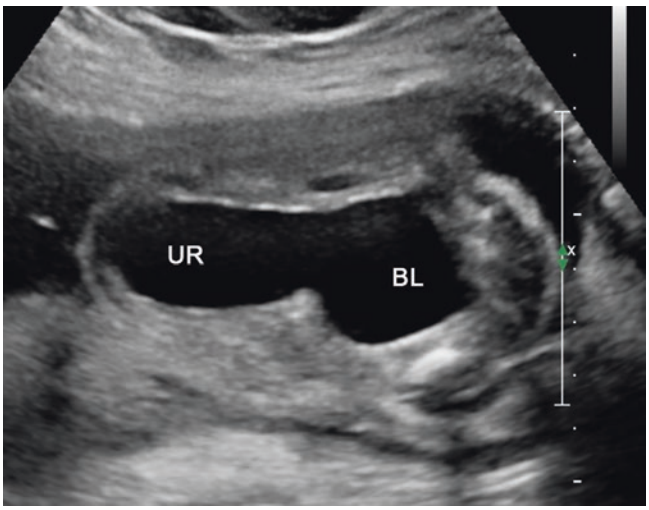

Fig. 4.17 Urachal cyst: Oblique coronal scan of fetal lower abdomen and pelvis showing over distended bladder (BL) with large urachal cyst (UC) extending from dome of bladder to umbilicus in a case of posterior urethral valves

4.2.12 Vesical Diverticulum

Vesical diverticulum is seen as cystic structure in fetal pelvis close to urinary bladder. Oblique scan may show continuity with bladder. When fetus micturates both bladder and diverticulum contract and empty confirming the diagnosis (Fig. 4.18).

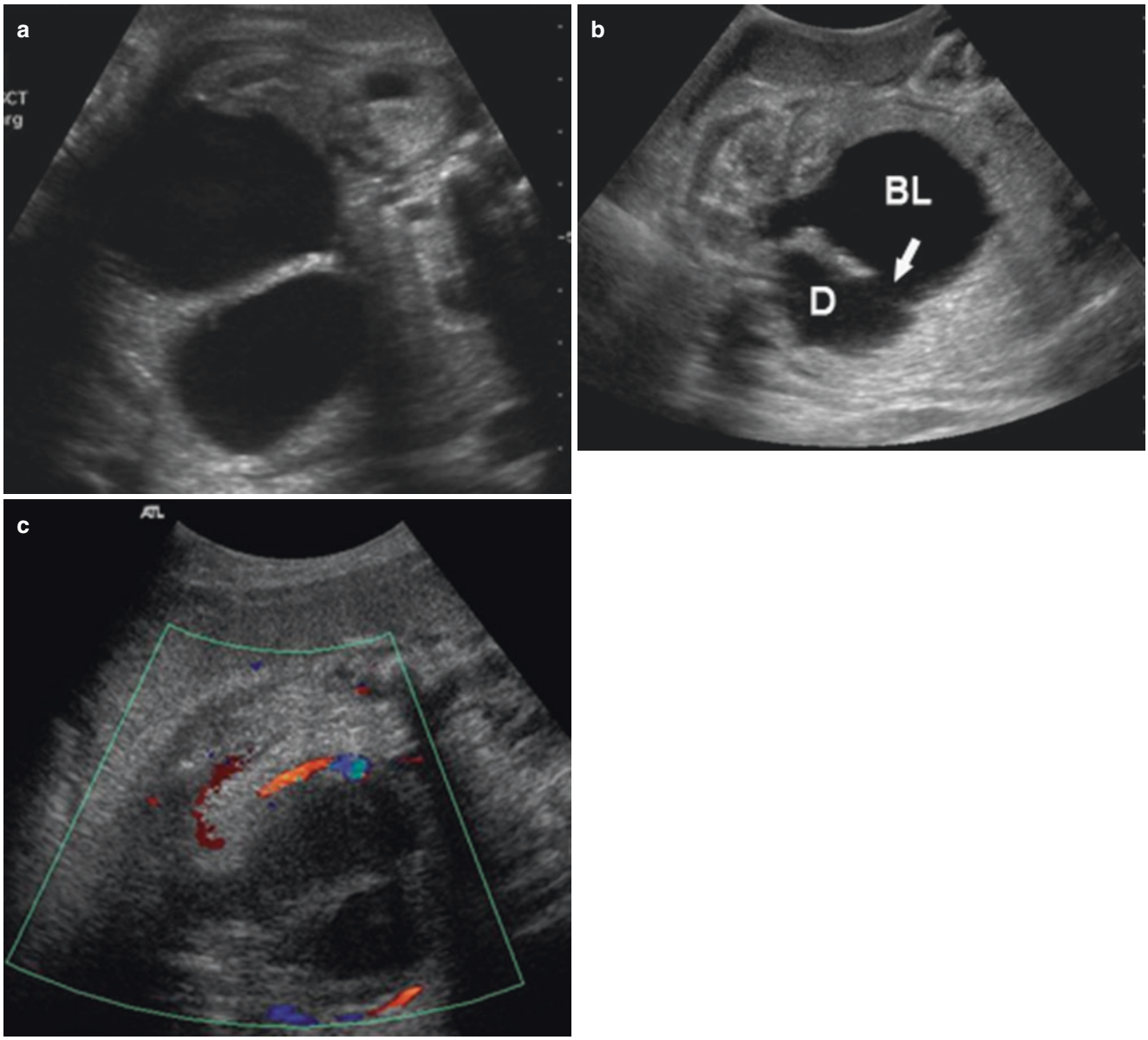

Fig. 4.18 Vesical diverticulum: (**a**) Axial scan of fetal pelvis showing two cystic structures in the pelvis. (**b**) Oblique scan shows that the diverticulum {D} communicates (arrow) with the urinary bladder (BL). (**c**) Axial scan after fetal micturition confirms that both the bladder and the diverticulum have contracted

4.2.13 Fetus in Fetu

Fetus in fetu is an anomalous condition where a mass of tissue resembling part of a fetus is seen in the fetal abdomen. One theory is that parts of a monozygotic twin are seen within the abdomen of the co-twin. While others consider it a well-developed teratoma. On sonography there is a well-defined solid and cystic mass with calcifications and part of axial skeleton, which differentiates it from a teratoma (Fig. 4.19). It is a benign condition and most often seen in retroperitoneum and so are fixed in location.

4.2.14 Umbilical Vein Varix

Umbilical vein varix represents focal dilatation of the extrahepatic intraabdominal umbilical vein. The diameter of umbilical vein normally increases linearly with gestational age. It has to measure more than 9 mm in width or ratio of more than 50% between dilated and a more distal normal intraabdominal portion of the vein to diagnose umbilical vein varix. It has been reported to be associated with chromosomal anomalies, cardiac anomalies, intrauterine fetal death due to thrombosis and fetal hydrops.

It is seen as an oval cystic mass in anterior midline of fetal upper abdomen. It is connected to the umbilicoportal vein. Colour Doppler Study, confirms that the varix is connected to umbilical vein. There is circular flow in the varix (Fig. 4.6). Associated anomalies of other systems and in particular cardiac anomaly has to be ruled out. It has to be followed up for development of hydrops due to thrombosis or anemia and fetal death due to thrombosis. When isolated, umbilical vein varix carries good prognosis with significantly low association with aneuploidy and mortality than previously reported.

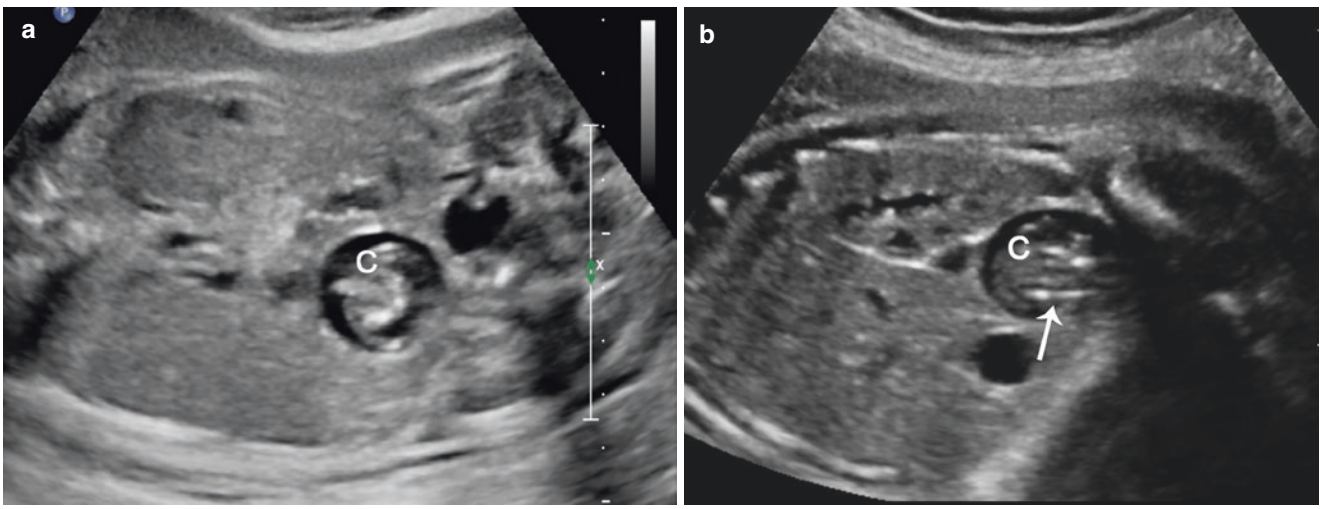

Fig. 4.19 Fetus in Fetu: (**a**) Gray Scale and (**b**) Longitudinal scan showing part of spine in the cyst indicating fetus in fetu. (**c**) Colour Doppler coronal scan of abdomen of a male fetus showing cyst (C) with solid areas and calcifications (arrow) with absent flow. (**d, e**) Postnatal scan showing the cyst with spine and ribs (solid arrows). (**f**) Colour Doppler showing no flow in the mass

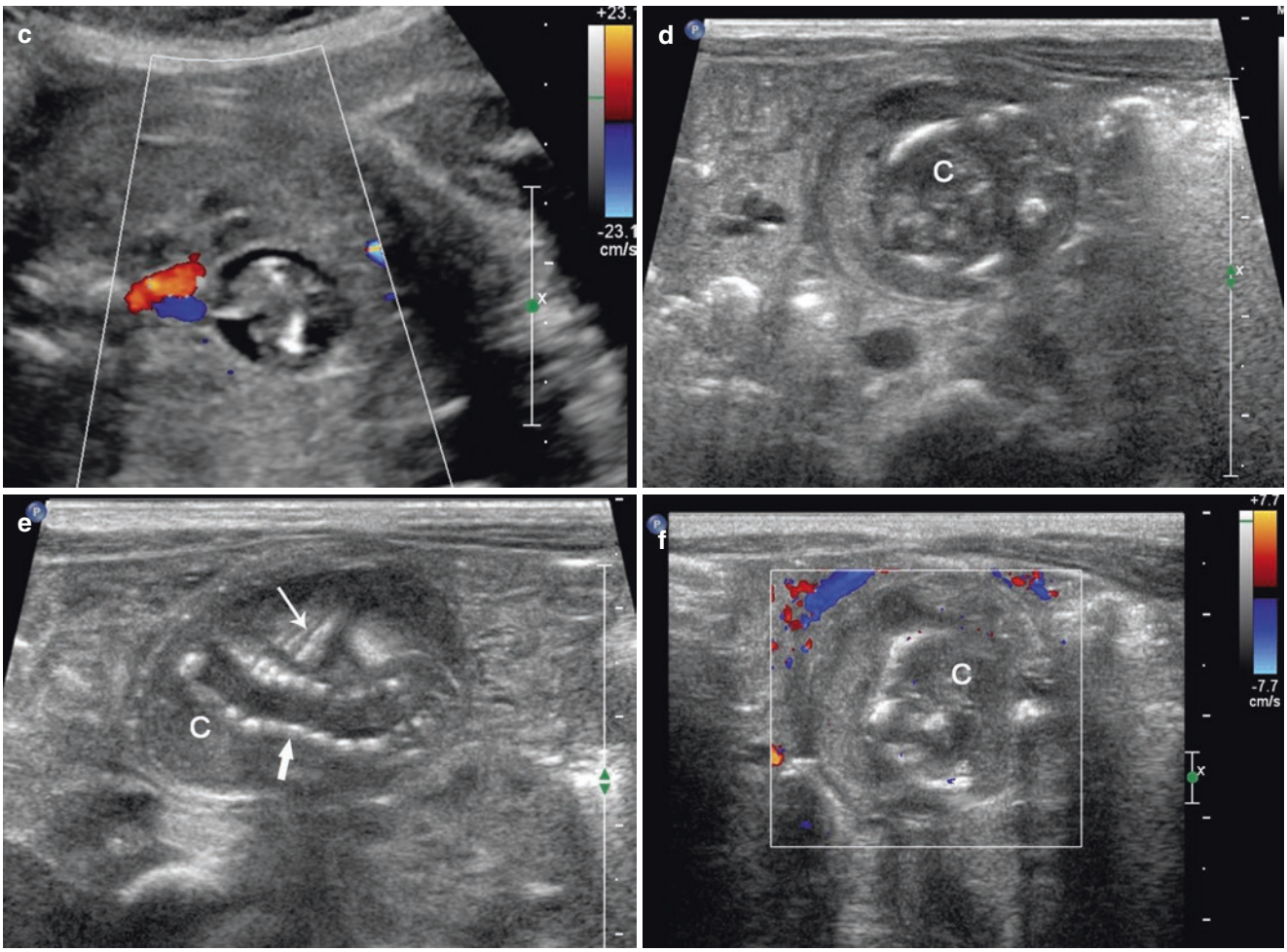

Fig. 4.19 (continued)

4.3 Solid Intraabdominal Masses in Fetus

4.3.1 Liver

Haemangioendothelioma is a very rare tumor of liver. It is usually seen in infants. It can be seen in the fetus usually in third trimester. On sonography it is seen either as an echopoor or heterogeneous mass of liver (Fig. 4.20). It has a predilection for the posterior part of right lobe. It may contain calcifications. On color Doppler study, there is increased vascularity. The hepatic artery and the hepatic vein are dilated. When it is large it can result in cardiac failure and hydrops or result in anemia/thrombocytopenia. Most of them decrease in size in postnatal life with or without calcifications. It cannot be differentiated from much rarer hepatoblastoma or mesenchymal hamartoma.

Hepatic hemangioma is another very rare tumor of fetal liver. It is seen as a well-defined echogenic mass in liver with absent vascularity on color Doppler study.

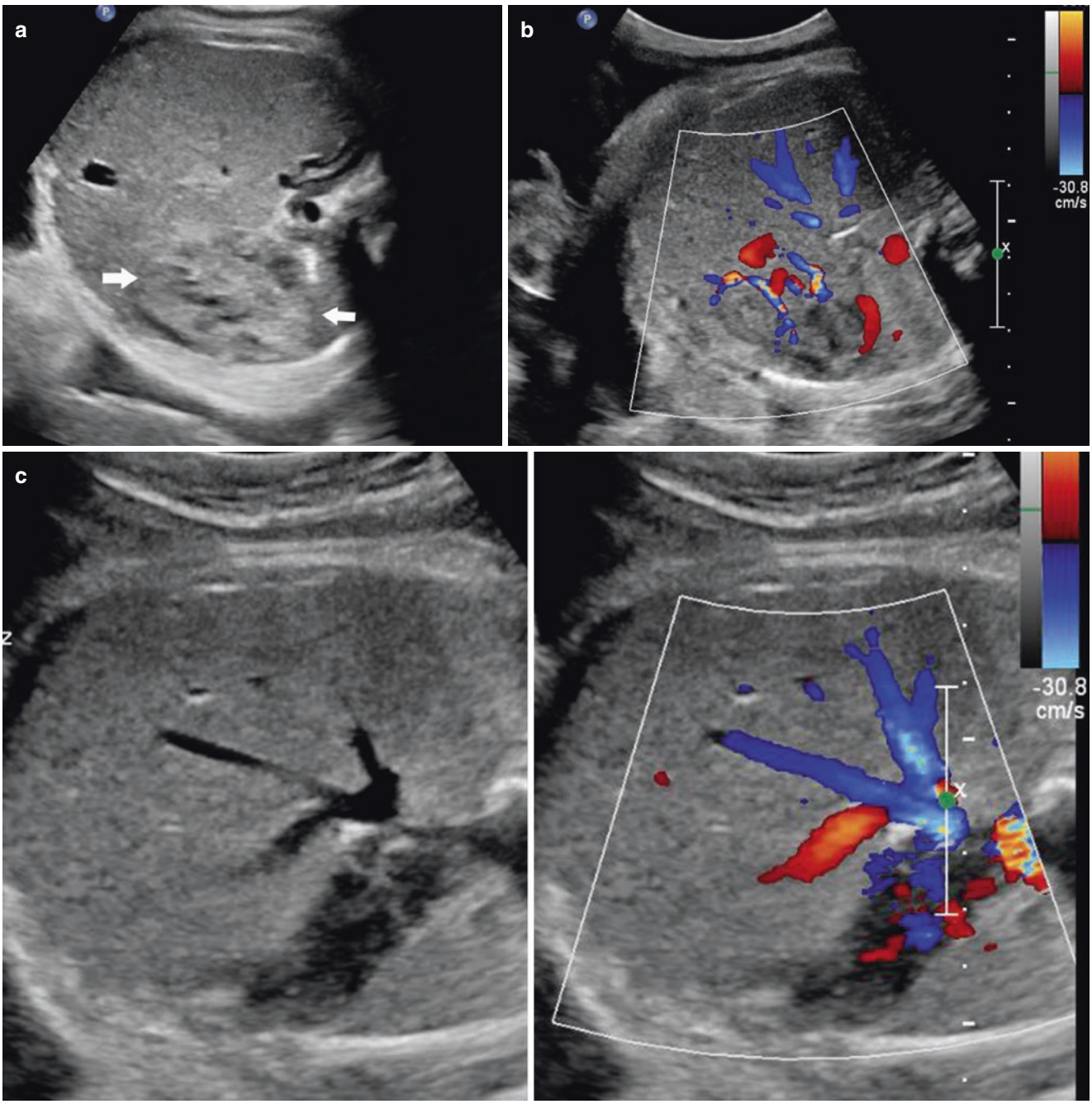

Fig. 4.20 Haemangioendothelioma of liver: (**a**) Axial scan of fetal upper abdomen shows a heterogeneous mass (arrow) in right lobe of liver with lack of an interphase with liver indicating its location in liver. (**b**–**d**) Colour Doppler images show increased vascularity in the mass, dilated right hepatic vein and celiac and hepatic arteries characteristic features of hemangioendothelioma

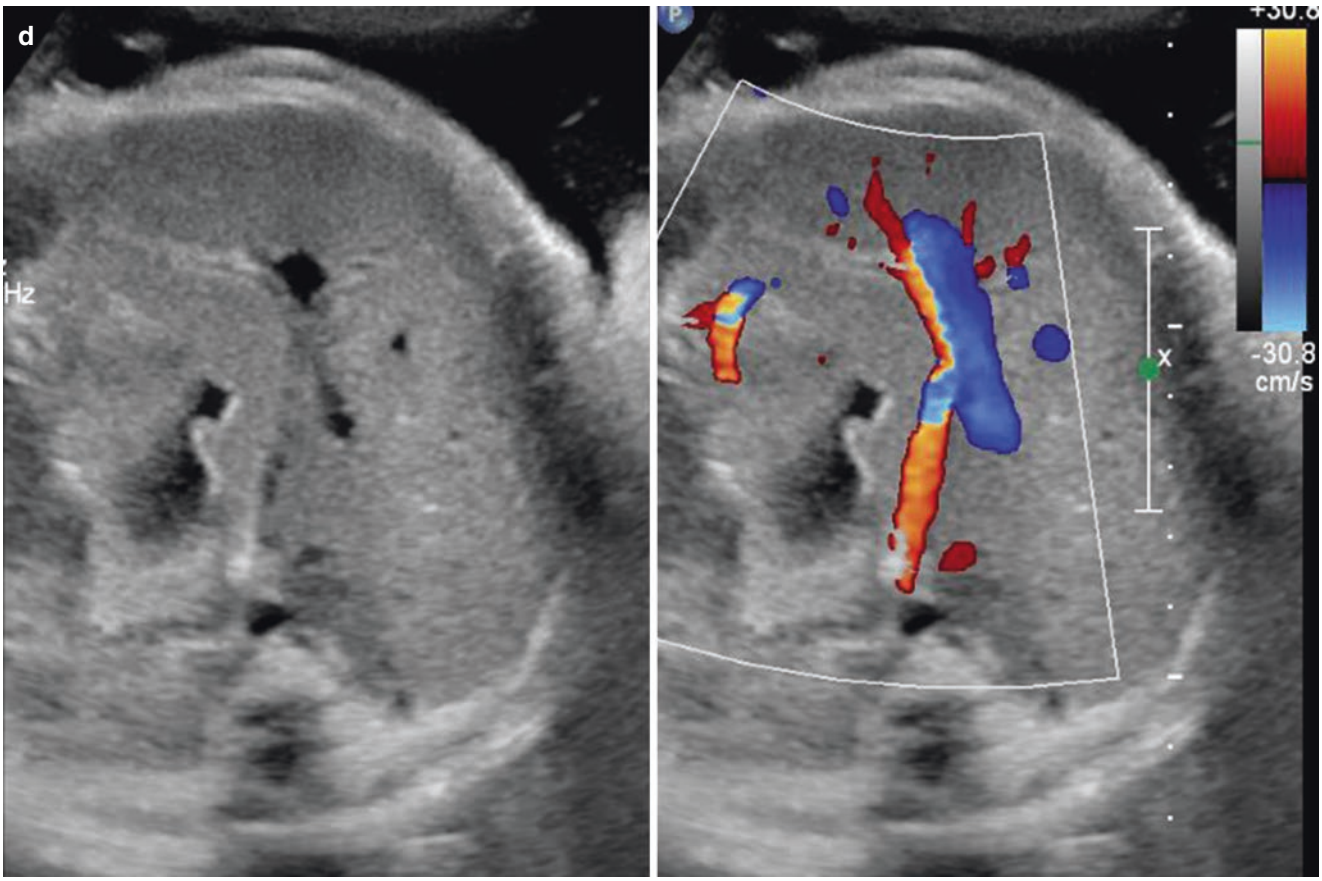

Fig. 4.20 (continued)

4.3.2 Adrenal Glands

Fetal adrenal glands are about 20 times relatively larger compared to adults. They can be seen in late second trimester and seen very well in third trimester. They are seen as pyramidal structures, the cortex echopoor compared to liver/spleen and medulla is echogenic (Fig. 4.21).

Adrenal Hemorrhage

Adrenal hemorrhage: Cause in the fetus is poorly understood. The right adrenal is involved in 75% of causes. The characteristic feature is change over time. Initially it is seen as a solid echogenic mass. Later it is seen as an heterogeneous echopoor mass (Fig. 4.22) when it is difficult to differentiate from neuroblastoma (Fig. 4.23). Then it can become cystic or shrink with or without calcifications (Fig. 4.22e).

Neuroblastoma

Neuroblastoma is the most common neoplasm of adrenal gland. It manifests usually in third trimester. It is usually seen as an echopoor or heterogeneous mass of adrenal gland. When it is large it pushes the kidney inferiorly (Fig. 4.23). On color Doppler study, a supplying vessel may be seen from the renal artery.

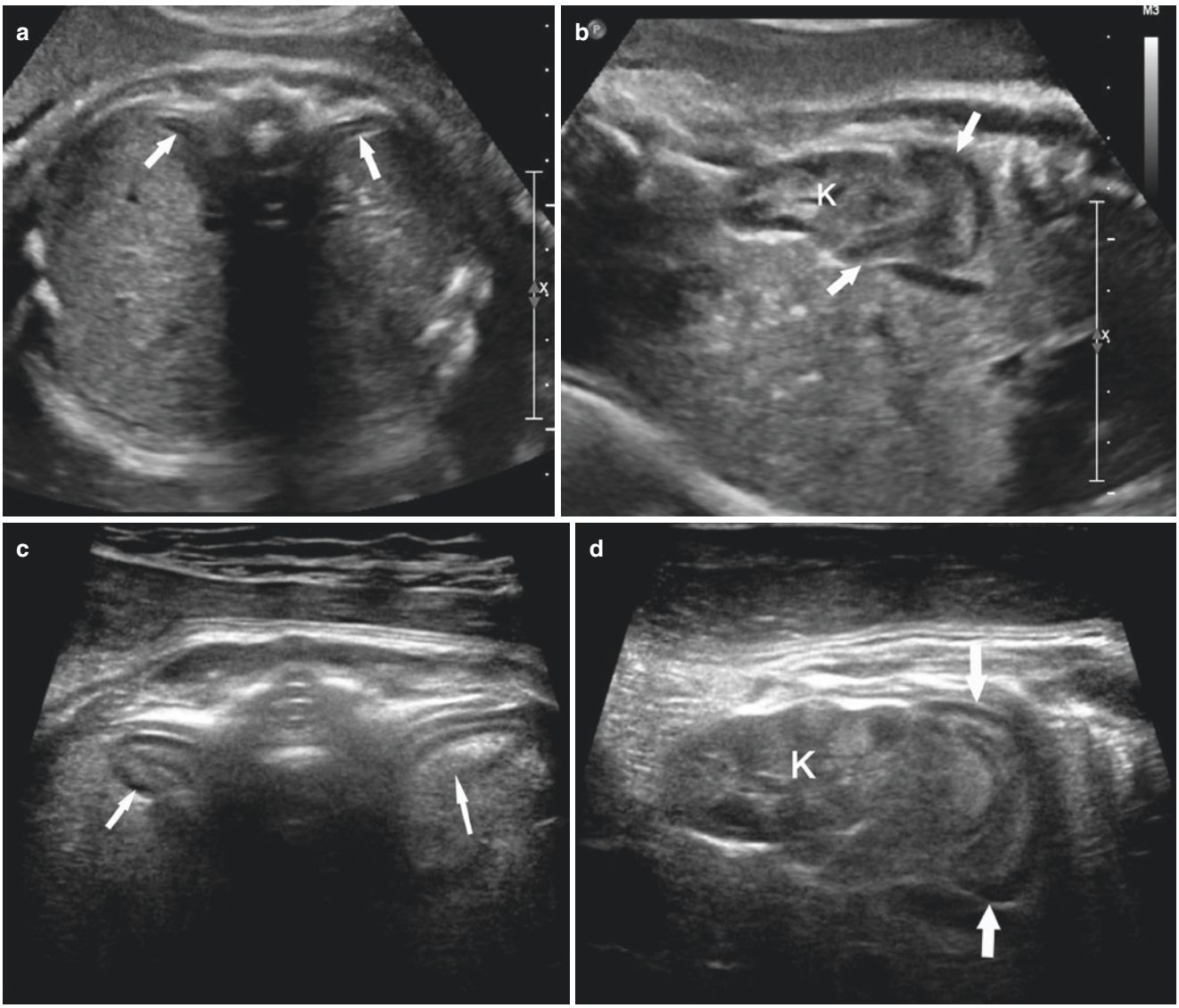

Fig. 4.21 Normal adrenal glands: (**a**) Axial scan of fetal abdomen from posterior aspect with convex probe and longitudinal scan with (**b**) convex probe and (**c**) high frequency probe showing the discoid adrenal glands with echogenic medulla and echopoor cortex (arrow). (**d**) high frequency probe showing the adrenal glands (arrow) capping the upper pole of kidney

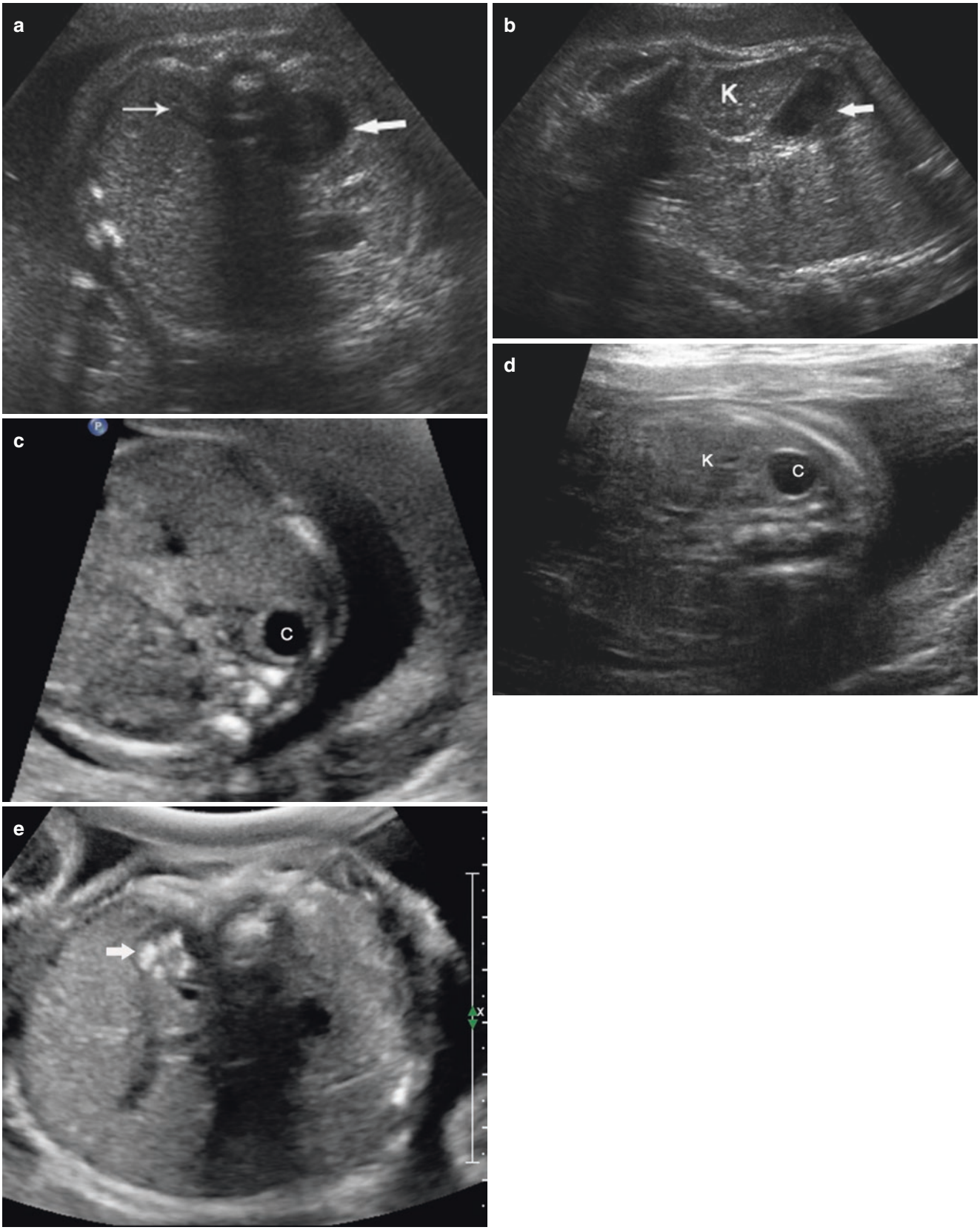

Fig. 4.22 Adrenal Hemorrhage: (**a**) Axial and (**b**) Longitudinal scan showing the heterogeneous cystic mass of adrenal gland suggestive of subacute hemorrhage. (**c**) Axial and (**d**) Longitudinal high frequency scan of the fetal adrenal gland after 4 week shows resolving hemorrhage as a cystic mass of adrenal (arrow). (**e**) Axial scan of another fetus of third trimester shows adrenal calcification—a sequel of hemorrhage

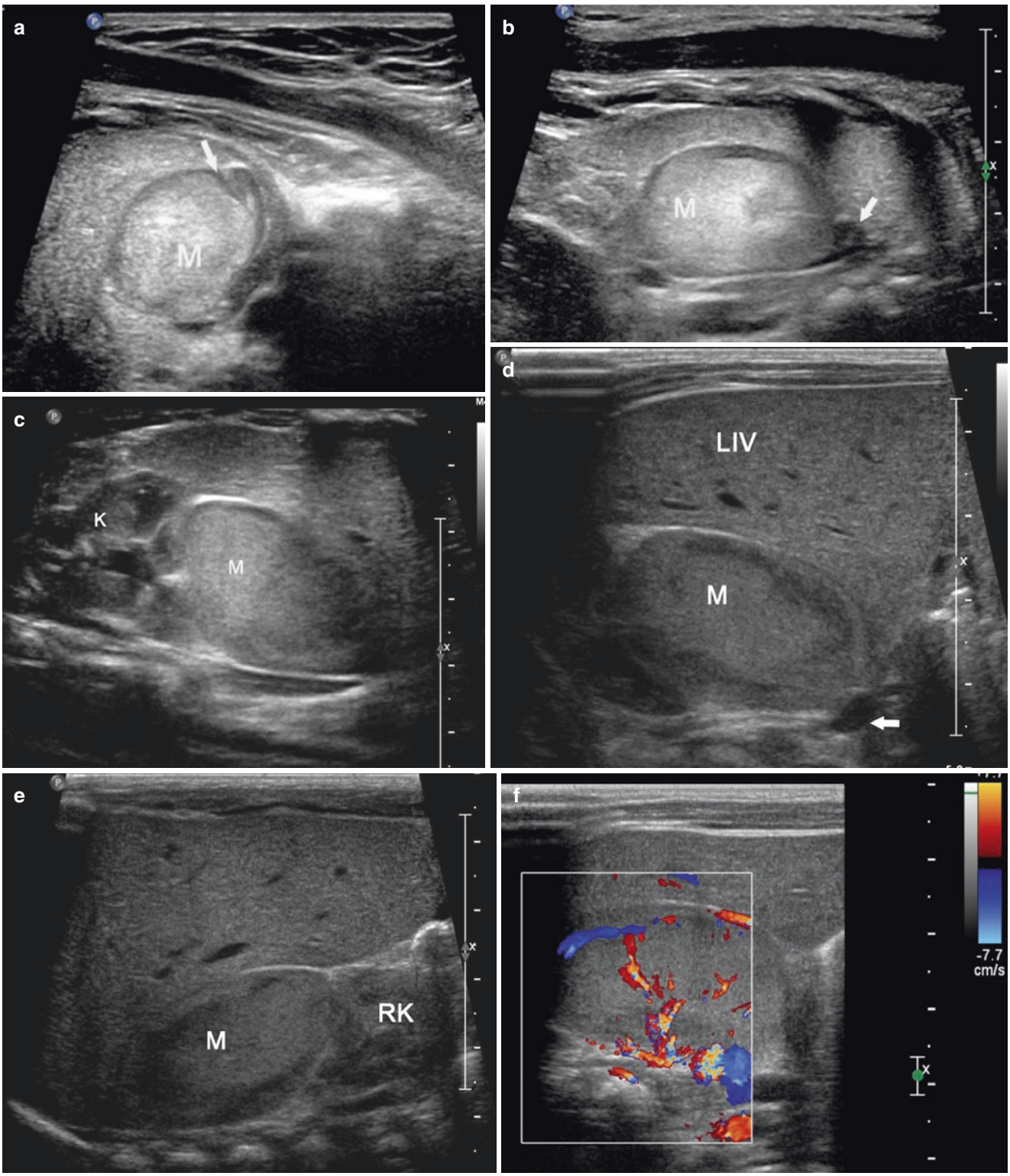

Fig. 4.23 Neuroblastoma: Axial (**a**) and Longitudinal (**b**) scan of fetal abdomen showing a solid mass (M) in adrenal area continuous with the adrenal (arrow). (**c**) Longitudinal scan showing the mass indenting and pushing the kidney down. Postnatal axial (**d**) and longitudinal (**e**) scans showing the adrenal mass posterior to inferior vena cava (arrow) and indenting on right kidney (RK). (**f**) Colour Doppler image showing the mass supplied by a vessels from renal artery. (**g**) Excised mass of neuroblastoma

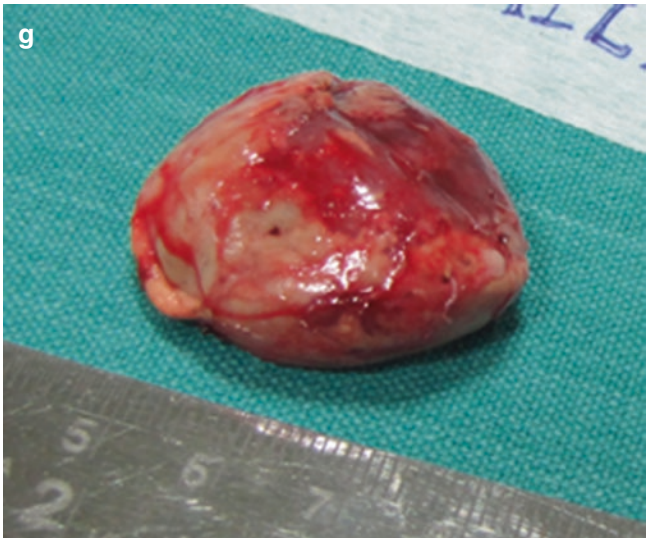

Fig. 4.23 (continued)

4.3.3 Infradiaphragmatic Bronchopulmonary Sequestration

About 10–15% of all bronchopulmonary sequestration are seen below the diaphragm with a 4:1 predilection for left side. It is seen as a well-defined echogenic mass in the space between stomach, spleen and upper pole of left kidney (Fig. 4.24). On color Doppler study, usually there is a feeding vessel arising from the thoracic aorta confirming the diagnosis. The features that help to differentiate it from adrenal neuroblastoma are: (1) It is more common on left side while adrenal neuroblastoma is more common on right side. (2) It is seen earlier in pregnancy compared to neuroblastoma. (3) It is more echogenic and (4) the feeding vessel is from thoracic aorta while it is from renal artery for neuroblastoma.

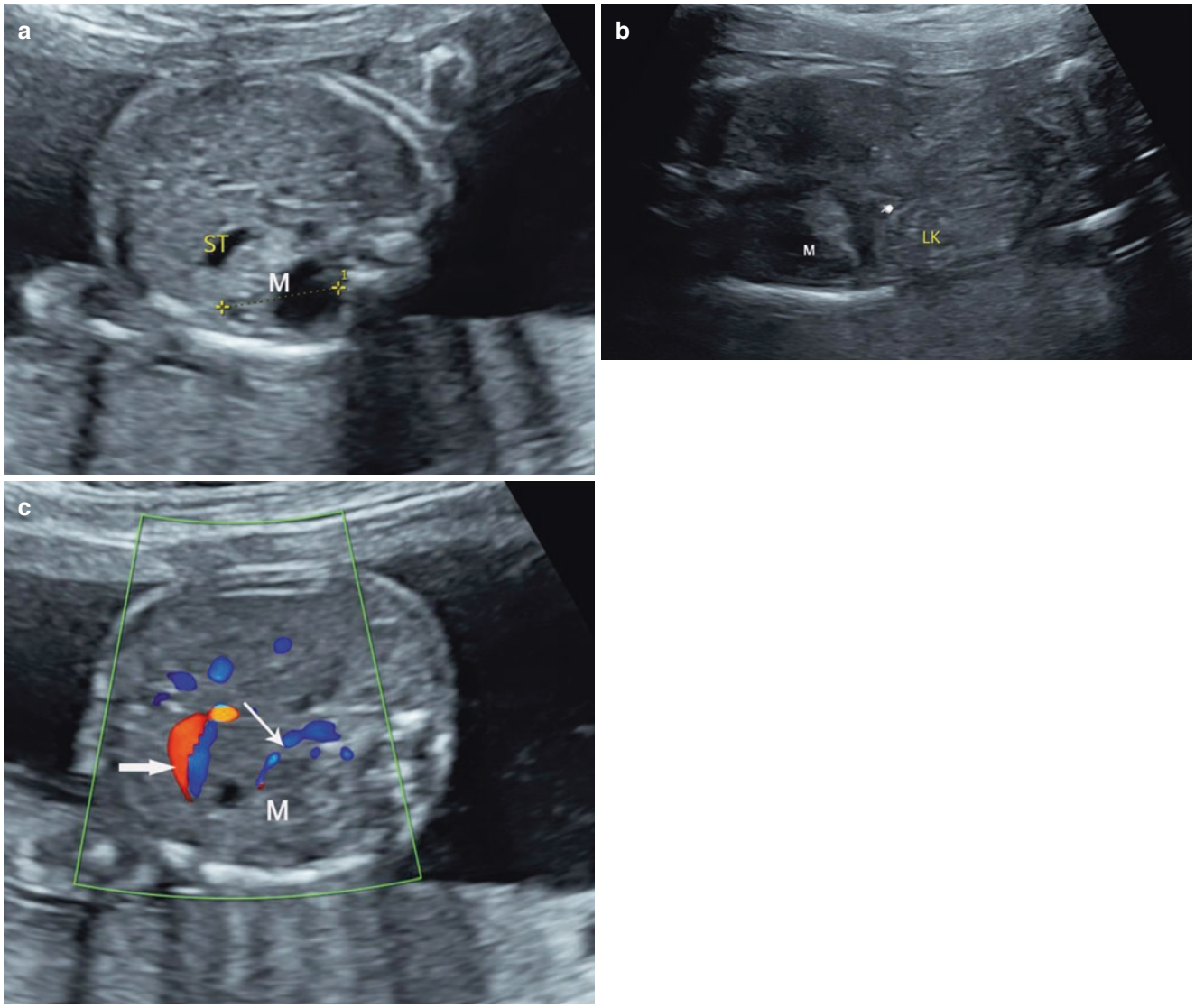

Fig. 4.24 Infradiaphragmatic Bronchopulmonary sequestration: (**a**) Axial scans of fetal upper abdomen showing a solid echogenic and cystic mass posterior to the stomach (ST). (**b**) Coronal scan shows the mass separate from normal adrenal (arrow) Left kidney (LK). (**c**) Colour Doppler image shows that the mass is posterior to splenic vessels, indicating that it is not arising from pancreas. There is a vessel (thin arrow) from aorta supplying it

4.3.4 Bronchopulmonary Foregut Malformation

In the axial section of fetal abdomen when an echogenic mass is seen posterior to the stomach an effort is made to identify the organ of origin. If spleen is seen separately and left adrenal is imaged normally, then bronchopulmonary sequestration should be considered. A tubular cystic structure representing the bronchus can be seen communicating with the stomach (Fig. 4.25). The bronchus can communicate with the stomach or esophagus.

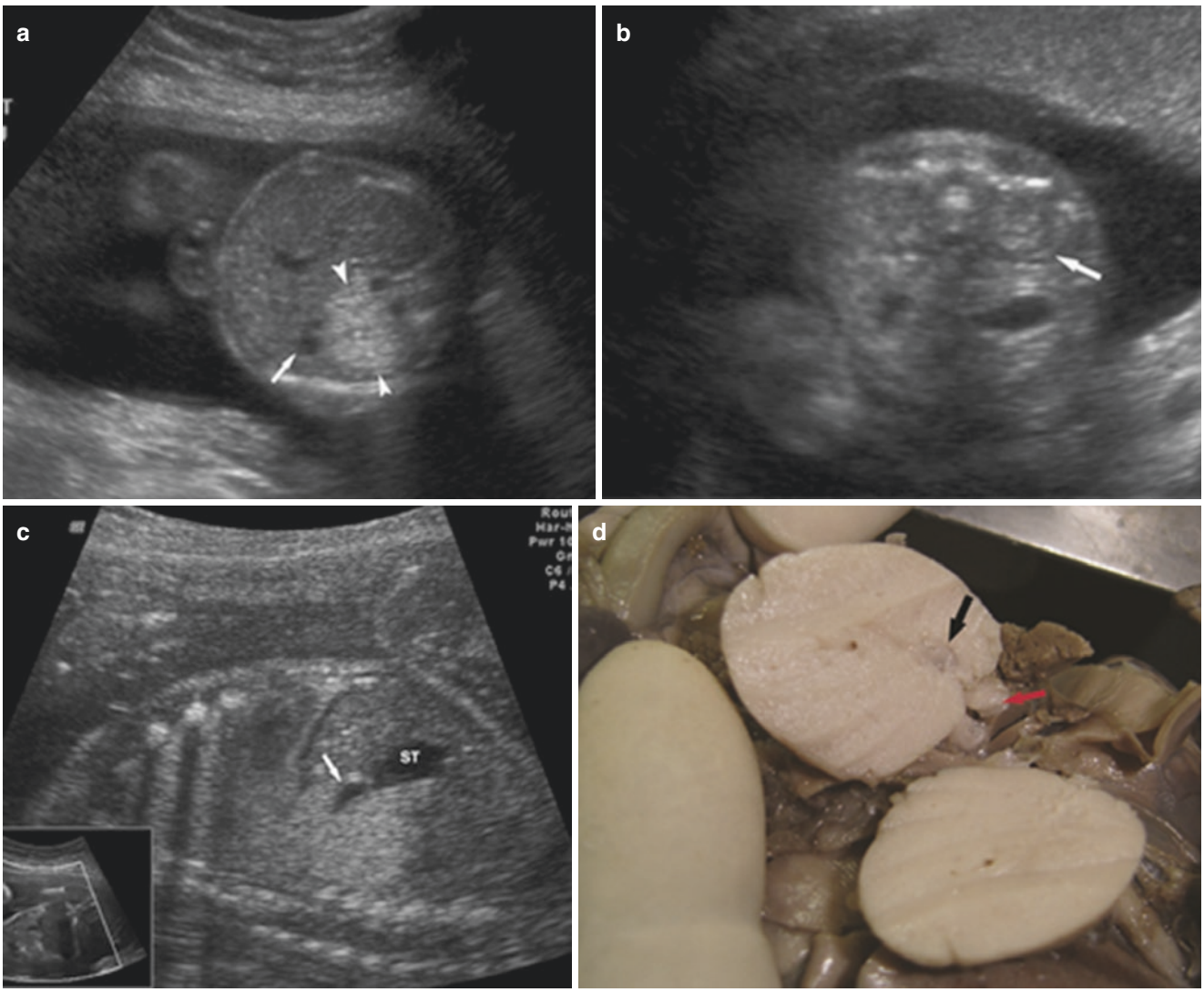

Fig. 4.25 Bronchopulmonary foregut malformation—(**a**) Axial scan of fetal upper abdomen shows an echogenic mass (arrow heads) posterior to stomach (arrow). (**b**) Scan showing the normal adrenal (arrow). (**c**) Oblique scan showing a tubular fluid filled structure (arrow) in center of the mass communicating with the lumen of stomach confirming the diagnosis (**d**) Cut section of the excised mass showing the bronchus (arrow)

4.4 Echoes in Gall Bladder

The gall bladder is seen well on sonography from second trimester onwards. It is seen as a pyriform cystic structure on right side of abdomen, a little below the section of abdominal circumference (Fig. 4.26). Echoes in gall bladder is due to sludge and resolve during pregnancy or early postnatal life.

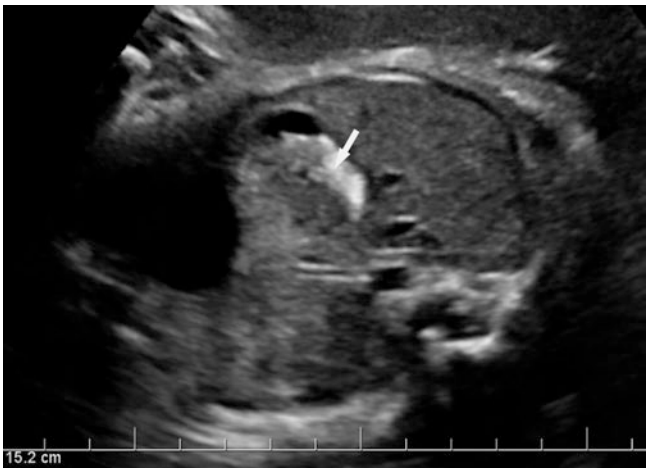

Fig. 4.26 Echoes in gall bladder: Oblique scan of fetal abdomen showing echogenic sludge in lumen of gall bladder (arrow)

4.5 Fetal Ascites

Fetal ascites refers to the accumulation of free fluid in the fetal peritoneal cavity. Fetal ascites can be part of hydrops fetalis or isolated.

4.5.1 Hydrops Fetalis

Hydrops fetalis is defined as the presence of extracellular fluid in at least two fetal body compartments. These compartments include ascites, pericardial effusion, pleural effusion, scalp and body wall edema. Hydrops fetalis can be due to heart failure, reduced oncotic pressure or obstruction of lymphatic flow. The etiologies of hydrops can be immune and non-immune categories. Immune hydrops is related to fetal isoimmunization due to Rh incompatibility between mother and fetus. Non immune fetal hydrops has several etiologies including fetal aneuploidy, cardiac anomaly, metabolic disorder, placental insufficiency, maternofetal viral infection, fetal anemia and cystic hygroma (Fig. 4.27).

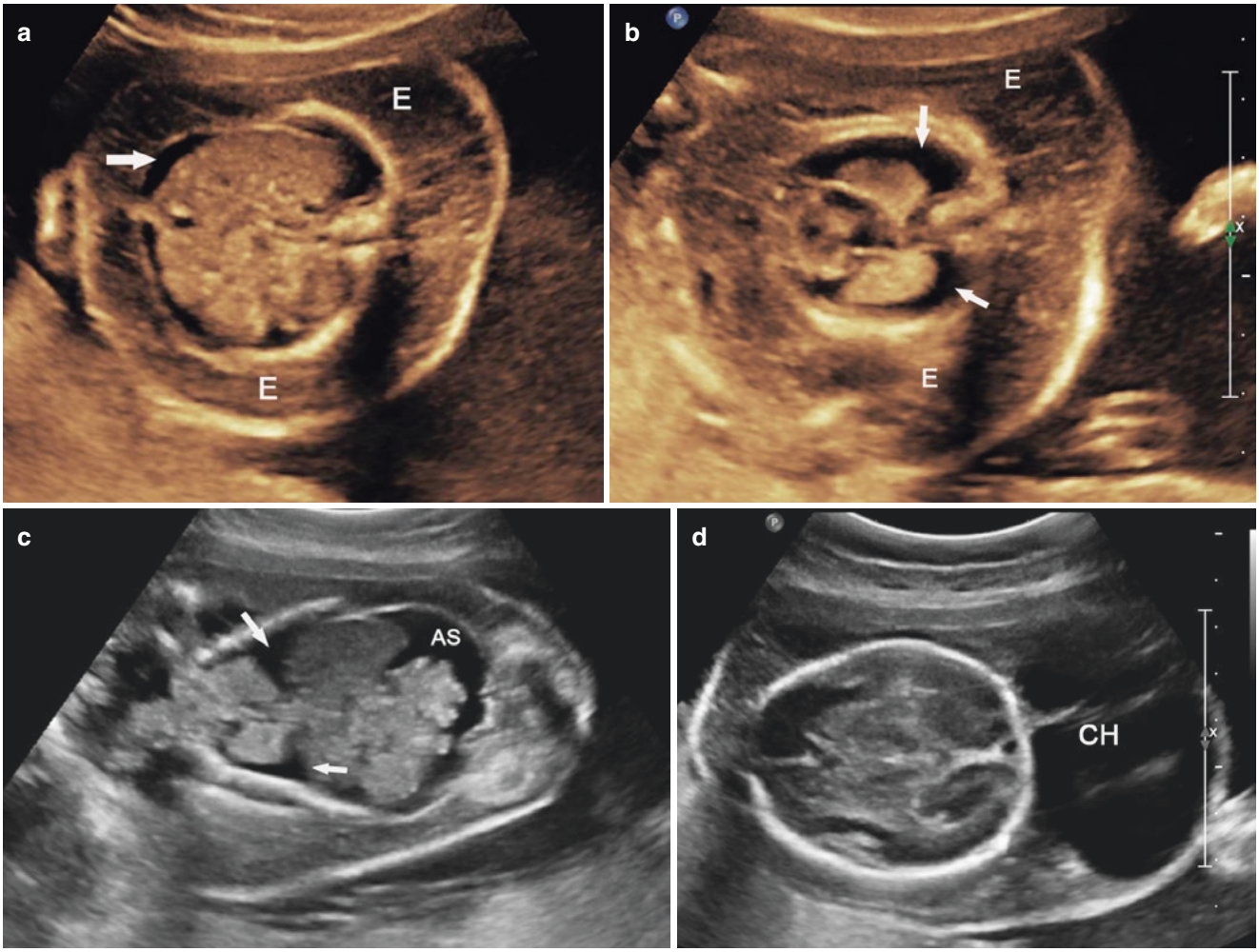

Fig. 4.27 Hydrops fetalis: Axial scan of (**a**) fetal abdomen (**b**) chest and (**c**) Coronal scan of chest and abdomen showing subcutaneous edema, pleural fluid and ascites. (**d**) head showing subcutaneous edema, in all sections, ascites, bilateral pleural fluid and cystic hygroma (CH)

4.5.2 Isolated Fetal Ascites

Isolated fetal ascites is defined as abnormal fluid accumulation in the abdominal cavity without fluid accumulation in any other serosal cavities or subcutaneous tissue. Isolated ascites can result from many different etiologies including meconium peritonitis, chromosomal anomaly, genitourinary tract abnormalities and viral infections. Few cases of isolated fetal ascites are discussed.

Meconium Peritonitis

Meconium peritonitis refers to a sterile chemical peritonitis due to intra-abdominal bowel perforation and spillage of fetal meconium into peritoneal cavity. It may be associated with bowel atresia, volvulus, intussusception and meconium ileus in cystic fibrosis. Spectrum of sonographic findings described in meconium peritonitis will vary depending on the underlying bowel disorder, the inflammatory response and time since perforation. Extrusion of the meconium into peritoneal cavity produces exudative ascites which outline the abdominal viscera. Ascites is echogenic due to presence of debris (Fig. 4.28). In case of male fetus ascites may extend to scrotum. Sometimes ascites is seen anteriorly in peritoneal cavity with matted echogenic bowel loops forming a posterior mass. The debris may show movement with fetal movement (Video 4.2). The ascites of meconium peritonitis can completely resolve during pregnancy, can get loculated in the form of meconium cyst or result in peritoneal calcifications. The meconium cyst is seen as a loculated fluid collection in peritoneal cavity with or without echogenic walls (Fig. 4.29). The calcifications occur during the healing process and appear as brightly echogenic linear or clumped bright echoes in the abdomen or pelvis, mostly along the periphery (Figs. 4.30 and 4.31). Calcification may be seen on surface of liver and under the diaphragm. On follow up of meconium peritonitis the fetus may show ileal atresia (Fig. 4.30).

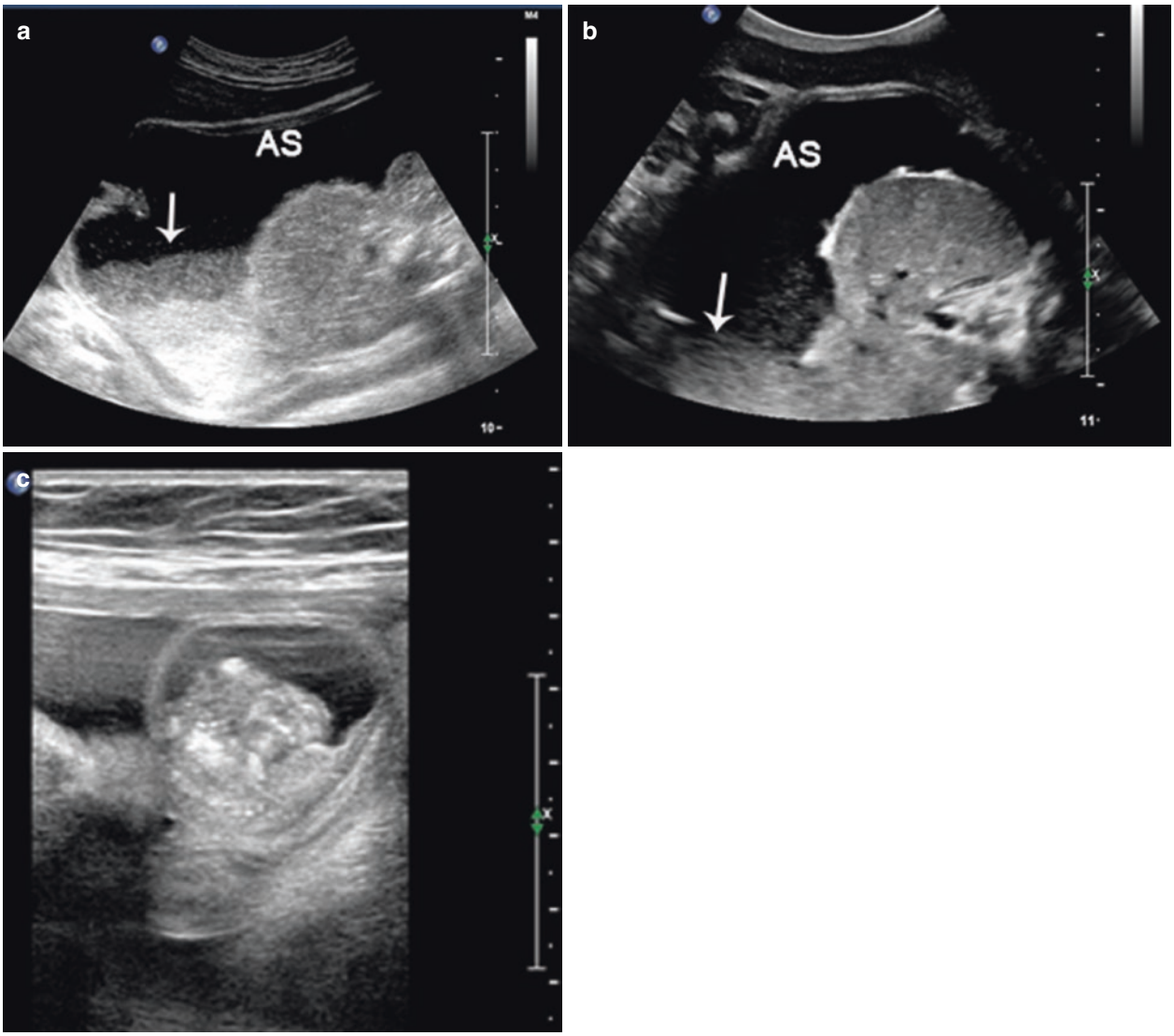

Fig. 4.28 Meconium Peritonitis: Axial scan of fetal abdomen showing ascites (AS) with debris (arrow) Video. (**a**) And ascites and calcifications on surface of liver (arrow) in (**b**). (**c**) Scan of scrotum showing the hydrocele with debris and calcifications

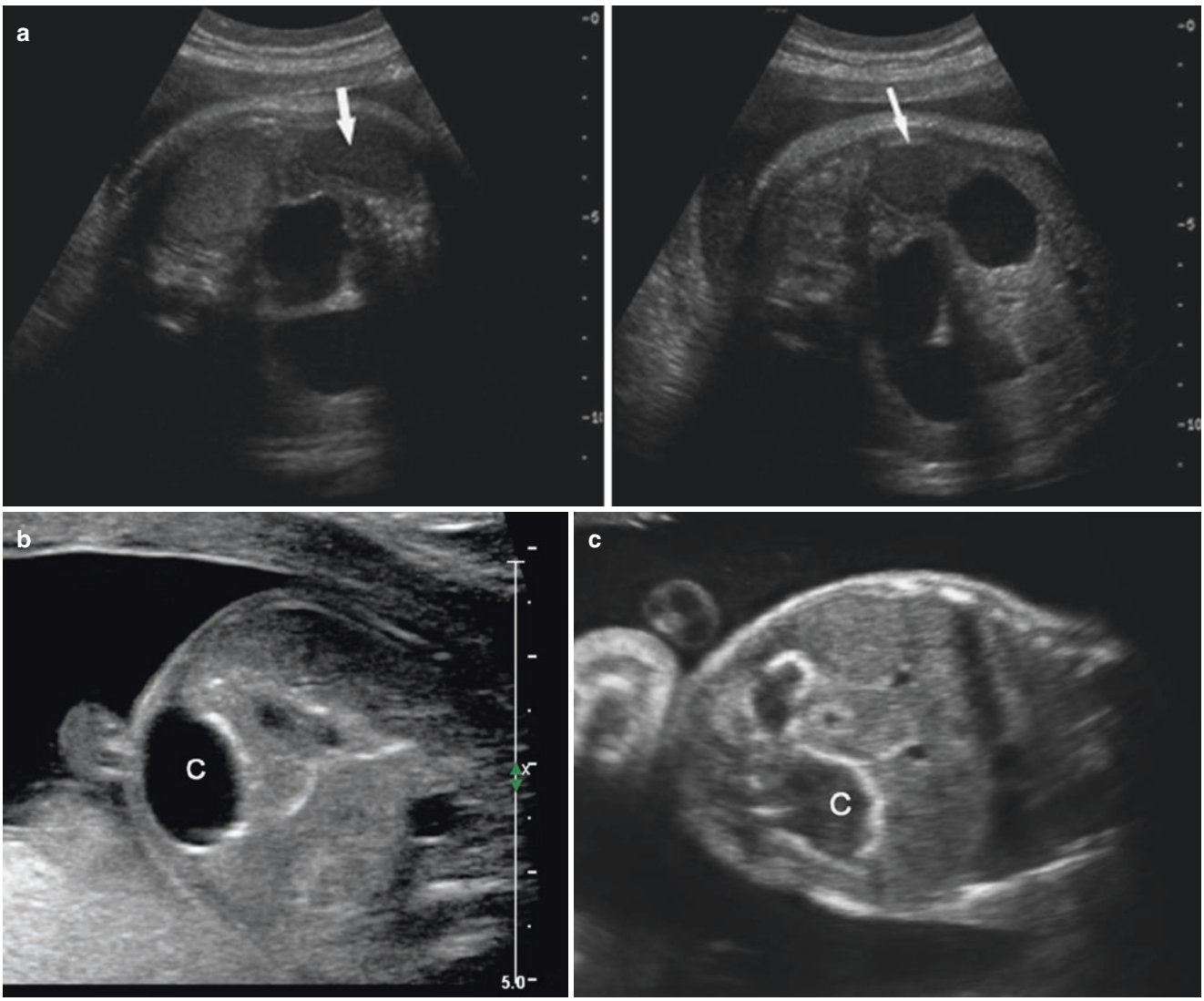

Fig. 4.29 Meconium cyst: (**a**) Axial and Coronal Scan of fetal abdomen showing meconium cyst with internal echoes (arrows). (**b**) Shows meconium cyst with part of the wall calcified. (**c**) Shows a meconium cyst with echogenic walls

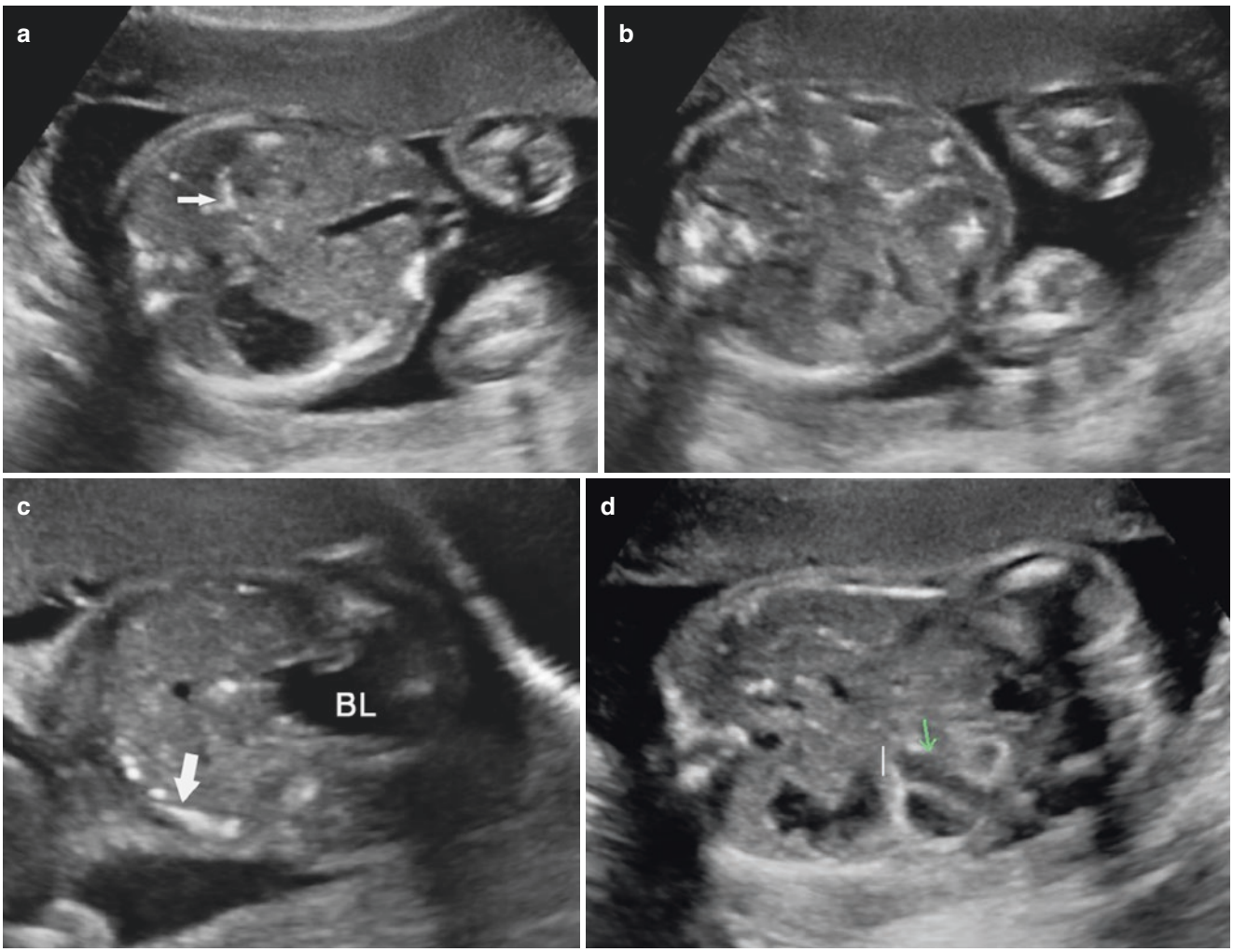

Fig. 4.30 Meconium Peritonitis with calcifications: Axial scan of (**a**) upper abdomen, (**b**) midabdomen and (**c**) coronal scan showing peritoneal calcifications in the periphery of abdomen, on the surface of liver and in between bowels. (**d**) Coronal scan showing dilated small bowel loop indicating an evolving ileal atresia

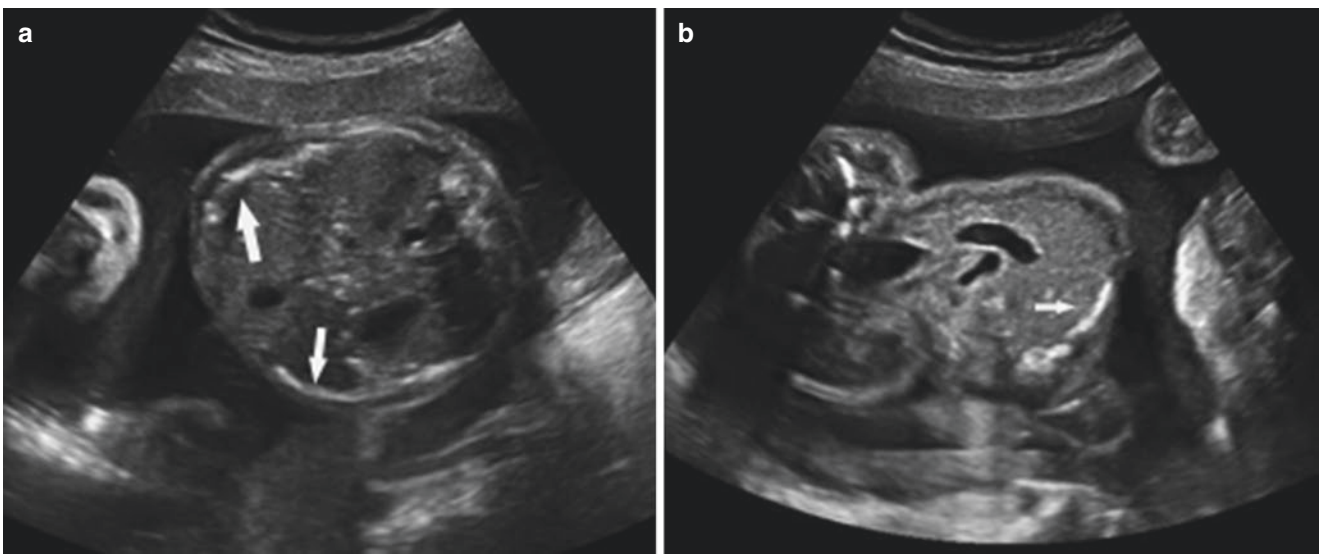

Fig. 4.31 Axial (**a**) and Coronal Scan (**b**) of another fetus showing peripheral calcifications and along under surface of diaphragm (arrows)

Urinary Ascites

Severe lower urinary tract obstruction can cause the rupture of fetal urinary bladder resulting in urinary ascites. Most common cause is posterior urethral valves. In some cases bladder rent closes spontaneously with reduced amount of ascites and increasing severity of hydroureteronephrosis. Imaging findings are ascites, hydroureteronephrosis and thickened bladder wall. The dilated posterior urethra is seen as the key hole appearance in posterior urethral valves. The rent in urinary bladder may or may not be visible (Fig. 3.54). In case the fetal bladder obstruction does not resolve spontaneously, drainage of bladder by vesico amniotic shunting can be performed after 17th week of gestation in order to prevent lung hypoplasia.

Congenital High Airway Obstruction Syndrome (CHAOS)

Congenital high airway obstruction syndrome is a very rare entity where the higher airway is intrinsically obstructed. The most common reason is laryngeal atresia. This obstruction causes fluid accumulation in lung resulting in enlargement of lungs. The heart is compressed between enlarged lungs and seen as micro and mesocardia. The diaphragm is inverted with convexity towards abdomen. Enlarged lungs lead to compression of inferior vena cava resulting in ascites and/or hydrops. Imaging findings are ascites, enlarged echogenic lungs, flattened diaphragm, mesocardia and microcardia (Fig. 4.32). The prognosis is poor.

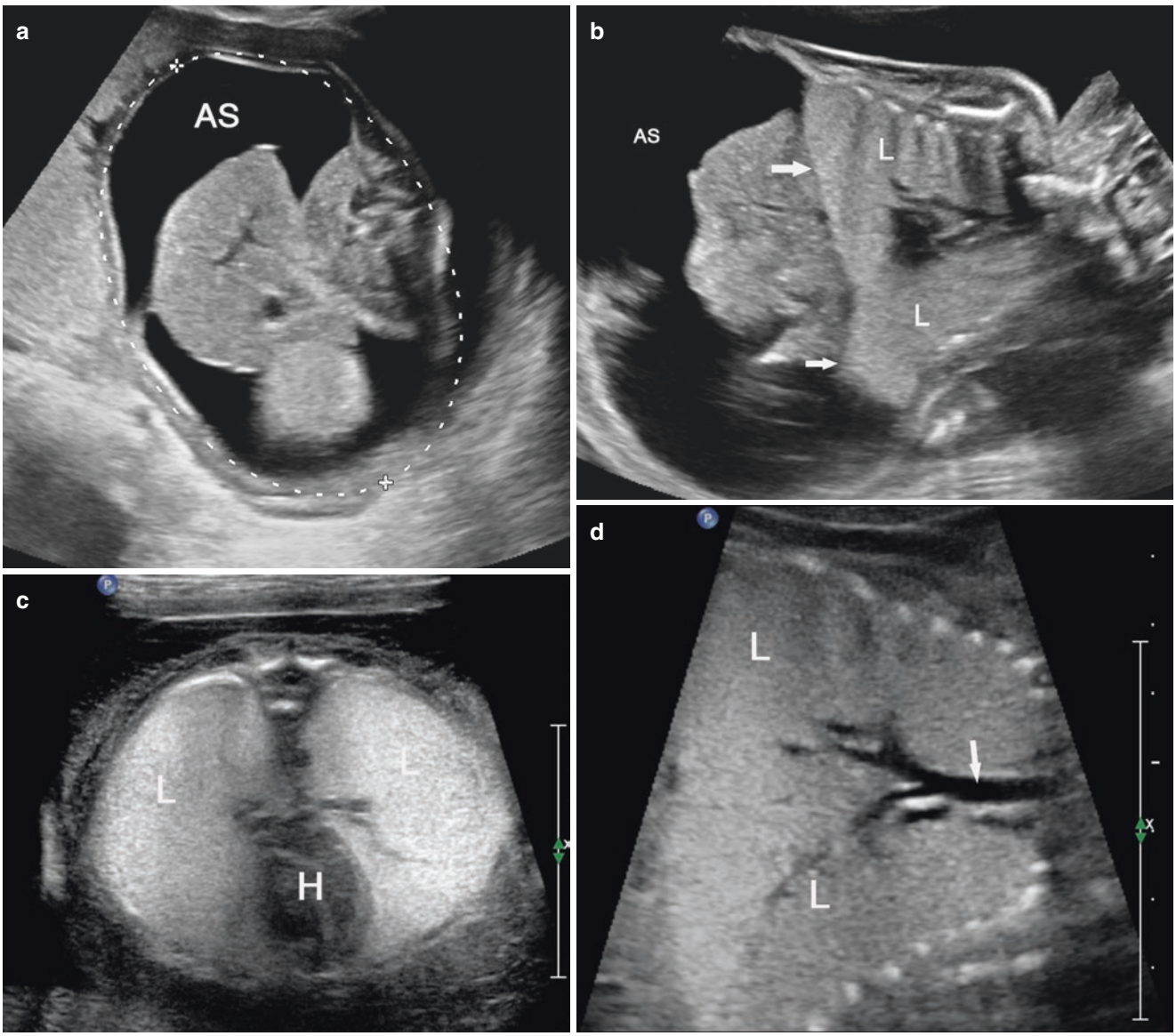

Fig. 4.32 Congenital High Airway Obstruction (CHAOS): (**a**) Axial scan of fetal abdomen showing ascites (AS). (**b**) Coronal scan of fetal chest and abdomen showing ascites and enlarged echogenic lungs (L) with inferiorly convex domes of diaphragm (arrows). (**c**) Axial scan of chest showing markedly enlarged echogenic lungs (L) with a central small heart (H). (**d**) Coronal scan of chest showing enlarged echogenic lungs lungs (L) with fluid distended trachea and bronchi (arrow)

Liver Fibrosis with Portal Hypertension

Biliary ducts are normally formed from remodeling and partial involution of cylindrical ductal plates. Insufficient remodeling and resorption leads to ductal plate malformation. Insult to the small interlobular ducts leads to congenital hepatic fibrosis. Imaging findings are ascites, small size of liver with irregular surface and coarse echopattern with portal hypertension. In portal hypertension, the portal and splenic veins are dilated with multiple collaterals. Color Doppler shows hepatofugal flow in portal vein with multiple collaterals (Fig. 4.33).

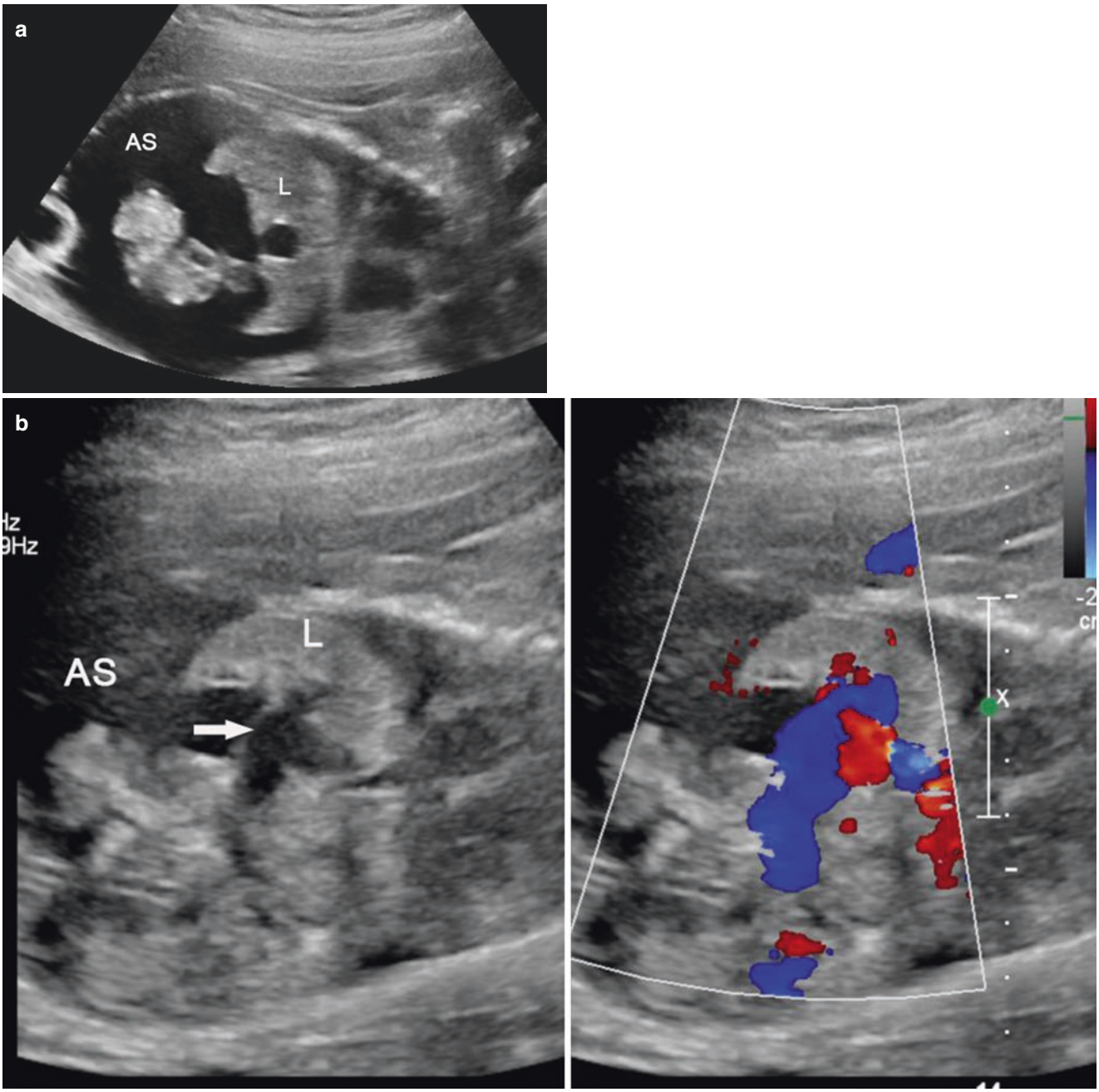

Fig. 4.33 Liver fibrosis with portal hypertension: (**a**) Coronal scan of fetal abdomen showing ascites (AS) and shrunken irregular liver (L). (**b**) Coronal gray Scale and Colour Doppler images showing the dilated portal vein (arrow) with hepatofugal flow. (**c**) Axial gray scale and colour Doppler images shows dilated tortuous vein on left side of abdomen indicating varices (arrow)

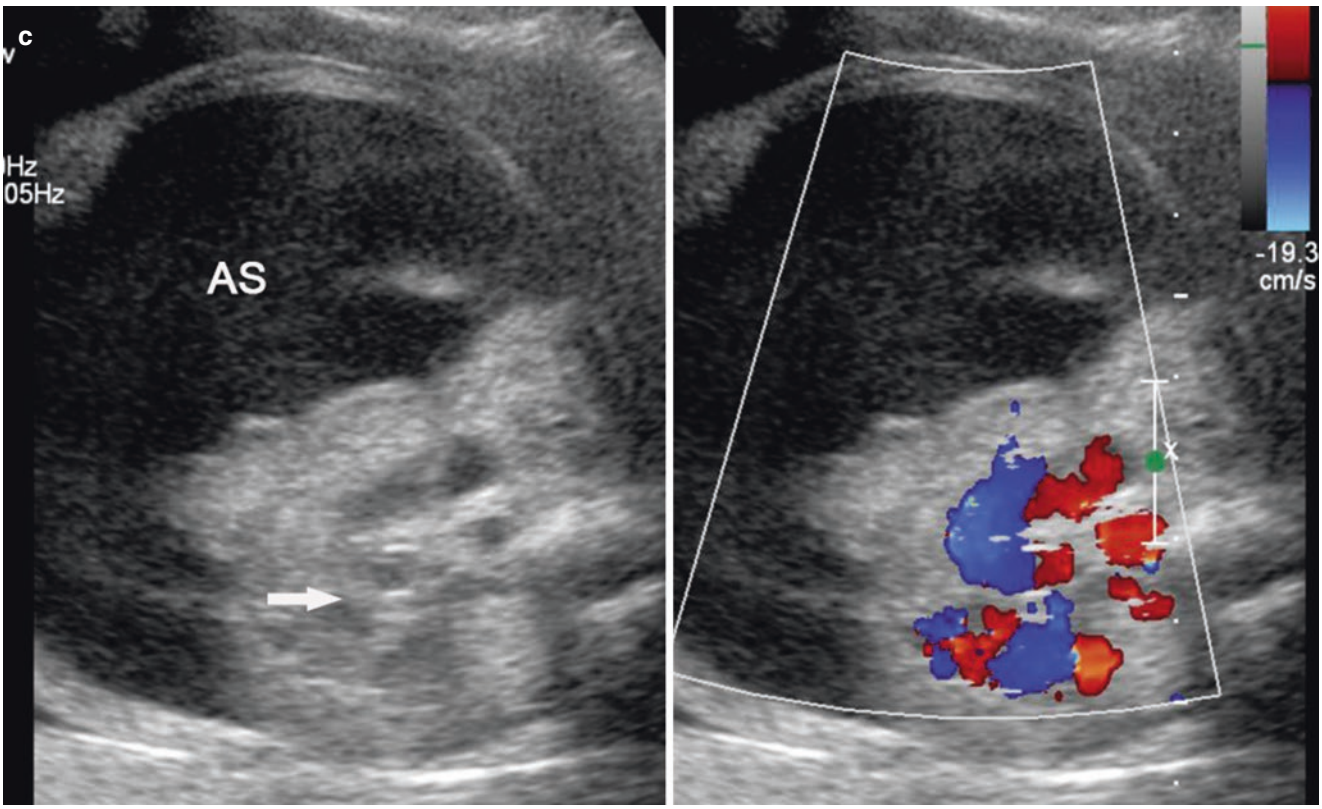

Fig. 4.33 (continued)

Suggested Reading

Agarwal R. Sonographic assessment of the fetal abdominal cystic lesions: a pictorial essay. Indian J Radiol Imaging. 1999;9(4):169–82.

Cho JY, Lee YH. Fetal tumors: prenatal ultrasonographic findings and clinical characteristics. Ultrasonography. 2014;33(4):240–51.

McNamara A, Levine D. Intraabdominal fetal echogenic masses: a practical guide to diagnosis and management. Radiographics. 2005;25(3):633–45.

Trinh TW, Kennedy AM. Fetal ovarian cysts: review of imaging spectrum, differential diagnosis, management, and outcome. Radiographics. 2015;35(2):621–35.

Tu CY. Ultrasound and differential diagnosis of fetal abdominal cysts. Exp Ther Med. 2017;13(1):302–6.

Fetal Abdominal Wall Sonography

5

5.1 Introduction

Abdominal wall defects (AWDs) consists of a spectrum of anomalies. The overall prevalence is about 6 per 10,000 births. Gastroschisis and omphalocele are common among AWDs, while other complex defects like bladder exstrophy, cloacal exstrophy, body stalk anomaly, Pentalogy of Cantrell, and abdominoschisis due to amniotic bands are uncommon. Many AWDs may be associated with other congenital abnormalities which influence prognosis and management. 60–100% of abdominal wall defects are diagnosed prenatally depending on the expertise. An increased understanding of the spectrum of fetal ventral wall defects will improve the prenatal diagnosis.

5.2 Embryology

By the end of second week of embryonic life, a bilaminar disc is formed. This disc has an epiblast facing the amniotic cavity and a hypoblast facing the yolk sac. Gastrulation occurs by the end of third week, when this bilaminar disc becomes a trilaminar disc. This disc comprises endoderm formed by the hypoblast, ectoderm formed by the epiblast and the mesoderm sandwiched in between. Further development of the embryo leads to craniocaudal folding and lateral folding resulting in the formation of ventral wall. This results in an outer tube (abdominal wall) surrounding an inner tube (gastrointestinal tract). During the eighth menstrual week, the midgut begins to elongate out of proportion to the increase in body length. To accommodate such a growth, the midgut herniates into the base of the umbilicus. Here the midgut undergoes a 90° counterclockwise rotation. This physiologic herniation may be detected sonographically and should not be mistaken for an anomaly. As the bowel returns into the abdominal cavity, it undergoes a further 180° counterclockwise rotation and the return is complete by 11th week.

5.2.1 Development of Cloaca

The cloaca develops as the terminal portion of the hindgut. During the sixth and seventh weeks of development, the urorectal septum begins to grow caudad towards the cloacal membrane and divides the cloaca into urogenital sinus anteriorly and the rectum posteriorly. Once the urorectal septum reaches the cloacal membrane, the membrane ruptures and two orifices are created. The urogenital sinus will undergo further differentiation to become the urinary bladder, urethra, and in the females, a portion of the vagina.

Electronic Supplementary Material The online version of this chapter (https://doi.org/10.1007/978-981-13-0932-8_5) contains supplementary material, which is available to authorized users.

S. B. Vijayaraghavan, *Atlas of Fetal Imaging*, https://doi.org/10.1007/978-981-13-0932-8_5

5.3 Physiological Herniation of Bowel in the Fetus

Physiological hernia of bowel in the fetus usually resolves by 11 weeks (CRL—45 mm). It should not be more than 1 cm into the cord and should never include the liver (Fig. 5.1). If there is any doubt during the first trimester, then a follow-up scan at 14 weeks should be done to document the return of bowel into the abdominal cavity.

5.4 Omphalocele

Omphalocele is a defect in the closure of the abdominal wall involving the cord insertion site. This defect results in herniation of abdominal contents into the base of the umbilical cord through a wide umbilical opening. Omphalocele occurs in 1 in 4000 live births. The incidence of omphalocele is higher in the first trimester due to a high spontaneous fetal loss or termination of pregnancy of early pickup of associated chromosomal or other structural abnormalities. The organs frequently seen in the omphalocele sac are small bowel loops, liver, rarely colon, spleen and kidneys. The herniated organs are wrapped in a two-layered sac of peritoneum and the amnion.

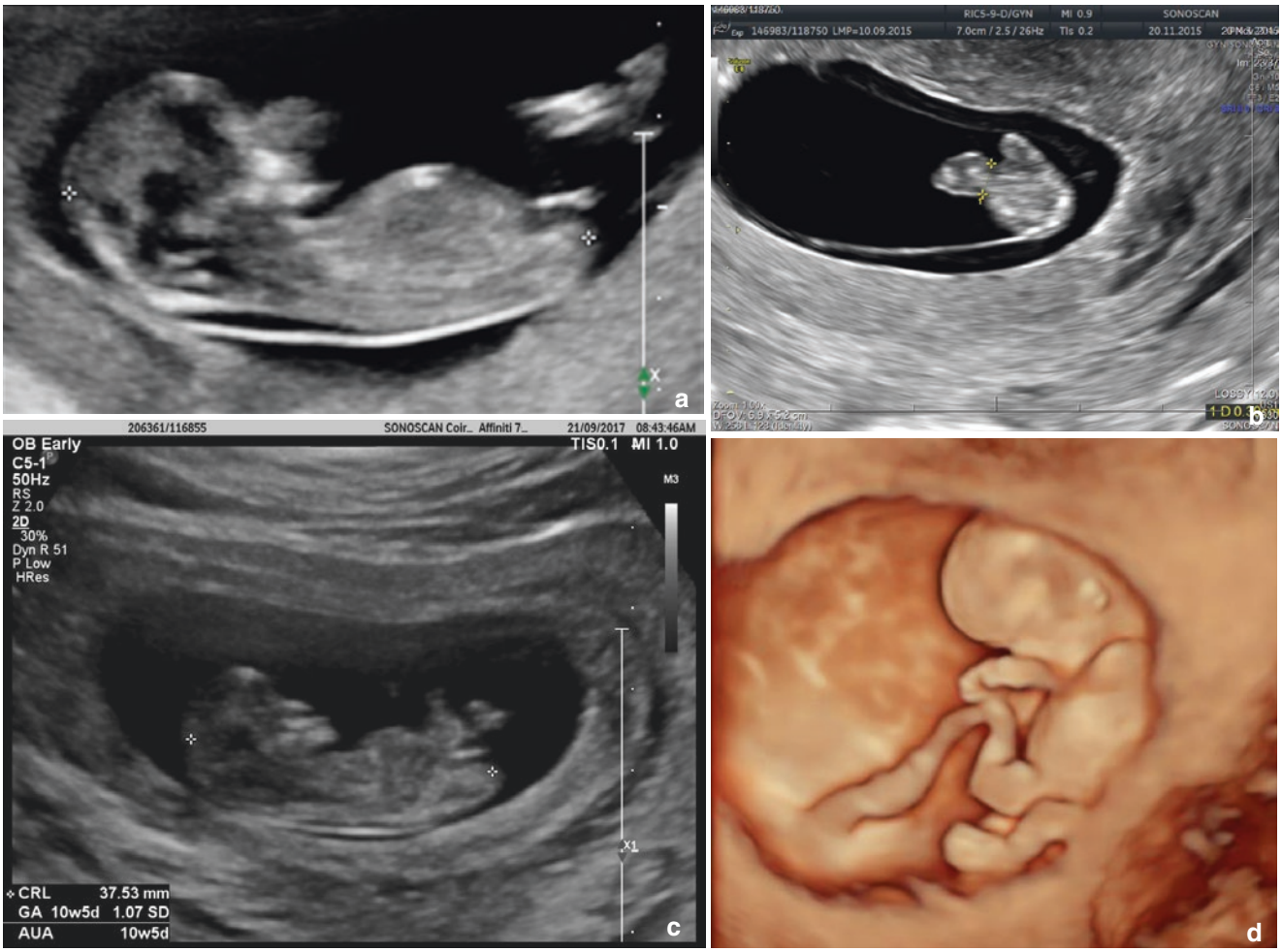

Fig. 5.1 Physiological herniation of bowel: (**a**) Longitudinal scan of fetus of 10 weeks gestation showing normal anterior abdominal wall; (**b**) axial section and (**c**) similar section of a fetus with physiological herniation of bowel; (**d**) 3D images of the same fetus

5.4.1 Ultrasound Features

An omphalocele is sonographically seen as a bulging structure arising from the anterior abdominal wall, containing some abdominal viscera (liver and/or bowel), and the cord insertion is noted on its convexity. Color Doppler is useful to show the cord insertion on convexity (Figs. 5.2 and 5.3).

5.4.2 Associated Genetic and Structural Abnormalities

There is a high incidence (15–40%) of genetic abnormalities of which trisomy 18 and 13 are common. The association with other structural anomalies or increased NT in the first trimester increase the possibility of genetic abnormalities.

5.4.3 Differential Diagnosis

Omphalocele should be differentiated from other abdominal wall defects and physiological herniation of gut in the cord that disappears by 11 weeks gestation. The herniated contents are contained in a sac in omphalocele whereas, in gastroschisis the bowel loops float freely in the amniotic fluid. The cord insertion site is normal in gastroschisis with a paramedian defect, while in an omphalocele, it inserts on the convexity of the sac. If a large omphalocele contains the whole of the liver, then this should be differentiated from the Limb Body Wall Complex (LBWC), which is characterized by evisceration of abdominal viscera outside the amniotic sac, major distortion of the body anatomy, with severe kyphoscoliosis and limb abnormalities. Cloacal exstrophy is another abnormality in which omphalocele extends caudally and is associated with bladder exstrophy and anomalies of the external genitalia. In the case of omphalocele, the recognition of a normal bladder in the pelvis rules out this very rare possibility of cloacal exstrophy.

5.4.4 Prognosis

The prognosis for prenatally diagnosed omphalocele is guarded.

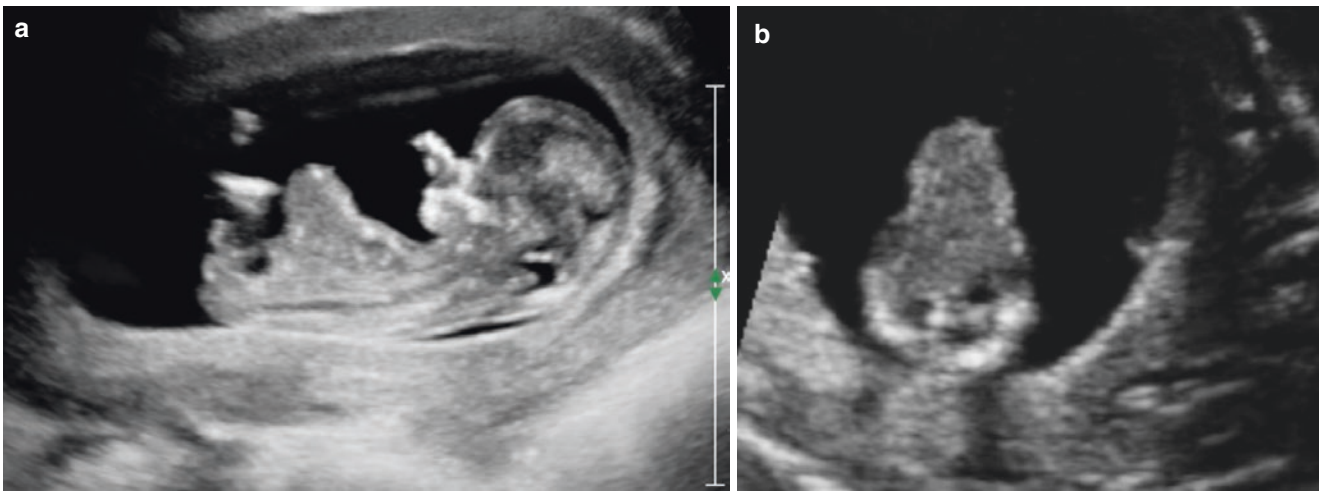

Fig. 5.2 Omphalocele in 15 weeks fetus: (**a**) Longitudinal and (**b**) axial scan showing the omphalocele

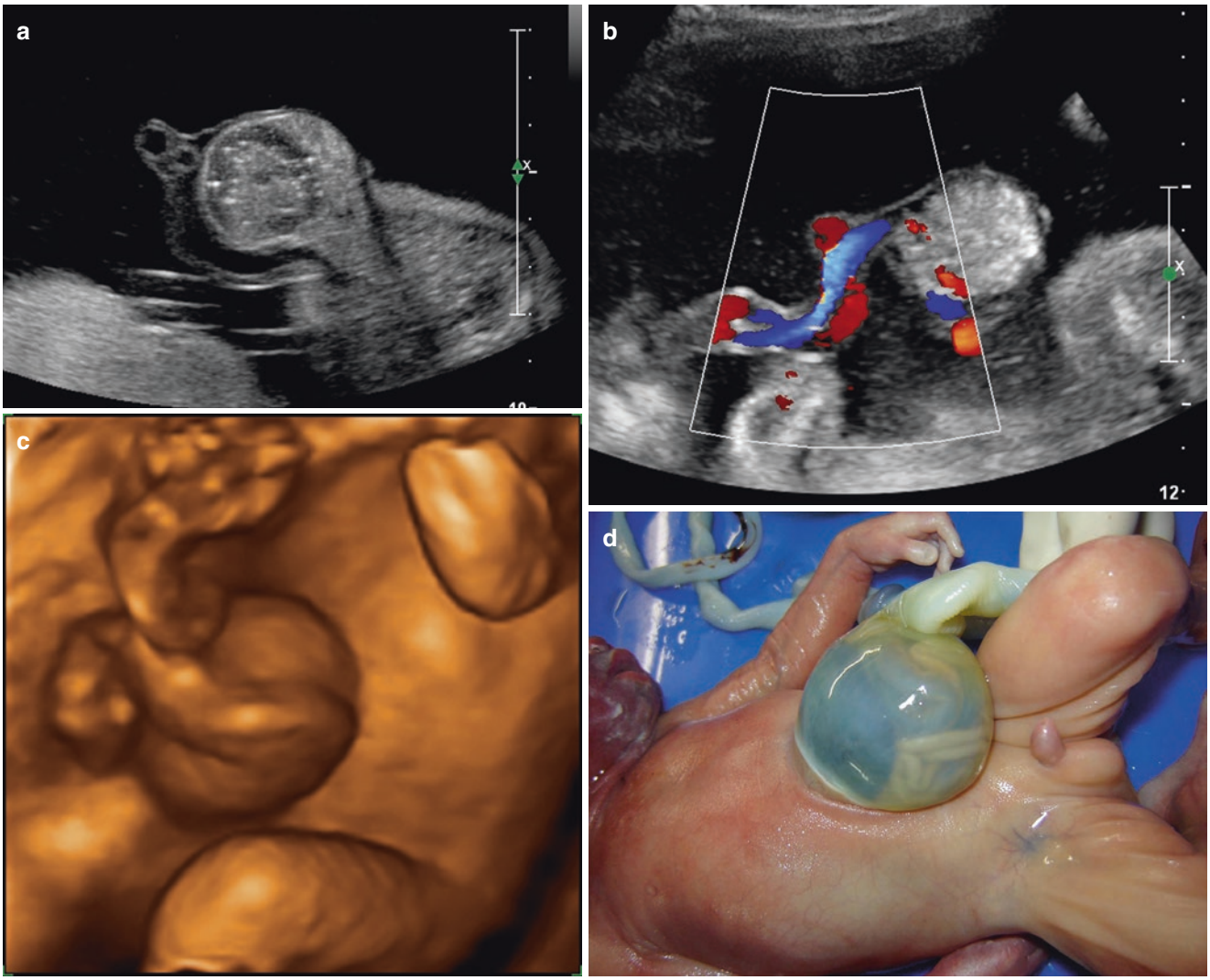

Fig. 5.3 Omphalocele in a 20 weeks fetus: (**a**) Axial scan and (**b**) colour Doppler scan and (**c**) 3D image showing the omphalocele and the insertion of the umbilical cord on the convexity. (**d**) Photograph of the abortus

5.5 Gastroschisis

In this AWD, the bowel herniates through a paramedian AWD, that is usually to the right of the cord insertion site and the herniated contents are not limited by a membrane. Incidence is 1 in 2000 live births. Young maternal age is associated with increased incidence.

5.5.1 Ultrasound Features

Prenatal diagnosis by ultrasound is based on the demonstration of the normally situated umbilical cord insertion and the herniated free-floating loops of intestine without any membranous covering. The stomach may be positioned abnormally with the gastric fundus pulled toward the defect. The free-floating bowel loops can appear thickened and edematous due to inflammation or as an echogenic mass (Figs. 5.4 and 5.5). Inflammation can progress to intestinal atresia. This may lead to the appearance of dilated bowel loops floating in the amniotic fluid and within the abdomen (Fig. 5.6). Gastroschisis is usually an isolated anomaly and has good prognosis.

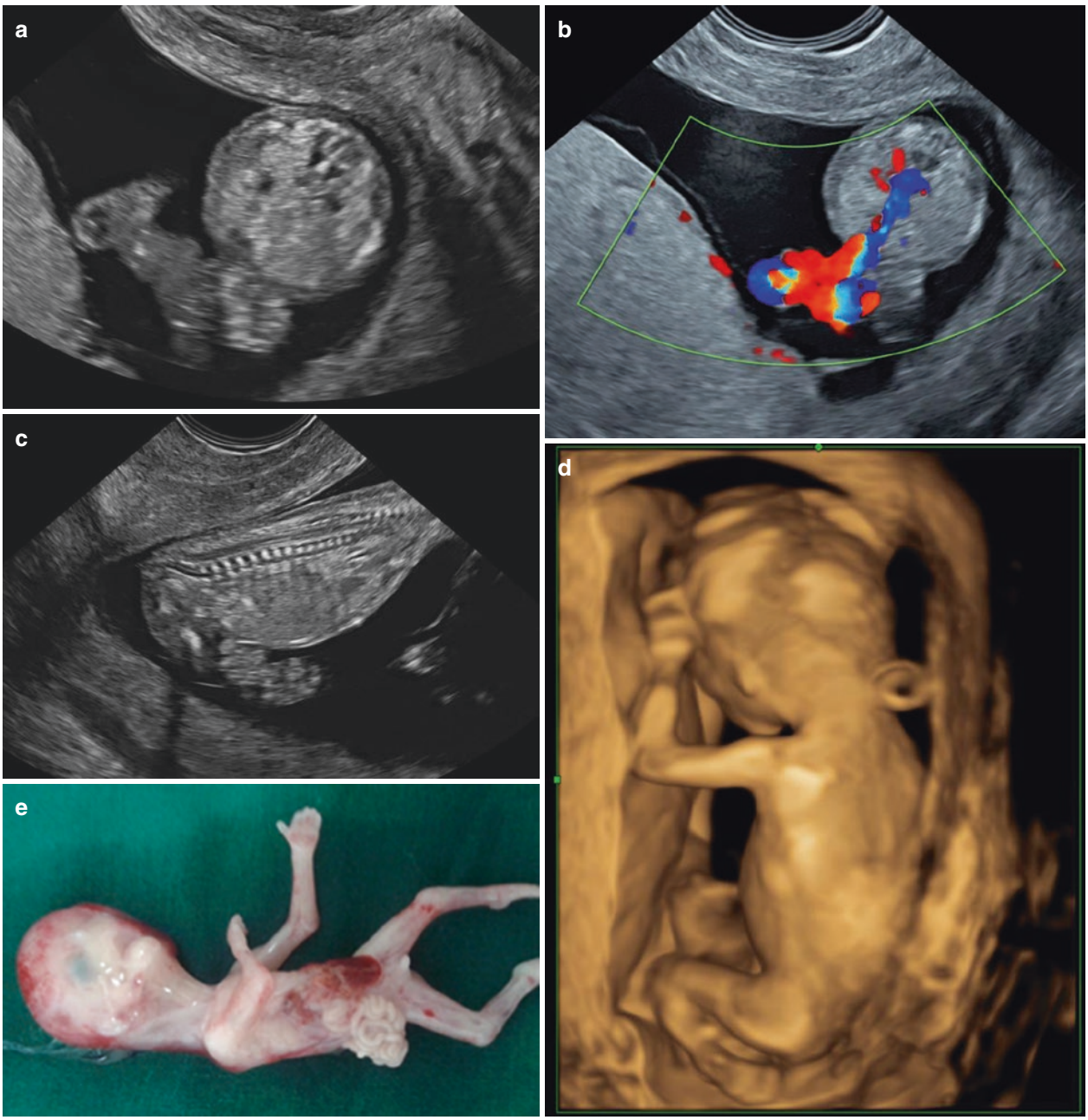

Fig. 5.4 Gastroschisis in a 13 weeks fetus: (**a**) Gray scale and (**b**) colour Doppler axial scan of the fetal abdomen showing the free floating bowel loops herniated through a defect to right of cord insertion; (**c**) longitudinal scan showing the free floating bowels in amniotic fluid; (**d**) 3D of the same fetus. (**e**) Abortus showing the gastroschisis

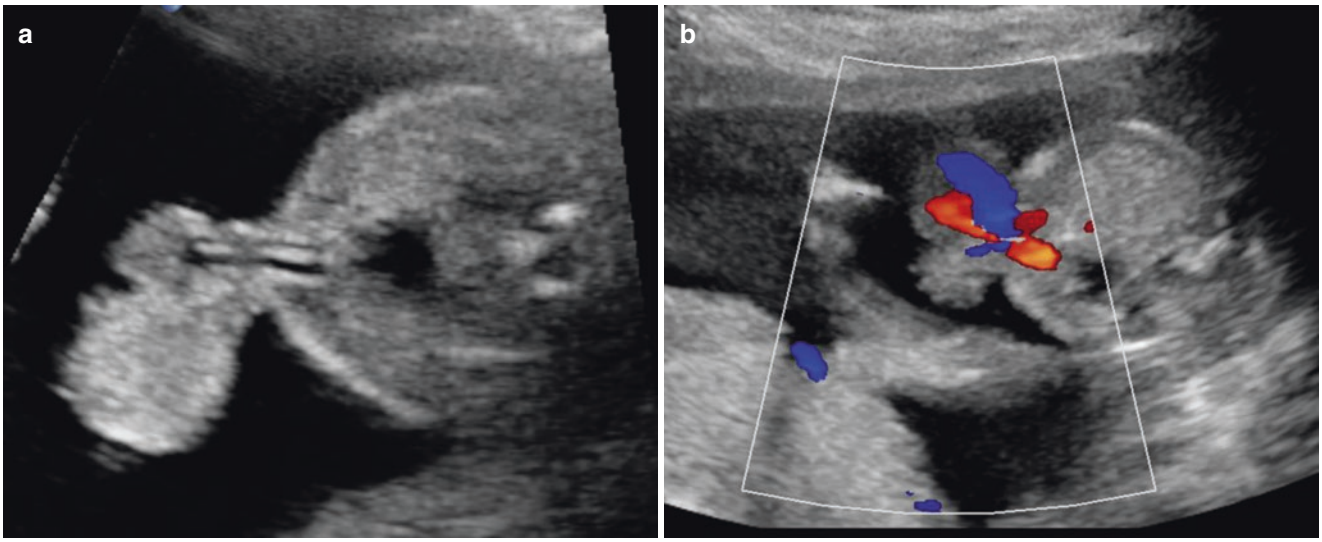

Fig. 5.5 Gastroschisis in a 20 weeks fetus: (**a**) Axial scan and (**b**) colour Doppler study of the fetal abdomen showing the matted bowels seen as an echogenic mass to right of cord insertion

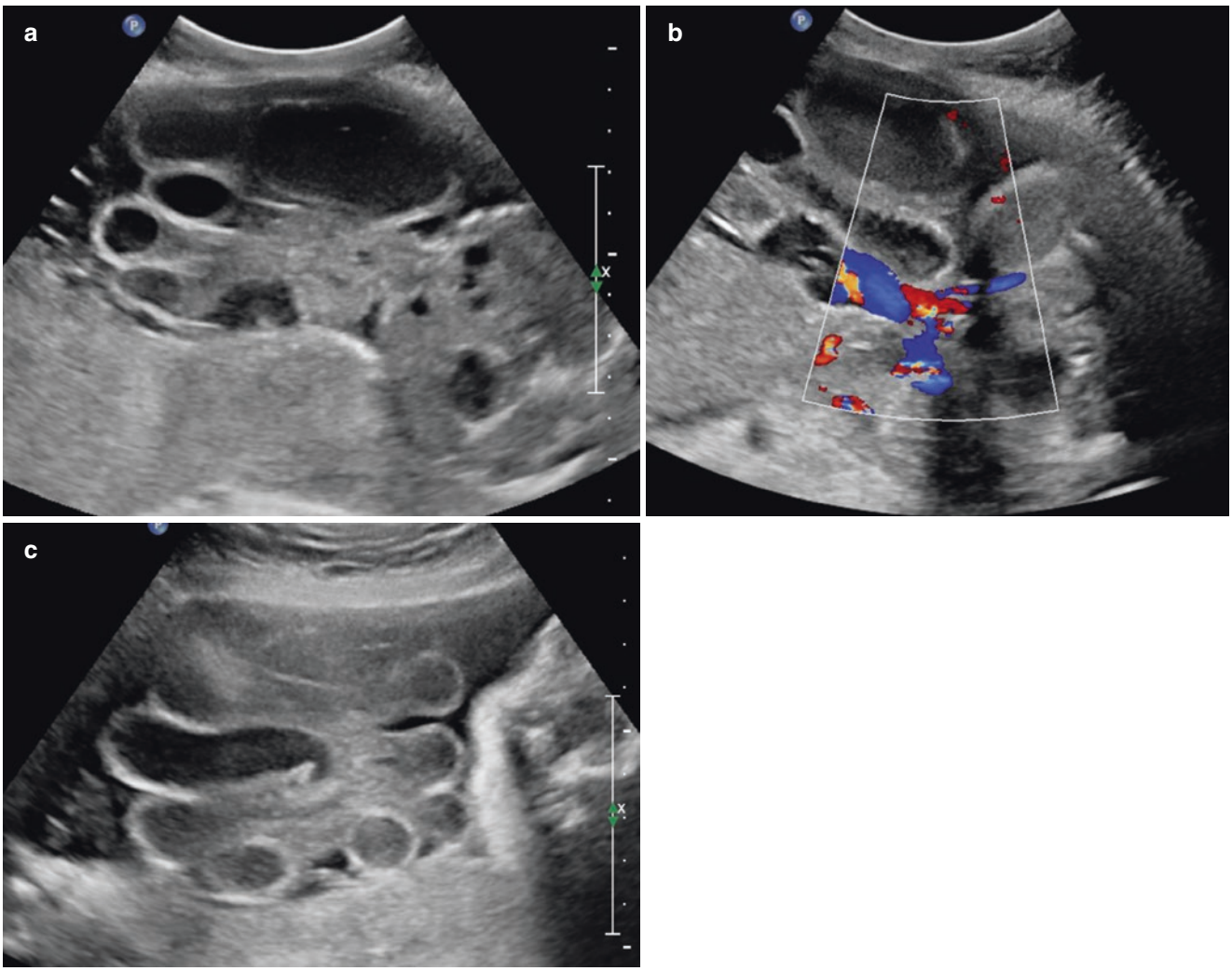

Fig. 5.6 Gastroschisis with small bowel atresia: (**a**) Axial scan and (**b**) colour Doppler scan showing the dilated small bowel loops floating in amniotic fluid herniated through a defect to right of cord insertion; (**c**) longitudinal scan showing dilated loops floating in the amniotic fluid

5.6 Umbilical Cord Hernia

Congenital hernia of the umbilical cord is a different type of ventral abdominal wall defect, in which the bowel usually herniates into the base of normally inserted umbilical cord through the umbilical ring. Its incidence is estimated to be 1 in 5000 and unlike omphalocele, it is not linked with chromosomal anomalies. Association with other anomalies is rare.

5.6.1 Ultrasound Features

A loop of bowel is seen herniating into the base of normally inserted umbilical cord through the umbilical ring and is seen in between the umbilical vessels (Fig. 5.7).

5.6.2 Outcome

Umbilical cord hernia is usually benign with a favorable outcome. However, prenatal diagnosis is useful to prevent inadvertent injury to the bowel during clamping of the cord at the time of delivery.

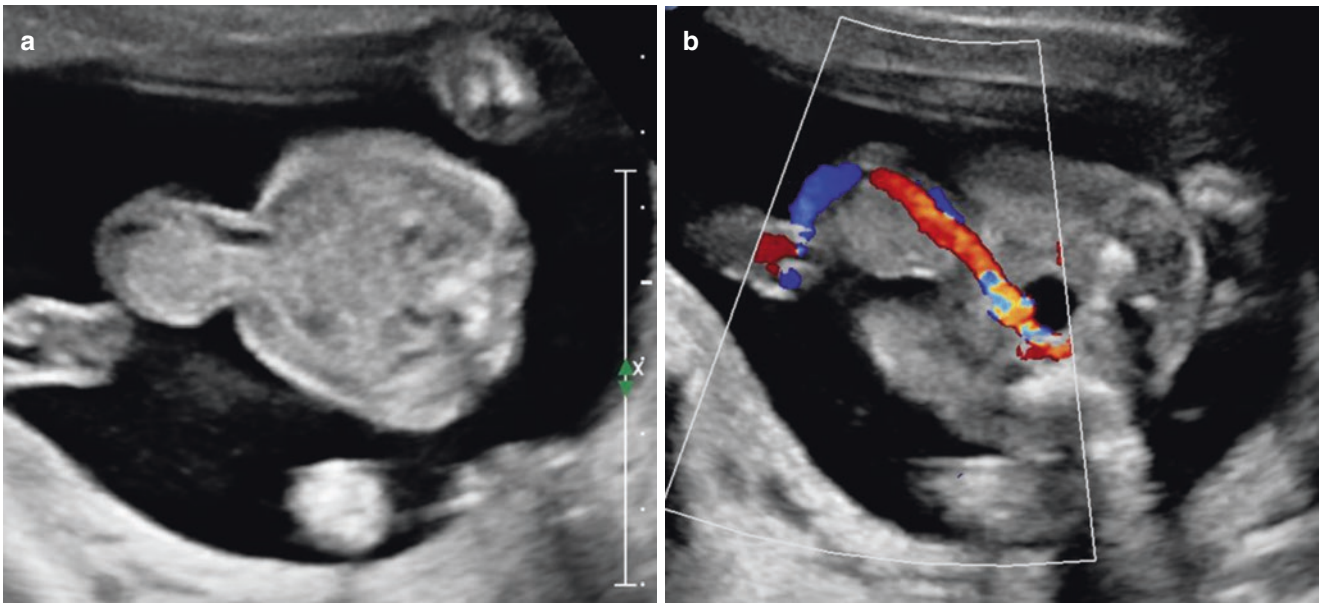

Fig. 5.7 Umbilical cord hernia: (**a**) Axial scan and (**b**) colour Doppler scan of fetal abdomen showing herniation of the loop of bowel into the base of umbilical cord by the side of cord vessels

5.7 Bladder and Cloacal Exstrophy

Bladder exstrophy and epispadias complex (BEEC) is an anterior midline defect with a variable expression involving the infraumbilical abdominal wall including the bony pelvis, urinary tract, and external genitalia. Bladder and cloacal exstrophy are two different expressions of a primary developmental defect. Exstrophy of the cloaca or OEIS complex is due to failure of fusion of the genital tubercles and pubic rami, incomplete development of the lumbosacral vertebrae with spinal dysraphism, imperforate anus, cryptorchidism and epispadias in males, anomalies of the mullerian duct derivatives in females and a wide range of urinary tract anomalies. Omphalocele is common and most patients have a single umbilical artery.

5.7.1 Aetiopathogenesis

At around 6 weeks, the urorectal septum divides the cloaca into urogenital sinus anteriorly and the hindgut posteriorly. Simultaneously, the mesoderm extends medially to form an infraumbilical abdominal wall. If this is deficient, the cloacal membrane can rupture anteriorly. Rupture after the urorectal septum has reached the urogenital membrane results in bladder exstrophy and rupture before the complete descent of the urorectal septum results in cloacal exstrophy.

5.7.2 Prenatal Ultrasound Findings

Bladder Exstrophy

Persistently non-visualized urinary bladder with normal amniotic fluid should raise the suspicion of bladder exstrophy. The redundant bladder mucosa is seen as a soft tissue mass at the lower abdominal wall inferior to cord insertion (Fig. 5.8).

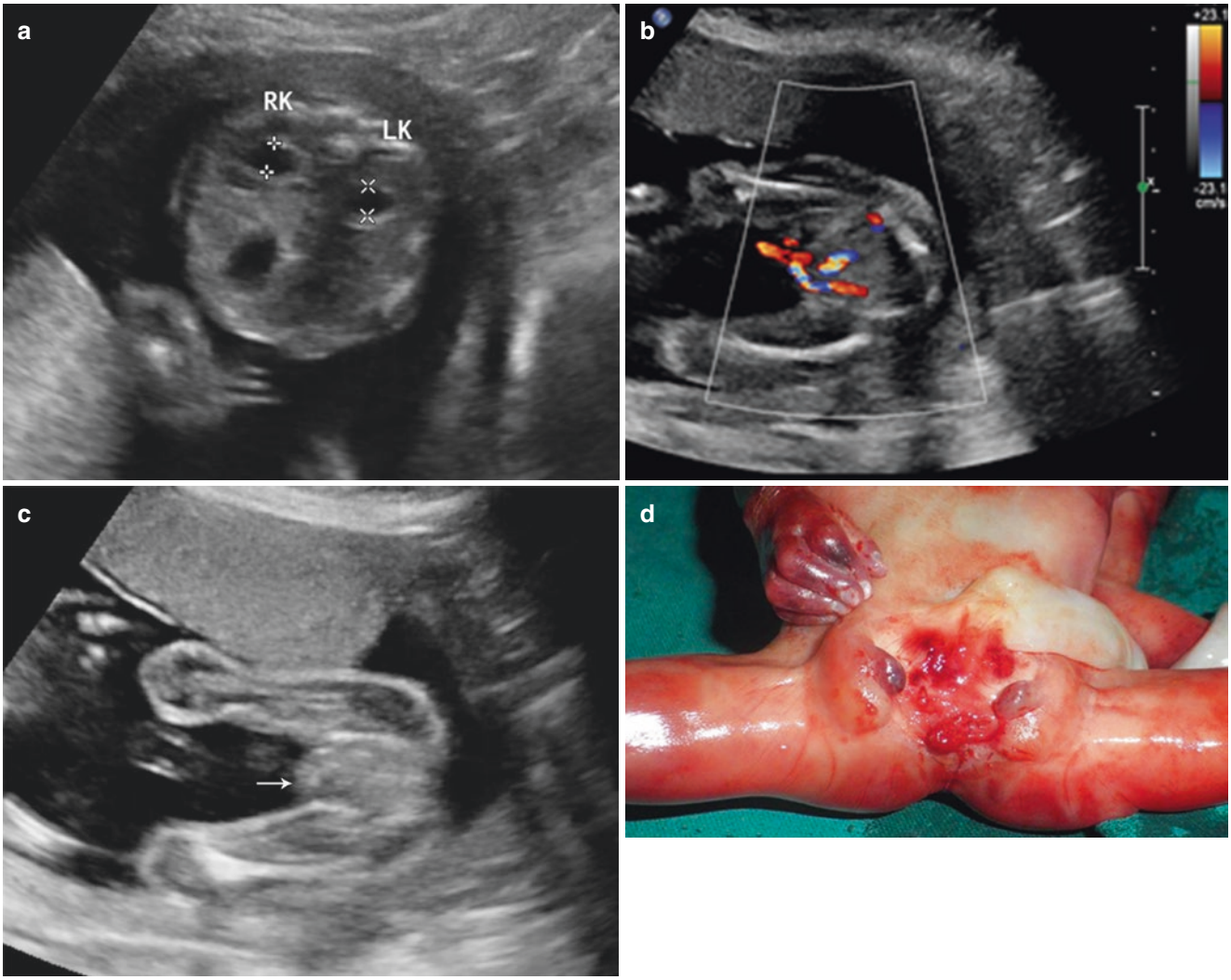

Fig. 5.8 Exstrophy of urinary bladder: (**a**) Axial scan showing the normal kidneys in a fetus with normal amniotic fluid volume. (**b**) Oblique coronal scan with color Doppler study of pelvis demonstrating absent urinary bladder between the umbilical arteries. (**c**) Oblique scan of fetal perineum and anterior abdominal wall demonstrating the irregular soft tissue mass (arrow) of lower abdominal wall below the cord insertion. (**d**) Photograph of abortus

Cloacal Exstrophy or OEIS Complex

Cloacal exstrophy is diagnosed when a persistently non-visualized bladder is associated with ventral wall defect, omphalocele, spinal defect, urinary tract anomaly along with ambiguous genitalia. The fetal anus is not seen. In the first trimester, a cystic mass is seen in the lower abdomen prior to the rupture of the cloacal membrane (Figs. 2.37, 5.9, and 5.10).

Karyotyping along with microarray should be done to detect genetic abnormalities and to detect fetal sex which may be difficult to determine by ultrasound imaging.

5.7.3 Outcome of Bladder and Cloacal Exstrophy

Outcome of bladder exstrophy is guarded as it involves multiple surgical procedures with problems of urinary incontinence and sexual function. Cloacal exstrophy is a lethal anomaly.

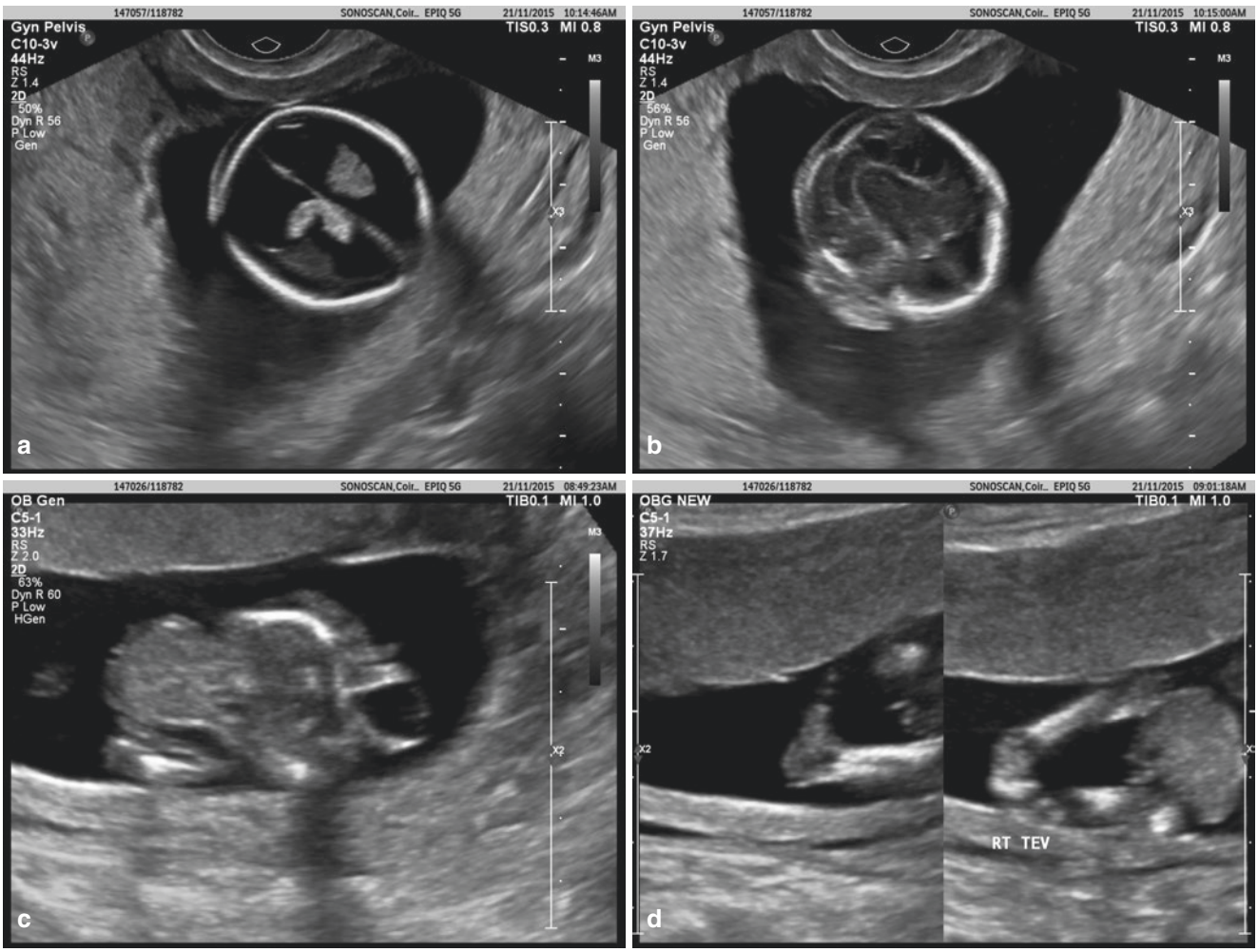

Fig. 5.9 Cloacal exstrophy: Axial scan of fetal head showing (**a**) bilateral lateral ventriculomegaly and (**b**) Arnold Chiari malformation; (**c**) axial scan of abdomen shows omphalocele and meningocele; (**d**) scan of lower limb shows talipes equinovarus deformity of one foot

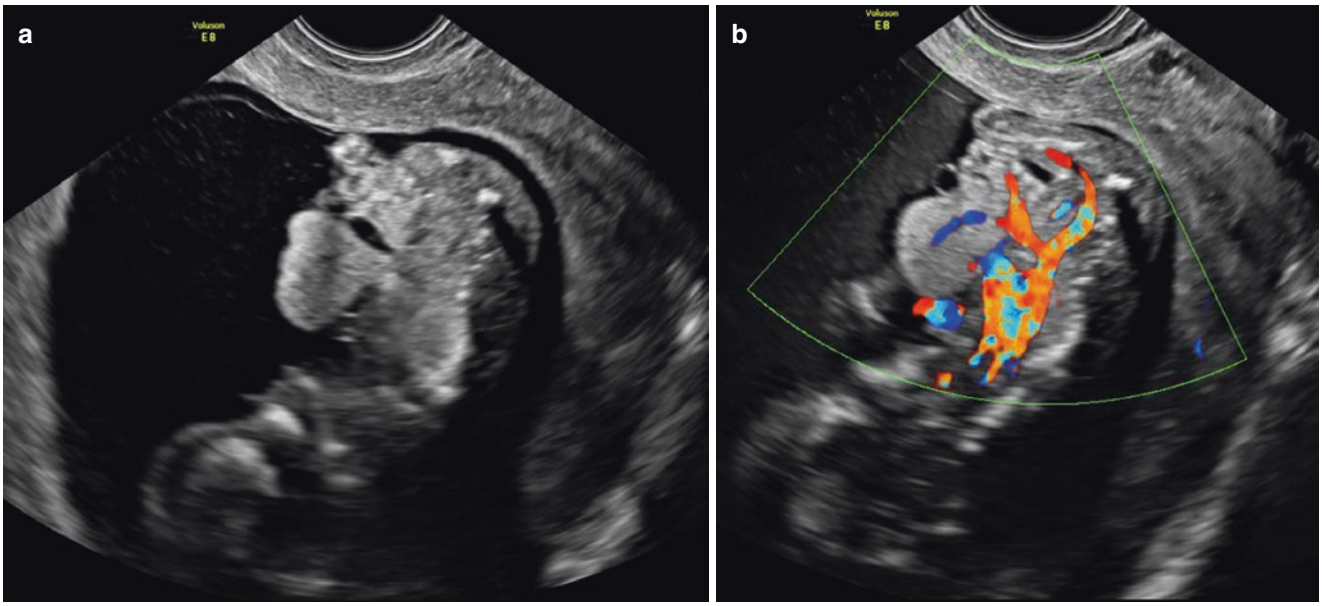

Fig. 5.10 Cloacal exstrophy in first trimester: (**a**) Longitudinal scan and (**b**) colour Doppler study, of at 13 weeks fetus showing the omphalocele, exstrophy of bladder and kyphoscoliosis of spine

5.8 Ectopia Cordis and Pentalogy of Cantrell

Ectopia cordis is defined as an anomaly in which the fetal heart lies outside the thoracic cavity either completely or partially. It is a rare congenital abnormality with an incidence of about 7 per 1 million live births. It is associated with omphalocele in Pentalogy of Cantrell. The Pentalogy of Cantrell is a rare anomaly characterized by a midline supraumbilical thoracoabdominal defect, a defect of the anterior diaphragm, a defect of the diaphragmatic pericardium and congenital cardiac anomalies.

5.8.1 Etiopathogenesis

Abnormal formation and migration of the ventral mesoderm during 14–18th post-fertilization days leads to a failure of fusion of the transverse septum of the diaphragm and lateral folds of the thorax.

5.8.2 Ultrasound Features

Diagnosis can be made as early as 10–12 weeks. The fetus shows a midline supraumbilical abdominal defect including herniated liver and ectopia cordis with a large omphalocele containing the intestines. Doppler and transvaginal ultrasound improves the precision in diagnosis (Fig. 5.11, Video 5.1 and Fig. 5.12, Video 5.2).

5.8.3 Associated Anomalies

A detailed search for the associated anomalies is mandatory since the prognosis mostly depends on the severity of these associated findings. Association with trisomy 13, 18 and Turner syndrome should be ruled out by invasive testing.

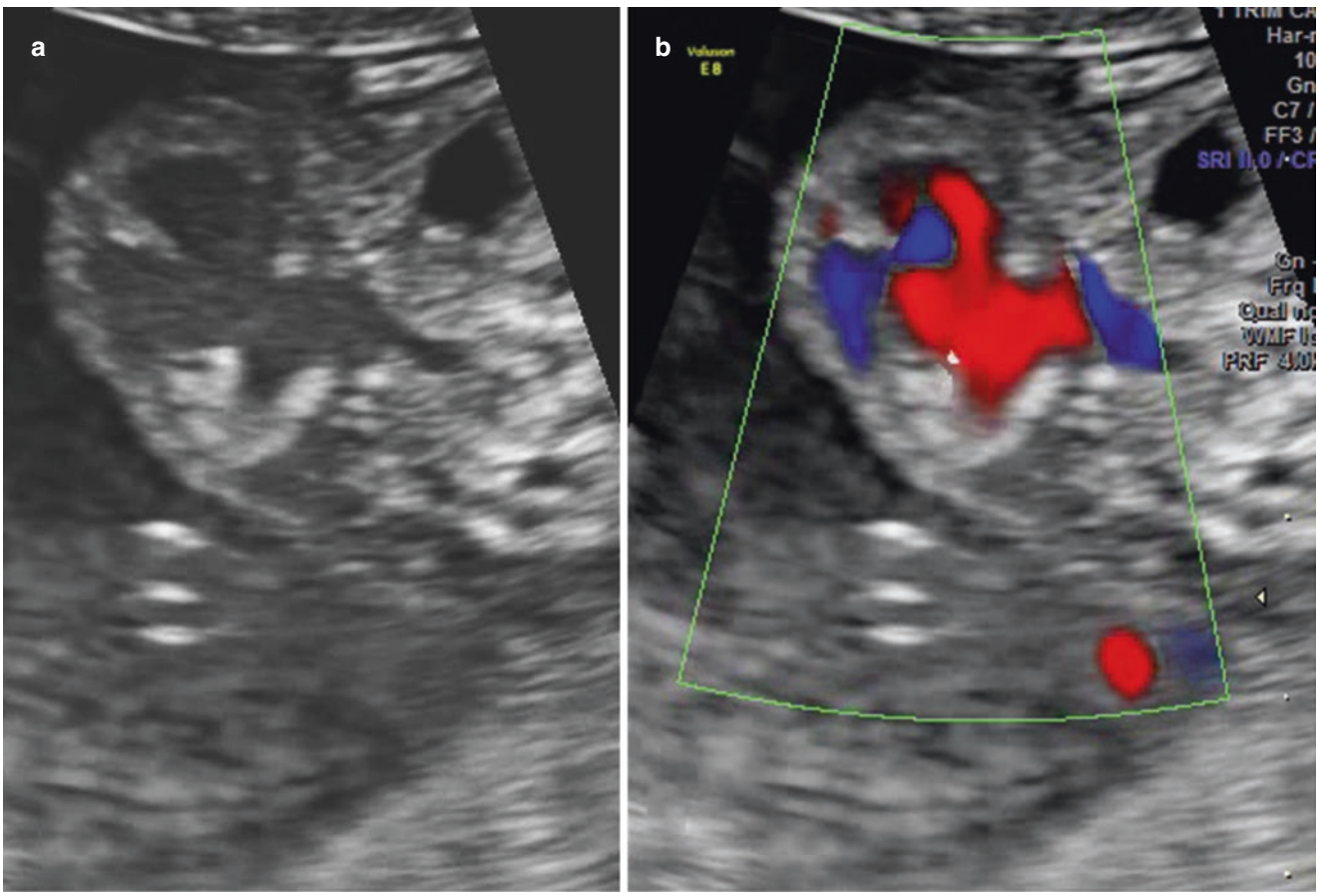

Fig. 5.11 Ectopia cordis in a 13 weeks fetus: (**a**) Gray scale and (**b**) colour Doppler study of axial scan of chest showing the fetal heart lying outside the chest (Video 5.1)

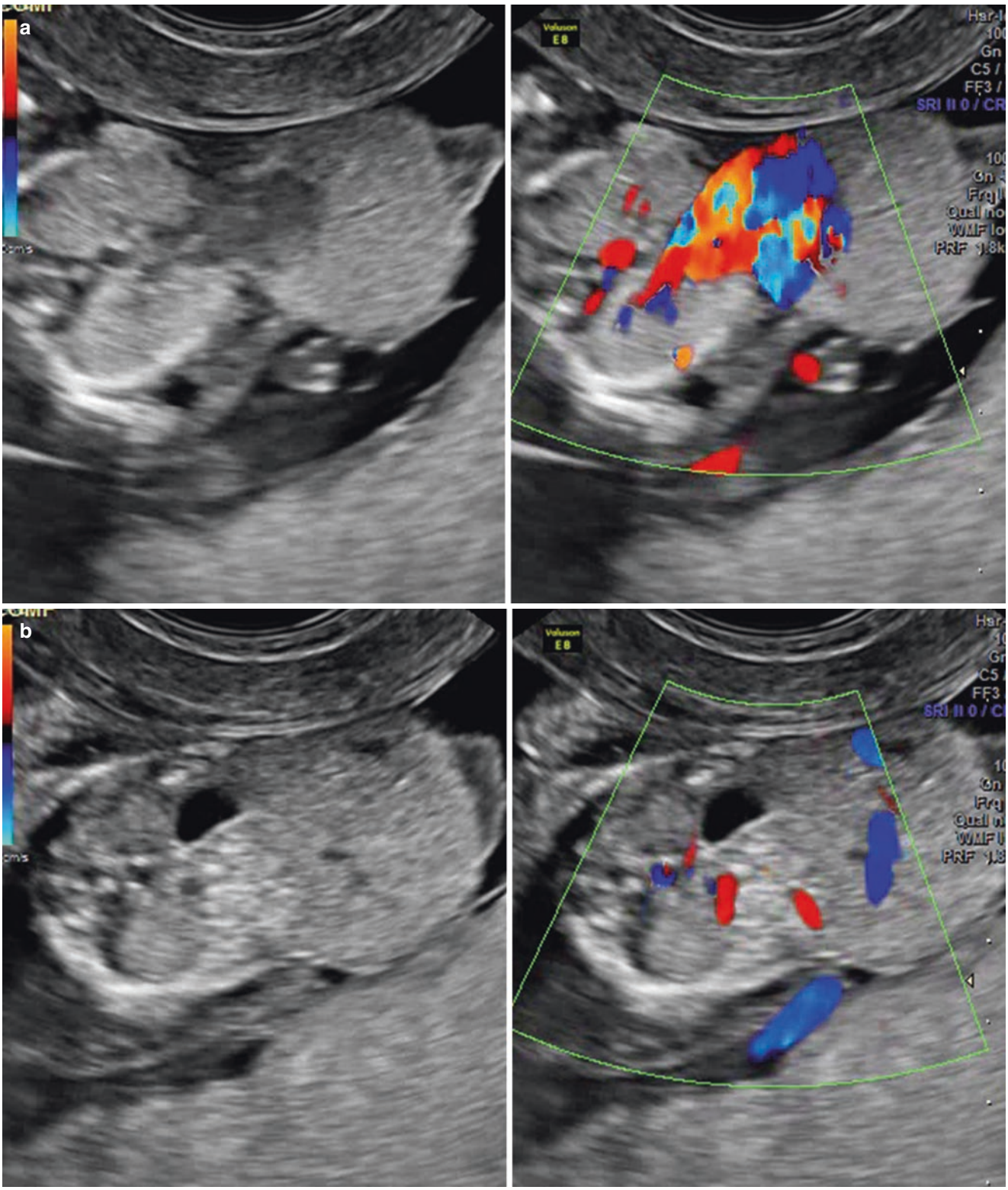

Fig. 5.12 Pentalogy of Cantrell: (**a**) Gray scale and colour Doppler study of axial scan of fetal chest showing ectopia cordis; (**b**) Gray scale and colour Doppler scan of axial scan of fetal abdomen showing the large omphalocele (Video 5.2)

5.9 Limb Body Wall Complex/Body Stalk Anomaly

Limb Body Wall Complex (LBWC)/Body stalk anomaly (BSA) is the rarest, most severe and invariably lethal abdominal wall defect. It is a severe defect where the abdominal wall does not develop and thus there is evisceration of abdominal structures into the extraembryonic coelom and as a result the fetus is attached to the placenta. This rare malformation syndrome has a reported prevalence of 0.12 cases per 10,000 births.

5.9.1 Aetiopathogenesis

Early maldevelopment of germinal disc causes multiple congenital anomalies. Other hypotheses are early amniotic rupture and vascular comprise.

5.9.2 Ultrasound Features

In the first trimester, fetal abdominal contents are seen eviscerated into the extra-embryonic coelom with a short or no cord. The fetal spine shows severe kyphoscoliosis (Figs. 5.13 and 5.14, Videos 5.3 and 5.4). In second trimester the fetus is seen in fixed position with the eviscerated abdominal contents adherent to placental surface. Cord insertion site cannot be identified. There are no free-floating bowel loops. The rest of the fetus shows movements (Fig. 5.15, Videos 5.5 and 5.6). In later gestation, oligoamnios is a prominent feature and it may be difficult to differentiate from omphalocele. High frequency scan will help to delineate the amniotic membrane and see the evisceration outside the amniotic membrane (Fig. 5.16).

5.9.3 Associated Anomalies

LBWC is a heterogeneous disease and is associated with varied internal anomalies. The central nervous system anomalies observed are anencephaly, encephalocele and alobar holoprosencephaly. Cardiovascular anomalies include primitive ventricle, common atrium atrial septal defects, common arterial trunk and membranous ventricular septal defect. The renal anomalies observed are unilateral or bilateral aplasia/hypoplasia of kidney. Genital abnormalities seen are abnormal external genitalia, absent gonad and exstrophy of bladder. Skeletal anomalies are most common and include club foot, oligodactyly, arthrogryposis, absent limb, single forearm bone, single lower leg bone, pesudosyndactyly, radial/ulnar hypoplasia, rotational defects and polydactyly. Karyotyping is usually normal.

5.9.4 Prognosis

LBWC is a lethal anomaly. Hence, it has to be differentiated from treatable causes like omphalocele or gastroschisis. But sometimes oligohydramnios may mask the underlying anomalies. High frequency probe is useful to demonstrate the amniotic membrane and evisceration of bowel. Early diagnosis followed by medical termination is the preferred treatment for this anomaly.

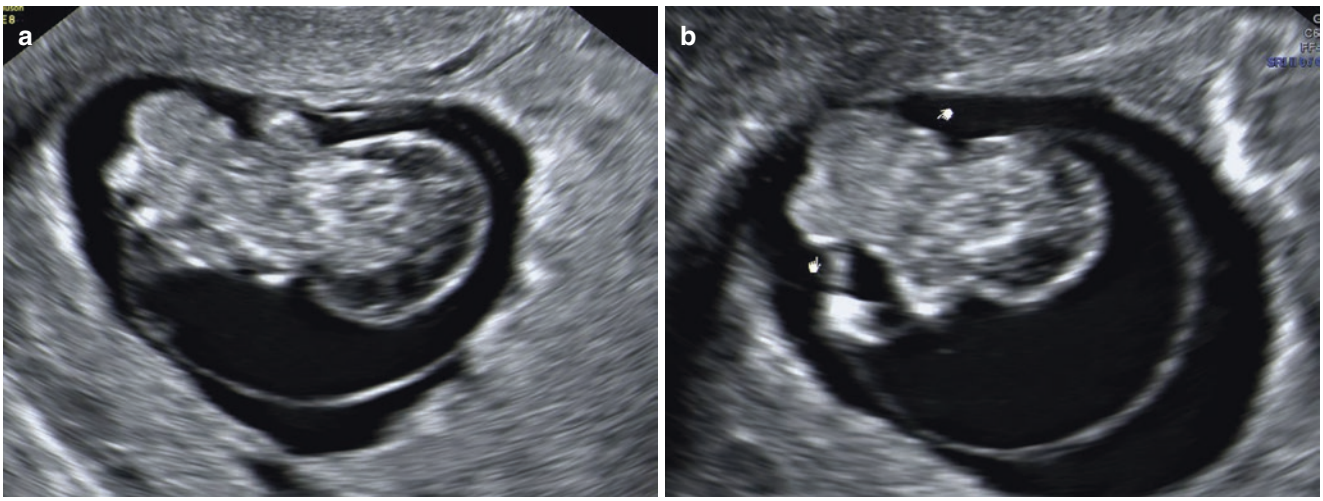

Fig. 5.13 Limb Body Wall Complex at 10 weeks: (**a**) Coronal scan of the fetus shows fetus in amniotic sac with scalp edema and evisceration of abdominal contents outside the amniotic sac. (**b**) Axial scan of the fetus clearly shows the eviscerated abdominal contents outside the amniotic sac (arrows)

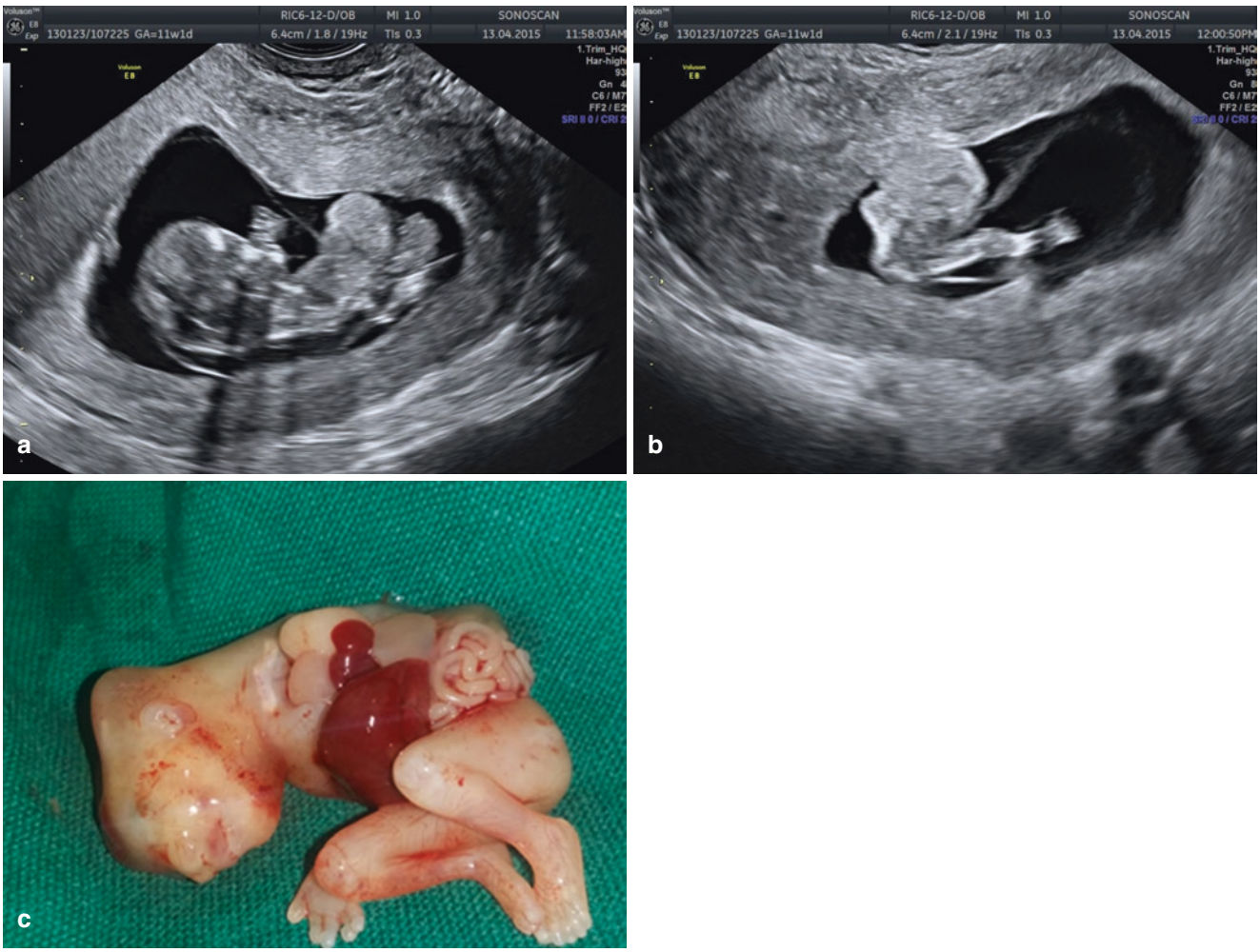

Fig. 5.14 Limb Body Wall Complex anomaly at 13 weeks: (**a**) Longitudinal and (**b**) axial scan of fetus shows evisceration of the viscera into the extraamniotic coelom. (**c**) Photograph of the abortus showing the anomaly (Videos 5.3 and 5.4)

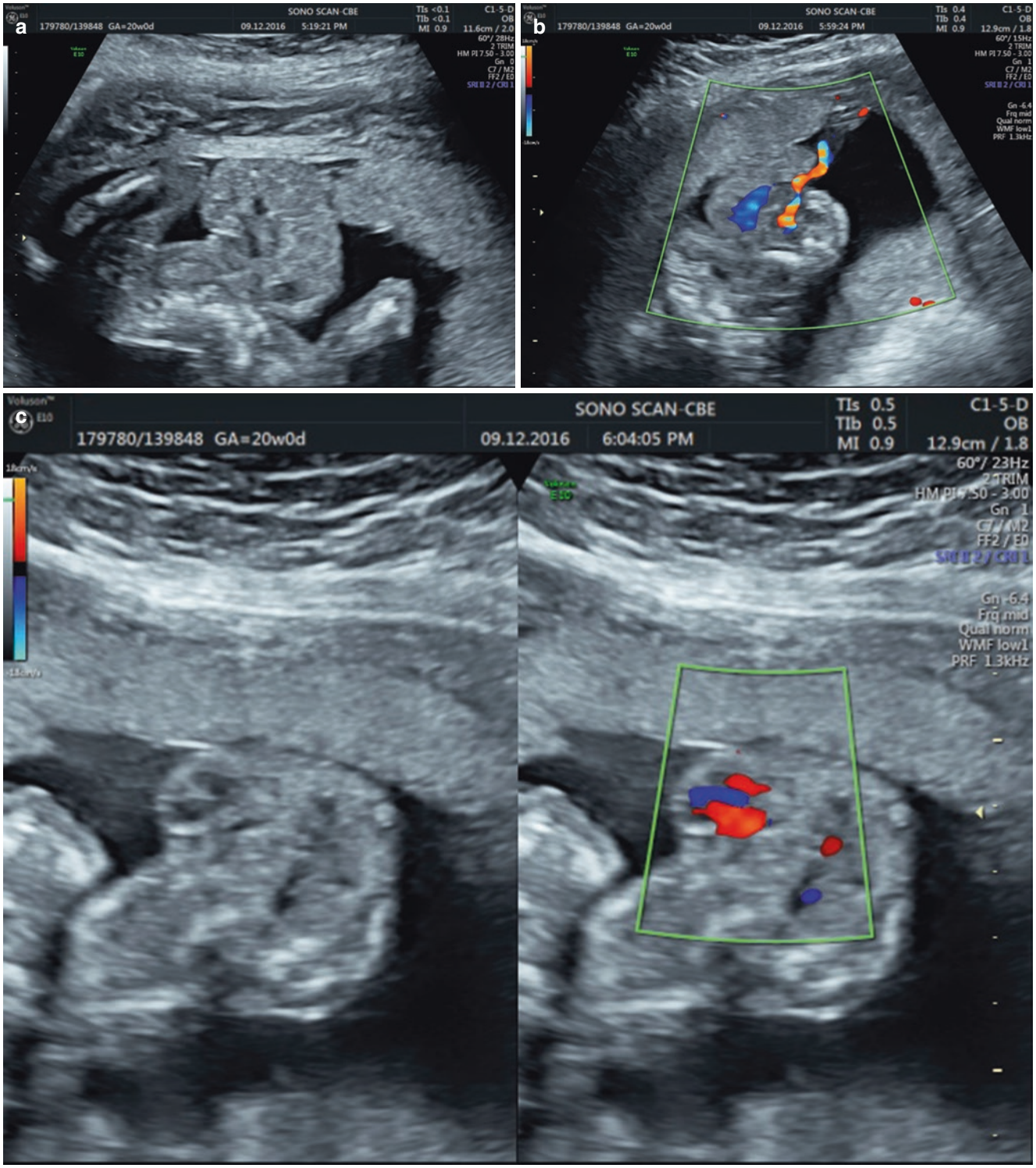

Fig. 5.15 Limb Body Wall Complex in early second trimester: (**a**) Oblique scan of fetus showing the evisceration of abdominal viscera into extraembryonic coelom close to the placenta. (**b**) Colour Doppler image showing the short umbilical cord. (**c**) Shows that the fetal heart is also eviscerated (video). Video showing that the eviscerated parts are fixed to the placenta while rest of the fetus shows movements (Videos 5.5 and 5.6)

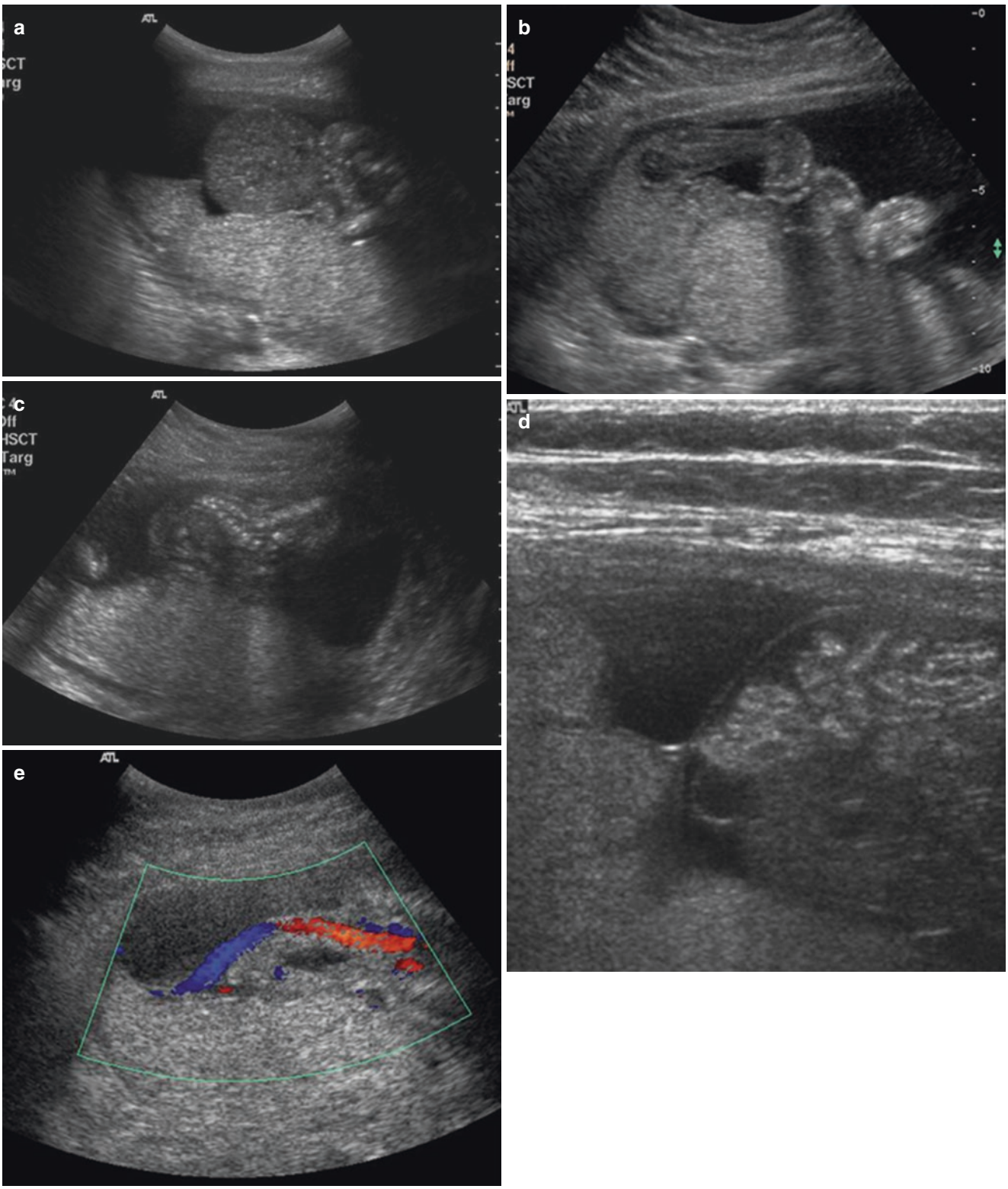

Fig. 5.16 Limb Body Wall Complex in late second trimester: (**a**) Longitudinal scan of fetus shows oligohydramnios which becomes a feature by this time of gestation and omphalocele. (**b**) Shows talipes equinovarus deformity of a foot. (**c**) Shows kyphoscoliosis of spine. (**d**) High frequency scan shows the amniotic membrane and that the bowels are outside the amniotic sac differentiating it from omphalocele. (**e**) Color Doppler scan shows short umbilical cord

5.10 Amniotic Band Syndrome

Amniotic band syndrome (ABS) is very rare and occurs in 0.5–1.0 of 10,000 births. Only a minority of cases involve the abdominal wall called abdominoschisis.

5.10.1 Aetiopathogenesis

The exogenous and endogenous theories are proposed to explain ABS. The exogenous theory by Torpin suggests rupture of the amnion without rupture of the chorion as the initial event. Subsequent oligohydramnios and attachment of the fetus to the "sticky" chorionic surface lead to entanglement of fetal parts and disruption defects. The endogenous theory suggests that vascular endothelial injury is the underlying pathogenesis of constriction bands and secondary limb amputation.

5.10.2 Ultrasound Features

The ultrasound features are highly variable depending upon the fetal body parts involved in amniotic bands. Earlier the amniotic rupture, more severe is the defect. The defects in amniotic band syndrome occur in a non-anatomic distribution and are described as "slash defects." Recognition of the slash appearance should lead to a careful search for bands, which may be difficult to see. Findings include fine linear echoes extending from the defect to the uterine wall. In abdominoschisis, the abdomimnal contents float in the amniotic fluid withoiut a clear encasing membrane and bands may also trap the umbilical cord. The cord insertion site may be hard to see, depending on the location of the band (Fig. 5.17).

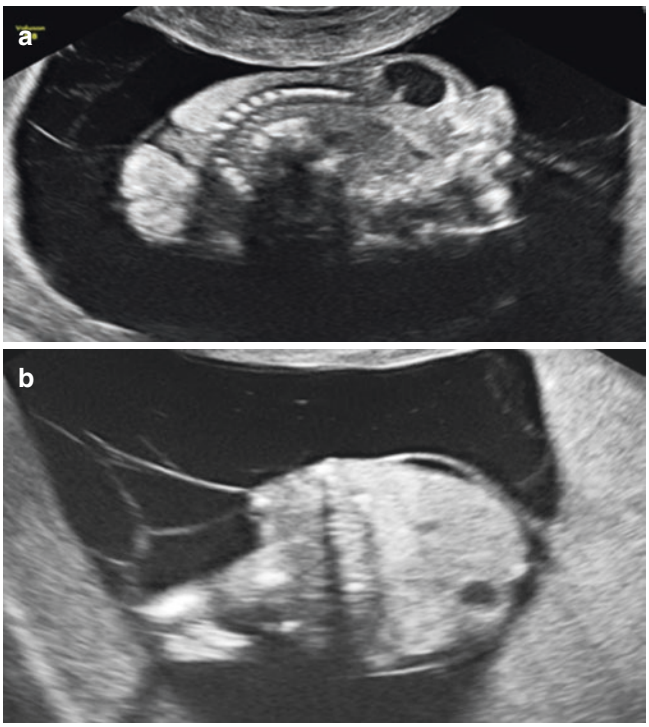

Fig. 5.17 Abdominoschisis in amniotic band syndrome: (**a**) Endovaginal sonography showing deformed cephalic pole with amniotic bands attached to it. (**b**) Shows eviscerated abdominal contents with amniotic band attached to it

5.11 Prognosis in ABS

The prognosis is poor in abdominoschisis.

5.12 Parasitic Twin

This is a very rare condition where an incomplete twin fetal part is attached to anterior abdominal wall. On Ultrasound axial section fetal abdomen shows part of trunk and lower limbs of the parasitic twin attached to anterior abdominal wall of an otherwise normal fetus (Fig. 5.18a, b and Video 5.7).

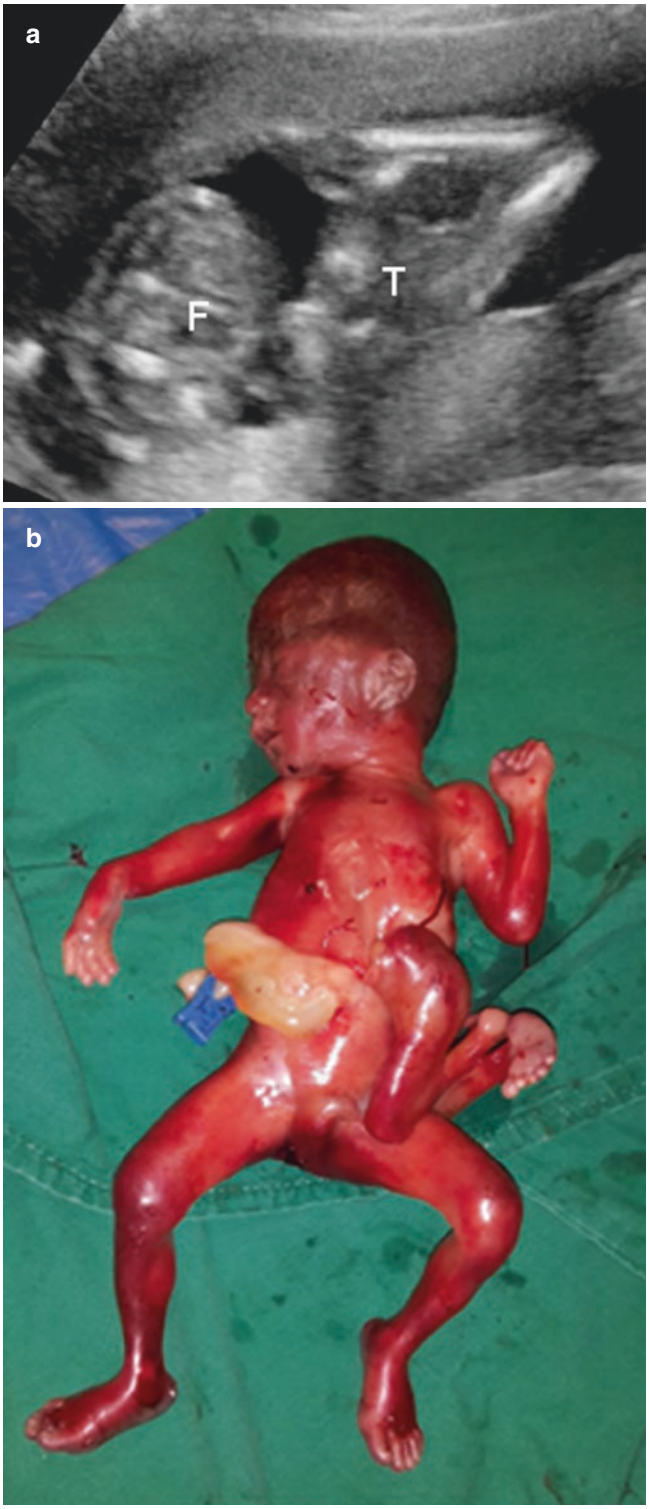

Fig. 5.18 Parasitic twin: (**a**) Axial scan of fetal abdomen showing trunk of parasitic twin (T) with lower limbs attached to the anterior abdominal wall of the fetus (F). (**b**) Photograph of the abortus (Video 5.7)

Conclusion

Abdominal wall defects are a complex group of congenital anomalies with a broad spectrum of manifestations and outcome. First step is evaluation of the cord insertion site in relation to the defect. The defects involving cord insertion are omphalocele, cloacal exstrophy, Pentalogy of Cantrell, abdominoschisis and body stalk anomaly. Omphalocele as an isolated defect has good prognosis. In cloacal exstrophy, the associated defect is inferior and in Pentalogy of Cantrell, the defect is superior. The defects with intact cord insertion are gastroschisis and bladder exstrophy. Absent urinary bladder is a finding in both bladder and cloacal exstrophy. Fixed fetal position and undefinable anatomic parts are hallmarks of abdominoschisis due to Amniotic Band syndrome and Body Stalk Anomaly. Recognition of more complex AWDs is vital in pregnancy counselling and management.

Suggested Reading

Brantberg A, Blaas HG, Haugen SE, Eik-Nes SH. Characteristics and outcome of 90 cases of fetal omphalocele. Ultrasound Obstet Gynecol. 2005;26(5):527–37.

Calzolari E, Bianchi F, Dolk H, Milan M, EUROCAT Working Group. Omphalocele and gastroschisis in Europe: a survey of 3 million births 1980–1990. Am J Med Genet. 1995;58:187–94.

Goetzinger KR, Tuuli MG, Longman E, et al. Sonographic predictors of postnatal bowel atresia in fetal gastroschisis. Ultrasound Obstet Gynecol. 2014;43:420–5.

Goyal A, Fishwick J, Hurrell R, Cervellione RM, Dickson AP. Antenatal diagnosis of bladder/cloacal exstrophy: challenges and possible solutions. J Pediatr Urol. 2012;8(2):140–4.

Khalil A, Arnaoutoglou C, Pacilli M, et al. Outcome of fetal exomphalos diagnosed at 11–14 weeks of gestation. Ultrasound Obstet Gynecol. 2012;39:401–6.

Mayer T, Black R, Matlack ME, Johnson DG. Gastroschisis and omphalocele: an eight year review. Ann Surg. 1980;192:783–7.

Pakdaman R, Woodward PJ, Kennedy A. Complex abdominal wall defects: appearances at prenatal imaging. Radiographics. 2015;35(2):636–49.

Raicevic M, Filipovic I, Sindjic-Antunovic S. Hernia of the umbilical cord associated with a patent omphalomesentric duct. J Postgrad Med. 2017;63:58–9.